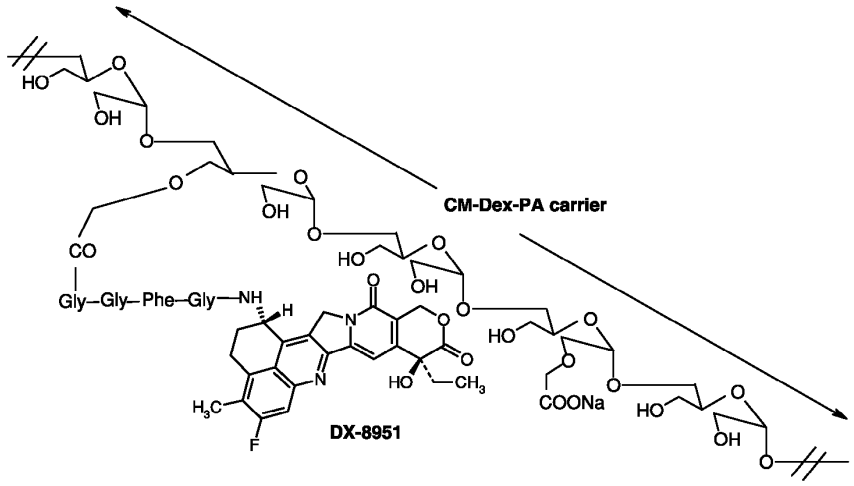


Figure 1. Partial structure of DE-310.

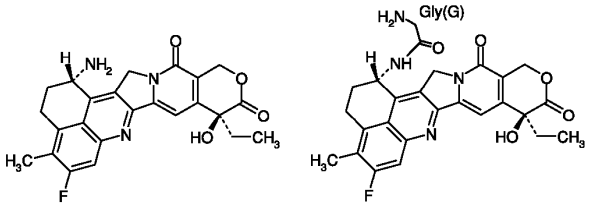


Figure 2. Chemical structures of DX-8951 and G-DX-8951.

and 0.38 ng/mL of free doxorubicin for 1 mL human plasma.

We have recently reported HPLC methods for the determination of DX-8951 in mouse and human plasma using a fluorometric detector (Oguma *et al.*, 2000, 2001a). The LLOQs of DX-8951 were 3 ng/mL for 100 µL of mouse plasma and 0.2 ng/mL for 500 µL of human plasma. It is thought that the sensitivity of HPLC is not adequate to analyze tissue samples, and the total analysis time is relatively long. Furthermore, we have developed an LC/MS/MS method for the determination of DX-8951 in human plasma (Oguma *et al.*, 2001b). It is suggested that the use of this LC/MS/MS method enables the chromatographic run time to be reduced, and is applicable for analyzing both released free drugs and conjugated drug in tumor tissue.

In this study, enzymatic digestion was used to treat samples for the analysis of a polymer-bounded compound in method II. We report here that enzymatic digestion with thermolysin is a very useful method for the determination of polymer-bounded compounds such as DX-8951. Our data suggest that phenylalanyl-glycyl-DX-8951 is released from conjugated DX-8951 after enzyme digestion. In addition, the peak areas derived from phenylalanyl-glycyl-DX-8951 are proportional to the concentrations of conjugated DX-8951. This tendency permits the determination of conjugated DX-8951 in biological samples. For the determination of free drug (not conjugated), it is suggested that two major compounds, DX-8951 and G-DX-8951, are released from conjugated DX-8951 by lysosomal enzymes of cathepsins in tumor tissue. In this paper, we describe methods for determining DX-8951 and G-DX-8951 (method I), and conjugated DX-8951 (method II) levels in tumor tissue by LC/MS/MS. The validations of these methods are also described.

EXPERIMENTAL

Chemicals. DE-310, DX-8951f and G-DX-8951 were synthesized at Daiichi Pharmaceutical Co., Ltd (Tokyo, Japan). D91-7117, (9*S*)-9-ethyl-2,3-dihydro-9-hydroxy-4-[(isopentylamino)methyl]-1*H*,2*H*-benzo[*de*]pyrano[3′,4′:6,7]indolizino[1,2-*b*]quinoline-10,13(9*H*,15*H*)-dione, was synthesized by Daiichi Pharmaceutical Co. Ltd (Tokyo) and used as an internal standard (IS). The methanol used was HPLC-grade (Wako Pure Chemical Industries Ltd, Osaka, Japan). The thermolysin used was biochemical-grade (Wako Pure Chemical Industries Ltd, Osaka, Japan). All other chemicals were of analytical reagent grade and used without purification. Water was purified by the Milli-Q system (Millipore, Milford, MA, USA).

Equipment. The chromatographic system comprised Waters 2795 Separation Modules (Waters, Milford, MA, USA) and a Symmetry C_{18} column (150 × 4.6 mm i.d.; Waters, Milford, MA, USA). The column temperature was kept at 45°C. The mobile phase for method I was an isocratic elution of methanol–0.1vol% trifluoroacetic acid (2:3, v/v). The mobile phase for method II was an isocratic elution of methanol–0.1vol% trifluoroacetic acid (9:11, v/v). The flow rate was 0.8 mL/min. An API-4000 mass spectrometer (Applied

Copyright © 2004 John Wiley & Sons, Ltd.

Biosystems/MDS Sciex, Concord, Canada) equipped with an atmospheric pressure chemical ionization (APCI) source was used. The mass spectrometer was operated in the positive-ion detection mode.

The temperature of the heated nebulizer was set at 500°C. The needle current was set at 2 μA. Nitrogen gas was used to obtain collision-induced detection (CID). The mass spectrometer was operated in the multiple reaction monitoring (MRM) mode. Ions were detected by monitoring the decay of the *m/z* 436 precursor ion to the *m/z* 419 product ion for DX-8951 [collision energy −40 V; Fig. 3(I)], the decay of the *m/z* 493 precursor ion to the *m/z* 419 product ion for G-DX-8951 [collision energy −40 V; Fig. 3(II)], the decay of the *m/z* 640 precursor ion to the *m/z* 493 product ion for phenylalanyl-glycyl-DX-8951 [collision energy −45 V; Fig. 3(III)], and the decay of the *m/z* 488 precursor ion to the *m/z* 401 product ion for D91-7117 [collision energy −40 V; Fig. 3(IV)]. Peak areas for all components were automatically integrated by using Analyst™ software, and peak-area ratios (area of analytes/area of IS) were plotted vs concentration by weighted linear regression (1/concentration^2).

The peak-area ratios (area of DX-8951, G-DX-8951/area of D91-7117) in method I were plotted vs concentration by weighted linear regression (1/concentration^2). The peak-areas of phenylalanyl-glycyl-DX-8951 in method II were plotted vs concentration by weighted linear regression (1/concentration^2).

Preparation of standard solutions

Standard solutions of DX-8951, G-DX-8951, and D91-7117 were prepared in 0.04 M Britton–Robinson buffer (pH 3) and diluted with the same buffer. The concentrations of these compounds were expressed as equivalents of their free bases. We analyzed the conjugated form to its carrier, conjugated DX-8951, using a standard solution of DE-310. Standard solutions of DE-310 were prepared in purified water and diluted with 0.1% Brij35 solution. This compound concentration was expressed as equivalents of DX-8951. These standard solutions were stored at 4°C under dark conditions.

Sample preparation. Tumor tissues as blank samples were isolated from Meth A tumor-bearing mice as follows: Balb/c male mice were transplanted subcutaneously with Meth A fibrosarcoma (1×10^6) cells. Subcutaneous tumor tissues obtained from the mice for analysis were homogenized in 10 vols of physiological saline (w/v).

For the analytical procedure of DX-8951 and G-DX-8951 (method I), 0.18 mL of a standard, or quality control (QC), or unknown sample and 0.03 mL of an internal standard (D91-7117, 0.5 μg/mL) were placed into a test tube. A 1 mL volume of 1 mol/L hydrochloric acid/methanol (1:99, v/v) was added to each tube and mixed, followed by centrifugation at 10,000 rpm for 5 min. The supernatants were transferred into test tubes and were evaporated to dryness under a stream of

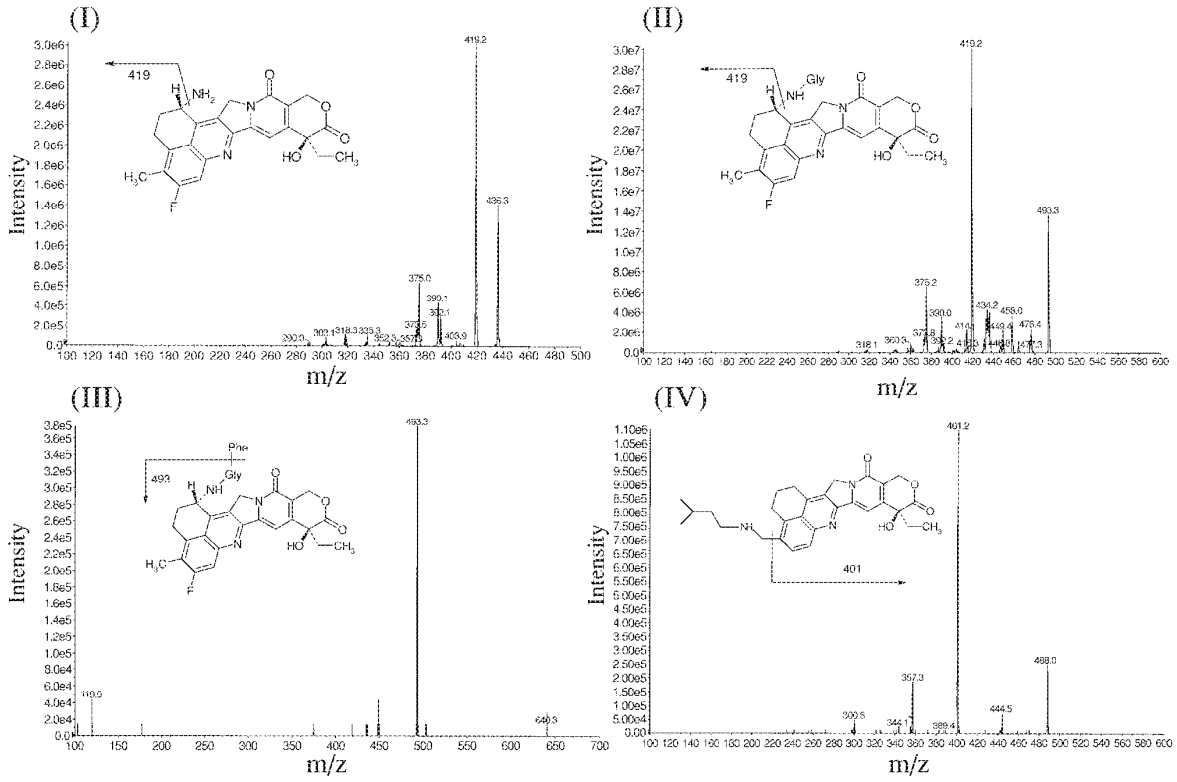


Figure 3. MS/MS full scan of product ions of (I) DX-8951, (II) G-DX-8951, (III) phenylalanyl-glycyl-DX-8951 and (IV) D91-7117 at the precursor ion of $[M+H]^+$.

Copyright © 2004 John Wiley & Sons, Ltd.

nitrogen gas at 40°C. The residues were reconstituted in 0.2 mL of mobile phase and mixed thoroughly. Each solution was applied to an Ultrafree-MC Centrifugal filters (UFC3 LTK, Millipore, USA) and centrifuged at 8000 rpm for 20 min. The filtrate solution, 0.08 mL, was injected onto the LC/MS/MS system.

To analyze conjugated DX-8951 (method II), 0.18 mL of a standard, QC, unknown sample and 0.07 mL of an internal standard (D91-7117, 2.5 μg/mL) were placed into a test tube. A 0.25 mL volume of 0.1 mol/L dipotassium hydrogenphosphate buffer (pH 8.5)–methanol (1:4, v/v) was added to each tube and mixed thoroughly by vortexing, followed by centrifugation at 10,000 rpm for 10 min. The supernatant (supernatant A) was removed to a test tube. To the remaining layer, 0.125 mL of 0.1 mol/L dipotassium hydrogenphosphate buffer (pH 8.5)–methanol (1:4, v/v) was added and mixed thoroughly by vortexing, followed by centrifugation at 10,000 rpm for 10 min. The supernatant (supernatant B) was removed to the test tube to combine with supernatant A. Thermolysin (6 mg) was dissolved in 0.75 mL of 0.1 mol/L Tris–hydrochloride buffer (pH 8.5)–0.1 mol/L calcium chloride solution (1:1, v/v). This enzymatic solution was added to the combined supernatants in the test tube. Each sample was placed on a shaker at 50°C for 2 h and then centrifuged at 3000 rpm for 5 min. The samples were applied to solid-phase extraction cartridges, pre-conditioned first with 2 mL of methanol, and then with 2 mL of purified water. The cartridge was washed with 2 mL of purified water. Then the analytes were eluted with 3 mL of 1 mol/L hydrochloric acid-methanol solution (1:99, v/v). The eluates were evaporated to dryness under a stream of nitrogen gas at 40°C. The residues were reconstituted in 0.2 mL of mobile phase and mixed thoroughly. The solutions were applied to Ultrafree-MC Centrifugal filters and centrifuged at 8000 rpm for 10 min. The filtrate solution, 0.04 mL, was injected onto the LC/MS/MS system.

Validation procedures. The absolute recoveries of DX-8951, G-DX-8951 and conjugated DX-8951 from tumor tissue homogenate solution were estimated by comparing the peak areas of extracted samples vs those of unextracted standard solutions. The selectivity of the assay was investigated by processing and analyzing six independent blank (drug-free) samples by the procedure described above. Calibration curves were constructed by plotting the peak area ratio of the analytes to IS against the concentration of the analyte. Each calibration curve consisted of nine calibration points ($n = 1$). The data were fitted to least squares linear regression with a weighting factor of $1/(\text{concentration})^2$. Intra-day precision evaluated as relative standard deviation (RSD) and accuracy of the method were determined by replicate analyses ($n = 5$) of QC samples. Inter-day precision (RSD) and accuracy were determined by replicate analyses ($n = 6$) of QC samples on three separate days. The lower limit of quantitation (LLOQ) was chosen as the concentration of the lowest calibration standard with an acceptable limit of variance (within 20% for both precision and accuracy). Stability during freezing and thawing was assessed using the QC samples after three freeze–thaw cycles. Stability in the autosampler was assessed using the QC samples after the reconstituted solutions were prepared and placed into the autosampler for 48 h, according to the method described above. Stability at room temperature was assessed by using the QC samples that had been placed on the bench top for 12 h. Stability during storage at −80°C was assessed using the QC samples that had been placed in a storage freezer set at −80 ± 5°C for 3 months.

Application of the method. To demonstrate their reliability, these methods were used to determine concentrations of DX-8951, G-DX-8951 and conjugated DX-8951 in tumor tissue samples. Meth A tumor-bearing mice were administrated a single intravenous infusion of DE-310 at a dose of 5.7 mg/kg/30 s that was 1/2 MTD (maximum tolerated dose) level for mice. Tumor tissue samples were collected from each animal at 12 h after the start of the infusion. Samples were stored at −80°C until analyzed.

RESULTS AND DISCUSSION

Recoveries

Recoveries of DX-8951 and G-DX-8951 from spiked tissue samples were determined at the concentrations of 1.36, 10.80 and 1350.27 ng/g for DX-8951, and 1.34, 10.65 and 1329.68 ng/g for G-DX-8951 in triplicate by method I. The mean recoveries of DX-8951 ranged from 86.8 to 99.0%. The mean recoveries of G-DX-8951 ranged from 90.5 to 94.6%, and that of IS was 97.3%.

Recoveries of conjugated DX-8951 from spiked tissue samples were determined at the concentrations of 73.7, 590 and 14700 ng/g (DX-8951 equivalent) in triplicate by method II. The mean recoveries of conjugated DX-8951 ranged from 70.5 to 77.2%, and that of IS was 88.7%. The recoveries of conjugated DX-8951 show a little lower. It is possible that the efficiency of enzymatic digestion using thermolysin is reduced in biological samples.

These extraction methods have been successfully applied to the extraction of DX-8951 G-DX-8951 and conjugated DX-8951 from tumor tissue.

Chromatography and selectivity

Chromatograms of tumor tissue extracts obtained from blank tumor tissue and blank tumor tissue spiked with DX-8951 (1.36 ng/g), G-DX-8951 (1.34 ng/g) and IS (100 ng/g) using method I are shown in Fig. 4. The retention times of DX-8951, G-DX-8951 and IS were approximately 5, 9 and 8 min, respectively. The overall chromatographic run times were within ca. 9 min.

Chromatograms of tumor tissue extracts obtained from blank tumor tissue and blank tumor tissue spiked with conjugated DX-8951 (73.7 ng/g) using method II are given in Fig. 5. The retention times of phenylalanyl–glycyl-DX-8951 and IS were approximately 14 and 7 min. The overall chromatographic run time was within ca. 14 min. These chromatograms indicated that no endogenous compounds interfered

Copyright © 2004 John Wiley & Sons, Ltd.

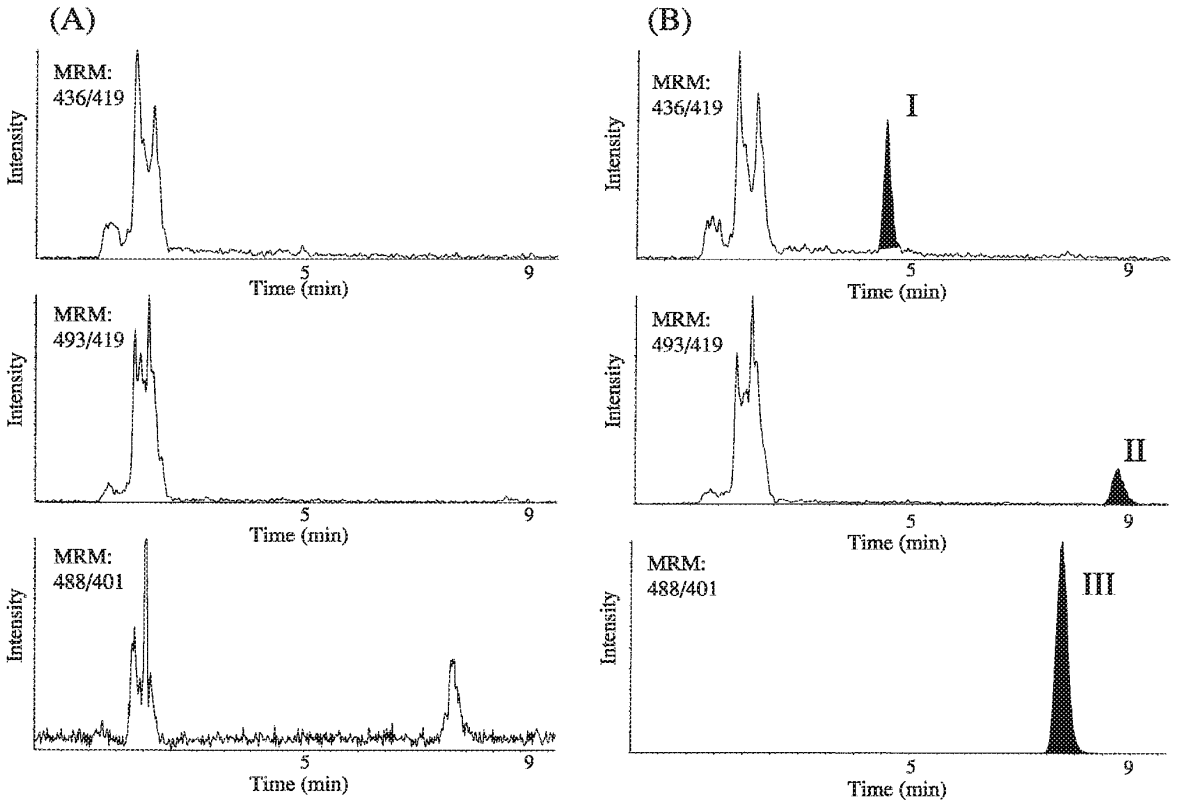


Figure 4. MRM chromatograms of (A) extract of blank tumor tissue and (B) extracts of blank tumor tissue spiked with DX-8951 (2.40 ng/mL), G-DX-8951 (3.08 ng/mL) and IS (33.92 ng/mL) using method I. [I = DX-8951, II = G-DX-8951 and III = IS.]

with the detection of DX-8951, G-DX-8951, and phenylalanyl-glycyl-DX-8951 at their retention times.

Calibration curves

Calibration curves for DX-8951 and G-DX-8951 in tumor tissue obtained on three separate days were linear over the concentration ranges of 1.36–2700.54 ng/g (DX-8951) and 1.34–2659.36 ng/g (G-DX-8951). The coefficients of determination (r^2) for DX-8951 and G-DX-8951 were not less than 0.9993 and 0.994, respectively.

Calibration curves for conjugated DX-8951 in tumor tissue obtained on three separate days were linear over the concentration range 73.7–73700 ng/g (DX-8951 equivalent). The coefficient of determination (r^2) was not less than 0.9978.

Precision and accuracy

The results of intra- and inter-assay precision and accuracy for DX-8951 and G-DX-8951 are shown in Table 1. The intra-assay precisions (RSD) of DX-8951 and G-DX-8951 estimates for the QC samples were less than 4.4 and 6.2%, respectively. The intra-assay accuracies of DX-8951 and G-DX-8951 were within −4.3 and −3.9%, respectively. The inter-assay precisions (RSD) of DX-8951 and G-DX-8951 were less than 6.7 and 7.4%, respectively. The inter-assay accuracies of DX-8951 and G-DX-8951 were within 4.4 and 2.7%, respectively.

The results of intra- and inter-assay precision and accuracy for conjugated DX-8951 are shown in Table 2. The intra-assay precision (RSD) of conjugated DX-8951 estimates for the QC samples was less than 5.0%. The intra-assay accuracy of conjugated DX-8951 was within −13.2%. The inter-assay precision (RSD) of conjugated DX-8951 estimates for the QC samples was less than 8.2%. The intra-assay accuracy of conjugated DX-8951 was within −9.2%. The accuracies of method II were shown to be slightly worse than those of method I. It is suggested that the pretreatment procedure of method II was slightly complicated in comparison with method I.

These results indicated that our described methods have satisfactory precision and accuracy.

Stability

The freeze–thaw stabilities of DX-8951 and G-DX-8951 were evaluated (Table 3). The mean accuracies of

Copyright © 2004 John Wiley & Sons, Ltd.

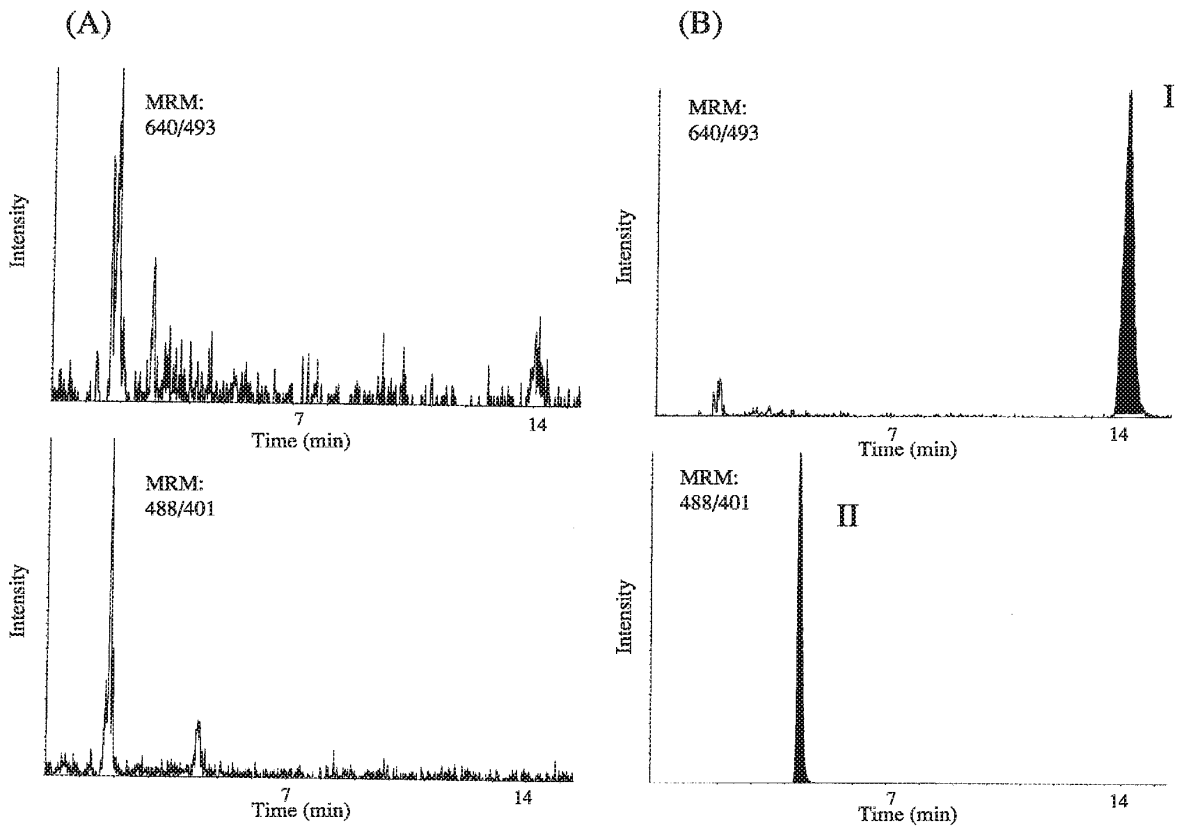


Figure 5. MRM chromatograms of (A) extract of blank tumor tissue and (B) extracts of blank tumor tissue spiked with Conjugated DX-8951 (2.40 ng/mL) and IS (33.92 ng/mL) using method II. [I = phenylalanyl-glycyl-DX-8951, II = IS.]

Table 1. Intra- and inter-assay precision and accuracy for DX-8951 and G-DX-8951 in tumor tissue using method I

Analytes	Nominal concentration (ng/g)	Intra-assay precision and accuracy			Inter-assay precision and accuracy		
		Mean (n = 5) (ng/g)	RSD (%)	Mean accuracy (%, n = 5)	Mean (n = 6) (ng/g)	RSD (%)	Mean accuracy (%, n = 6)
DX-8951	1.36	1.34	3.0	−1.5	1.33	2.3	−2.2
	10.80	10.34	1.8	−4.3	10.93	5.9	1.2
	1350.27	1318.34	4.4	−2.4	1410.26	6.7	4.4
G-DX-8951	1.34	1.30	6.2	−3.0	1.34	4.5	0.0
	10.65	10.23	3.7	−3.9	10.94	7.4	2.7
	1329.68	1303.64	1.7	−2.0	1323.84	1.6	−0.4

Table 2. Intra- and inter-assay precision and accuracy for conjugated DX-8951 in tumor tissue using method II

Analyte	Nominal concentration[a] (ng/g)	Intra-assay precision and accuracy			Inter-assay precision and accuracy		
		Mean (n = 5) (ng/g)	RSD (%)	Mean accuracy (%, n = 5)	Mean (n = 6) (ng/g)	RSD (%)	Mean accuracy (%, n = 5)
Conjugated DX-8951	73.7	67.8	5.0	−8.0	75.7	8.2	2.7
	590.0	512.0	1.6	−13.2	536.0	7.8	−9.2
	14700.0	14700.0	4.1	0.0	15300.0	3.9	4.1

[a] Equivalent to DX-8951.

Copyright © 2004 John Wiley & Sons, Ltd.

Table 3. Stability of DX-8951 and G-DX-8951 in tumor tissue

Analytes	Nominal concentration (ng/g)	After three cycles of freeze–thaw Mean accuracy (%, $n = 3$)	After storage at room temperature for 12 h Mean accuracy (%, $n = 3$)	After storage at −80°C for 3 months Mean difference[a] (%, $n = 3$)
DX-8951	2.71	−6.4	9.4	−7.8
	1350.27	−3.3	−0.6	3.0
G-DX-8951	2.66	7.8	5.2	−12.8
	1329.68	11.7	14.0	−3.8

[a] Difference from the concentrations on the first day.

Table 4. Stability of conjugated DX-8951 in tumor tissue

Analyte	Nominal concentration (ng/g)	After three cycles of freeze–thaw Mean accuracy (%, $n = 3$)	After storage at room temperature for 12 h Mean accuracy (%, $n = 3$)	After storage at −80°C for 3 months Mean difference[a] (%, $n = 3$)
Conjugated	147.0	−6.1	−3.6	8.2
DX-8951	14700.0	−3.9	−13.9	0.0

[a] Difference from the concentrations on the first day.

DX-8951 and G-DX-8951 after three cycles were within −6.4 and 11.7%, respectively. The room temperature stabilities of DX-8951 and G-DX-8951 in tumor tissue were evaluated (Table 3). The mean accuracies of DX-8951 and G-DX-8951 after storage for 12 hours were within 9.4 and 14.0%, respectively. After storage at −80°C for 3 months, the concentrations of QCs of DX-8951 and G-DX-8951 were comparable with those of freshly prepared QCs (Table 3). The mean differences of DX-8951 and G-DX-8951 between the stored and fresh samples were within −7.8 and −12.8%, respectively.

The freeze–thaw stabilities of conjugated DX-8951 were evaluated (Table 4). The mean accuracy of conjugated DX-8951 after three cycles was within −6.1%. The room temperature stabilities of conjugated DX-8951 in tumor tissue were evaluated (Table 4). The mean accuracy of conjugated DX-8951 after storage for 12 h was within −13.9%. After storage at −80°C for 3 months, the concentrations of QCs of conjugated DX-8951 were comparable with those of freshly prepared QCs (Table 4). The mean difference of conjugated DX-8951 between the stored and fresh samples was within 8.2%.

These results showed that no significant degradation occurred during three freeze–thaw cycles, and that these analytes were stable in tumor tissue kept for 12 h at room temperature, and for at least 3 months at −80°C.

Analysis of samples

The suitability of these analytical methods was demonstrated by the determination of DX-8951, G-DX-8951 and conjugated DX-8951 in tumor tissue samples after the start of infusion (5.7 mg/kg) of DE-310. The chromatograms of the tumor tissue samples are shown in Figs 6 and 7. These two methods are applicable to determine the compounds in tumor tissues.

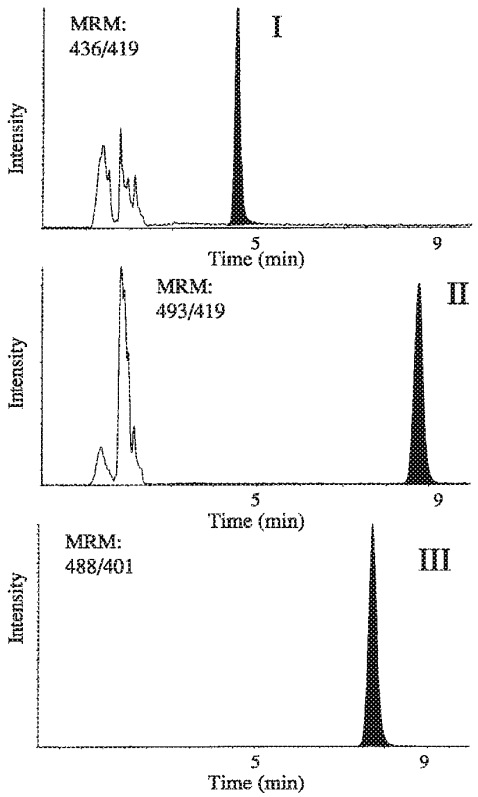


Figure 6. MRM chromatogram of DX-8951 and G-DX-8951 in a tumor tissue sample obtained 12 h after intravenous infusion of DE-310 (5.7 mg/kg). [I = DX-8951, II = G-DX-8951 and III = IS.]

Copyright © 2004 John Wiley & Sons, Ltd.

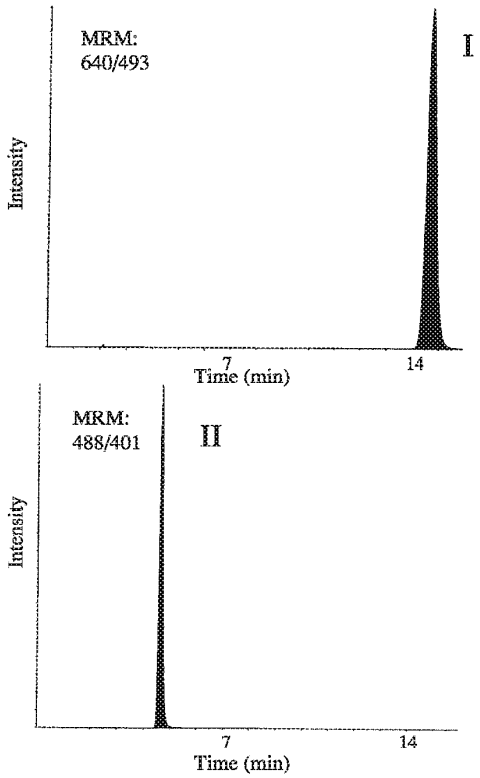


Figure 7. MRM chromatogram of Conjugated DX-8951 in a tumor tissue sample obtained 12 h after intravenous infusion of DE-310 (5.7 mg/kg). [I = phenylalanyl-glycyl-DX-8951, II = IS.]

CONCLUSION

Sensitive and selective analytical methods for the determination of DX-8951 G-DX-8951 and conjugated DX-8951 in tumor tissue were established by LC/MS/MS. These methods proved to be useful for pre-clinical pharmacokinetics studies of DE-310.

REFERENCES

Fraier D, Frigerio E, Pianezzola E, Benedetti MS, Cassidy J and Vasey P. A sensitive procedure for the quantitation of free and N-(2-hydroxypropyl) methacrylamide polymer-bound doxorubicin (PK1) and some of its metabolites, 13-dihydrodoxorubicin, 13-dihydrodoxorubicinone and doxorubicinone, in human plasma and urine by reversed-phase HPLC with fluorimetric detection. *Journal of Pharmaceutical and Biomedical Analysis* 1995; **13**: 625–633.

Fraier D, Frigerio E, Brianceschi G, Casati M, Benecchi A and James C. Determination of MAG-camptothecin, a new polymer-bound camptothecin derivative, and free camptothecin in dog plasma by HPLC with fluorimetric detection. *Journal of Pharmaceutical and Biomedical Analysis* 2000; **22**: 505–514.

Inoue K, Kumazawa E, Kuga H, Susaki H, Masubuchi N and Kajimura T. CM-dextran-polyalcohol-camptothecin conjugate: DE-310 with a novel carrier system and its preclinical data. *Advances in Experimental Medicine and Biology* 2003; **519**: 145–153.

Maeda H. The enhanced permeability and retention (EPR) effect in tumor vasculature: the key role of tumor-selective macromolecular drug targeting. *Advances in Enzyme Regulation* 2001; **41**: 189–207.

Maeda H, Wu J, Sawa T, Matsumura Y and Hori K. Tumor vascular permeability and EPR effect in macromolecular therapeutics: a review. *Journal of Control of Release* 2000; **65**: 271–284.

Matsumura Y and Maeda H. A new concept for macromolecular therapeutics in cancer chemotherapy: mechanism and antitumor agent smancs. *Cancer Research* 1986; **46**: 6387–6392.

Oguma T, Ohshima Y and Nakaoka M. Sensitive high-performance liquid chromatographic method for the determination of the lactone form and the lactone plus hydroxy-acid forms of the new camptothecin derivative DX-8951 in human plasma using fluorescence detection. *Journal of Chromatography B* 2000; **740**: 237–245.

Oguma T, Yamada M, Konno T, Inukai K and Nakaoka M. High-Performance liquid chromatographic analysis of lactone and hydroxy acid of new antitumor drug, DX-8951 (exatecan), in mouse plasma. *Biological and Pharmaceutical Bulletin* 2001a; **24**: 176–180.

Oguma T, Konno T, Inaba A and Nakaoka M. Validation study of assay method for DX-8951 and its metabolite in human plasma and urine by high-performance liquid chromatography/atmospheric pressure chemical ionization tandem mass spectrometry. *Biomedical Chromatography* 2001b; **15**: 108–115.

Schoemaker NE, Frigerio E, Fraier D, Scellens JH M, Rosing H, Jansen S and Beijnen JH. High-performance liquid chromatographic analysis for the determination of a novel polymer-bound camptothecin derivative (MAG-camptothecin) and free camptothecin in human plasma. *Journal of Chromatography B* 2001; **763**: 173–183.

Copyright © 2004 John Wiley & Sons, Ltd.

OnCusp
Ex. 1002

Clinical Significance of *TROP2* Expression in Colorectal Cancer

Takahiro Ohmachi,[1,2,3] Fumiaki Tanaka,[1,3] Koshi Mimori,[1,3] Hiroshi Inoue,[1,3] Katsuhiko Yanaga,[2] and Masaki Mori[1,3]

Abstract

Purpose and Experimental Design: To identify cancer-related genes, the expression profiles of colorectal cancer cells and normal epithelial cells were examined and compared using laser microdissection and cDNA microarray analysis. From these combined techniques, several cancer-related genes, including *TROP2*, were identified. *TROP2* is known as a calcium signal transducer and is highly expressed in several types of tumors. However, no studies have investigated the significance of *TROP2* expression in colorectal cancer. Thus, the expression status of *TROP2* was investigated in 74 colorectal cancer samples by quantitative real-time reverse transcription-PCR and immunohistochemical studies.

Results: Laser microdissection and cDNA microarray analysis showed that there were 84 overexpressed genes in cancer cells. One of the highly overexpressed genes was *TROP2*. Quantitative real-time reverse transcription-PCR showed that *TROP2* expression in cancer samples was significantly higher than in normal samples ($P < 0.001$). The samples were divided into high ($n = 26$) and low ($n = 48$) *TROP2* expression groups. The cases with high *TROP2* expression showed a higher frequency of liver metastasis ($P = 0.005$) and more cancer-related death ($P = 0.046$). Those cases also had an inclination of deeper depth of invasion ($P = 0.064$) and more lymph node metastasis ($P = 0.125$). Interestingly, the patients with high *TROP2* expression tumors had poorer prognosis ($P = 0.0036$). Multivariate analysis showed that *TROP2* expression status was an independent prognostic factor (relative risk, 2.38; 95% confidence interval, 1.29-4.74; $P < 0.01$).

Conclusion: *TROP2* is one of the cancer-related genes that correlates with biological aggressiveness and poor prognosis of colorectal cancer. Thus, *TROP2* is a possible candidate gene for diagnosis and molecular target therapy of colorectal cancer.

Colorectal cancer is one of the most prevalent cancers in the world. In Japan, the disease rate of colorectal cancer patients has doubled over the past 20 years, with ~75 of 100,000 people suffering from the disease today. Additionally, colorectal cancer has been the second cause of death in neoplastic disease (1). Recently, molecular target therapy and cancer immunotherapy for solid cancers have been introduced to the clinic (2–5). However, indications for these therapies are limited due to the low frequency of target gene expression, unstable effectiveness, and/or severe side effects (5, 6). Thus, there is a pressing need to explore novel cancer-specific genes to serve as molecular targets for therapy and cancer specific immunotherapy.

In this study, the gene expression profiles were compared between cancer cells and normal epithelial cells using the combined techniques of laser microdissection and cDNA microarray analysis to explore cancer-related or cancer-specific genes. From this analysis, several cancer-related genes were identified. Among them, *TROP2* showed markedly different expression between cancer cells and normal epithelial cells.

Fornaro et al. cloned the *TROP2* gene, which encodes a 35,709-Da type 1 transmembrane protein with a single transmembrane domain and is homologous to *TROP1/KSA/GA733-2*. Moreover, *TROP2*, a cell surface receptor, has been shown to play a role in regulating the growth of carcinoma cells (7). *TROP2* is also responsible for gelatinous drop-like corneal dystrophy (8). *TROP2* is expressed at high levels in human trophoblast cells and it has been reported as one of the highly specific genes to the tumors, such as ovarian and bladder cancers (9–12). On the other hand, our institute developed tumor-specific immunotherapy using *MAGE* peptide-pulsed dendritic cells (13). We are planning to expand the therapy using other tumor-specific genes. Depending on the outcome of this analysis, *TROP2* may become a candidate gene. In addition, the clinical significance of the gene has not been studied in colorectal cancer. Thus, we investigated *TROP2*

Authors' Affiliations: [1]Department of Surgery and Molecular Oncology, Medical Institute of Bioregulation, Kyushu University, Beppu, Japan; [2]Department of Surgery, Jikei University School of Medicine, Tokyo, Japan, and [3]Core Research for Evolutional Science and Technology, Japan Science and Technology Agency, Saitama, Japan

Received 9/7/05; revised 2/4/06; accepted 3/15/06.

Grant support: Core Research for Evolutional Science and Technology, Japan Science and Technology Agency; Uehara Memorial Foundation; Japan Society for the Promotion of Science Grant-in-Aid for Scientific Research (grants 17015032, 17109013, 17591411, 17591413, 17015032, and 16390381).

The costs of publication of this article were defrayed in part by the payment of page charges. This article must therefore be hereby marked *advertisement* in accordance with 18 U.S.C. Section 1734 solely to indicate this fact.

Requests for reprints: Masaki Mori, Department of Surgery and Molecular Oncology, Medical Institute of Bioregulation, Kyushu University, 4546 Tsurumihara, Beppu 874-0838, Japan. Phone: 81-977-27-1650; Fax: 81-977-27-1651; E-mail: mmori@beppu.kyushu-u.ac.jp.

©2006 American Association for Cancer Research.

doi:10.1158/1078-0432.CCR-05-1961

Table 1. Overexpressed genes in colorectal cancer

Gene name	Symbols	Systematic code	Locus	Fold overexpression
Dipeptidase 1 (renal)	*DPEP1*	J05257	16q24,3	17.59
Teratocarcinoma-derived growth factor 1	*CRIPTO*	AU124747	3p21,31	8.35
Human megakaryocyte-enhanced gene transcript 1 protein	*MEGT1*	AF195764	6p21,33	8.22
Cell surface glycoprotein Trop-2	*TROP2*	BG259957	1p32,1	7.84
Integrin β_3 (platelet glycoprotein IIIa, antigen CD61)	*CD61*	NM_000212	17q21,32	7.12
Matrix metalloproteinase-7 (matrilysin, uterine)	*MMP7*	NM_002423	11q21-q22	6.71
Phosphoprotein C8FW	*TRIB3*	BG387820	20p13	6.56
Human cell surface glycoprotein CD44 (CD44) gene	*CD44*	L05411	11p13	6.08
Epiregulin	*EREG*	BG235918	4q13,3	5.71
Matrix metalloproteinase-11 (stromelysin 3)	*MMP11*	AW301093	22q11,23	5.70
Human clone PP1195 unknown mRNA	.....	AF217970	8p23,1	4.80
Human cDNA FLJ20093fis, clone COL04263	ANKRD10	AK000100	13q34	4.73
Cadherin 3, type 1, P-cadherin (placental)	*CDH3*	NM_001793	1q22,1	4.63
Fatty acid – binding protein 6, ileal (gastrotropin)	*FABP6*	X90908	5q23,35	4.48
KIAA0546 protein	.....	AB011118	12q15	4.36
Ataxia telangiectasia group D – associated protein	*TRIM29*	AF230388	11q22-q23	4.24
TAR (HIV) RNA-binding protein 1	*TARBP1*	U38847	1q42,3	4.06
Expressed sequence tags	*PPAT*	AA442070	4q12	3.82
Expressed sequence tags	*AK126318*	BE672109	17q23,2	3.68
Human mRNA; cDNA DKFZp564C053	.....	AL049246	3q23	3.60
Solute carrier family 12, member 2	*SLC12A2*	U30246	5q23,2	3.58
Human Na,K-ATPase α-1 subunit gene	*ATP1A1*	M30309	1p13,1	3.56
Ectodermal-neural cortex (with BTB-like domain)	*ENC1*	BC000418	5q12-13,3	3.47
Bone morphogenetic protein 7 (osteogenic protein 1)	*BMP7*	BE395650	20q13,31	3.42
Solute carrier family 7, member 5	*SLC7A5*	M80244	16q24,2	3.42
Human DNA for apoER2	*LRP8*	D86407	1p32,3	3.41
Human mRNA for KIAA0761 protein	*MCLC*	AB018304	1p13,3	3.40
Human activin β-A subunit	*INHBA*	X57579	7p14,1	3.39
Deleted in lymphocytic leukemia, 2	*DLEU2*	AW978447	13q14,2	3.38
Human mRNA for nuclear pore complex protein	*NUP107*	AJ296745	12q15	3.33
Growth factor receptor-bound protein 7	*GRB7*	AU148656	17q12	3.32
Human mRNA for KIAA0619 protein	*ROCK2*	AB014619	2p25,1	3.32
Meiotic recombination (Saccharomyces cerevisiae) 11 homologue A	*MRE11A*	AF073362	11q21	3.29
Chromosome 20 open reading frame 119	*TOMM34*	AK026760	20q13,12	3.26
ZFM1 protein alternatively spliced product	*SF1*	D26121	11q13	3.24
Mevalonate kinase (mevalonic aciduria)	*MVLK*	BG474232	12q24,11	3.22
Oviductal glycoprotein 1, 120 kDa (mucin 9, oviductin)	*OVGP1*	NM_002557	1p13,2	3.16
Zinc finger protein 195	*BRD1*	AW025438	1p22,1	3.14
Centromere protein F (350/400 kDa, mitosin)	*CENPF*	U19769	1q41	3.12
Cadherin 6, type 2, K-cadherin (fetal kidney)	*CDH6*	AU149929	5p16,1-p14	3.09
Solute carrier family 11, member 2	*SLC11A2*	AI868673	12q13,12	3.08

(Continued on the following page)

expression in clinical samples of colorectal cancer to determine its clinicopathologic significance.

Materials and Methods

Tissue sampling, laser microdissection, and cDNA microarray analysis. The samples of cancer tissues and noncancerous tissues were obtained from 16 patients with colorectal cancer who underwent surgical resection in Kyushu University Hospital (Beppu, Japan). Written informed consent was obtained from all patients. Tumors and adjacent normal tissues were immediately embedded in Tissue-Tek OCT compound medium (Sakura, Tokyo, Japan) and were kept frozen at −80°C until laser microdissection was done. Serial 8-μm frozen sections were generated by a cryostat. Sections were mounted onto a foil-coated glass slide, 90 FOIL-SL25 (Leica Microsystems, Wetzlar, Germany) for laser microdissection. Slides were stained with H&E at room temperature and dehydrated with ethanol. The Application Solutions Laser Microdissection System (Leica Microsystems) was introduced for laser microdissection to obtain the cancer cells and normal epithelial cells and to discard the mesenchymal tissues. Laser microdissection was done for several sequential sections and total RNA was extracted from each section (14). As the extracted total RNA was insufficient for hybridization to the cDNA microarray, the RNA was subjected to T7-based RNA amplification (15). The purity and concentration of the amplified RNA were determined by an Agilent

Table 1. Overexpressed genes in colorectal cancer (Cont'd)

Gene name	Symbols	Systematic code	Locus	Fold overexpression
Zinc finger, X-linked, duplicated A	*ZXDA*	AL031115	Xp11.1	3.07
Runt-related transcription factor 1	*RUNX1*	D43969	21q22.12	3.06
Expressed sequence tags	*TORD9*	AA844124	14q32	3.03
Spectrin, α, erythrocytic 1 (elliptocytosis 2)	*SPTA1*	AA703344	1q23.1	3.02
Human transcription factor SL1 (by similarity)	*TAF1A*	AK001054	1q41	3.01
Glycoprotein glucosyltransferase precursor (by similarity)	*UGCGL2*	AK001735	13q32.1	2.98
Formyl peptide receptor-like 1	*FPRL1*	BG541691	19q13.41	2.93
Guanine nucleotide binding protein 4	*GNG4*	AW593228	1q42.3	2.93
Prostaglandin E receptor 4 (subtype EP4)	*PTGER4*	NM_000958	5p13.1	2.93
Human cDNA FLJ10517fis, clone NT2RP2000812	*ASPM*	AK001379	1q31.3	2.92
Human G-protein-coupled receptor gene	*GPR19*	U55312	12p132	2.88
Human mRNA; cDNA DKFZp566P1124	----	AL110236	11q14.1	2.87
Human thiazide-sensitive NaCl cotransporter	*SLC12A3*	U44128	16q13	2.87
KIAA0410 gene product	*NUPL1*	BI599177	13q12.13	2.87
High-mobility group protein isoform I-C	*HMGA2*	BG250825	12q14.3	2.83
Human, paired box gene 9	*PAX9*	BC001159	14q13.3	2.82
Guanidinoacetate N-methyltransferase	*GAMT*	NM_000156	19p13.3	2.81
Karyopherin α3	*KPNA3*	D89618	13q14.2	2.80
KIAA0008 gene product	*DLG7*	BI087140	14q22.3	2.79
Nucleophosmin/nucleoplasmin 3	*NPM3*	AI631542	10q24.31	2.77
Zinc finger protein 200	*ZNF200*	NM_003454	16p13.3	2.75
Ras-related associated with diabetes	*RRAD*	AI186786	16q22.1	2.73
Human metabotropic glutamate receptor 8	*GRM8*	U92459	7q31.33	2.70
Zinc finger protein homologous to Zfp91 in mouse	*ZFP91*	AB057443	11q12.1	2.70
Human G-protein-coupled receptor GPR86	*GPR86*	AF295368	3q25.1	2.67
Nuclear receptor subfamily 1, group I, member 3	*NR1I3*	Z30425	1q23.3	2.66
Human homeobox gene	*HOXB*	AF287967	17q21.32	2.62
Human interleukin-17	*IL17*	U32659	6p12	2.62
Zinc finger protein 184 (Kruppel-like)	*ZNF184*	BG254958	6p22.1	2.61
Macaque *somatostatin I*	*SST*	M19318	3q27.3	2.60
Expressed sequence tags	*PTPN22?*	AA401425	1p13.2	2.58
Human ZNF43	*ZNF43*	X59244	19p12	2.57
Homer, neuronal immediate early gene, 1B	*HOMER1*	BI858644	5q14.1	2.55
Homo sapiens *clone 23903 mRNA sequence*	----	AF035281	7q36.1	2.55
Natural killer cell group 7 sequence	*NKG7*	S69115	19q13.41	2.55
Expressed sequence tags	----	AI025099	19p13.2	2.54
Human mRNA for CSR1	*SCARA3*	AB007829	8p21.1	2.53
Neuronal pentraxin II	*NPTX*	BC000924	7q22.1	2.52
KIAA0322 protein	*NEDL1*	AB002320	7p14.1-p13	2.51
Cyclin E1	*CCNE1*	BG761079	19q12	2.50
Death-associated transcription factor 1	*DATF1*	AB002331	20q13.33	2.50
Human DNA for single-minded gene 2	----	D85922	21q22.13	2.50
RasGAP-related protein	*IQGAP2*	AAB37765	5q13.3	2.50

2100 Bioanalyzer (Agilent Technologies, Palo Alto, CA) as described previously (14). In brief, high-quality amplified RNA run on a bioanalyzer typically has the shape of a hump peak and one marker peak, indicating no contamination of rRNA. Of 16 cancer and 16 normal microdissected and T7-based amplified RNA samples, 8 samples from the cancer sections and 10 samples from the normal sections were determined to be of sufficient quality. Each 8 RNA samples from cancer sections and the mixture of 10 RNA samples from normal epithelium were hybridized competitively to a cDNA microarray containing 12,814 genes. A list of genes on this cDNA microarray is available from http://www.agilent.com/chem/genelists.

Microarray analysis. After subtracting the local and global background signals, the expression values were calculated as the intensity of the dye-normalized red (Cy5) and green (Cy3) channel signals. The data flagged as poor quality according to the Agilent data extraction software were removed from the analysis. All data calculated by data extraction software were imported to the Rosetta Luminator system version 2.0 (Rosetta Biosoftware, Kirkland, WA). Candidate genes were selected that fulfilled the following criteria: the control (Cy3) intensity was <700, the fold changes were >2.5, and the P was <0.01 (14). Moreover, within the selected genes that met these criteria, genes that were up-regulated in three or more RNA samples (eight total samples) were further analyzed.

Semiquantitative real-time PCR. The semiquantitative real-time reverse transcription-PCR assay used 74 operatively resected paired cancer and normal samples that were not used for microarray analysis. Total RNA was extracted from each bulk sample and cDNA was

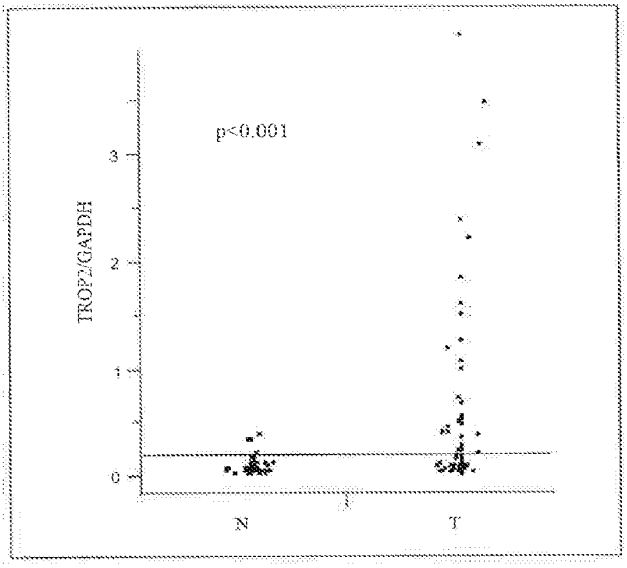


Fig. 1. Quantitative reverse transcription-PCR analysis showed substantial differences in *TROP2* expression between cancer and normal samples of 74 clinical cases. The cancer samples showed higher *TROP2* expression than the normal samples ($P < 0.001$). *Horizontal line*, expression value of 0.2 (P, Student's t test).

synthesized from 8.0 μg total RNA as described previously (16). The purity and concentration of total RNA were determined using an Agilent 2100 Bioanalyzer. The following primers were used to amplify the *TROP2* gene: sense primer 5′-GCCTACTACTTCGACAGGGACA-3′ and antisense primer 5′-CAGTTCGTTGATCTCCACCTTC-3′. The *glyceraldehyde-3-phosphate dehydrogenase* (sense primer 5′-TTGGTATCGTGGAAGGACTCA-3′ and antisense primer 5′-TGTCATCATATTTGGCAGGTTT-3′) gene was used as an internal control. The reaction was done in a LightCycler system (Roche Applied Science, Indianapolis, IN) using the LightCycler FastStart DNA Master SYBR Green I kit (Roche Diagnostics, Mannheim, Germany). Details of each reaction are described elsewhere (17). Briefly, thermal cycling for all genes was initiated with a denaturation step of 95°C for 10 minutes and then consisted of 40 cycles at 95°C for 10 seconds, 65°C (60°C for *glyceraldehyde-3-phosphate dehydrogenase*) for 10 seconds, and 72°C for each optimal length (1 second/25 bp). All calculated concentrations of target genes were divided by the amount of the endogenous reference (*glyceraldehyde-3-phosphate dehydrogenase*) to obtain the normalized *TROP2* expression values. Each assay was done in triplicate.

Immunohistochemistry. Of 74 cases, immunohistochemical staining was done in 34 selected cases. Immunohistochemical studies of *TROP2* were done on formalin-fixed, paraffin-embedded surgical sections. After deparaffinization and blocking, the antigen-antibody reaction was incubated overnight at 4°C. The LSAB2 kit (DAKO, Kyoto, Japan) was applied to detect the signal of the *TROP2* antigen-antibody reaction. All sections were counterstained with hematoxylin. The purified goat polyclonal antibody against the purified recombinant human *TROP2* extracellular domain (R&D Systems, Inc., Minneapolis, MN) was used at 5 μg/mL.

Statistical analysis. Quantitative real-time reverse transcription-PCR data were calculated with JMP 5 for Windows software (SAS Institute, Inc., Cary, NC). Differences between groups were estimated using the Student's t test and the χ^2 test. The survival curves were estimated by the Kaplan-Meier method and the comparison between the curves was made by the log-rank test. The relative risk (RR) was calculated using the Cox proportional hazards model. A probability level of 0.05 was chosen for statistical significance.

Results

Microarray analysis. In the microarray analysis, 84 genes were identified that had a higher expression level in cancer cells than in normal epithelial cells. Among these genes, some are involved with signal transduction (27.4%), transcription (16.7%), transport (13.1%), metabolism (4.8%), cell adhesion (4.8%), secretion (3.6%), apoptosis (3.6%), and an unknown function (16.7%; Table 1). Of these genes, some were already reported as associated with colorectal cancer aggressiveness, such as *MMP7* (18, 19), *MMP11* (20, 21), *CD44* (22–24), *CD61* (25, 26), *CRIPTO* (27, 28), *ENC1* (29), *SLC7A5* (30), *DPEP1* (31), and *activin A* (32, 33).

TROP2 expression in colorectal cancer samples and corresponding normal tissues. Quantitative real-time reverse transcription-PCR was done on 74 paired samples to show *TROP2* mRNA expression in clinical samples. Quantitative real-time reverse transcription-PCR showed that *TROP2* expression in cancer samples was significantly higher (averaged expression values of cancer were 8.34-fold higher; $P < 0.0001$) than those in normal samples (Fig. 1). Figure 2 shows the results of immunohistochemical studies of *TROP2* expression in representative clinical samples of well-differentiated adenocarcinoma (Fig. 2A), moderately differentiated adenocarcinoma (Fig. 2B), poorly differentiated adenocarcinoma (Fig. 2C), and mucinous adenocarcinoma (Fig. 2D). The majority of the *TROP2* expression was observed in the cancer cells, the minority in stromal cells, and none in the normal colonic epithelium. Immunohistochemical studies revealed that the staining was strong ($n = 7$), moderate ($n = 9$), or weak ($n = 18$) in the tumor cells, whereas very weak or none in the normal cells in all 34 cases. There was a significant difference in immunohistochemical staining between the tumor and the normal samples ($P < 0.01$), and the data are similar to those obtained from mRNA expression analysis. All 16 tumors with strong or moderate immunohistochemical expression showed higher mRNA expression values (>0.2). The expression of *TROP2* mRNA relatively associated with protein expression.

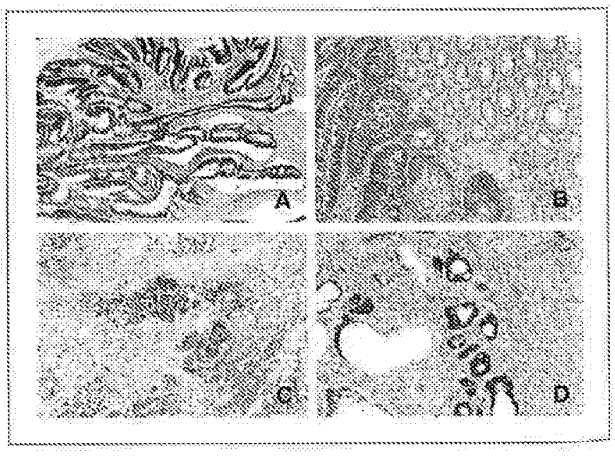


Fig. 2. Immunohistochemistry of *TROP2* expression in representative examples of colorectal cancer. *A*, well-differentiated adenocarcinoma. *B*, moderately differentiated adenocarcinoma. *C*, poorly differentiated adenocarcinoma. *D*, mucinous adenocarcinoma. *TROP2* protein is strongly expressed in cancer cells. (Original magnification, ×40.)

Table 2. Clinicopathologic variables and *TROP2* mRNA expression in 74 colorectal cancers

Variables	Expression		*P*
	High ($n = 26$)	Low ($n = 48$)	
Age	66.6 ± 3.8	67.5 ± 2.8	0.701
Sex			
Male	14	30	0.470
Female	12	18	
Histologic cell type			
Well	6	18	0.420
Moderately	19	29	
Poorly and others	1	1	
Tumor site*			
Right colon	9	13	0.498
Left colon	17	35	
Serosal invasion			
Absent	14	36	0.064
Present	12	12	
Lymph node metastasis			
Absent	12	31	0.125
Present	14	17	
Lymphatic permeation			
Absent	13	29	0.388
Present	13	19	
Venous permeation			
Absent	18	39	0.241
Present	8	9	
Liver metastasis			
Absent	17	44	0.005†
Present	9	4	
Cancer-related death			
Alive	17	41	0.046†
Death	9	7	

*Relative to splenic flexure.
†Cox proportional model.

Among the undifferentiated cell types, several regions of the cancer had strong immunohistochemical staining for *TROP2* (Fig. 2C and D).

High TROP2 expression correlates with clinicopathologic variables. The experimental samples were divided into two groups [the high expression group with *TROP2* expression values (>0.2; $n = 26$) and the remaining samples in the low expression group ($n = 48$)] to investigate *TROP2* expression in association with clinicopathologic variables (Table 2). The border of the two groups was defined by an upper limit, including 95% of the expression values of the normal samples. The incidence in liver metastasis was significantly higher ($P = 0.005$) in the high expression group (9 of 26, 34.6%) than in the low expression group (4 of 48, 8.3%), and the incidence of cancer death was significantly higher ($P = 0.046$) in the high expression group (9 of 26, 34.6%) than in the low expression group (7 of 48, 14.6%). The high expression group also had inclinations of deeper invasion ($P = 0.064$) and more lymph node metastasis ($P = 0.125$) than the low expression group.

Survival analysis. The 5-year actuarial overall survival rates in patients with high *TROP2* mRNA expression levels and those with low levels were 48.5% and 83.3%, respectively. Moreover, the high expression group also showed poorer prognosis in the Kaplan-Meier survival curve ($P = 0.0036$; Fig. 3). Table 3 revealed the result of RR and the 95% confidence interval (95% CI) by the Cox proportional hazards model. Table 3A shows the univariate analysis for all clinicopathologic variables. Regarding these variables, lymph node metastasis (RR, 2.711; 95% CI, 1.526-5.681; $P = 0.0004$), liver metastasis (RR, 2.409; 95% CI, 1.381-4.059; $P = 0.003$), depth of invasion (RR, 2.127; 95% CI, 1.276-3.675; $P = 0.0041$), histologic grade (RR, 2.097; 95% CI, 1.098-5.313; $P = 0.0225$), and high *TROP2* expression (RR, 2.026; 95% CI, 1.216-3.501; $P = 0.0071$) were statistically significant. Table 3B shows the result of multivariate analysis in the final model, which included lymph node metastasis, depth of invasion, histologic grade, tumor site, and lymphatic permeation. In this model, the variable of high *TROP2* expression was an independent prognostic predictor for the patients with colorectal cancer (RR, 2.38; 95% CI, 1.29-4.74; $P = 0.005$; Table 3B). Of the variables that were entered in the multivariate analysis, the variable of liver metastasis was excluded because there was a significant correlation with the variable of high *TROP2* expression.

Discussion

For further understanding of cancer biology, it is important to identify cancer-related genes. To find such genes, a combination of techniques, laser microdissection and cDNA microarray analysis, was applied to clinical samples. Laser microdissection can isolate cancer cells from tumor tissue that consists of mixed populations of carcinoma cells and stromal cells, such as fibroblasts, macrophages, and lymphocytes (16). RNA extracted from these tissues was subjected to rigorous procedures for quality to ensure its utility in cDNA microarray analysis. Almost 50% to 60% of the frozen surgical samples passed the RNA quality check according to our experience. Through using both laser microdissection and microarray analysis, 84 cancer-related genes were identified that were overexpressed in cancer cells compared with normal cells in the colon.

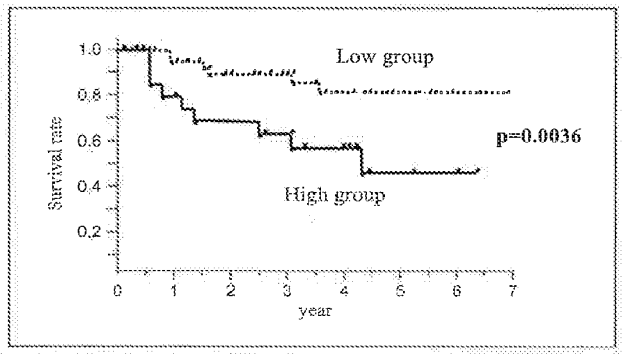


Fig. 3. Kaplan-Meier survival curves of patients with colorectal cancer according to the status of *TROP2 expression*. Patients with high *TROP2* mRNA expression (*bold line*) showed significantly poorer prognosis than those with low *TROP2* mRNA expression (*dotted line*; $P = 0.0036$, log-rank test).

Table 3.

Variable	RR (95% CI)	P^*
(A) Univariate analysis		
Lymph node metastasis (present)	2.71 (1.53-5.68)	0.000
Liver metastasis (present)	2.41 (1.38-4.06)	0.003
Serosal invasion (present)	2.13 (1.28-3.68)	0.004
Histologic cell type†	2.10 (1.10-5.31)	0.023
High *TROP2*	2.03 (1.22-3.50)	0.007
Tumor site‡ (right colon)	1.55 (0.92-2.59)	0.098
Lymphatic permeation (present)	1.54 (0.93-2.67)	0.095
Gender (female)	1.30 (0.78-2.20)	0.310
Age at surgery (>65 y)	1.27 (0.74-2.41)	0.402
Venous permeation (present)	1.13 (0.59-1.93)	0.686
(B) Multivariate analysis		
High *TROP2*	2.38 (1.29-4.74)	0.005
Lymph node metastasis (present)	2.04 (1.08-4.48)	0.027
Histologic cell type†	2.00 (0.97-5.29)	0.060
Tumor site (right colon)‡	1.99 (1.06-3.89)	0.031
Serosal invasion (present)	1.70 (0.98-3.08)	0.059
Lymphatic permeation (present)	0.92 (0.50-1.70)	0.788

*Cox proportional model.
†Indicates moderately and poorly differentiated adenocarcinoma.
‡Relative to splenic flexure.

This study showed that *TROP2* was one of the most highly expressed genes in colorectal cancer cells compared with normal colon tissue. *TROP2* is reported to be highly expressed in several types of cancers. For example, Nakajima et al. revealed that *TROP2* is overexpressed in esophageal cancer, and the titer of serum *TROP2* antibody correlated with tumor size (34). With respect to colon cancer, Kanai et al. studied the expression of mRNA of genes altered by 5-azacytidine treatment in cancer cell lines and found that *TROP2* was overexpressed in clinical colorectal cancers (35). However, they did not investigate the correlation between the *TROP2* expression status and the clinicopathologic factors. Our study of a comparison of both groups showed a significant difference in liver metastasis, and this was associated with cancer-related death. Although there were no significant differences in the other pathologic factors examined, there was a tendency in serosal invasion between the groups. Therefore, these results suggest that high *TROP2* expression has an association with biological aggressiveness of colorectal cancer.

The reason why the cancers with high *TROP2* expression show aggressive behavior is unclear. There are some studies suggesting the biological mechanism of high *TROP2* expression associated with the aggressiveness of cancer. Fornaro et al. suggested that *TROP2* not only acts as a calcium signal transducer but also has a receptor function activity. *TROP2* has homology to serum insulin-like growth factor-II–binding proteins and has a conservative structure for potential cytoplasmic phosphorylation sites (7). Basu et al. revealed that the phosphorylation occurred on Ser^{303} by protein kinase C (36).

We are investigating the predicted function of *TROP2* gene and taking notice of its intracellular domain of phosphatidylinositol 4,5-bisphosphate–binding sequence. Phosphatidylinositol 4,5-bisphosphate is the most important lipid in the cytoplasmic leaflet of the plasma membrane and is responsible for a wide range of membrane-related phenomena that consist of the functions of endocytosis, exocytosis, cytoskeletal attachment, enzyme activation, actin-binding protein, production of three second messengers, ion-channel activation, and binding site for PH and other domains (37). El Sewedy et al. investigated that the phosphatidylinositol 4,5-bisphosphate–binding site of *TROP2* has an ability of being phosphorylated by protein kinase C (38); thus, the signal transduction through *TROP2* has a possibility of causing the aggressiveness of cancer cells. Consequently, we assume that the *TROP2* gene has a receptor activity and influences the aggressive behavior of colorectal cancer cells during tumor progression. To investigate its biological function, we are planning the following experiments: (*a*) Establishment of the transfectant of the *TROP2* gene to clarify the dominant proliferation and progression of invasiveness. (*b*) Interference of the *TROP2* gene expression by small interfering RNA (or short hairpin RNA) to examine the alteration of its proliferation and invasiveness. (*c*) Verification of the binding activity between *TROP2* and phosphatidylinositol 4,5-bisphosphate and exploration of the alteration of the binding activity by protein kinase C. (*d*) Utilization of the transfectant with mutant *TROP2* gene, which lacks the phosphatidylinositol 4,5-bisphosphate–binding site to compare the result of *in vitro* analysis with that of experiment 1. Thus, high *TROP2* expression would contribute to biological aggressiveness of cancer cells through paracrine and autocrine signaling pathway. Nonetheless, more precise understanding of the mechanism that is responsible for the aggressiveness is necessary.

Because *TROP2* is overexpressed in colon cancer cells and not expressed in normal cells, it is a novel target for treatment. In fact, Mangino G et al. showed that *TROP2* is one of the target molecules recognized by human CTLs (39). We investigated the effectiveness of cancer-specific immunotherapy using *MAGE* antigen as a dendritic cell therapy (13, 40–42). However, the patients that can be treated with this therapy are limited because the patients must meet conditions, such as adequate HLA typing and positive *MAGE* gene expression in the tumor. The percentage of such patients is ~10% to 40% in several types of cancers. If *TROP2* can become an immunotherapeutic molecular target, the combined specific immunotherapy with *MAGE* and *TROP2* genes would be a powerful new treatment modality for colorectal cancer patients.

In conclusion, our results indicated that *TROP2* mRNA and protein were overexpressed in colorectal cancer cells and high *TROP2* expression status correlated with liver metastasis and poor prognosis. These findings suggest that *TROP2* is one of the cancer-related genes that are associated with cancer aggressiveness and is one of the predictors of survival in patients with colorectal cancer. The overexpression of this gene has a possible role for assessment of the postoperative adjuvant therapy of colorectal cancer patients. Furthermore, this gene will be useful not only for diagnostics but also molecular targeted therapy.

Acknowledgments

We thank Dr. S. Tanaka for helpful discussion and T. Shimooka, K. Ogata, M. Oda, M. Kasagi, and Y. Nakagawa for excellent technical assistance.

References

1. Tsukuma H, Ajiki W, Oshima A. Cancer incidence in Japan. GanTo Kagaku Ryoho 2004;31:840–6.
2. Weitz J, Koch M, Debus J, Hohler T, Galle PR, Buchler MW. Colorectal cancer. Lancet 2005;365:153–65.
3. McWilliams RR, Erlichman C. Novel therapeutics in colorectal cancer. Dis Colon Rectum 2005;48:1632–50.
4. Wu DH, Liu L, Chen LH. Antitumor effects and radiosensitization of cytosine deaminase and thymidine kinase fusion suicide gene on colorectal carcinoma cells. World J Gastroenterol 2005;11:3051–5.
5. Aggarwal S, Chu E. Current therapies for advanced colorectal cancer. Oncology 2005;19:589–95.
6. Roberts RB, Arteaga CL, Threadgill DW. Modeling the cancer patient with genetically engineered mice: prediction of toxicity from molecule-targeted therapies. Cancer Cell 2004;5:115–20.
7. Fornaro M, Dell'Arciprete R, Stella M, et al. Cloning of the gene encoding Trop-2, a cell-surface glycoprotein expressed by human carcinomas. Int J Cancer 1995;62:610–8.
8. Tsujikawa M, Kurahashi H, Tanaka T, et al. Identification of the gene responsible for gelatinous drop-like corneal dystrophy. Nat Genet 1999;21:420–3.
9. Alberti S, Miotti S, Stella M, et al. Biochemical characterization of Trop-2, a cell surface molecule expressed by human carcinomas: formal proof that the monoclonal antibodies T16 and MOv-16 recognize Trop-2. Hybridoma 1992;11:539–45.
10. Miotti S, Canevari S, Menard S, et al. Characterization of human ovarian carcinoma-associated antigens defined by novel monoclonal antibodies with tumor-restricted specificity. Int J Cancer 1987;39:297–303.
11. Fradet Y, Cordon-Cardo C, Thomson T, et al. Cell surface antigens of human bladder cancer defined by mouse monoclonal antibodies. Proc Natl Acad Sci U S A 1984;81:224–8.
12. Lipinski M, Parks DR, Rouse RV, Herzenberg LA. Human trophoblast cell-surface antigens defined by monoclonal antibodies. Proc Natl Acad Sci U S A 1981;78:5147–50.
13. Sadanaga N, Nagashima H, Mashino K, et al. Dendritic cell vaccination with MAGE peptide is a novel therapeutic approach for gastrointestinal carcinomas. Clin Cancer Res 2001;7:2277–84.
14. Nishida K, Mine S, Utsunomiya T, et al. Global analysis of altered gene expressions during the process of esophageal squamous cell carcinogenesis in the rat: a study combined with a laser microdissection and a cDNA microarray. Cancer Res 2005;65:401–9.
15. Pabon C, Modrusan Z, Ruvolo MV, et al. Optimized T7 amplification system for microarray analysis. Biotechniques 2001;31:874–9.
16. Mori M, Mimori K, Yoshikawa Y, et al. Analysis of the gene-expression profile regarding the progression of human gastric carcinoma. Surgery 2002;131:S39–47.
17. Ogawa K, Utsunomiya T, Mimori K, et al. Clinical significance of human kallikrein gene 6 messenger RNA expression in colorectal cancer. Clin Cancer Res 2005;11:2889–93.
18. Min Y, Adachi Y, Yamamoto H, et al. Insulin-like growth factor I receptor blockade enhances chemotherapy and radiation responses and inhibits tumour growth in human gastric cancer xenografts. Gut 2005;54:591–600.
19. Yoshimoto M, Itoh F, Yamamoto H, Hinoda Y, Imai K, Yachi A. Expression of MMP-7 (PUMP-1) mRNA in human colorectal cancers. Int J Cancer 1993;54:614–8.
20. Skoglund J, Emterling A, Arbman G, Anglard P, Sun XF. Clinicopathological significance of stromelysin-3 expression in colorectal cancer. Oncology 2004;67:67–72.
21. Thewes M, Pohlmann G, Atkinson M, Mueller J, Putz B, Hofler H. Stromelysin-3 (ST-3) mRNA expression in colorectal carcinomas: Localization and clinicopathologic correlations. Diagn Mol Pathol 1996;5:284–90.
22. Furuta K, Zahurak M, Goodman SN, Hamilton SR, August JT. CD44 expression in the stromal matrix of colorectal cancer: association with prognosis. Clin Cancer Res 1998;4:21–9.
23. Wielenga VJ, Heider KH, Offerhaus GJ, et al. Expression of CD44 variant proteins in human colorectal cancer is related to tumor progression. Cancer Res 1993;53:4754–8.
24. Heider KH, Hofmann M, Hors E, et al. A human homologue of the rat metastasis-associated variant of CD44 is expressed in colorectal carcinomas and adenomatous polyps. J Cell Biol 1993;120:227–33.
25. Etoh T, Ueo H, Inoue H, et al. Clinical significance of K-Ras mutations in intraoperative tumor drainage blood from patients with colorectal carcinoma. Ann Surg Oncol 2001;8:407–12.
26. Vontalfen A, Wiedle G, Borisch B, Birrer S, Luder P, Imhof BA. Integrin α(v)β(3) expression in colon carcinoma correlates with survival. Mod Pathol 2001;14:1126–32.
27. Saeki T, Stromberg K, Qi CF, et al. Differential immunohistochemical detection of amphiregulin and cripto in human normal colon and colorectal tumors. Cancer Res 1992;52:3467–73.
28. Ciardiello F, Kim N, Saeki T, et al. Differential expression of epidermal growth factor-related proteins in human colorectal tumors. Proc Natl Acad Sci U S A 1991;88:7792–6.
29. Fujita M, Furukawa Y, Tsunoda T, Tanaka T, Ogawa M, Nakamura Y. Up-regulation of the ectodermal-neural cortex 1 (ENC1) gene, a downstream target of the β-catenin/T-cell factor complex, in colorectal carcinomas. Cancer Res 2001;61:7722–6.
30. Tamai S, Masuda H, Ishii Y, Suzuki S, Kanai Y, Endou H. Expression of L-type amino acid transporter 1 in a rat model of liver metastasis: positive correlation with tumor size. Cancer Detect Prev 2001;25:439–45.
31. Melver CM, Lloyd JM, Hewett PJ, Hardingham JE. Dipeptidase 1: a candidate tumor-specific molecular marker in colorectal carcinoma. Cancer Lett 2004;209:67–74.
32. Wildi S, Kleeff J, Maruyama H, Maurer CA, Buchler MW, Korc M. Overexpression of activin A in stage IV colorectal cancer. Gut 2001;49:408–17.
33. Zhou S, Buckhaults P, Zawel L, et al. Targeted deletion of Smad4 shows it is required for transforming growth factor β and activin signaling in colorectal cancer cells. Proc Natl Acad Sci U S A 1998;95:2412–6.
34. Nakashima K, Shimada H, Ochiai T, et al. Serological identification of TROP2 by recombinant cDNA expression cloning using sera of patients with esophageal squamous cell carcinoma. Int J Cancer 2004;112:1029–35.
35. Kanai Y, Ushijima S, Saito Y, Nakanishi Y, Sakamoto M, Hirohashi S. MRNA expression of genes altered by 5-azacytidine treatment in cancer cell lines is associated with clinicopathological parameters of human cancers. J Cancer Res Clin Oncol 2001;127:697–706.
36. Basu A, Goldenberg DM, Stein R. The epithelial/carcinoma antigen EGP-1, recognized by monoclonal antibody RS7-3G11, is phosphorylated on serine 303. Int J Cancer 1995;62:472–9.
37. McLaughlin S, Murray D. Plasma membrane phosphoinositide organization by protein electrostatics. Nature 2005;438:605–11.
38. El Sewedy T, Fornaro M, Alberti S. Cloning of the murine TROP2 gene: conservation of a PIP_2-binding sequence in the cytoplasmic domain of TROP-2. Int J Cancer 1998;75:324–30.
39. Mangino G, Grazia Capri M, Barnaba V, Alberti S. Presentation of native TROP-2 tumor antigens to human cytotoxic T lymphocytes by engineered antigen-presenting cells. Int J Cancer 2002;101:353–9.
40. Tanaka S, Harada M, Mine T, et al. Peptide vaccination for patients with melanoma and other types of cancer based on pre-existing peptide-specific cytotoxic T-lymphocyte precursors in the periphery. J Immunother 2003;26:357–66.
41. Tanaka F, Fujie T, Tahara K, et al. Induction of antitumor cytotoxic T lymphocytes with a MAGE-3-encoded synthetic peptide presented by human leukocytes antigen-A24. Cancer Res 1997;57:4466–8.
42. Tanaka F, Fujie T, Go H, et al. Efficient induction of antitumor cytotoxic T lymphocytes from a healthy donor using HLA-A2-restricted MAGE-3 peptide *in vitro*. Cancer Immunol Immunother 1997;44:21–6.

Clarke, Modet & Cº
COLOMBIA

May 9, 2017

umedas@oslaw.org
nozawak@oslaw.org
hkobayashi@oslaw.org

OHNO & PARTNERS
Attn: Shinsuke UMEDA, Ph.D.
Marunouchi Kitaguchi Bldg. 21F
1-6-5, Marunouchi, Chiyoda-ku,
Tokyo, 100-0005
JAPAN

EXTENSIBLE DEADLINE: AUGUST 1, 2017

Ref: COLOMBIA
Patent Application No. **NC2016/0000187** in the name of **DAIICHI SANKYO COMPANY LIMITED**
Y/Ref.: SHU/PD20-9008CO
O/Ref.: P-2016/12118

Dear Sirs:

Please be informed that the company **LABORATORIOS LEGRAND S.A.** has filed opposition against the application of the reference. The basic points of this are described below:

1. Opposition filed by LABORATORIOS LEGRAND S.A.

1.1 Clarity and conciseness (Art. 30 of Decision 486/00)

The opponent states that:

- Claims 1 to 16 do not specifically define the technical characteristics of the antibody-drug conjugate. According to the opponent, the main claims indicates different drug-linker structures which comprises an undetermined amount of compounds.

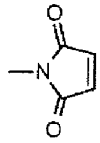
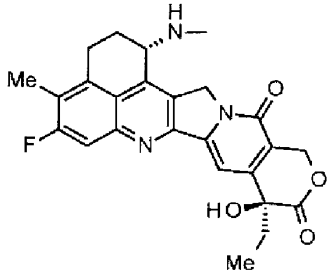
- Although the claims include formulas and sequences of the antibody, all the possible molecules for which a protection is sought are not divulged. Besides, the molecules are defined in terms of substitutions and results to be

achieved which are not be accepted as technical characteristics of the invention.

- Claim 1 mentions as essential and technical characteristics the compound of formula I, the drug-linker structures and the antibodies (such as trastuzumab). However, as indicated in section 1.3, the state of the art anticipates this type of conjugates, as well as the antitumor agents, antibodies such as trastuzumab, and the **succinimid** part of the linker.

- Claim 1 lacks clarity and conciseness since it is not clear the preamble and the characterizing part, so that t claims protection for subject matter which is widely known in the state of the art, such as anti-HER2 antibodies (that may be trastuzumab) and /or camptothecin derivatives.

- Claims 11 to 16 lack clarity since they refer to the reducing condition in the method:

> "*A method for preparing anti-HER2 antibody-drug conjugate, wherein the anti-HER2 antibody is treated in a reducing condition and thereafter reacted with a compound selected from the compound group shown below:*
> *(maleimid-N-yl)-CH_2CH_2-C(=O)-NH-CH_2CH_2O-CH_2CH_2-O-CH_2CH_2-C(=O)-GGFG-NH-$CH_2CH_2CH_2$-C(=O)-(NH-DX),*
> *(maleimid-N-yl)-$CH_2CH_2CH_2CH_2CH_2$-C(=O)-GGFG-NH-CH_2-O-CH_2-C(=O)-(NH-DX), or*
> *(maleimid-N-yl)-$CH_2CH_2CH_2CH_2CH_2$-C(=O)-GGFG-NH-CH_2CH_2-O-CH_2-C(=O)-(NH-DX),*
> *wherein (maleimid-N-yl)- is a group represented by the following formula:*
> *[Formula 4]*
>
> 
>
> *wherein the nitrogen atom is a connecting position,*
> *-(NH-DX) is a group represented by the following formula:*
> *[Formula 5]*
>
> 
>
> *wherein the nitrogen atom of the amino group at position 1 is a connecting position, and*

wherein the anti-HER2 antibody comprises a heavy chain and a light chain selected from the group;
a heavy chain consisting of an amino acid sequence consisting of positions 1 to 449 of SEQ ID NO: 1 and a light chain consisting of an amino acid sequence consisting of positions 1 to 214 of SEQ ID NO: 2, and
a heavy chain consisting of the amino acid sequence of SEQ ID NO: 1 and a light chain consisting of the amino acid sequence of SEQ ID NO: 2"

In addition, the sequences may be selected among different segments of the amino acid sequences SEQ ID NO: 1 and 2.

- Regarding claim 9, the opponent indicates the description of the medicament is too general refers to several compositions comprising antibody-drug conjugates.

1.2 Unity of Invention (Art. 25 of Decision 486/00)

According to the examiner, the method disclosed in claims 11 to 16 refer to regions which are not related to the structure or function of the conjugates disclosed in claims 1 to 11. In this way, the application lacks unity of invention.

1.3 Inventive step (Art. 18 of Decision 486/00)

The opponent is of the opinion that current application lacks of inventive step in view of the following documents:

No.	Document	Affected requirement
Govindan et al	US 2016/0287722 A1	Inventive step

According to the description, the objective technical problem which the present invention solves is decreasing the toxicity of the cancer treatment with an antitumor by means of a conjugate between an antitumor compound, a linker and an anti-HER2 antibody (which may be trastuzumab). However, this had been already disclosed in the state of the art, for instance, in *Govindan et al*.

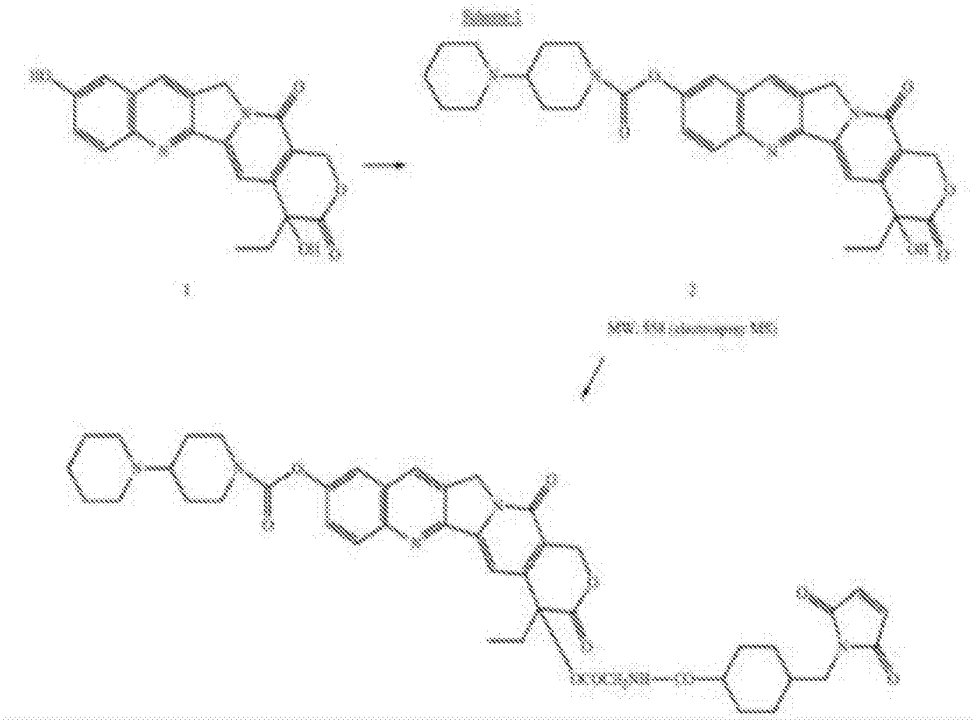
"*[0010] In one embodiment, the invention relates to an immunoconjugate comprising:*
[0011] (a) a targeting moiety;
[0012] (b) a chemotherapeutic moiety; and
[0013] (c) a linker binding to the targeting moiety via a thiol group, and to the chemotherapeutic moiety via an intracellularly-cleavable moiety other than a hydrazone. In another embodiment, the invention relates to an immunoconjugate comprising:
[0014] (a) targeting moiety;
[0015] (b) a chemotherapeutic moiety; and
[0016] (c) a linker binding to the targeting moiety via a thiol group, and to the chemotherapeutic moiety via an intracellularly-cleavable moiety other

than a hydrazone; wherein said linker comprises an amino acid moiety and a thiol-reactive moiety and is linked to the chemotherapeutic moiety via the amino acid moiety and to the targeting moiety via the thiol-reactive moiety.
[0017] Another embodiment of the invention is a method of treating cancer, a malignancy, an autoimmune disease, an infection, or an infectious lesion with the immunoconjugates described herein"

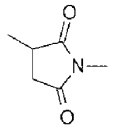
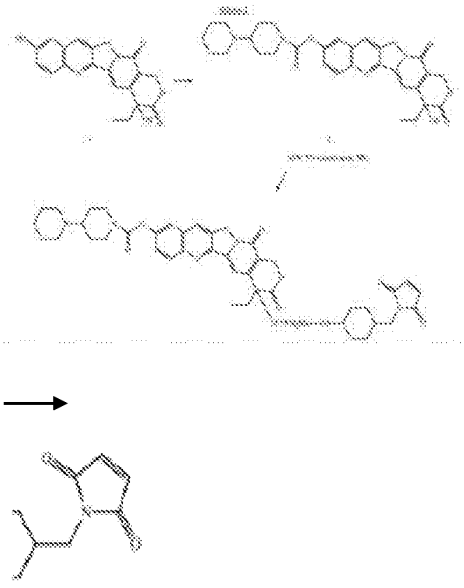
As shown, *Govindan et al*. discloses all the essential characteristics of the claimed antibody-drug conjugate. In addition, in paragraph [0052]:

"[0052] *In a preferred embodiment of the present invention, antibodies, such as mAbs, are used that recognize or bind to markers or tumor-associated antigens that are expressed at high levels on target cells and that are expressed predominantly or only on diseased cells versus normal tissues, and antibodies that internalize rapidly. Antibodies useful within the scope of the present invention include mAbs with properties as described above (and show distinguishing properties of different levels of internalization into cells and microorganisms), and contemplate the use of, but are not limited to, in cancer, the following mAbs: LL1 (anti-CD74), LL2 (anti-CD22), RS7 (anti-epithelial glycoprotein-1(EGP-1)), PAM-4 and KC4 (both anti-MUC1), MN-14 (anti-carcinoembryonic antigen (CEA, also known as CD66e), Mu-9 (anti-colon-specific antigen-p), Immu 31 (an anti-alpha-fetoprotein), TAG-72 (e.g., CC49), Tn, J591 (anti-PSMA (prostate-specific membrane antigen)), G250 (an anti-carbonic anhydrase IX mAb) and L243 (anti-HLA-DR). Other useful antigens that may be targeted using these conjugates include HER-2/neu, BrE3, CD19, CD20 (e.g., C2B8, hA20, 1F5 Mabs) CD21, CD23, CD80, alpha-fetoprotein (AFP), VEGF, EGF receptor, P1GF, MUC1, MUC2, MUC3, MUC4, PSMA, gangliosides, HCG, EGP-2 (e.g., 17-1A), CD37, HLA-DR, CD30, Ia, A3, A33, Ep-CAM, KS-1, Le(y), 5100, PSA (prostate-specific antigen), tenascin, folate receptor, Thomas-Friedenreich antigens, tumor necrosis antigens, tumor angiogenesis antigens, Ga 733, IL-2, IL-6, T101, MAGE, antigen to which L243 binds, CD66 antigens, i.e. CD66a-d or a combination thereof*" (emphasis added)

Similarly, the camptothecin derivatives with 4-(N-maleimidomethyl)-cyclohexane-1-carbonyl are disclosed in *Govindan et al*.



In addition, the linker would have been anticipated since the core succinimid had been divulged in *Govindan et al*.

Colombian application No. NC2016/0000187	***Govindan et al.***
Claim 1 -(Succinimid-3-yl-N)-$CH_2CH_2CH_2CH_2CH_2$-C(=O)-GGFG-NH-CH_2-O-CH_2-C(=O)-(NH-DX), -(Succinimid-3-yl-N)-$CH_2CH_2CH_2CH_2CH_2$-C(=O)-GGFG-NH-CH_2CH_2-O-CH_2-C(=O)-(NH-DX), or -(Succinimid-3-yl-N)-CH_2CH_2-C(=O)-NH-CH_2CH_2-O-CH_2CH_2-O-CH_2CH_2-C(=O)-GGFG-NH-$CH_2CH_2CH_2$-C(=O)-(NH-DX), -(Succinimid-3-yl-N)- has a structure represented by the following formula: [Formula 2] 	

In this regard, although the linker structure is not identical, there is no information disclosed in the description allowing to identify a surprising effect achieved by including the specific linker. Therefore, the technical effect is obvious in view of the teachings disclosed in the prior art.

In conclusion, for the opponent the claimed invention is obvious when considering the teachings disclosed in *Govindan et al*.

2. Technical Advice

After having reviewed the instant application and the opponent's arguments, we would like to draw your kind attention to the following facts:

Please note that according to our current practice, a defense brief may be filed for responding to the arguments of the opponents against the clarity, unity of invention and inventiveness of the present invention. In the defense brief, it could be included an amended claim set that allows to compare the characteristics of the invention with the state of the art.

Regarding the clarity, please note that set of claims has been amended based on the specific objections indicated by the Colombian examiner in the first formal office action and in order to comply the local requirements. In this way, we suggest maintaining the claims and waiting for the issuance of the substantive office action so that we could evaluate if the examiner indicated new objections and it is necessary to further amend the claims.

In connection to the unity of invention, in our opinion, an objection to the unity of the invention can only be stablished once the patentability assessment has been conducted. In this way, we do not consider valid the arguments indicated by the opponent regarding this requirement.

With respect to the arguments against the inventive step of the claimed invention in view of the teachings disclosed in *Govindan et al.*, if you consider pertinent, it could be filed arguments demonstrating that the technical characteristics disclosed in the set of claims would have not been obviously derived from the teachings disclosed in the cited document. Specifically, it would be helpful to expose technical data and arguments proving an advantage or unexpected technical effect achieved by the specific characteristics of the antibody-drug conjugate which could not be anticipated by th skilled person in the art. Please let us know if said data is available.

Please be advised that in case a response to the opposition is not filed, the application will be evaluated considering the arguments submitted by the opponent. After substantive examination, it will be issued an office action indicating the examiner's position and the arguments and documents which indeed affects the patentability of the invention, if any.

Please let us know how to proceed.

Deadline

Please be informed that the deadline for filing a response to the office action is **August 1, 2017**, which is extendable once, for 60 working days. Nonetheless, as we need a certain amount of time in order to prepare the response, we appreciate receiving your instructions by **July 25, 2017**. Otherwise, if we do not receive your instructions by the mentioned date, we will request the indicated extension of time. The costs involved on an extension of time are: official fee USD $42, professional fees USD $207 plus VAT (19%).

►IMPORTANT NOTE: Since failure to reply to an Office Action leads to the lapse of the application, in the absence of your instructions until July 25, 2017, we shall automatically file a time extension and will charge for this service.

Divisional applications

Please be advised that according to our current practice, a divisional application can be filed anytime during prosecution of the parent application, before the issuance of a final decision. However, we clarify that a divisional application cannot contain subject matter which has been already evaluated by the Colombian examiner or overlaps subject matter of the parent application; otherwise, the division will be rejected by the Colombian PTO. In addition, as a recent adopted practice, when filing a divisional application, it is mandatory to limit the scope of the description (including the examples) to the specific subject matter claimed in the divisional claims.

If you have any comments or questions, please do not hesitate to contact us.

Very truly yours,

Paola Rúa
Patent Engineer
prua@clarkemodet.com.co

REYES & REYES
ABOGADOS

Señor
SUPERINTENDENTE DE INDUSTRIA Y COMERCIO
E. S. D.

REF:	**EXPEDIENTE NC2016/0000187**
TÍTULO SOLICITADO:	**"CONJUGADO DE ANTICUERPO-FÁRMACO ANTI-RECEPTOR 2 DEL FACTOR DE CRECIMIENTO EPIDERMAL (HER2)"**
PUBLICACIÓN:	**Gaceta 780 de 30 dic 2016 de 2015**
PRIORIDAD:	**JA 2014-017777 31/01/2014** **JA 2014-168944 22/08/2014** **JA 2014-227886 10/11/2014**
SOLICITANTE:	**DAIICHI SANKYO COMPANY,LIMITED**
APODERADO:	**CAROLINA MERCEDES DAZA MONTALVO**
TRÁMITE:	**PRESENTACION DE OPOSICIÓN**

JUAN PABLO REYES VILLAMIZAR, mayor de edad, identificado como aparece al pie de mi firma, abogado en ejercicio, titular de la tarjeta profesional número 92189 del Consejo Superior de la Judicatura, obrando en calidad de apoderado de la sociedad **LABORATORIOS LEGRAND S.A.,** en ejercicio de lo dispuesto por el artículo 42 de la Decisión 486 de 2000, muy respetuosamente me permito formular la siguiente

I. PETICIÓN

Sírvase negar el beneficio patentario a la solicitud contenida en el expediente **NC2016/0000187**, por no cumplir con lo dispuesto en la Decisión 486 de 2000, con base en los fundamentos que se expondrán a continuación.

REYES & REYES
A B O G A D O S

II. LEGÍTIMO INTERÉS

Asiste a **LABORATORIOS LEGRAND S.A.,** legítimo interés para presentar esta oposición, pues la eventual concesión de la solicitud restringiría injustificadamente el empleo de ciertas sustancias, derivados y procesos que a nuestro juicio carecen de nivel inventivo, en detrimento de sus legítimos intereses comerciales. De igual manera mis clientes están interesados, por su misma condición de industrias farmacéuticas, en evitar la concesión de privilegios de patente que incumplan los requisitos materiales de patentabilidad establecidos en las normas vigentes, y que supongan un riesgo para la libre competencia.

III. FUNDAMENTOS DE LA OPOSICIÓN

La solicitud colombiana en trámite **NC2016/0000187**, referida a un conjugado de anticuerpo-fármaco caracterizado porque un compuesto antitumoral está conjugado a un anticuerpo anti-HER2 en forma de una estructura fármaco-enlazador, no cumple los requisitos materiales para otorgársele el privilegio de patente de invención, tal como puede determinarse al valorar los siguientes argumentos:

Falta de claridad y concisión

La solicitud carece de concisión ya que las 16 reivindicaciones no definen específicamente las características técnicas esenciales del conjugado de anticuerpo-fármaco que busca protección, esto debido a que en las reivindicaciones principales se presentan diferentes enlazadores al anticuerpo seleccionables que a su vez comprenden una cantidad no determinada de compuestos.

Aunque las reivindicaciones incluyen las fórmulas y las secuencias del anticuerpo, éstas no definen todas y cada una de las posibles moléculas que buscan protección según las alternativas divulgadas, además, se encuentran definidas a partir de sustituciones y resultados opcionales lo que no aporta a la identificación de la molécula objeto de la solicitud en trámite. Por lo tanto, las modalidades pretendidas tampoco encuentran sustento por la descripción.

REYES & REYES
A B O G A D O S

Ahora bien, la reivindicación principal de la presente invención reclama como **características técnicas esenciales** tanto el compuesto de fórmula I, los enlazantes y anticuerpos (como Trastuzumab), idea que está alejada de la realidad pues como se verá más adelante, el estado de la técnica anticipaba este tipo de conjugados, así como los agentes antitumorales, los anticuerpos como trastuzumab, y la parte **succinimid** del agente enlazante.

La forma de redacción de la reivindicación principal no es clara ni concisa y tiende a confundir al lector, no es claro cual es la parte caracterizante de dicha invención, y por el contrario trata de reclamar derechos sobre materia que es ampliamente conocida como son los anticuerpos anti-HER2 (podría tratarse de trastuzumab) y/o derivados de campotecina.

Adicional a lo anterior, la solicitud en estudio tampoco cumple con el criterio de claridad por cuanto no se define la condición reductora en el método de las reivindicaciones 11 a 16:

> *11. Un método para preparar un conjugado de anticuerpo anti-HER2, caracterizado porque el anticuerpo anti-HER2 se trata en una **condición reductora** y después se hace reaccionar con un compuesto seleccionado del grupo de compuestos mostrado a continuación:*
> *(maleimid-N-il)-CH2CH2-C(=O)-NH-CH2CH2O-CH2CH2-O-CH2CH2-C(=O)-GGFG-NH-CH2CH2CH2-C(=O)-(NH-DX),*
> *(maleimid-N-il)-CH2CH2CH2CH2CH2-C(=O)-GGFG-NH-CH2-O-CH2-C(=O)-(NH-DX), or*
> *(maleimid-N-il)-CH2CH2CH2CH2CH2-C(=O)-GGFG-NH-CH2CH2-O-CH2-C(=O)-(NH-DX),*
> *en donde (maleimid-N-il)- es un grupo representado por la siguiente fórmula:*
> *(…)*
> *en donde el anticuerpo anti-HER2 comprende una cadena pesada una cadena ligera seleccionada del grupo:*
> *una cadena pesada que consiste en una secuencia de aminoácidos que consiste en las posiciones 1 a 449 de SEQ ID NO: 1 y una cadena ligera que consiste en una secuencia de aminoácidos que consiste en las posiciones 1 a 214 de SEQ ID NO: 2 y*
> *una cadena pesada que consiste en la secuencia de aminoácidos de SEQ ID NO: 1 y una cadena ligera que consiste en la secuencia de aminoácidos de SEQ ID NO: 2.*

y en donde adicionalmente las secuencias pueden ser seleccionadas entre diferentes segmentos de la cadena de aminoácidos de las SEQ ID NO: 1 y 2.

REYES & REYES
ABOGADOS

Por lo tanto la materia objeto de las reivindicaciones excede lo desarrollado y corresponde a una extrapolación no razonable de las moléculas evaluadas.

De acuerdo a lo anterior, la solicitud falla en cumplir con lo dispuesto por el Artículo 30 de la D. 486 que precisa lo siguiente: *- Las reivindicaciones definirán la materia que se desea proteger mediante la patente. Deben ser claras y concisas y estar enteramente sustentadas por la descripción.*

Por otro lado, las reivindicaciones 11 – 16 que establecen el método de producción de un conjugado de anticuerpo anti-HER2, incluyen regiones funcionalmente diferentes que no se relacionan ni en su estructura ni en su función entre los conjugados de las reivindicaciones 1 – 11, por lo que la solicitud además incumple con el requisito de unidad de invención tal como lo determina el Art. 25 de la D. 486: *-La solicitud de patente sólo podrá comprender una invención o un grupo de invenciones relacionadas entre sí, de manera que conformen un único concepto inventivo.*

En este sentido, la solicitud no sólo comprende diferentes categorías desligadas entre sí de las características esenciales, sino que además incluye una cantidad no determinada de posibles invenciones al sumar a un método ya bastante amplio en el que se incluyen además moléculas comerciales, tales como el anticuerpo Trastuzumab, dentro de las secuencias reclamadas y que son objeto de evaluación en toda la memoria descriptiva de la solicitud.

Por otro lado, la solicitud en trámite pretende la protección de un medicamento de acuerdo a las siguientes características:

> *9. Un fármaco antitumoral y/o fármaco anticancerígeno caracterizado porque contiene el conjugado de anticuerpo-fármaco de conformidad con la reivindicación 1.*

Sin embargo, se considera que tal descripción no es clara ni concisa y podría cobijar un sinnúmero de composiciones que comprenden conjugados con compuestos antitumorales. Así las cosas, la materia de las reivindicaciones y en general la solicitud en estudio no puede ser objeto de patente pues incumple las normas mínimas de presentación, como es la claridad, concisión, soporte y unidad de invención.

REYES & REYES
A B O G A D O S

La solicitud carece de nivel inventivo

Según la descripción, la solicitud trata de resolver el problema técnico objetivo de disminuir la toxicidad del tratamiento del cáncer con un antitumoral mediante un conjugado entre un compuesto antitumoral, un agente enlazante y anticuerpo anti-HER2 (podría ser trastuzumab):

> *En este contexto, los inventores crearon un enlazador con una estructura específica y exitosa en la obtención de un conjugado de anticuerpo-fármaco en el cual el anticuerpo anti-HER2 y exatecano son conjugados entre sí mediante el enlazador, y se confirma un excelente efecto antitumoral presentado por el conjugado para de este modo, completar la presente invención.*

Materia que ya había sido revelada en el estado de la técnica, prueba de ello se encuentra en el siguiente documento publicado anteriormente a la fecha de presentación de la solicitud en estudio y que cito a continuación:

- Publicación Americana US 2016/0287722 A1 ***"Immunoconjugates with an Intracellularly-Cleavable Linkage"*** *Serengulam V. Govindan, Summit, NJ [US] 2016-10-*06, objeta el nivel inventivo de la solicitud en trámite ya que describe conjugados terapéuticos con mejorada capacidad de marcar varios tipos de células cancerígenas que contienen motivos diana y motivos terapéuticos:

SUMMARY OF THE INVENTION

[0010] In one embodiment, the invention relates to an immunoconjugate comprising:

[0011] (a) a targeting moiety;

[0012] (b) a chemotherapeutic moiety; and

[0013] (c) a linker binding to the targeting moiety via a thiol group, and to the chemotherapeutic moiety via an intracellularly-cleavable moiety other than a hydrazone. In another embodiment, the invention relates to an immunoconjugate comprising:

REYES & REYES
A B O G A D O S

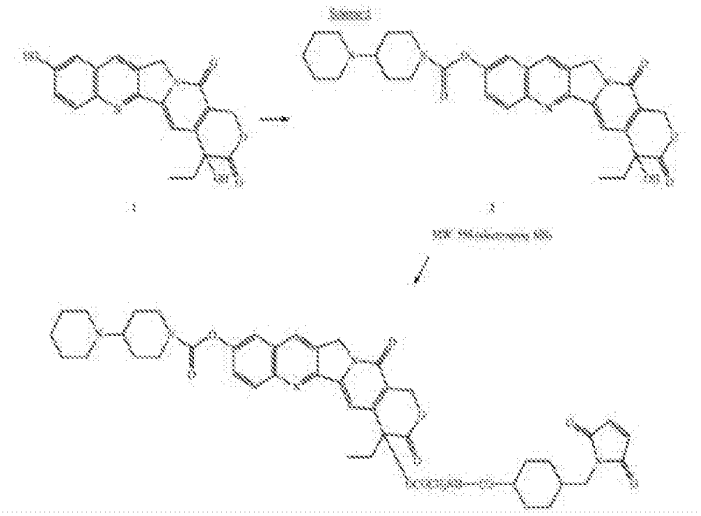
[0014] (a) targeting moiety;
[0015] (b) a chemotherapeutic moiety; and
[0016] (c) a linker binding to the targeting moiety via a thiol group, and to the chemotherapeutic moiety via an intracellularly-cleavable moiety other than a hydrazone; wherein said linker comprises an amino acid moiety and a thiol-reactive moiety and is linked to the chemotherapeutic moiety via the amino acid moiety and to the targeting moiety via the thiol-reactive moiety.
[0017] Another embodiment of the invention is a method of treating cancer, a malignancy, an autoimmune disease, an infection, or an infectious lesion with the immunoconjugates described herein.

Como se puede ver en el sumario, *Govindan et al* revela las características esenciales del conjugado de anticuerpo reclamado, tales como el motivo diana, el motivo quimioterapéutico, el ligador o enlazante que comprende un grupo tiol, en el que se unen los anticuerpos anti-HER2 entre otros anticuerpos, tal como se puede observar en el siguiente fragmento:

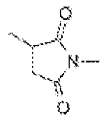
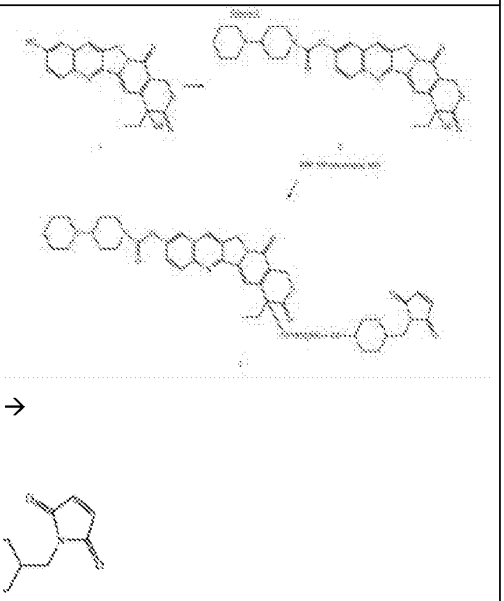
[0052] In a preferred embodiment of the present invention, antibodies, such as mAbs, are used that recognize or bind to markers or tumor-associated antigens that are expressed at high levels on target cells and that are expressed predominantly or only on diseased cells versus normal tissues, and antibodies that internalize rapidly. Antibodies useful within the scope of the present invention include mAbs with properties as described above (and show distinguishing properties of different levels of internalization into cells and microorganisms), and contemplate the use of, but are not limited to, in cancer, the following mAbs: LL1 (anti-CD74), LL2 (anti-CD22), RS7 (anti-epithelial glycoprotein-1(EGP-1)), PAM-4 and KC4 (both anti-MUC1), MN-14 (anti-carcinoembryonic antigen (CEA, also known as CD66e), Mu-9 (anti-colon-specific antigen-p), Immu 31 (an anti-alpha-fetoprotein), TAG-72 (e.g., CC49), Tn, J591 (anti-PSMA (prostate-specific membrane antigen)), G250 (an anti-carbonic anhydrase IX mAb) and L243 (anti-HLA-DR). Other useful antigens that may be targeted using these conjugates include HER-2/neu, BrE3, CD19, CD20 (e.g., C2B8, hA20, 1F5 Mabs) CD21, CD23, CD80, alpha-fetoprotein (AFP), VEGF, EGF receptor, PlGF, MUC1, MUC2, MUC3, MUC4, PSMA, gangliosides, HCG, EGP-2 (e.g., 17-1A), CD37, HLA-DR, CD30, Ia, A3, A33, Ep-CAM, KS-1, Le(y), 5100, PSA (prostate-specific antigen), tenascin, folate receptor, Thomas-Friedenreich antigens, tumor necrosis antigens, tumor angiogenesis antigens, Ga 733, IL-2, IL-6, T101, MAGE, antigen to which L243 binds, CD66 antigens, i.e. CD66a-d or a combination thereof. The CD66

REYES & REYES
ABOGADOS

De igual forma, los compuestos derivados de hidroxicamptotecina con 4-(N-maleimidometil) ciclohexano – 1 carbonil se divulgaban previamente en dicho documento:



Además, se desea resaltar que el agente enlazante se habría anticipado ya que el núcleo ***succimid*** había sido revelado por *Govindan*:

Solicitud Colombiana NC2016/0000187	US 2016/0287722 A1
Rv1: -(Succinimid-3-il-N)-CH2CH2CH2CH2CH2-C(=O)-GGFG-NH-CH2-O-CH2-C(=O)-(NH-DX), -(Succinimid-3-il-N)-CH2CH2CH2CH2CH2-C(=O)-GGFG-NH-CH2CH2-O-CH2-C(=O)-(NH-DX), o -(Succinimid-3-il-N)-CH2CH2-C(=O)-NH-CH2CH2-O-CH2CH2-O-CH2CH2-C(=O)-GGFG-NH-CH2CH2CH2-C(=O)-(NH-DX), (Succinimid-3-il-N)- tiene estructura representada por la siguiente fórmula: [Fórmula 3] 	 →

REYES & REYES
ABOGADOS

Ahora bien, aunque la estructura del enlazante no es idéntica, se observa que en la descripción no existe información suficiente que permita identificar un efecto sorprendente o novedoso obtenido por dicho enlazante, en comparación a otros enlazantes conocidos en el estado de la técnica, y se considera que el efecto logrado era obvio al emplear un anticuerpo como por ejemplo trastuzumab para dirigir el compuesto citotóxico hacia las células diana.

En conclusión, la reivindicación principal ya era conocida en el estado de la técnica si se tiene en cuenta:

- El compuesto antitumoral derivado de campotecinas así como su uso en conjugados de este tipo
- Anticuerpos anti-HER2 (podría tratarse de trastuzumab) así como su uso en conjugados
- La parte succinimid era ya usado por otros autores como Govindan

y dado que no existen datos que indiquen que el agente enlazador es el responsable de mejorar o aumentar el efecto biológico del tratamiento antitumoral no es posible considerar que la presente solicitud sea inventiva.

Rogamos se analicen los argumentos expuestos con el rigor y detenimiento habituales y que en consecuencia se decrete, además de la negación de la solicitud en comento, el archivo del expediente que la contiene

IV. FUNDAMENTOS DE DERECHO

Son fundamentos de derecho el Capítulo I, (Requisitos de Patentabilidad) y el artículo 42 (Oposiciones) de la Decisión 486 de 2000.

V. SOLICITUD DE PLAZO EXTRA PARA SUSTENTAR LA OPOSICIÓN

En desarrollo de lo dispuesto por el artículo 42, inciso 2º de la Decisión 486, solicito comedidamente a su Despacho el plazo adicional de sesenta días para sustentar la presente oposición. Para los anteriores efectos, me permito anexar la constancia de pago correspondiente.

REYES & REYES
A B O G A D O S

V. PRUEBAS

Ruego que se tenga como tal, sin perjuicio de las que puedan presentarse al vencimiento de la prórroga solicitada, y de aquellas que el Despacho considere oficiosamente, el siguiente:

D1. US 2016/0287722 A1 ***"Immunoconjugates with an Intracellularly-Cleavable Linkage"*** *Serengulam V. Govindan, Summit, NJ [US] 2016-10*-06, portada, p 1–3, reivindicaciones

VI. ANEXOS

Para efectos del trámite correspondiente, me permito anexar al presente escrito los siguientes anexos:

1. Certificado de existencia y representación legal de **LABORATORIOS LEGRAND S.A.**.
2. Poder para actuar.
3. Constancia de pago de las tasas de tramitación de oposición.
4. Las mencionadas en el acápite de pruebas

VII. NOTIFICACIONES

El suscrito recibirá notificaciones en la secretaría de su Despacho o en mi oficina localizada en la Carrera 17 No. 88-23, Oficina 205, Fax (1) 621.25.42 de esta ciudad. Laboratorios Legrand S.A. las recibirá en la secretaría de su Despacho o en la Carrera 19-A No. 90-13, Oficina 901 de Bogotá D.C.
Señor Superintendente,

JUAN PABLO REYES VILLAMIZAR
C.C. 80.419.709 de Usaquén
T.P.A. 92.189 de C.S.J.

本複製物は、特許庁が著作権法第４２条第２項第１号の規定により複製したものです。
取扱にあたっては、著作権侵害とならないよう十分にご注意ください。

P.X

osimertinib, and osimertinib active metabolites, and to assess anti-tumor activity (RECIST v1.1). Clinicaltrials.gov identifier: NCT03255083. Result: Not applicable. Conclusion: Not applicable. Keywords: Axl, EGFR mutation, drug resistance

P3.04-013
Phase 1 Study of the Anti-HER3 Antibody Drug Conjugate U3-1402 in Metastatic or Unresectable EGFR-Mutant NSCLC

P. Jänne,[1] H. Yu,[2] M. Vigliotti,[3] N. Shiplotsky,[1] J. Singh,[3] F. Guevara,[3] C. Yu[3] [1]Lowe Center for Thoracic Oncology, Dana-Farber Cancer Institute, Boston, MA/US, [2]Memorial Sloan-Kettering Cancer Center, New York, NY/US, [3]Daiichi Sankyo, Inc, Basking Ridge, NJ/US

Background: While the treatment of EGFR-mutant NSCLC has significantly improved with the use of EGFR tyrosine kinase inhibitors, there remain limited treatment options for many patients who develop resistance to these agents. The HER3/ERBB3 oncogene is overexpressed in many cancers, including NSCLC, and higher expression is correlated with poorer outcomes. U3-1402 is a novel antibody-drug conjugate (ADC) comprised of a recombinant fully human anti-HER3 antibody (patritumab) covalently conjugated via a cleavable peptide linker to a derivative of the topoisomerase I inhibitor exatecan. After U3-1402 binds to HER3 on the tumor cell surface, it is internalized and leads to apoptosis via inhibition of topoisomerase I. This ADC achieves a high drug-to-antibody ratio of ~8:1. **Method:** Trial Design: This is a multicenter, open-label Phase 1 study of U3-1402 in metastatic or unresectable non-squamous NSCLC subjects harboring EGFR-activating mutation who (a) are T790M mutation-negative after disease progression during treatment with erlotinib, gefitinib, or afatinib or (b) develop disease progression while on osimertinib. Eligible subjects are at least 18 years of age, have ECOG PS 0 or 1, have radiological documentation of disease progression while receiving continuous treatment with erlotinib, gefitinib, afatinib, or osimertinib, have at least one measurable lesion per RECIST v1.1, have adequate bone marrow and organ function, do not have LVEF <45% by either ECHO or MUGA scan, do not have mean QTc prolongation to > 470 ms for females and > 450 ms for males, and do not have spinal cord compression or clinically active brain metastases. This study includes two parts: Dose Escalation and Dose Expansion. In Dose Escalation, subjects receive U3-1402 via intravenous infusion in 21-day cycles. In Dose Escalation, escalation of U3-1402 dosing between subjects is based on dose-limiting toxicity data in subjects, guided by the modified Continuous Reassessment Method (mCRM) using a Bayesian logistic regression model (BLRM) following the escalation with overdose control (EWOC) principle. In Dose Expansion, subjects receive U3-1402 at the recommended dose for expansion determined in Dose Escalation. Primary objective is to determine the safety, tolerability, and recommended dose for expansion of U3-1402. Secondary objectives are to assess the pharmacokinetic parameters of U3-1402, total anti-HER3 antibody, and MAAA-1181a (drug payload), and to assess antitumor activity of U3-1402 (RECIST v1.1). **Clinicaltrials.gov identifier:** NCT03260491. **Result:** Not applicable. **Conclusion:** Not applicable. **Keywords:** EGFR mutation, antibody drug conjugate, HER3

P3.05-001
Breath Analysis for Early Detection of Lung Cancer: The LuCID Study

M. Van Der Schee,[1] J. Dickson,[2] M. Ruparel,[2] S. Janes,[2] S. Dragonieri,[3] L. Fuller,[4] S. Grundy,[5] D. Baldwin,[6] P. Crosbie,[7] A. Prasad,[8] M. Haris,[9] A. Barlow,[10] L. Calvert,[11] A. Wight,[12] J. Bennett,[13] M. Gaga,[14] S. Chee,[15] V. Conteh,[16] M. Ledson,[17] C. Hodkinson,[1] J. Boschmans,[1] R. Smith,[1] R. Parris,[1] D. Apthorp,[1] S. Kitchen,[1] M. Allsworth,[1] B. Boyle,[1] R. Rintoul[18] [1]Owlstone Medical Ltd, Cambridge/GB, [2]University College London, Lungs for Living Research Center, London/GB, [3]Bari University Hospital, Bari/IT, [4]South Tyneside NHS Foundation Trust, South Shields/GB, [5]Aintree University Hospitals NHS Foundation Trust, Liverpool/GB, [6]Nottingham University Hospitals NHS Trust, Pb/GB, [7]University Hospital of South Manchester NHS Foundation Trusts, Manchester/GB, [8]Buckinghamshire Healthcare NHS Trust, Amersham/GB, [9]Royal Stoke University Hospital NHS Trust, Stoke on Trent/GB, [10]West Hertfordshire Hospitals NHS Trust, Watford/GB, [11]North West Anglia NHS Foundation Trust, Peterborough/GB, [12]Wirral University Teaching Hospital, Birkenhead/GB, [13]Glenfield Hospital, University Hospitals of Leicester NHS Trust, Leicester/GB, [14]Athens Chest Hospital, Athens/GR, [15]University Hospital Southampton NHS Foundation Trust, Southampton/GB, [16]Barnet Hospital, Royal Free London NHS Foundation Trust, London/GB, [17]Liverpool Heart & Chest, Liverpool/GB, [18]Thoracic Oncology, Papworth Hospital NHS Foundation Trust, Cambridge/GB

Background: There is an urgent need for methods to detect lung cancer earlier. If detected early, over half of lung cancer patients could be cured with existing treatments. Therefore, our greatest opportunity lies in increasing rates of early diagnosis through improved cancer screening. Exhaled breath contains over 1,000 Volatile Organic Compounds (VOCs), which are the products of metabolic activity, hence they directly reflect the current state of cells and represent a valuable source of information about the health of an individual. As the earliest stages of tumor development are characterized by profound changes in cellular metabolic activity, VOCs are potential non-invasive biomarkers for early detection of lung cancer. The LuCID study aims to collect breath samples and evaluate VOCs in exhaled breath as non-invasive biomarkers for early detection of lung cancer. **Method:** LuCID is an international multi-center prospective case-control cohort study (ClinicalTrials.gov ID NCT02612532) currently in progress, evaluating breath VOCs in patients with a clinical suspicion of lung cancer. A clinical suspicion is based on symptoms and/or suspicious finding on incidental imaging. Using tidal breathing, patients breathe into the ReCIVA Breath Sampler for 7 minutes to collect alveolar- and bronchial-enriched breath fractions on stable sorbent tubes for later analysis by Gas Chromatography-Mass Spectrometry and Field Asymmetric Ion Mobility Spectrometry (FAIMS, Owlstone Medical Ltd). A classification algorithm will be constructed from chemical spectral data, and undergo internal and external blinded validation to provide a ROC-curve detailing diagnostic accuracy. The LuCID study has an adaptive trial design, recruiting up to 2,600 patients depending on interim results. **Result:** The LuCID study has recruited 980 patients to date from 20 centers (mean age 67.5, SD 12.0). Of patients with completed follow-up (n=802), 33% have histologically confirmed lung cancer (of those with lung cancer: 40% early stage 1a-2b, 60% advanced stage 3a-4). Non-Small Cell Lung Cancer (NSCLC) comprised 87% of these cancers, and Small Cell Lung Cancer 9%. NSCLC were further categorized as adenocarcinoma (50%), squamous cell carcinoma (38%), with the remaining 12% belonging to other categories. **Conclusion:** The LuCID study is evaluating the analysis of exhaled VOC biomarkers as a new diagnostic modality for early detection of lung cancer. Successful completion of the LuCID study will pave the way for the development of a non-invasive, easy-to-implement test that could markedly improve screening and early detection rates, reducing lung cancer morbidity and mortality. **Keywords:** Screening, breath analysis, Biomarkers

P3.05-002
The Effect of Nodule Size on the Sensitivity of the LuCED® Test for Lung Cancer

M. Meyer, R. Katdare, C. Presley, D. Wilbur, J. Zulueta, A. Nelson
Vislangate, Phoenix, AZ/US

Background: The LuCED® test is based on analysis of sputum by the Cell-CT® platform that computes 3D images of cells with isometric resolution, allowing orientation-independent measurements of 704 3D structural biomarkers to generate a probabilistic score to identify abnormal cells, that was consistent by tumor histology and stage. Early

本複製物は、特許庁が著作権法第４２条第２項第１号の規定により複製したものです。
取扱にあたっては、著作権侵害とならないよう十分にご注意ください。

L7 ANSWER 9 OF 14 EMBASE COPYRIGHT (c) 2018 Elsevier B.V. All rights
Full Text | Citing References
reserved on STN
AN 0052876845 EMBASE
DN 620146686
TI Phase 1 study of the anti-HER3 antibody drug conjugate U3-1402 in metastatic or unresectable EGFR-mutant NSCLC.
AU Janne, P. (correspondence)
CS Lowe Center for Thoracic Oncology, Dana-Farber Cancer Institute, Boston, MA, United States.
AU Yu, H.
CS Memorial Sloan-Kettering Cancer Center, New York, NY, United States.
AU Vigliotti, M.; Shipitofsky, N.; Singh, J.; Guevara, F.; Yu, C.
CS Daiichi Sankyo, Inc., Basking Ridge, NJ, United States.
SO Journal of Thoracic Oncology, (November 2017) Vol. 12, No. 11, Supp. Supplement 2, pp. S2290. Abstract Number: P3.04-013.
Meeting Info: 18th World Conference on Lung Cancer of the International Association for the Study of Lung Cancer, IASLC 2017. Yokohama, Japan. 15 Oct 2017-18 Oct 2017
ISSN: 1556-1380
PB Elsevier Inc..
CY Netherlands
DT Journal; Conference; (Conference Abstract)
FS CONF
FS Intellectual Indexing
LA English
SL English
ED Entered Embase: 12 Jan 2018
Last Updated on Embase: 12 Jan 2018
Indexing Added: 12 Jan 2018
First Entered Embase or Embase Alert: 12 Jan 2018
AB Background: While the treatment of EGFR-mutant NSCLC has significantly improved with the use of EGFR tyrosine kinase inhibitors, there remain limited treatment options for many patients who develop resistance to these agents. The HER3/ERBB3 oncogene is overexpressed in many cancers, including NSCLC, and higher expression is correlated with poorer outcomes. U3-1402 is a novel antibody-drug conjugate (ADC) comprised of a recombinant fully human anti-HER3 antibody (patritumab) covalently conjugated via a cleavable peptide linker to a derivative of the topoisomerase I inhibitor exatecan. After U3-1402 binds to HER3 on the tumor cell surface, it is internalized and leads to apoptosis via inhibition of topoisomerase I. This ADC achieves a high drug-to-antibody ratio of w8:1. Method: Trial Design: This is a multicenter, open-label Phase 1 study of U3-1402 in metastatic or unresectable non-squamous NSCLC subjects harboring EGFR-activating mutation who (a) are T790M mutation-negative after disease progression during treatment with erlotinib, gefitinib, or afatinib or (b) develop disease progression while on osimertinib. Eligible subjects are at least 18 years of age, have ECOG PS 0 or 1, have radiological documentation of disease progression while receiving continuous treatment with erlotinib, gefitinib, afatinib, or osimertinib, have at least one measurable lesion per RECIST v1.1, have adequate bone marrow and organ function, do not have LVEF <45% by either ECHO or MUGA scan, do not have mean QTc prolongation to >470 ms for females and >450 ms for males, and do not have spinal cord compression or clinically active brain metastases. This study includes two parts: Dose Escalation and Dose Expansion. In Dose Escalation, subjects receive U3-1402 via intravenous infusion in 21-day cycles. In Dose Escalation, escalation of U3-1402 dosing between subjects is based on dose-limiting toxicity data in subjects, guided by the modified Continuous Reassessment Method (mCRM) using a Bayesian logistic regression model (BLRM) following the escalation with overdose control (EWOC) principle. In Dose Expansion, subjects receive U3-1402 at the recommended dose for expansion determined in Dose Escalation. Primary objective is to determine the safety, tolerability, and recommended dose for expansion of U3-1402. Secondary objectives are to assess the pharmacokinetic parameters of U3-1402, total anti-HER3 antibody, and MAAA-1181a (drug payload), and to assess antitumor activity of U3-1402 (RECIST v1.1). Clinicaltrials.gov identifier: NCT03260491. Result: Not applicable. Conclusion: Not applicable.
TI Phase 1 study of the anti-HER3 antibody drug conjugate U3-1402 in metastatic or unresectable EGFR-mutant NSCLC.
AB Background: While the treatment of EGFR-mutant NSCLC has significantly

本複製物は、特許庁が著作権法第４２条第２項第１号の規定により複製したものです。
取扱にあたっては、著作権侵害とならないよう十分にご注意ください。

improved with the use of EGFR tyrosine kinase inhibitors, there remain limited treatment options for many patients who develop resistance to these agents. The HER3/ERBB3 oncogene is overexpressed in many cancers, including NSCLC, and higher expression is correlated with poorer outcomes. U3-1402 is a novel antibody-drug conjugate (ADC) comprised of a recombinant fully human anti-HER3 antibody (patritumab) covalently conjugated via a cleavable peptide linker to a derivative of the topoisomerase I inhibitor exatecan. After U3-1402 binds to HER3 on the tumor cell surface, it is internalized and leads to apoptosis via inhibition of topoisomerase I. This ADC achieves a high drug-to-antibody ratio of w8:1. Method: Trial Design: This is a multicenter, open-label Phase 1 study of U3-1402 in metastatic or unresectable non-squamous NSCLC subjects harboring EGFR-activating mutation who (a) are T790M mutation-negative after disease progression during treatment with erlotinib, gefitinib, or afatinib or (b) develop disease progression while on osimertinib. Eligible subjects are at least 18 years of age, have ECOG PS 0 or 1, have radiological documentation of disease progression while receiving continuous treatment with erlotinib, gefitinib, afatinib, or osimertinib, have at least one measurable lesion per RECIST v1.1, have adequate bone marrow and organ function, do not have LVEF <45% by either ECHO or MUGA scan, do not have mean QTc prolongation to >470 ms for females and >450 ms for males, and do not have spinal cord compression or clinically active brain metastases. This study includes two parts: Dose Escalation and Dose Expansion. In Dose Escalation, subjects receive U3-1402 via intravenous infusion in 21-day cycles. In Dose Escalation, escalation of U3-1402 dosing between subjects is based on dose-limiting toxicity data in subjects, guided by the modified Continuous Reassessment Method (mCRM) using a Bayesian logistic regression model (BLRM) following the escalation with overdose control (EWOC) principle. In Dose Expansion, subjects receive U3-1402 at the recommended dose for expansion determined in Dose Escalation. Primary objective is to determine the safety, tolerability, and recommended dose for expansion of U3-1402. Secondary objectives are to assess the pharmacokinetic parameters of U3-1402, total anti-HER3 antibody, and MAAA-1181a (drug payload), and to assess antitumor activity of U3-1402 (RECIST v1.1). Clinicaltrials.gov identifier: NCT03260491. Result: Not applicable. Conclusion: Not applicable.

Proc. Natl. Acad. Sci. USA
Vol. 87, pp. 4905–4909, July 1990
Biochemistry

Molecular cloning and expression of an additional epidermal growth factor receptor-related gene

(receptor tyrosine kinase/sequence/amphiregulin/ERBB2/ERBB3)

GREGORY D. PLOWMAN, GENA S. WHITNEY, MICHAEL G. NEUBAUER, JANELL M. GREEN, VICKI L. MCDONALD, GEORGE J. TODARO, AND MOHAMMED SHOYAB

Oncogen, 3005 First Avenue, Seattle, WA 98121

Contributed by George J. Todaro, March 21, 1990

ABSTRACT **Epidermal growth factor (EGF), transforming growth factor α (TGF-α), and amphiregulin are structurally and functionally related growth regulatory proteins. These secreted polypeptides all bind to the 170-kDa cell-surface EGF receptor, activating its intrinsic kinase activity. However, amphiregulin exhibits different activities than EGF and TGF-α in a number of biological assays. Amphiregulin only partially competes with EGF for binding EGF receptor, and amphiregulin does not induce anchorage-independent growth of normal rat kidney cells (NRK) in the presence of TGF-β. Amphiregulin also appears to abrogate the stimulatory effect of TGF-α on the growth of several aggressive epithelial carcinomas that overexpress EGF receptor. These findings suggest that amphiregulin may interact with a separate receptor in certain cell types. Here we report the cloning of another member of the human EGF receptor (HER) family of receptor tyrosine kinases, which we have named "*HER3/ERRB3*." The cDNA was isolated from a human carcinoma cell line, and its 6-kilobase transcript was identified in various human tissues. We have generated peptide-specific antisera that recognizes the 160-kDa HER3 protein when transiently expressed in COS cells. These reagents will allow us to determine whether HER3 binds amphiregulin or other growth regulatory proteins and what role HER3 protein plays in the regulation of cell growth.**

Epidermal growth factor (EGF), transforming growth factor α (TGF-α), and amphiregulin (1–3) all bind to the 170-kDa cell-surface EGF receptor (EGF-R), resulting in activation of its intrinsic kinase activity (3–6). Amphiregulin was originally identified from phorbol ester-treated human breast carcinoma cells (MCF-7) on its ability to inhibit the growth of several carcinoma cell lines while stimulating the proliferation of normal cells (7). The secreted form of amphiregulin is a 78-amino acid glycoprotein that is proteolytically cleaved from a larger transmembrane precursor (4). Amphiregulin contains a motif that is 38% identical with EGF and conserves most residues implicated as involved in binding to the EGF-R (3, 4). In addition, mature amphiregulin contains a distinct NH_2-terminal sequence of 43 predominantly hydrophilic amino acids, not present in other EGF-like proteins. Because related ligands often bind structurally similar receptors (8–10), we speculated that EGF, TGF-α, or amphiregulin may differentially interact with a homolog of EGF-R. After failing to show any interaction between these three secreted growth factors and HER2/neu, a known EGF-R-related protein, we initiated a search for other members of this family of receptor tyrosine kinases. This report describes the cloning and expression of human EGF receptor (HER)3,* a candidate receptor for EGF-like growth factors.

The publication costs of this article were defrayed in part by page charge payment. This article must therefore be hereby marked "*advertisement*" in accordance with 18 U.S.C. §1734 solely to indicate this fact.

MATERIALS AND METHODS

Cell Culture. All cells were obtained from ATCC and grown in Dulbecco's modified Eagle's medium (DMEM)/10% heat-inactivated fetal bovine serum.

cDNA Cloning. Total cellular RNA was extracted from A-431 (subclone A3), and MDA-MB-361 cells, and poly(A)$^+$ RNA was isolated. First-strand cDNA synthesis (11) was performed on A-431-A3 RNA with reverse transcriptase by using a 72-fold degenerate primer mixture based on the amino acid sequence (in one-letter code) YMIMVKCWMI (ARRD1). A cDNA library was constructed in λgt10, and 3.0×10^5 recombinants were screened in duplicate on nitrocellulose filters. Filters were first probed at low stringency with ^{32}P-labeled ARRD2, a 96-fold degenerate oligonucleotide. The filters were then stripped and reprobed at high stringency with ^{32}P-labeled EGFR300, a cDNA fragment corresponding to amino acids 863–944 of EGF-R (12). Of 69 clones that differentially hybridized to ARRD2 and EGFR300, three were found to encode an EGF-R-related protein (HER3), six clones encoded HER2 protein, and 10 clones spanned various regions of EGF-R. One HER3 clone was used as a probe to screen a λgt10 cDNA library derived from oligo(dT)-primed MDA-MB-361 RNA, and three additional cDNA clones were isolated—one with a 4.5 kilobase (kb) insert (pHER3-3b). To obtain the 5′-cDNA clone, we used the polymerase chain reaction (PCR) as follows. Single-stranded cDNA, synthesized from MDA-MB-361 RNA with S729ERR as primer, was dA-tailed and used as template for PCR amplification by using S720ERR, XSCT17, and XSC as primers (13). All cDNA clones and several PCR-generated clones were sequenced on both strands by using T7 polymerase with oligonucleotide primers (14).

The oligonucleotide mixtures (including their degeneracy or length and corresponding amino acid residues) used for priming and screening the λgt10 library were as follows (sequences in parentheses are in one-letter amino acid code):

ARRD1 5′–ATCATCCARCAYTTDACCATDATCATRTA–3′,
(72-fold, YMIMVKCWMI)
ARRD2 5′–GCCATCCAYTTDATNGGNAC–3′,
(96-fold, VPIKWMA)
S729ERR 5′–TCGTCGACTCCTTCACCACTATCTCA–3′,
(26-mer, EIVVKD)
S720ERR 5′–TGGCGTCGACCTATCTCAGCATCTCGGT–3′,
(28-mer, DRDAEIV)
XSCT17 5′–GACTCGAGTCGACATCGATTTTTTTTTTTTTTT–3′,
(35-mer)
XSC 5′–GACTCGAGTCGACATCG–3′,
(17-mer).

Abbreviations: EGF, epidermal growth factor; EGF-R, EGF receptor; TGF-α, transforming growth factor α; HER, human EGF receptor; PCR, polymerase chain reaction; nt, nucleotide(s).

*The sequence reported in this paper has been deposited in the GenBank data base (accession no. M34309).

OnCusp
Ex. 1002

Degenerate residues are as follows: D = A, G, or T; N = A, C, G, or T; R = A or G; Y = C or T.

Expression of HER3 in COS Cells. The complete 4.1-kb *HER3* coding sequence was reconstructed and inserted into a pCDM8 (Invitrogen, San Diego) -based expression vector. The resulting plasmid (cHER3x) was grown in competent *Escherichia coli* MC1061/P3 bacteria (15) and was introduced into COS-1 cells by using the DEAE-dextran method (15).

Immunoblotting. Cell pellets were harvested 72–96 hr after transfection; one hundred μg of protein was separated by using 7% SDS/PAGE and analyzed by immunoblotting with polyclonal antisera generated against synthetic peptides (16) specific to the kinase domain of HER3 (PPDDKQLLYSEAKT, amino acids 841–854; GAEPYAGLRLAEVPD, amino acids 889–903; sequences shown using single-letter code).

RESULTS

Amphiregulin Purified from MCF-7 Cells Is Not a Ligand for HER2/neu. EGF-R shares structural homology with HER2/neu, the protein product of *ERBB2* protooncogene: 83% amino acid identity exists in the cytoplasmic kinase domain, and 42% homology is present in the extracellular ligand-binding domain, where 49 of 50 cysteines are conserved (12, 17). Therefore, we sought to establish whether amphiregulin interacted with this putative receptor and homolog of EGF-R, because the ligand for HER2/neu has not been identified. Experiments were performed on cells expressing high levels of human (SKBR-3 and BT474) HER2 or rat (B104-1-1 and DHFR-G8) neu protein. Direct binding, *in vitro* kinase assays, proliferation assays, *in vivo* phosphorylation, and receptor down-regulation assays (18) all showed no association between the 78-amino acid form of amphiregulin and HER2/neu (G.D.P., M.S., Y. Yarden, G.J.T., and R. Weinberg, data not shown). The ligand for HER2/neu remains elusive.

Isolation of cDNA Clones Encoding an EGF-R-Related Gene. Northern (RNA) blot analysis of A-431 and human placental RNA provides evidence for the existence of other EGF-R-related transcripts (12, 17). A subclone of the A-431 cell line (A-431-A3) was isolated after growth in soft agar and was characterized to have 30-fold-increased sensitivity to amphiregulin inhibition as compared with the parental line, yet had no alteration in the number or affinity of EGF-Rs as measured by binding competition assays (7). Poly(A)$^+$ RNA was prepared from these cells, and a cDNA library was constructed by specific priming with a 72-fold degenerate oligonucleotide complementary to a stretch of 10 amino acids unique to the kinase domains of EGF-R and HER2/neu. A 96-fold degenerate oligonucleotide probe, based on an upstream region of 7 amino acids conserved in EGF-R and HER2/neu, was used to screen the cDNA library at low-stringency conditions. EGF-R clones were eliminated by rehybridization at high stringency with a short EGF-R cDNA probe spanning the same region of the kinase domain. Sixty-nine clones were partially sequenced, revealing three clones that encoded a closely related, yet distinct, member of the ERBB/EGF-R subfamily of receptor tyrosine kinases. A survey of several human tumor cell lines identified the breast carcinoma cell line, MDA-MB-361, to be a more abundant source of the 6-kb transcript than A-431-A3 cells, so it was used to isolate overlapping cDNA clones spanning the entire coding sequence of *HER3*. The HER3 transcript was also detected in several primary breast carcinomas and in normal colon, kidney, breast, and brain RNA (data not shown).

The nucleotide sequence for *HER3* contains an open reading frame coding for 1342 amino acids beginning with a consensus-initiating methionine at nucleotide (nt) 199 (Fig. 1). The amino acids downstream of this methionine have the characteristics of a signal sequence; the mature protein is predicted to begin at Ser-20, followed by 1323 amino acids with a calculated M_r of 146,000. The 4026-nt coding region is flanked by 198 nt of 5′ and 755 nt of 3′ untranslated sequences. No poly(A) tail is present, suggesting this is a partial cDNA sequence.

Structural Domains of HER3. HER3 has all the structural features of receptor tyrosine kinase (19), with a single hydrophobic stretch of 32 amino acids characteristic of a transmembrane region that separates the sequence into a 612-residue extracellular ligand-binding domain and a 677-amino acid COOH-terminal cytoplasmic domain strongly homologous with other members of the tyrosine kinase family (Figs. 2 and 3). The ligand-binding domain can be divided into four subdomains (I–IV), including two cysteine-rich regions (II, IV) that conserve all 48 cysteines present in the corresponding regions of the EGF-R (12) and two flanking domains (I and III) that may define specificity for ligand binding (21). HER3 shares 40–50% identity with EGF-R and 40–45% identity with HER2/neu in each of these subdomains (12, 17). There are 10 potential *N*-linked glycosylation sites in the extracellular domain of HER3, conserving 5 of 12 potential sites in EGF-R and 3 of 8 sites in HER2/neu. The cytoplasmic domain includes the following: a stretch of basic residues flanking the membrane-spanning region; a consensus ATP-binding site (Gly-Xaa-Gly-Xaa-Xaa-Gly-Xaa$_n$-Lys), and sequences homologous to other members of the tyrosine kinase family (22); an acidic helical motif similar to the domain of EGF-R that confers receptor internalization and ligand-dependent calcium influx (23); and a hydrophilic COOH-terminal tail containing 13 tyrosines (Fig. 3). The kinase domain of HER3 is most similar to EGF-R and HER2/neu (60 and 62%) and shared lower homology (26–34%) with representatives of other classes of tyrosine kinases (Fig. 2). EGF-R and HER2/neu have 83% amino acid sequence identity between their kinase domains, suggesting that, in this domain, they are more closely related to each other than they are to HER3.

The cytoplasmic domain of HER3 also has several unique features (Fig. 3). Protein kinase C-induced phosphorylation of EGF-R occurs primarily on Thr-654, whereas Thr-669 has been implicated as a major site for phosphorylation of EGF-R in response to EGF (24, 25). Both of these residues are conserved in HER2/neu, but both are altered in HER3 (Ala-657 and Asp-672). Recent studies using EGF-R mutants have shown that preventing phosphorylation at either residue has no effect on EGF binding; however, in certain cell lines, phosphorylation of EGF-R Thr-654 by phorbol esters appears to block EGF-induced mitogenesis (24, 25). HER3 already contains these "mutations" and may lack this negative control mechanism induced by protein kinase C.

Two additional atypical amino acid changes are present in the HER3 kinase domain (Fig. 3). A sequence comparison of protein kinases reveals certain residues that are either highly or completely conserved (22). HER3 contains most of these amino acids including Gly-697, Gly-699, Val-704, Lys-723, Asn-820, Asp833–Phe834–Gly835, Glu-862, Asp-874, Gly-879, and Arg-936; however, HER3 has nonconservative substitutions at Cys-721, His-740, and Asn-815. The latter two amino acids are present as glutamate and aspartate, respectively, in all known protein kinases—serine/threonine as well as tyrosine kinases (Figs. 2 and 3). Strict conservation of these residues suggests that they are important for catalytic activity, and the amino acid changes at these positions in HER3 indicate it might have altered kinase activity.

The COOH-terminal 353 amino acids of HER3 contain 13 tyrosines, several of which are flanked by numerous charged residues. These features are characteristic of the autophosphorylation domains of EGF-R (26) and HER2/neu (27), yet this region of HER3 shares no significant primary sequence homology to either of these two family members and is ≈30–50% longer. The sequence Tyr-Glu-Tyr-Met is repeated

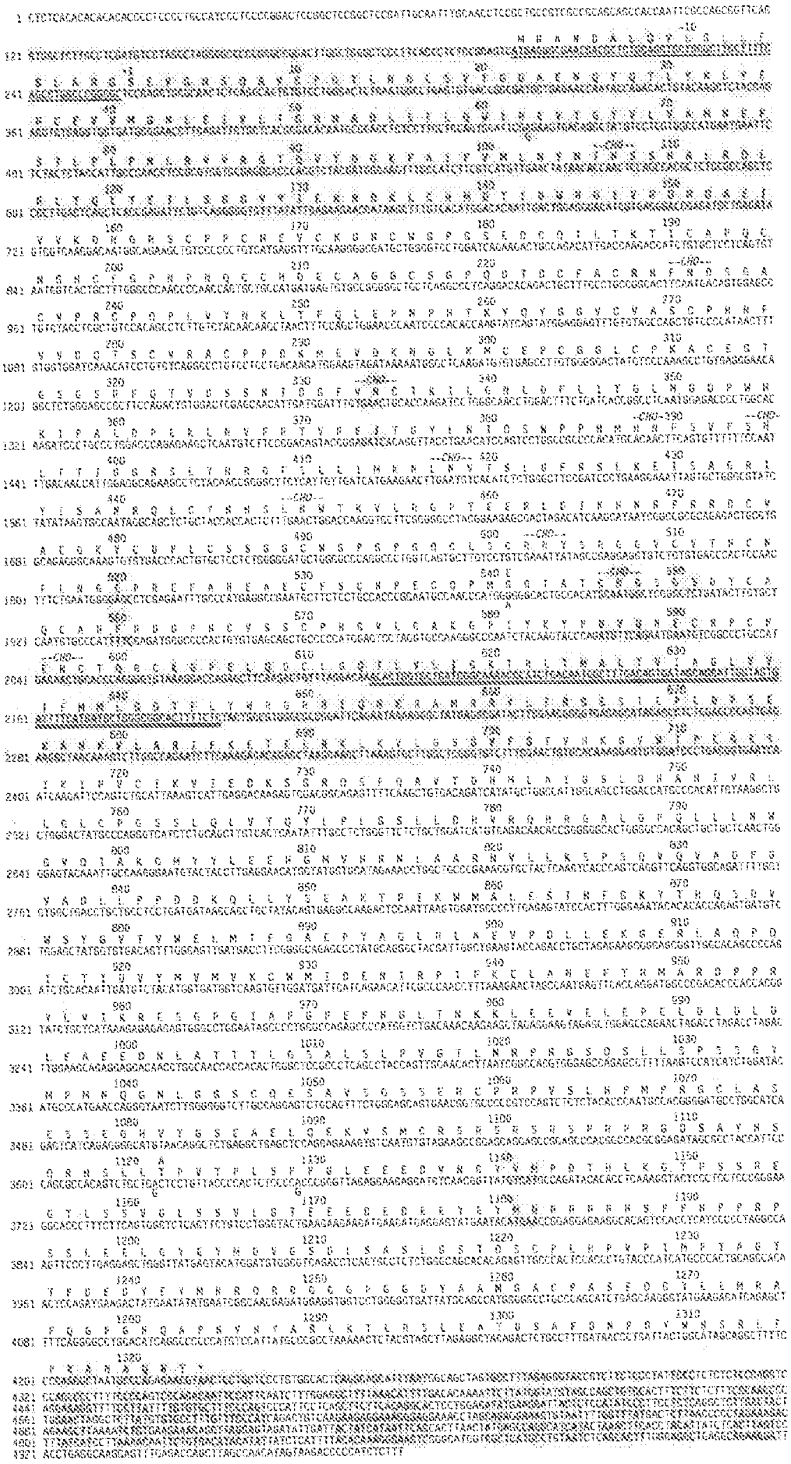


FIG. 1. Nucleotide sequence and deduced amino acid sequence of human HER3 (1342 residues). Nucleotides are numbered at left, and amino acids (in one-letter code) are numbered above the sequence. The 19-residue signal sequence is singly underlined, and the predicted NH_2 terminus of the mature protein is indicated by +1. The transmembrane domain is doubly underlined at amino acids 614–645. Potential N-linked glycosylation sites (Asn-Xaa-Ser or Asn-Xaa-Thr) are denoted with -CHO-. No poly(A) tail was present in the clones. This sequence represents a consensus based on cDNA and PCR clones isolated from MDA-MB-361 RNA and was used in subsequent expression constructs. Clonal sequence differences are listed below the consensus residue, including Ade-441 to guanine in one of four PCR clones, Gua-1877 to adenine from one A-431 cDNA clone, Ade-3619 to guanine in one cDNA clone, and Ade-3642 to guanine in one cDNA clone.

three times in this domain of HER3, possibly the result of gene duplication.

Expression of HER3 in COS Cells. To determine the biochemical properties of HER3, we inserted its complete coding sequence into an expression vector under the control of the cytomegalovirus immediate-early promoter (15). This vector (cHER3κ) was transfected into COS cells, and the transiently expressed protein was detected by immunoblot analysis using antisera specific to the cytoplasmic domain of HER3. The recombinant protein migrated with an apparent

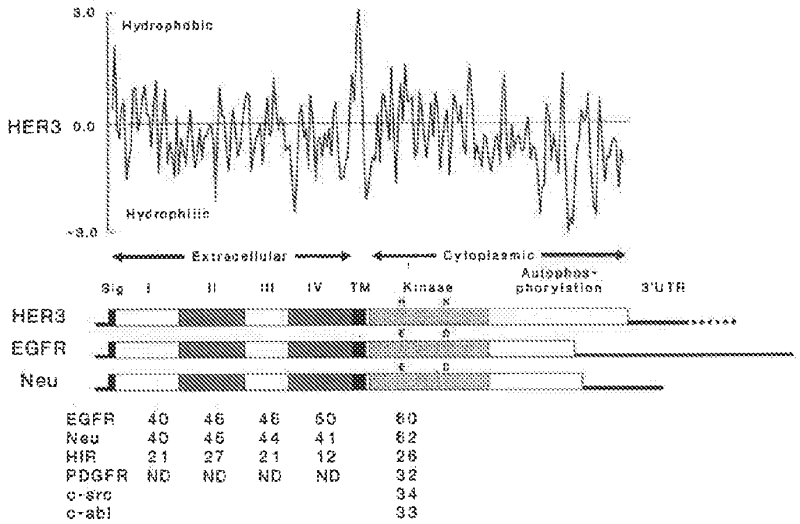


FIG. 2. Hydropathy profile (20) of HER3 and comparison of protein domains for HER3 (1342 amino acids), EGF-R (1210 amino acids), and HER2 (Neu) (1255 amino acids). Signal peptide and transmembrane domains are represented by filled boxes, the cysteine-rich extracellular subdomains are hatched, and the cytoplasmic tyrosine kinase domain is stippled. Amino acids unique to the HER3 kinase domain (histidine, asparagine) compared with other protein kinases (glutamic and aspartic residues) are indicated using the single-letter code. The percent amino acid sequence identity between HER3 and representatives of other classes of tyrosine kinases are indicated. Sig, signal peptide; I, II, III, and IV, extracellular domains; TM, transmembrane domain; 3′ UTR, 3′ untranslated region; HIR, insulin receptor; PDGFR, platelet-derived growth factor receptor; ND, not determined.

M, of 160,000, slightly less than the EGF-R (Fig. 4). The abundance of EGF-R in COS cells complicated efforts to assess whether EGF-like ligands bind HER3. Stable expression of HER3 in cells lacking EGF-R will allow us to determine whether EGF, TGF-α, or amphiregulin interact with this putative receptor.



FIG. 3. Protein sequence comparison between members of the human EGF-R family. Sequences are displayed using the single-letter code, and identical residues are denoted with dots. Gaps were introduced for optimal alignment and are shown by a dash. Signal sequences are bounded by single lines, transmembrane domains are bounded by double lines, and sequences used to derive the probes and primers (ARRD1, ARRD2) used for cloning are underlined. Cysteine residues are marked with stars, the potential ATP-binding site is shown with circled crosses (Gly-Xaa-Gly-Xaa-Xaa-Gly beginning at residue 697 and Lys-723), COOH-terminal tyrosines are denoted with open triangles, and additional residues of HER3 referred to in the text are marked with arrows (Ala-657, Cys-721, His-740, and Asn-815). Neu, HER2/neu.

5451 of 14295

OnCusp
Ex. 1002

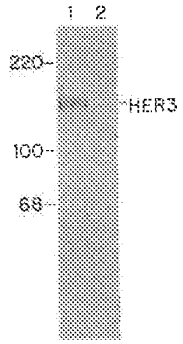


FIG. 4. Immunoblot analysis of the recombinant HER3 transiently expressed in COS cells. Lanes: 1, HER3-transfected COS cells; 2, cDM8 mock-transfected COS cells. Note presence of a 160-kDa band.

DISCUSSION

Previous biochemical and biological evidence suggested that members of the EGF/TGF-α/amphiregulin family are not functionally equivalent (3, 28). For example, TGF-α has an activity comparable to that of EGF in many *in vitro* assays: TGF-α and EGF bind with similar affinity to EGF-R, resulting in autophosphorylation of EGF-R; both ligands induce similar changes in intracellular pH and calcium levels; and both transduce comparable proliferative signals in many cell types; however, TGF-α appears more potent than EGF in several *in vivo* assays, including the promotion of bone resorption, wound healing, and angiogenesis (28). Likewise, amphiregulin can be distinguished from EGF/TGF-α based on EGF-R binding studies and by a number of biological assays (3).

The identification of another member of the EGF-R subclass of receptor tyrosine kinases reveals a greater repertoire by which the EGF/TGF-α/amphiregulin family of ligands might exert their diverse growth regulatory signals. Conceivably, some differences in biological activity between amphiregulin and EGF/TGF-α may result from the ability of amphiregulin to interact differentially with members of the EGF-R family. Because EGF-R and HER2/neu have been shown to act synergistically (29), HER3 may interact with either of these two receptors. Moreover, the disparity in response to these ligands may be reflected in the less conserved cytoplasmic region of HER3 compared with EGF-R and HER2/neu. The COOH-terminal region of EGF-R appears to act as a competitive inhibitor for exogenous substrate phosphorylation and thereby serves to fine-tune its kinase activity (26, 27). The more conserved homology between the cytoplasmic regions of EGF-R and HER2/neu, as opposed to HER3, suggests these two receptors share a more similar function, whereas the distinctiveness of HER3 indicates it may be subject to different regulation and might signal an alternate biochemical response.

During review of this manuscript, the sequence of a cDNA encoding ERBB3 was reported (30). The amino acid sequence of ERBB3 is identical to that of HER3 except for two residues; both Gly-541 and Gly-1045 of HER3 were deduced to be glutamic acid (Glu-541, Glu-1045) in ERBB3. We have noted four polymorphic purine residues among our HER3 cDNA clones (see Fig. 1). Two of these differences alter the deduced amino acid sequence (Glu-541 and Ala-1122), with one change corresponding to a difference between the HER3 and ERBB3 sequences.

The isolation of HER3 cDNA will facilitate the investigation on its function in normal cells and in various proliferative disorders including neoplasia. Site-directed mutagenesis and expression of modified HER3 in mammalian cells will make possible the unraveling of the biochemical mechanism of its putative ligand(s), including amphiregulin. The generation of chimeric receptors consisting of different domains of the three EGF-R family members as well as other receptor tyrosine kinases will further help to define the signal-transduction pathways used by these receptors and their cognate ligands. Conceivably, the multiplicity of receptor and ligand types provides an organism with a better means to regulate homeostasis under various physiological and pathological conditions.

We thank Tony Purchio for his advice and critical comments on this manuscript.

1. Savage, C. R., Jr., Inagami, T. & Cohen, S. (1972) *J. Biol. Chem.* **247**, 7612–7621.
2. Marquardt, H., Hunkapiller, M. W., Hood, L. E. & Todaro, G. J. (1984) *Science* **223**, 1079–1082.
3. Shoyab, M., Plowman, G. D., McDonald, V. L., Bradley, J. G. & Todaro, G. J. (1989) *Science* **243**, 1074–1076.
4. Plowman, G. D., Green, J. M., McDonald, V. L., Neubauer, M. G., Disteche, C. M., Todaro, G. J. & Shoyab, M. (1990) *Mol. Cell. Biol.* **10**, 1969–1981.
5. Todaro, G. J., Fryling, C. & DeLarco, J. E. (1980) *Proc. Natl. Acad. Sci. USA* **77**, 5258–5262.
6. Carpenter, G., Stoscheck, C. M., Preston, Y. A. & DeLarco, J. E. (1983) *Proc. Natl. Acad. Sci. USA* **80**, 5627–5630.
7. Shoyab, M., McDonald, V. L., Bradley, J. G. & Todaro, G. J. (1988) *Proc. Natl. Acad. Sci. USA* **85**, 6528–6532.
8. Ullrich, A., Gray, A., Tam, A. W., Yang-Feng, T., Tsubokawa, M., Collins, C., Henzel, W., Le Bon, T., Kathuria, S., Chen, E., Jacobs, S., Francke, U., Ramachandran, J. & Fujita-Yamaguchi, Y. (1986) *EMBO J.* **5**, 2503–2512.
9. Matsui, T., Heidaran, M., Miki, T., Popescu, N., La Rochelle, W., Kraus, M., Pierce, J. & Aaronson, S. (1989) *Science* **243**, 800–804.
10. Chang, M. S., Lowe, D. G., Lewis, M., Hellmiss, R., Chen, E. & Goeddel, D. V. (1989) *Nature (London)* **341**, 68–72.
11. Gubler, U. J. & Hoffman, B. J. (1983) *Gene* **25**, 263–269.
12. Ullrich, A., Coussens, L., Hayflick, J. S., Dull, T. J., Gray, A., Tam, A. W., Lee, J., Yarden, Y., Libermann, T. A., Schlessinger, J., Downward, J., Mayes, E. L. V., Whittle, N., Waterfield, M. D. & Seeburg, P. H. (1984) *Nature (London)* **309**, 418–425.
13. Frohman, M. A., Dush, M. K. & Martin, G. R. (1988) *Proc. Natl. Acad. Sci. USA* **85**, 8998–9002.
14. Tabor, S. & Richardson, C. C. (1987) *Proc. Natl. Acad. Sci. USA* **84**, 4767–4771.
15. Seed, B. & Aruffo, A. (1987) *Proc. Natl. Acad. Sci. USA* **84**, 3365–3369.
16. Gentry, L. E. & Lawton, A. (1986) *Virology* **152**, 421–431.
17. Coussens, L., Yang-Feng, T. L., Liao, Y. L., Chen, E., Gray, A., McGrath, J., Seeburg, P. H., Libermann, T. A., Schlessinger, J., Francke, U., Levinson, A. & Ullrich, A. (1985) *Science* **230**, 1132–1139.
18. Yarden, Y. & Weinberg, R. A. (1989) *Proc. Natl. Acad. Sci. USA* **86**, 3179–3183.
19. Yarden, Y. & Ullrich, A. (1988) *Biochemistry* **27**, 3113–3119.
20. Kyte, J. & Doolittle, R. F. (1982) *J. Mol. Biol.* **157**, 105–132.
21. Lax, I., Johnson, A., Howk, R., Sap, J., Bellot, F., Winkler, M., Ullrich, A., Vennstrom, B., Schlessinger, J. & Givol, D. (1988) *Mol. Cell. Biol.* **8**, 1970–1978.
22. Hanks, S. K., Quinn, A. M. & Hunter, T. (1988) *Science* **241**, 42–52.
23. Chen, W. S., Lazar, C. S., Lund, K. A., Welsh, J. B., Chang, C. P., Walton, G. M., Der, C. J., Wiley, H. S., Gill, G. N. & Rosenfeld, M. G. (1989) *Cell* **59**, 33–43.
24. Livneh, E., Dull, T. J., Berent, E., Prywes, R., Ullrich, A. & Schlessinger, J. (1988) *Mol. Cell. Biol.* **8**, 2302–2308.
25. Countaway, J. L., Northwood, I. C. & Davis, R. J. (1989) *J. Biol. Chem.* **264**, 10828–10835.
26. Honegger, A., Dull, T. J., Bellot, F., Obberghen, E. V., Szapary, D., Schmidt, A., Ullrich, A. & Schlessinger, J. (1988) *EMBO J.* **7**, 3045–3052.
27. Margolis, B. L., Lax, I., Kris, R., Dombalagian, M., Honegger, A., Howk, R., Givol, D., Ullrich, A. & Schlessinger, J. (1989) *J. Biol. Chem.* **264**, 10667–10671.
28. Derynck, R. (1988) *Cell* **54**, 593–595.
29. Kobai, Y., Myers, J. N., Wada, T., Brown, V. I., LeVea, C. M., Davis, J. G., Dobashi, K. & Greene, M. I. (1989) *Cell* **58**, 287–292.
30. Kraus, M. H., Issing, W., Miki, T., Popescu, N. C. & Aaronson, S. A. (1989) *Proc. Natl. Acad. Sci. USA* **86**, 9193–9197.

Int. J. Cancer: 76, 671–676 (1998)
© 1998 Wiley-Liss, Inc.

Publication of the International Union Against Cancer
Publication de l'Union Internationale Contre le Cancer

HUMAN TROP-2 IS A TUMOR-ASSOCIATED CALCIUM SIGNAL TRANSDUCER

Elisabetta RIPANI[1], Andrea SACCHETTI[2], Daniela CORDA[2] and Saverio ALBERTI[1]*

[1]*Unit of Experimental Oncology, Department of Cell Biology and Oncology, Istituto di Ricerche Farmacologiche Mario Negri, Consorzio Mario Negri Sud, Santa Maria Imbaro (Chieti), Italy*

[2]*Laboratory of Cellular and Molecular Endocrinology, Department of Cell Biology and Oncology, Istituto di Ricerche Farmacologiche Mario Negri, Consorzio Mario Negri Sud, Santa Maria Imbaro (Chieti), Italy*

Trop-2/EGP-1/GA733-1 is a recently identified cell surface glycoprotein highly expressed by human carcinomas. The cytoplasmic tail of Trop-2 possesses potential serine and tyrosine phosphorylation sites and a phosphatidyl-inositol binding consensus sequence. Thus, we investigated whether Trop-2 might be a functional signaling molecule. Using the fluorescent probe Fura-2, we assayed the cytoplasmic calcium levels in human cancer cells stimulated with anti-Trop-2 or control antibodies. Three anti-Trop-2 MAbs, Rs7-7G11, MOv16 and 162-46.2 specifically induced a transient intracellular calcium level increment in up to 40% of the experiments performed. Polyclonal antisera recognizing recombinant Trop-2 molecules possessed a much lower stimulation efficiency. The average latency of antibody-induced Ca^{2+} rise for OvCa-432 cells was 64 ± 26 sec. Internal Ca^{2+} concentrations reached peaks of 190 ± 24 nM vs. basal levels of 61 ± 4 nM and returned to baseline within 193 ± 37 sec. Similar values were obtained in MCF-7 cells. For comparison, stimulation of P2-purinergic receptors on MCF-7 and OvCa-432 cells induced a Ca^{2+} rise in most cases, leading to average internal Ca^{2+} concentrations of 297 ± 41 and 391 ± 39 nM, respectively. Our findings show that Trop-2 transduces an intracellular calcium signal, are consistent with the hypothesis that it acts as a cell surface receptor and support a search for a physiological ligand. *Int. J. Cancer* 76:671–676, 1998.
© *1998 Wiley-Liss, Inc.*

Trop-2/EGP-1/GA733-1 is a monomeric cell surface glycoprotein expressed at high levels by normal human multistratified epithelia and trophoblast and by the majority of human carcinomas (Alberti *et al.*, 1992; Stein *et al.*, 1994). We have cloned the human (Fornaro *et al.*, 1995) and the murine (El-Sewedy *et al.*, 1998) TROP2 genes (Leij *et al.*, 1994; Szala *et al.*, 1990). Interestingly, the cytoplasmic tails of the human and murine Trop-2 possess potential serine and tyrosine phosphorylation sites and a phosphatidyl-inositol binding consensus sequence (El-Sewedy *et al.*, 1998). Thus, we speculate that Trop-2 might be a novel cell-surface receptor, that might play a regulatory role in the growth of carcinoma cells. Consistent with the hypothesis that Trop-2 might be a signal transducer, it has been shown that the cytoplasmic serine 303 of Trop-2/EGP-1 can be phosphorylated by PKC (Basu *et al.*, 1995), although the events following the phosphorylation were not investigated. Cytosolic Ca^{2+} plays an important role in the regulation of the differentiated function of several nucleated cell types (Tsien and Tsien, 1990; Meldolesi *et al.*, 1991). Importantly, it participates in the regulation of the cell cycle in proliferating cells and of tumor cells in particular (Dixon *et al.*, 1997). Thus, it was of interest to investigate whether Trop-2/EGP-1/GA733-1 could mediate an intracellular calcium signaling. No physiological ligand for Trop-2 has been identified. However, specific antibodies can cross-link cell surface receptors and induce signaling (Leitenberg *et al.*, 1995; Holland and Owens, 1997). Thus, we tested if the cross-linking of Trop-2 with specific MAbs could elicit a cytosolic calcium signal.

MATERIAL AND METHODS

Cells

The human OvCa-432 ovarian carcinoma and MCF-7 mammary carcinoma cell lines (Alberti *et al.*, 1992) were grown in RPMI-1640 medium (GIBCO, Grand Island, NY). The C3H mouse L fibrosarcoma cells were maintained in DMEM (GIBCO), with 1 g/l glucose and sodium pyruvate. RPMI-1640 and DMEM were supplemented with glutamine, penicillin, streptomycin and 10% FCS (culture medium). L cell transfectants were maintained in DMEM/HAT culture medium. The day before Ca^{2+} measurements, cells were collected in PBS-EDTA, filtered through a 20 µm pore nylon mesh (Filcon, Torino, Italy) to remove cell aggregates and seeded on sterile glass coverslips coated with poly-D-lysine (Sigma, St. Louis, MO) (Bizzarri and Corda, 1994).

Production of recombinant Trop-2 protein

The coding region of TROP2/EGP-1/GA733-1 between the leader sequence and the transmembrane region (Fornaro *et al.*, 1995) was amplified by PCR using specific primers. After subcloning in the galactose-inducible pQE-10 vector (Qiagen, Chatsworth, CA), the correctness of the resulting open reading frame and the absence of PCR-induced mutations was confirmed by DNA sequencing. The TROP2 constructs were transformed in XL1-blue *Escherichia coli* strain and synthesis of the recombinant Trop-2 was induced by IPTG 0.2 mM for 5 hr (Studier *et al.*, 1990). The 6 histidine-tagged recombinant Trop-2 was purified by affinity chromatography on chelated Ni^{2+} columns (Qiagen), in denaturing conditions and following the manufacturer's instructions. Purity of the recombinant Trop-2 protein to be used for animal immunization was verified by PAGE.

Antibodies

The MOv-16 MAb was a gift of Dr. M. I. Colnaghi (Milano, Italy). The T16 hybridoma was supplied by Dr. C.E. Klein (Würzburg, Germany). The RS7-3G11 MAb was a kind gift of Dr. R. Stein (Newark, NJ). The 162-46.2 anti-Trop-2 and T16 hybridomas were grown as ascites in BALB/c or nude mice (Alberti *et al.*, 1992; Stein *et al.*, 1994). The anti-CD5 (Leu-1, Becton-Dickinson, Mountain View, CA) and PK-136 MAb were used as controls (Fig. 1) (Ledbetter *et al.*, 1985; Koo and Peppard, 1984). The MAbs were purified either by affinity chromatography on protein-A Sepharose or by ion-exchange chromatography (Alberti *et al.*, 1992). Three micrograms of MAb in 300 µl final volume were used in most assays (*see* Results). Polyclonal anti-sera recognizing Trop-2 were obtained either by immunizing rabbits with the recombinant Trop-2 protein produced in *E. coli* or by immunizing

Abbreviations: ATP: adenosine trisphosphate; $[Ca^{2+}]_i$: free cytosolic calcium concentration; FITC: fluorescein-isothiocyanate; MAb: monoclonal antibody; PAGE: polyacrylamide gel electrophoresis; SM: staining medium; SEM: standard error of the mean.

Grant sponsor: Italian Association for Cancer Research and the Italian National Research Council; Grant number: 94.01319.39.

*Correspondence to: Consorzio Mario Negri Sud, 66030 Santa Maria Imbaro (Chieti), Italy. Fax: (39)872-578-240.
E-mail: Alberti@CMNS.MNEGRI.IT

Received 8 August 1997; Revised 29 November 1997

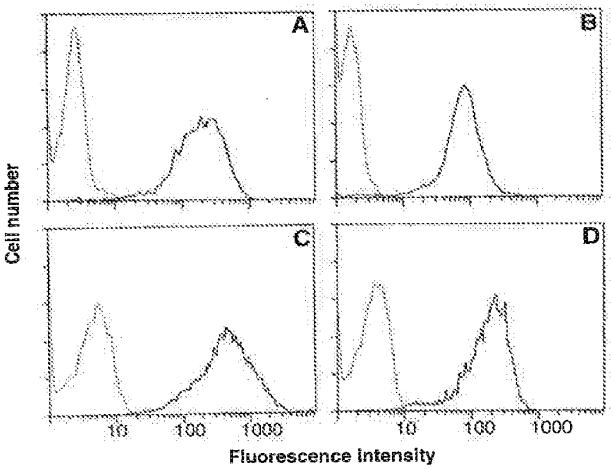


FIGURE 1 – Immunofluorescence analysis of OvCa-432 (*a*, *c*) and MCF-7 (*b*, *d*) cells. Cells were stained with T16 MAb (*a*, *b*) or with anti-Trop-2 polyclonal antisera (*b*, *d*) (solid line). Dotted lines indicate staining with control antibodies.

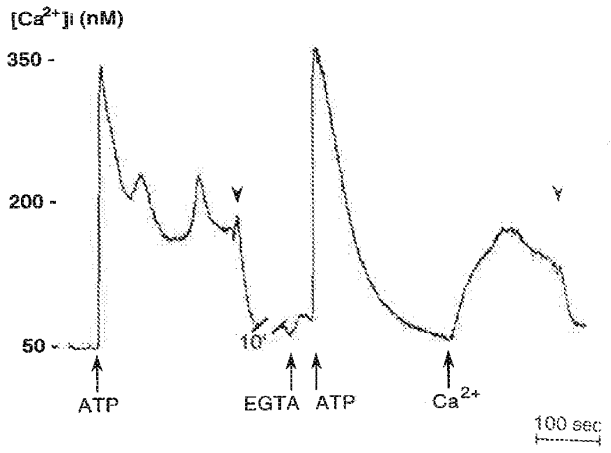


FIGURE 2 – Increase of $[Ca^{2+}]_i$ in OvCa-432 cells stimulated with 5 μM ATP. Arrows indicate, respectively, the addition of ATP, of 2 mM EGTA in PBS w/o Ca^{2+} and Mg^{2+}, of ATP in PBS/EGTA and of 0.9 mM Ca^{2+} in PBS/ATP. Arrowheads indicate washes. $[Ca^{2+}]_i$ levels are indicated.

mice with mouse L cells transfected with Trop-2. Pre-immune sera from the same animals were used as controls. The titers in bleedings were confirmed by Western blot or slot blot analysis over recombinant Trop-2 proteins. Immunofluorescence FACS analysis of Trop-2 transfectants and control L cells and of Trop-2 expressing and non-expressing human carcinoma cell lines confirmed the specificity of the antisera obtained. Polyspecific stimulations were performed either with polyclonal antisera (3 μg) or with mixed polyclonal antisera (1.5 μg) and anti-Trop-2 MAb (MOv16, T16, 162–46.2, 0.5 μg each). Goat anti-mouse or anti-rabbit immunoglobulin (Serotec, Oxford, UK) were used to enhance the extent of cross-linking induced by the anti-Trop-2 antibodies. All antibodies were salt-exchanged to PBS in spin columns. Antibodies in PBS were subsequently sterilized by ultracentrifugation and stored frozen until use. All antibody preparations were spun prior to use at 15,000 × *g*, 4°C for 30 min to remove aggregates that could cause non-specific stickiness to cell membranes.

Flow cytometry immunofluorescence analysis

Cell staining was performed essentially as described (Alberti *et al.*, 1994) (Fig. 1). Briefly, cell suspensions (200 μl) were incubated with saturating amounts of the appropriate MAb for 30 min on ice, washed and, if necessary, incubated with 1 μg of fluorescein-isothiocyanate (FITC)-conjugated secondary antibody for 30 min on ice. After washing, the cells were re-suspended in medium with 0.5 μg/ml of propidium iodide to allow gating of dead cells. Fluorescence analysis was made on a fluorescence-activated cell sorter (FACS-STAR, Becton Dickinson, Sunnyvale, CA) (Alberti *et al.*, 1992; 1994).

Measurement of cytosolic Ca^{2+}

$[Ca^{2+}]_i$ recordings were performed on cells adhering to glass coverslips (Bizzarri and Corda, 1994). Briefly, 1–5 × 10^6 cells were seeded on poly-d-lysine coated 24 × 24 mm coverslips the day before the recording. Coverslips were washed twice with HEPES-buffered PBS with Ca^{2+} and Mg^{2+}, 0.1 mg/ml BSA, pH 7.4 and incubated in the same buffer with 2–5 μM Fura-2 AM (Boehringer Mannheim, Germany), at room temperature for 30–80 min depending on the cell line. The coverslips were then transferred to a perfusion chamber mounted on the stage of a Zeiss IM35 microscope and maintained at 37°C. Ca^{2+} recordings were performed as previously described (Bizzarri and Corda, 1994) using a dual excitation spectrofluorimeter at 340/380 nm (model CMIT111, Spex Industries, Edison, NJ) with emission at 505 nm. Groups of 2–5 cells were selected and their $[Ca^{2+}]_i$ was recorded for 1–2 min to ensure stability of the signal. Control antibodies were added and the cell signals were recorded for further 6–8 min to ensure the absence of non-specific signaling. After washing, anti-Trop-2/ESP-1/GA733-1 antibodies were added and the signal was recorded for 10 min. If no signal was apparent after 5 min, goat anti-mouse or anti-rabbit antisera were added after washing to increase the level of Trop-2 cross-linking. Adenosine trisphosphate (ATP) (Sigma) was mostly used at a final concentration of 5 μM (Dixon *et al.*, 1997; Popper and Batra, 1993). Measured 340/380 nm ratio values were then converted to free calcium concentration (Bizzarri and Corda, 1994). At the end of the recordings, 4 μM ionomycin and 50 mM EGTA were added to obtain maximum ratio (R_{max}), minimum ratio (R_{min}), and the constant β (the ratio of the fluorescence measured at 380 nm in Ca^{2+}-free *vs.* Ca^{2+}-saturating solution), as described by Bizzarri and Corda (1994). The calcium signaling parameters are presented as mean ± SEM throughout. Each of the traces presented in Figures 2–4 is representative of several recordings performed (Tables I and II).

RESULTS

Production of recombinant Trop-2 and of polyclonal anti-Trop-2 antisera

Since it was unclear whether the available anti-Trop-2 MAb would have been able to elicit a calcium signal, polyclonal anti-human Trop-2 antibodies were produced both in mice and in rabbits. The coding region of Trop-2 between the leader sequence and the transmembrane region (Fornaro *et al.*, 1995) was expressed in *E. coli* and purified to essential homogeneity by affinity chromatography. The purity of the recombinant Trop-2 protein for animal immunization was verified by PAGE. The antibody titers in the sera from immunized rabbits were verified by slot blot, Western blot and flow cytometry analysis (Fig. 1). Anti-Trop-2 antisera did not significantly label cells transfected with Trop-1/Ep-CAM (Fornaro *et al.*, 1995; Litvinov *et al.*, 1994) (not shown), confirming that the Trop-2 responses did not depend on a co-expression of Trop-1. Bacteria do not preserve the glycosylation pattern of

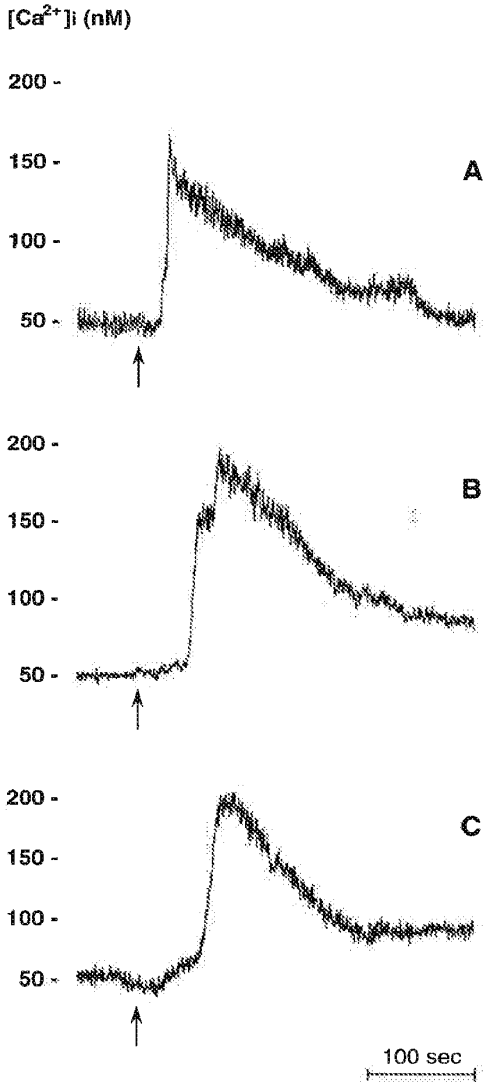


FIGURE 3 – $[Ca^{2+}]_i$ recordings in OvCa-432 (*a*, *b*) and MCF-7 (C) cells. (*a*) Increase of $[Ca^{2+}]_i$ in OvCa-432 cells stimulated with MAb 162-46.2. (*b*) Increase of $[Ca^{2+}]_i$ in OvCa-432 cells stimulated with MAb MOv16. (*c*) Increase of $[Ca^{2+}]_i$ in MCF-7 cells stimulated with MAb MOv16. Arrows indicate the addition of the antibody. $[Ca^{2+}]_i$ levels are indicated.

eukaryotic molecules and glycosylation could mediate ligand recognition and affect signaling (Ding *et al.*, 1995). Thus, polyclonal antisera were also produced against native glycosylated Trop-2 molecules by injecting C3H mice with plasma cell membranes from L cells transfected with Trop-2. Extensive adsorption of the sera on untransfected mouse L cells effectively removed anti-L cell reactivity, as determined by flow cytometry.

Flow cytometry analysis

All the cell lines monitored for $[Ca^{2+}]_i$ levels, *i.e.*, OvCa-432 and MCF-7 cells and transfected L cells, were confirmed to express high levels of Trop-2 by flow cytometry analysis (Fig. 1). The anti-Trop-2 reactivity of the Rs7-7G11 MAb (Stein *et al.*, 1994) was demonstrated by specific staining of Trop-2 transfected L cells.

Measurement of cytosolic Ca^{2+} cell labeling of coverslip-adherent cells

Preliminary experiments determined for both OvCa-432, MCF-7 and L cells conditions for efficient Fura-2 AM labeling and signal stimulation. Three to ten micrograms of purified antibodies or 3-10 μl of antisera in 300 μl final volume were used. Three μg proved routinely sufficient for specific stimulation of OvCa-432 cells and were used throughout. For comparison, 0.2 μg of anti-Trop-2 are sufficient to stain 5×10^4 OvCa-432 cells essentially to saturation, as assayed by flow cytometry. Preliminary experiments indicated that both OvCa-432 and MCF-7 cells are sensitive to fluid shear stress and temperature fluctuations and these can provoke spontaneous rises in calcium levels (Grierson and Meldolesi, 1995). Thus, temperature control (37°C) was accurately maintained, antibody solutions were kept at 37°C and slowly added

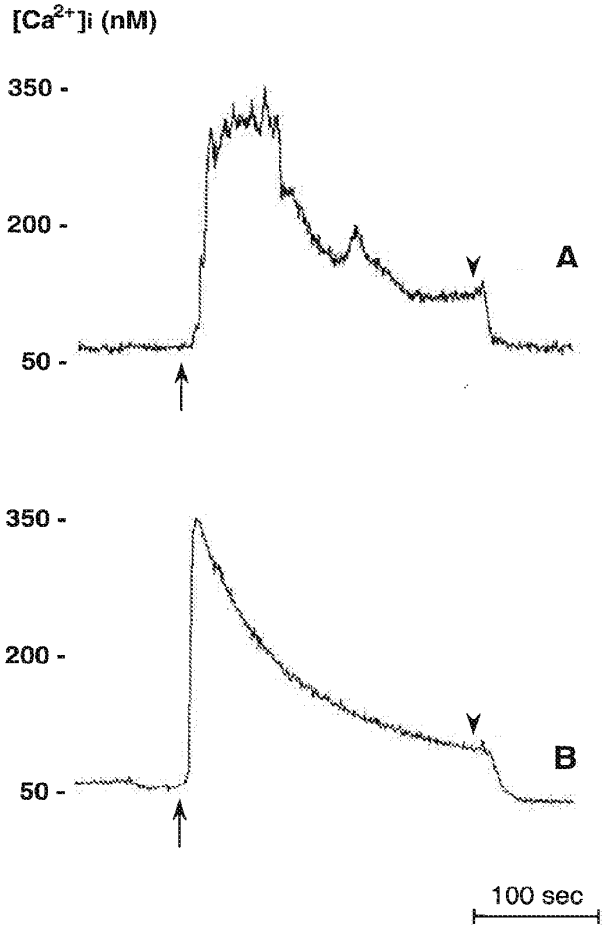


FIGURE 4 – $[Ca^{2+}]_i$ recordings in OvCa-432 cells. (*a*) Increase of $[Ca^{2+}]_i$ in OvCa-432 cells stimulated with mAb MOv16. (*b*) Increase of $[Ca^{2+}]_i$ in OvCa-432 cells stimulated with 5 μM ATP. The first arrow indicates the addition of the antibodies, the second indicates washing with PBS/BSA. $[Ca^{2+}]_i$ levels are indicated.

OnCusp
Ex. 1002

TABLE I – INDUCTION OF CYTOSOLIC CALCIUM MOBILIZATION AFTER CROSS-LINKING WITH ANTI-TROP-2/GA733-1/EGP-1 ANTIBODIES

Target cells	OvCa-432	MCF-7
Rs7-7G11[1,2]	40% (2/5)	ND
MOv16[2]	19% (16/62)	10% (3/30)
162-46.2[2]	8% (2/25)	0% (0/12)
T16[2]	0% (0/20)	0% (0/10)
Control MAb[3,4]	0% (0/112)	0% (0/30)
Anti-Trop-2 polyclonals	9% (1/11)	8% (1/12)
Anti-Trop-2 polyclonals and MAb	11% (1/9)	ND[5]
Pre-immune sera[4]	0% (0/20)	0% (0/12)
ATP	100% (26/26)	92% (25/27)

[1]Increase of $[Ca^{2+}]_i$/number of total experiments, percentage. The ratios of the absolute numbers are indicated in parenthesis.–[2]MAb anti-Trop-2 (Alberti *et al.*, 1992; Stein *et al.*, 1994).–[3]PK136, anti-NK-1.1 (Koo and Peppard, 1984) and Leu-1, anti-CD5 (Ledbetter *et al.*, 1983).–[4]Control MAb and/or pre-immune sera were added before each measurement.–[5]ND: not done.

TABLE II – CHARACTERISTICS OF THE CALCIUM SIGNAL INDUCED BY ANTI-TROP-2/GA733-1/EGP-1 MAb OR ATP

Cell lines	$[Ca^{2+}]_i$ nM		Seconds	
	Basal[1]	Peak[2]	Latency[3]	Return to baseline[4]
OvCa @Trop-2	64 ± 4	191 ± 24	65 ± 26	193 ± 37
ATP	61 ± 4	391 ± 39	≤2	440 ± 39
MCF-7 @Trop-2	71 ± 7	264 ± 75	77 ± 23	137
ATP	59 ± 4	297 ± 41	≤2	400 ± 46

[1]Basal $[Ca^{2+}]_i$ levels are indicated (± SEM).–[2]Peak $[Ca^{2+}]_i$ levels ± SEM.–[3]Latency between stimulus and response. When latency was too short to be correctly quantified, it is indicated as 2 sec or less.–[4]Time necessary to return to baseline levels.

to the cells and the stability of cell fluorescence was ensured for several minutes before proceeding with the assay. A large number of recordings (n ≥ 69) indicate that the basal $[Ca^{2+}]_i$ of the OvCa-432 cells is 63 ± 3 nM and that of the MCF-7 cells is 58 ± 6 nM.

Measurement of cytosolic Ca^{2+} ATP stimulation

ATP is a physiological stimulus that efficiently signals through an elevation of the $[Ca^{2+}]_i$ levels in several transformed human epithelial cell lines (Dixon *et al.*, 1997; Popper and Batra, 1993). Thus, stimulation by ATP was used throughout as an indicator of integrity of cell calcium signalling and for comparison with the characteristics of the antibody induced calcium rises. ATP responses in MCF-7 cells have been characterised and are dependent on a P_{2u} purinergic receptor (Dixon *et al.*, 1997). However, no similar evidence was available for the OvCA-432 cells. Thus, we investigated if ATP can induce a calcium signal in OvCa-432 cells and how it compares with signaling in MCF-7. Concentrations of ATP ≥ 0.5 μM induce cytosolic calcium rises in the OvCA-432 cells and 5 μM ATP reproducibly caused efficient stimulation, in good agreement with results obtained with other human cancer cell lines (Dixon *et al.*, 1997; Popper and Batra, 1993). ATP 5 μM induces in the OvCA-432 cells $[Ca^{2+}]_i$ levels of 330 ± 40 nM over the basal level (net increase 545±73 % vs the basal). For comparison, the same concentrations of ATP induce a 238 ± 40 nM rise over the basal level in the MCF-7 cells (net increase 416 ± 82% *vs.* the basal) (Figs. 2, 4, Table II). The response to ATP in the OvCa-432 cells has 2 components, similarly to what has been observed in MCF-7 cells. A first component is fast and of short duration and probably depends on IP_3 stimulation of Ca^{2+} release from internal stores, whereas the second one is more prolonged and is due to extracellular calcium entry (Fig. 2). Indeed, as Ca^{2+} is removed by washing and addition of 2 mM EGTA, the second component is eliminated and is restored by subsequent addition of Ca^{2+} (Fig. 2) ($n = 6$).

Measurement of cytosolic Ca^{2+}, stimulation with anti-Trop-2 antibodies

Most of the anti-Trop-2/EGP-1/GA733-1 stimulation assays were performed on highly Trop-2 expressing human cell lines, *i.e.*, the ovarian carcinoma OvCa-432 and the mammary carcinoma MCF-7 (Fig. 1). One hundred and twelve independent recordings were performed on OvCa-432 and 64 were obtained on MCF-7 cells stimulated with anti-Trop-2 antibodies. Significant rises in $[Ca^{2+}]_i$ were frequently observed using anti-Trop-2 antibodies. The cells used in the assays did not respond to antibodies with irrelevant binding specificities (Table I), thus excluding signaling through IgG Fc receptors. Moreover, since some MAbs that efficiently bound Trop-2 did not signal (Table I), non-specific effects by antibodies bound to the cell membrane were also excluded. Since all the analyses were performed on small groups of cells, both the frequency and the intensity of the increases of $[Ca^{2+}]_i$ induced by anti-Trop-2 MAb represent an average of the responses of the different cells (Bizzarri and Corda, 1994). The efficiency of response varied widely among the different anti-Trop-2 MAbs used, the highest being for the MOv16 and Rs7-7G11 MAbs on OvCa-432 cells (Table I). However, no significant differences were detectable among cytoplasmic calcium profiles obtained with different MAbs (Fig. 3 and data not shown). Polyspecific stimulations were also attempted, either with polyclonal antisera or with polyclonal antisera mixed with anti-Trop-2 MAb. However, they all proved quite unefficient (Table I). Since Trop-2 is glycosylated (Alberti *et al.*, 1992) and glycosylation could significantly affect signaling (Leconte *et al.*, 1994; Ding *et al.*, 1995), mouse polyclonal antisera directed against native Trop-2 molecules were also produced. However, these did not perform significantly better than the rabbit anti-recombinant Trop-2 antisera (data not shown). Since polyclonal antisera efficiently bound to Trop-2 (Fig. 1), these findings suggest competition between different anti-Trop-2 epitope specificities (Alberti *et al.*, 1992; Stein *et al.*, 1994), because of competitive binding (Alberti *et al.*, 1992) or of negative signaling by some antibodies. The addition of anti-immunoglobulin antisera induced Ca^{2+} signaling in about 30% of the cells unresponsive to anti-Trop-2 MAb alone, suggesting that the frequency of Ca^{2+} responses depends on the intensity of cross-linking. The antibody-induced Ca^{2+} rises showed a latency ranging from less than 2 sec to about 200 sec (Table II). Calcium levels reached their peak values in 6 to 150 sec and returned to baseline levels between 32 and 300 sec. The antibody-induced Ca^{2+} rises over the basal level are of 127 ± 22 nM (net increase 195 ± 29% *vs.* basal) for the OvCa-432 cells (range 35–268 nM) and of 192 ± 82 nM (net increase 285 ± 143% *vs.* basal) for the MCF-7 cells (range 143–274 nM) (Table II). Preliminary analysis indicates that Trop-2 can transduce signals also in the absence of extra-cellular Ca^{2+}, suggesting that one component of Trop-2 signaling is induction of Ca^{2+} release from intracellular stores (data not shown). Interestingly, comparison with ATP calcium signals indicates that the highest peaks of $[Ca^{2+}]_i$ induced by anti-Trop-2 antibodies are quite close to those induced by ATP. Thus, since multiple cells were analyzed in each recording, the lower average $[Ca^{2+}]_i$ rises by anti-Trop-2 MAb *vs.* ATP is due at least in part to the different efficiency of recruitment of signaling units (20–40% for antibodies *vs.* 90% for ATP) (Bizzarri and Corda, 1994). In other words, antibodies only rarely recruited all the cells under observation, whereas this was quite often the case for ATP.

DISCUSSION

The human Trop-2/GA733-1/EGP-1 is a cell surface glycoprotein expressed at high levels by normal human multistratified epithelia and trophoblast and by the majority of human carcinomas (Alberti *et al.*, 1992; Stein *et al.*, 1994). Interestingly, the cytoplasmic tail of Trop-2/GA733-1/EGP-1 can be phosphorylated on serine 303 (Basu *et al.*, 1995), suggesting a role of this molecule in

5456 of 14295

OnCusp
Ex. 1002

signal transduction. Thus, we have tested the hypothesis that Trop-2 could act as a signal transducer in transformed cells. Cross-linking of cell surface receptors is probably critical for signaling (Lemmon *et al.*, 1997) and antibodies directed against cell surface receptors can be efficient cross-linkers and signal inducers (Holland and Owens, 1997; Leitenberg *et al.*, 1995). Thus, since a physiological ligand for Trop-2 has not been identified yet, we assayed the intracellular Ca^{2+} levels after an antibody-mediated cross-linking.

Remarkably, anti-Trop-2 MAb induced significant and frequent rises in the cytoplasmic $[Ca^{2+}]_i$ whereas no responses were elicited by control MAb (Table I). Similarly to other MAb-stimulated cell surface signaling molecules (Holland and Owens, 1997; Leitenberg *et al.*, 1995) and references therein), the percentages of responses varied widely among the MAbs used, with the highest percentage for the MOv16 (20% of responses) and the RS-7G11 (40% of responses). Possible reasons for this include binding of the various MAbs to different epitopes of Trop-2/EGP-1/GA733-1 (Stein *et al.*, 1994) or to the same epitope but with grossly different affinity. However, MOv-16, T16 and 162-46.2 are all high affinity MAbs and bind to the same or closely spaced epitopes of Trop-2 (Alberti *et al.*, 1992). An alternative possibility is that the different MAbs might induce a different relative orientation of the bound Trop-2, which might affect signalling to downstream cytoplasmic molecules.

The finding of responses in up to 40% of the cases and of induced increases of 200–300% over the basal $[Ca^{2+}]_i$ when using anti-Trop-2 antibodies indicates an efficient signaling ability. In the majority of experiments the stimulated calcium increase appeared within 1–2 min after the administration of the antibodies, whith the latest responses appearing within 3–4 min. Taking into account the time necessary for diffusion and binding, these time frames are consistent with a fast signaling after the cross-linking of Trop-2. Both OvCa-432 and MCF-7 cells express markedly heterogeneous levels of Trop-2. Thus, it would be of interest to determine if the signaling capacity of Trop-2 depends on its cell surface density. The increase in free cytosolic calcium concentration due to the activation of cell surface receptors is caused by the opening of Ca^{2+} channels or by the release of Ca^{2+} from intracellular stores, or both (Meldolesi *et al.*, 1991; Tsien and Tsien, 1990). We have shown for OvCa-432 that ATP induces a biphasic response with an initial mobilization of Ca^{2+} from internal stores, and a subsequent channel-mediated entry of extracellular Ca^{2+} (Tsien and Tsien, 1990; Meldolesi *et al.*, 1991; Popper and Batra, 1993). The Ca^{2+} signaling mediated by the cross-linking of Trop-2 appears similar to that of purinergic receptors. Consistently, preliminary analysis indicates that Trop-2 can transduce signals in the absence of extra-cellular Ca^{2+}, indicating that it can induce Ca^{2+} release from intracellular stores (data not shown).

Since Trop-2/EGP-1/GA733-1 transduces a calcium signal in different cell lines and with good efficiency, we speculate that this is a physiological function of Trop-2. The homologous Trop-1/Ep-CAM has been proposed to be an adhesion molecule (Litvinov *et al.*, 1994), although Trop-1 self-recognition has been questioned (Fornaro *et al.*, 1995). Thus, our findings support a search for a physiological ligand for Trop-2/EGP-1/GA733-1, since it might be involved in cell adhesion to a substrate or to other cells. Different adhesion molecules, *e.g.*, integrins (Schwartz *et al.*, 1993), can transduce a signal through an increase in cytoplasmic Ca^{2+}, similarly to Trop-2. Remarkably, signaling by integrins can regulate several responses linked to adhesion to a substrate, including cell growth (Assoian, 1997). A similar role for Trop-2 would be of interest and would be consistent with the high expression of this molecule in tumour cells. The recent finding that human cancer cells can express an oncogenic chimaeric mRNA between Cyclin D1, a master regulator of the G_1-S transition in the cell cycle, and TROP2/EGP-1/GA733-1 (data not shown) also support a role of Trop-2 in tumor growth.

ACKNOWLEDGEMENTS

We thank Drs. R. Dell'Arciprete, R. Ciccocioppo and A.M. Naglieri for help during the course of this work and Ms. A.L. DeFrancesco for technical assistance. This work was supported by the Italian Association for Cancer Research (AIRC, Milano, Italy) and the Italian National Research Council (Convenzione CNR—Consorzio Mario Negri Sud and ACRO contract 94.01319.39).

REFERENCES

Alberti, S., Miotti, S., Stella, M., Klein, C.E., Fornaro, M., Ménard, S. and Colnaghi, M.I., Biochemical characterization of Trop-2, a cell surface molecule expressed by human carcinomas: formal proof that the monoclonal antibodies T16 and MOv-16 recognize Trop-2. *Hybridoma*, **11**, 539–545 (1992).

Alberti, S., Nutini, M. and Herzenberg, L.A., DNA methylation prevents the amplification of TROP1, a tumor associated cell surface antigen gene. *Proc. natl. Acad. Sci. (Wash.)*, **91**, 5833 (1994).

Assoian, R.K., Anchorage-dependent cell cycle progression. *J. Cell Biol.*, **136**, 1–4 (1997).

Basu, A., Goldenberg, D.M. and Stein, R., The epithelial/carcinoma antigen EGP-1, recognized by monoclonal antibody RS7-3G11, is phosphorylated on serine 303. *Int. J. Cancer*, **62**, 472–479 (1995).

Bizzarri, C. and Corda, D., Norepinephrine, unlike ATP, induces all-or-none increase in cytosolic calcium in thyroid cells. The role of inositol-trisphosphate-sensitive stores and calcium channels. *Europ. J. Biochem.*, **219**, 837–844 (1994).

Dexi, D.X., Vera, J.C., Heaney, M.L., and Golde, D.W., N-glycosylation of the human granulocyte-macrophage colony-stimulating factor receptor alpha subunit is essential for ligand binding and signal transduction. *J. Biol. Chem.*, **270**, 24580–24584 (1995).

Dixon, C.J., Bowler, W.B., Fleetwood, P., Ginty, A.F., Gallagher, J.A. and Carron, J.A., Extracellular nucleotides stimulate proliferation in MCF-7 breast cancer cells via P2-purinoceptors. *Brit. J. Cancer*, **75**, 34–39 (1997).

Ilyas-Szendy, T., Fornaro, M. and Alberti, S., Cloning of the murine Trop-2 gene. Conservation of a PIP-2 binding sequence in the cytoplasmic domain of Trop-2. *Int. J. Cancer*, **75**, 324–331 (1998).

Fornaro, M., Dell'Arciprete, R., Stella, M., Bucci, C., Nutini, M., Capri, M.G. and Alberti, S., Cloning of the gene encoding TROP-2, a cell-surface glycoprotein expressed by human carcinomas. *Int. J. Cancer*, **62**, 610–618 (1995).

Grierson, J.P. and Meldolesi, J., Shear stress-induced $(Ca^{2+})_i$ transients and oscillations in mouse fibroblasts are mediated by endogenously released ATP. *J. biol. Chem.*, **270**, 4453–4456 (1995).

Holland, J. and Owens, T., Signaling through intercellular adhesion molecule 1 (ICAM-1) in a B cell lymphoma line. *J. biol. Chem.*, **272**, 9108–9112 (1997).

Koo, G.C. and Peppard, J.R., Establishment of monoclonal anti-Nk-1.1 antibody. *Hybridoma*, **3**, 301–303 (1984).

Leconte, I., Carpentier, J.L. and Clauser, E., The functions of the human insulin receptor are affected in different ways by mutation of each of the four *N*-glycosylation sites in the beta subunit. *J. biol. Chem.*, **269**, 18062–18071 (1994).

Ledbetter, J.A., Martin, P.J., Spooner, C.E., Wofsy, D., Tsu, T.T., Beatty, P.G. and Gladstone, P., Antibodies to Tp67 and Tp44 augment and sustain proliferative responses of activated T cells. *J. Immunol.*, **135**, 2331–2336 (1985).

De Leij, L., Helrich, W., Stein, R. and Mattes, M.J., SCLC-cluster-2 antibodies detect the pancarcinoma/epithelial glycoprotein EGP-2. *Int. J. Cancer*, **8 (Suppl.)**, 60–63 (1994).

Leitenberg, D., Constant, S., Li, D.D., Smith, B.R. and Bottomly, K., CD4 and CD45 regulate qualitatively distinct patterns of calcium mobilization in individual CD4+ T cells. *Europ. J. Immunol.*, **25**, 2445–2451 (1995).

Lemmon, L.A., Pinchasi, D., Zhou, M., Lax, I. and Schlessinger, J., Kit receptor dimerization is driven by bivalent binding of stem cell factor. *J. biol. Chem.*, **272**, 6311–6317 (1997).

OnCusp
Ex. 1002

LITVINOV, S.V., VELDERS, M.P., BAKKER, H.A.M., FLEUREN, G.J. and WARNAAR, S.O., Ep-CAM: a human epithelial antigen is a homophilic cell-cell adhesion molecule. *J. Cell Biol.*, **125**, 437–446 (1994).

MELDOLESI, J., CLEMENTI, E., FASOLATO, C., ZACCHETTI, D. and POZZAN, T., Ca^{2+} influx following receptor activation. *Trends Pharmacol. Sci.*, **12**, 289–292 (1991).

POPPER, L.D. and BATRA, S., Calcium mobilization and cell proliferation activated by extracellular ATP in human ovarian tumor cells. *Cell Calcium*, **14**, 209–218 (1993).

SCHWARTZ, M.A., BROWN, E.J. and FAZELI, B., A 50-kDa integrin-associated protein is required for integrin-regulated calcium entry in endothelial cells. *J. biol. Chem.*, **268**, 19931–19934 (1993).

STEIN, R., BASU, A., GOLDENBERG, D.M., LLOYD, K.O. and MATTES, M.J., Characterization of cluster 13: the epithelial/carcinoma antigen recognized by MAb RS7. *Int. J. Cancer*, **8**, 98–102 (1994).

STUDIER, F.W., ROSENBERG, A.H., DUNN, J.J. and DUBENDORFF, J., Use of T7 RNA polymerase to direct expression of cloned genes. *Methods Enzymol.*, **185**, 60–89 (1990).

SZALA, S., BROEHLICH, M., SCOLLON, M., KASAI, Y., STEPLEWSKI, Z., KOPROWSKI, H. and LIENNENBACH, A.J., Molecular cloning of cDNA for the carcinoma-associated antigen GA733-2. *Proc. nat. Acad. Sci. (Wash.)*, **87**, 3542–3546 (1990).

TSIEN, R.W. and TSIEN, R.Y., Calcium channels, stores, and oscillations. *Ann. Rev. Cell Biol.*, **6**, 715–760 (1990).

OnCusp
Ex. 1002

14 Preclinical and Clinical Development of Exatecan (DX-8951f)

A Hexacyclic Camptothecin Analog

Eric K. Rowinsky, MD

CONTENTS

INTRODUCTION
STRUCTURE
PRECLINICAL ACTIVITY
PRECLINICAL PHARMACOLOGY
PRECLINICAL TOXICOLOGY
PHASE I DEVELOPMENT IN PATIENTS WITH ADVANCED MALIGNANCIES
DISEASE-DIRECTED (PHASE II–III) EVALUATIONS
DE-310, A MACROMOLECULAR CARRIER OF DX-8951
CONCLUSION
REFERENCES

1. INTRODUCTION

The principal rationale for synthesizing exatecan (DX-8951f, Daiichi Pharmaceutical Co., Ltd, Japan) was to exploit physicochemical features of the camptothecins (CPTs) anticipated to yield an increased therapeutic advantage compared with currently available CPT analogs such as topotecan and irinotecan. The overall therapeutic profile sought in these efforts was greater and broader antitumor activity, decreased toxicity, and intrinsic activity without requiring metabolic activation, which may accentuate the fundamentally large interindividual variability in the pharmacologic behav-

Camptothecins in Cancer Therapy
Edited by: V. R. Adams and T. G. Burke © Humana Press Inc., Totowa, NJ

ior of the CPT analogs and consequently in their antitumor and toxicologic profiles. Exatecan has completed Phase I clinical development on a broad range of schedules and is currently undergoing more focused disease-directed Phase II and Phase III evaluations. Additionally, DE-310, a unique polymer prodrug of exatecan, which was developed to achieve protracted systemic exposure to the active drug after a single dose, is also undergoing early clinical development.

2. STRUCTURE

Exatecan (DX-8951f; (1*S*, 9*S*)-1-amino-9-ethyl-5-fluoro-1, 2, 3, 9, 12, 15-hexahydro-9-hydroxy-4-methyl-10*H*, 13*H*-benzo [*de*] pyrano [3', 4':6,7] indolizino[1,2-*b*]quinoline-10, 13-dione monomethane sulfonate (salt) dihydrate is a water-soluble, fluorinated, hexaphilic synthetic derivative of CPT that, in contrast to irinotecan, has intrinsic activity without undergoing metabolic activation. The chemical structure of the anhydrous base form of the drug, referred to as DX-8951, is shown in Fig. 1. The 20S stereoisomeric form is active, whereas the 20R form is inactive. The chemical structure of exatecan has been modified to render the molecule water-soluble by adding a ring structure between rings A (in position 9) and B (in position 7), and a fluorine in position 11. Similar to all CPT derivatives that inhibit topoisomerase I (TOP-I), the A-ring of the lactone form of the drug is hydrolyzed to form an open-ring hydroxy-acid species. The two species coexist in solution according to a reversible pH-dependent equilibrium, with an acidic pH favoring the formation of the closed-ring lactone form.

3. PRECLINICAL ACTIVITY

Interest in exatecan was first generated after the agent demonstrated 3 times greater potency than SN-38, the active metabolite of irinotecan, 10 times greater potency than topotecan, and 20 times greater potency than CPT at inhibiting TOP-I extracted from murine P388 leukemia; IC_{50} (concentration that inhibits 50%) values of 0.975, 2.71, 9.52, and 23.5 μg/mL were reported for exatecan1f, SN-38, topotecan, and CPT, respectively *(1)*. The inhibition of human TOP-I by the lactone was approximately 300-fold greater than that by the hydroxy-acid form. Exatecan was also approximately five times more potent than SN-38 at inhibiting DNA synthesis. Furthermore, in a study of the relative antitumor properties of the CPT analogs against a panel of 32 cell lines derived from human breast, gastric, colon, ovarian, cervical, lung, and hematopoietic neoplasms, the IC_{50} values of exatecan averaged 6- and 28-fold lower than SN-38 and topotecan, respectively *(1,2)*. A summary of the relative IC_{50} values of exatecan and the other CPT analogs according to tumor type is shown in Table 1. In the human tumor cloning assay, exatecan inhibited the growth of clonogenic

OnCusp
Ex. 1002

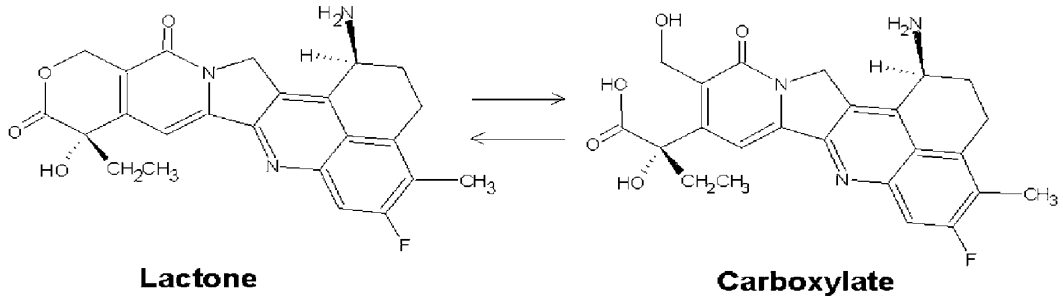


Fig. 1. Structure of the active exatecan lactone (left) undergoing reversible pH-dependent hydrolysis to its inactive open-ring form.

Table 1
In Vitro Cytotoxicity Against A Series of 32 Cancer Cell Lines: Summary According to Tumor Type

	IC_{50} (ng/mL)			
Tumor type	*Exatecan*	*SN-38*	*Topotecan*	*CPT*
Breaast	2.02	6.57	64.1	12.5
Colon	2.92	15.1	92.5	21.8
Stomach	1.53	15.1	30.6	13.0
Lung	0.87	7.37	35.3	9.99
Others	4.33	36.2	82.9	26.1
Summary	2.09	12.1	89.5	15.3

ID_{50}, drug concentration at which the growth is inhibited by 50%.

cells derived from patients with head and neck, non-small-cell lung, liver, lung, breast, colon, ovary, and prostate carcinomas in a dose-dependent manner, and exatecan and topotecan were not completely cross-resistant *(3)*.

Exatecan has shown activity against a wide range of human tumor xenografts in nude mice, including gastric, pancreatic, colon, breast, ovary, and lung cancers *(1,4,5)*. In addition, the agent demonstrated impressive antitumor activity against an intracranial xenograft of human RH30 rhabdomyosarcoma and various other pediatric solid neoplasms, murine lung and liver metastasis xenograft models, and both early and late stages of human acute myelogenous leukemia in a severe combined immunodeficient mouse model *(5–11)*. Exatecan also produced notable activity that was superior to gemcitabine in both orthotopic and traditional xenografts of human pancreatic cancer *(12)*. Although exatecan treatment resulted in impressive antitumor activity on both single and divided dosing administra-

Table 2
Comparison of the Antitumor Effects of Exatecan and CPT-11 Against Various Human Tumor Xenografts

		Exatecan total (75 mg/kg)		*Irinotecan (320 mg/kg)*	
Tumor type	*No. of tumors*	*>IR (80%)*	*>IR (58%)*	*>IR (80%)*	*>IR (58%)*
Gastric cancer	2	2 (100%)	2 (100%)	1 (50%)	2 (100%)
Colon cancer	6	6 (100%)	6 (100%)	4 (67%)	5 (83%)
Lung cancer	5	4 (80%)	5 (100%)	1 (20%)	2 (40%)
Breast cancer	2	2 (100%)	2 (100%)	2 (100%)	2 (100%)
Renal cancer	1	0 (0%)	0 (0%)	0 (0%)	0 (10%)
Total	16	14 (88%)	15 (94%)	8 (50%)	11 (69%)
$p<0.05$ $p = 0.10$					

IR, dose at which the specified percentage of tumor growth inhibition is produced by the drug as a single agent.

tion schedules, superior efficacy was generally noted against human tumor xenografts when the agent was administered on divided dosing schedules *(1,4)*. For example, in studies involving the in vivo homologous Meth A mouse fibrosarcoma model, a cyclical dosing pattern resulted in superior antitumor activity at lower doses of exatecan compared with a single dosing schedule. A comparison of the antitumor effects of exatecan and irinotecan at equitoxic doses against various human tumor xenografts is depicted in Table 2.

Several in vitro and in vivo investigations using human tumor cell lines and drug-resistant variants have demonstrated that exatecan, in contrast to topotecan and SN-38, is not affected by mechanisms of drug resistance conferred by overexpression of P-glycoprotein (Pgp) or breast cancer resistance protein, as well as decreased levels of TOP-I mRNA or protein *(9,12–18)*. In fact, exatecan is not a substrate for the Pgp multidrug transporter that confers multidrug resistance, whereas both topotecan and SN-38 are weak substrates for Pgp *(9,12–15)*. The impressive and distinctly different preclinical antitumor spectra of exatecan may, in part, be due to the fact that the agent is not a substrate for the Pgp multidrug transporter, in contrast to topotecan, 9-aminocamptothecin, and SN-38, which are weak substrates for the efflux pump *(13–16)*. The lack of cross-resistance of Pgp-overexpressing neoplasms to exatecan is indicated by the results of a study in which the agent exhibited similar antitumor activity against human lung cancer PC-6 and its multidrug resistance Pgp-overexpressing variant, PC-6/vincristine as shown in Table 3 *(9)*. Similarly, exatecan demonstrated roughly equiva-

OnCusp
Ex. 1002

Table 3
Comparison of the Antitumor Effects and Relative Resistance of Exatecan and Other Topoisomerase I-Targeting Agents Against Parental (PC-6) and Pgp Overexpressing (PC-6/Vincristine) Cancer Cell Lines

	IC_{50} (ng/mL)		
Agent	*PC*	*6 PC-6/Vincristine*	*Resistance ratio*
Exatecan	0.089	0.069	0.8
SN-38	0.655	0.751	1.1
Topotecan	1.73	4.36	2.5
Vincristine	0.284	107	380
Cisplatin	13.8	69	0.5

ID_{50}, dose associated with inhibition growth by 50%; Pgp, P-glycoprotein.

lent potencies against PC-6 and a SN-38–resistant subline characterized by impaired SN-38 accumulation without Pgp overexpression, and the antitumor activities of exatecan were similar against human pancreatic cancers SUIT-2 and KP-1N and their respective sublines that had acquired resistance to CPT-11 in vivo and SN-38 in vitro, presumably because of reduced levels of TOP-I mRNA and protein *(8)*. The magnitude of accumulation of drug within the cell was demonstrated to be a determinant of sensitivity to exatecan in vitro, and this phenomenon appears, in part, to be the basis for differential activity between CPT analogs *(8)*. Exatecan treatment has also been demonstrated to induce BRCP in vitro, but BRCP overexpression, which conferred resistance to 9-aminocamptothecin, SN-38, and irinotecan, was responsible for negligible to no resistance to exatecan *(17,18)*. Similarly, neither overexpression of Pgp, multidrug-resistance protein-1, or lung cancer–resistance protein conferred resistance to exatecan in a wide array of experimental human colon and ovarian cancers *(19)*. There is only one clear model of tumor resistance to exatecan, in which drug resistance relates to qualitative changes in the expression of TOP-I *(9,20)*. Evidence implicates "modifier" proteins such as ubiquitin, SUMO-1, and others, which bind to critical domains of TOP-I *(16,20)*. In addition, higher levels of the DNA repair protein O(6)-methylguanine-DNA methyltransferase have been demonstrated to be associated with resistance to exatecan and other CPT analogs, and treatment of drug resistance cells, presumptively because of increased O(6)-methylguanine-DNA methyltransferase activity, by a nontoxic O(6)-methylguanine-DNA methyltransferase inhibitor-augmented drug activity *(21)*.

4. PRECLINICAL PHARMACOLOGY

In preclinical pharmacology studies of exatecan in dogs and rodents using radiolabeled drug (^{14}C-exatecan) and high-performance liquid chromatography for differential quantification of lactone and total drug, the half-life ($t_{1/2}$) of the lactone ranged from approximately 20 to 30 minutes, and systemic exposure to the lactone was approximately 50% of total drug exposure *(22–28)*. In both species, the clearance rates of total drug and lactone were similar: lactone exposure accounted for approximately 50% of total exatecan exposure, and the pharmacokinetics of both total drug and lactone were dose-independent. Tissue distribution studies revealed exatecan uptake in all tissues; however, drug concentrations in brain were very low, suggesting that exatecan is not transported across an intact blood-brain barrier. Exatecan was also shown to be highly bound to plasma proteins in all species, and spectrometric studies indicated that the lactone is selectively stabilized by albumin under physiologic conditions. In vitro, plasma proteins were determined to be approximately 93, 86, 96, and 93% in rats, dogs, monkeys, and humans, respectively.

In rats treated with a single intravenous (iv) dose of ^{14}C-exatecan, urine and fecal recovery averaged 15% and 78% of the administered dose, respectively *(22–25)*. The majority of exatecan was metabolized to hydroxylated metabolites. The same hydroxylated metabolites have predominated after coincubation of exatecan and liver microsomes of multiple species, including humans, in vitro. These studies, and other in vitro and in vivo studies, have indicated that exatecan is highly metabolized to a 4-hydroxymethyl metabolite (UM-1) and a 3-hydroxy metabolite (UM-2), the structures of which are shown in Figure 2. The cytochrome P450 microsomal isoenzymes CYP3A4 and CYP1A2 are principally involved in metabolism of exatecan to UM-1 and UM-2, respectively *(22–28)*. The antitumor activities of both hydroxylated metabolites against P388 and PC-6 cancer cell lines were demonstrated to be substantially less than exatecan *(22,23,25,26,28)*. The hydroxylation of exatecan has been demonstrated to be inhibited in vitro by several known CYP3A substrates, including ketoconazole, nifedipine, erythromycin, and fentanyl *(22)*. There were no gender-related differences in exatecan metabolism, but an interindividual variation of hydroxylation, consisting of a 5.6-fold difference between the lowest and highest rates of hydroxylation in 29 human liver microsomal samples, was demonstrated *(22,23)*.

5. PRECLINICAL TOXICOLOGY

The toxicity profile of exatecan has been evaluated in mice, rats, and dogs before clinical trials *(22,25,26)*. The toxicity profile was consistent across all animal species. Rapidly proliferative tissues, including hematopoietic

OnCusp
Ex. 1002

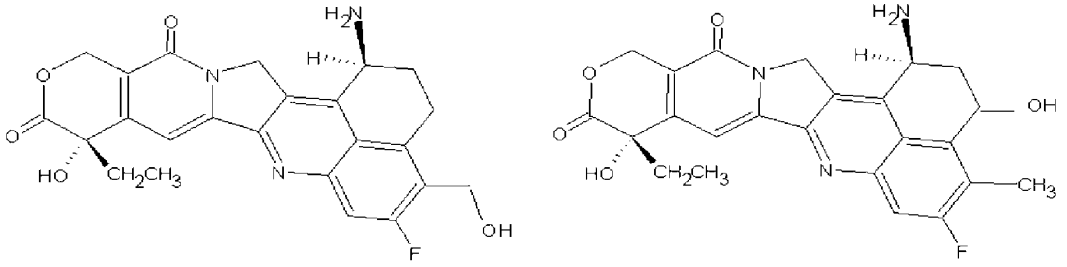


Fig. 2. Structures of the principal metabolites of exatecan 3-hydroxy metabolite (UM-1) (left) and a 3-hydroxy metabolite (UM-2) (right).

(neutropenia, thrombocytopenia, anemia, lymphopenia), gastrointestinal (vomiting diarrhea), lymph nodes, and reproductive tissues, have been most prone to the toxic effects of exatecan, and noncumulative myelosuppression, particularly neutropenia, was been the principal dose-limiting effect of exatecan on both single- and divided-dosing regimens in both rodents and dogs. In addition to being dose-dependent, hematologic toxicity appeared schedule-dependent, with more frequent (divided) dosing schedules associated with greater toxicity at equivalent doses. Similar to other CPT analogs, there has been considerable interspecies differences in drug tolerance, with dogs being more susceptible to toxicity than rodents. Therefore, the human equivalent of one-third of the low toxic dose in dogs was used to determine the starting dose for each corresponding schedule of administration in human clinical trials.

6. PHASE I DEVELOPMENT IN PATIENTS WITH ADVANCED MALIGNANCIES

6.1. Overall Clinical Scheme

The safety, dosing limits, and pharmacokinetics of multiple exatecan administration schedules were evaluated in phase I clinical evaluations according to a parallel and integrated development plan that linked studies in the United States, Europe, and Japan. The principal objective of this approach was to select an optimal dosing regimen for subsequent disease-directed clinical investigations. To achieve this goal, a core protocol was established to standardize clinical data evaluation including toxicity and efficacy criteria, definitions of unacceptable or dose-limiting toxicity (DLT) and maximum tolerated dose (MTD), inclusion and exclusion criteria, and supportive therapy paradigms. Another goal was to readily permit exchange of data in a timely manner among the three global regions so that all investigators had ready access to the data for decision making as dose escalation was in

progress. Data were collected and processed in compliance with the International Committee on Harmonization guidelines.

Six phase I studies were initially conducted outside of Japan according to three schedules of administration and two durations of iv infusion *(25,26,29–36)*. Two studies were duplicated in Japan; however, these studies were directed to evaluate the pharmacokinetics of the exatecan lactone and total exatecan *(29,31)*, whereas the other studies were limited to measurements of total exatecan because of logistical considerations regarding the analysis of the exatecan lactone.

For each study, the starting dose was chosen as one-third of the toxic dose low for the corresponding schedule in the dog, which was the most sensitive species. There was no standardization of the method of dose escalation, because both modified Fibonacci and modified continual reassessment methods were employed. Interestingly, there were no significant differences between the methods in the number of dose escalation steps required to delineate and recommend phase II doses. However, MTDs were determined separately for heavily pretreated (HP) and minimally pretreated (MP) patients because the extent of prior treatment appeared to be a major determinant for the severity of the neutropenia, which was the principal toxicity. The definitions of HP and MP patients were derived prospectively, largely based on the results of prior Phase I studies of other TOP-I-targeting agents and chemotherapeutics in which neutropenia was the principal DLT *(37–39)*. HP patients were defined as those who had received more than six courses of alkylating-agent containing chemotherapy (or more than four courses of carboplatin), radiation therapy to more than 25% of hematopoietic reserves, and two or more courses of mitomycin C or nitrosourea. All toxic effects were graded according to the National Cancer Institute Common Toxicity Criteria, version 1.0. DLT was defined as grade 4 neutropenia (absolute neutrophil count [ANC] <500/μL) associated with fever (≥38.4°C) or lasting longer than 5 days), any grade 3 nonhematologic toxicity (excluding nausea and vomiting), grade 4 vomiting with maximum supportive care, any grade 3 or higher event requiring intensive care treatment, or the inability to start a second course after a 2-week treatment delay because of toxicity. The MTD was defined as the highest dose at which no more than 20% of patients experienced DLT during the first course.

6.2. Overall Pharmacokinetic Scheme

Initial analytical assays to measure plasma and urinary concentrations of exatecan and metabolites used high-performance liquid chromatography, but more sensitive liquid chromatographic/mass spectrometry/mass spectrophotometry assays were subsequently derived and validated *(23–28)*. The pharmacokinetics of exatecan were determined in all phase I studies using standard noncompartmental and compartmental pharmacokinetic

methods. Compartmental analyses were performed to obtain more robust estimations of individual pharmacokinetic parameters. Initially, the individual data sets in each study were fit with either two- or three-compartment models using nonlinear least-squares regression *(40)*. The "goodness" of model fit (i.e. two- versus three-compartment model) was guided by inspection of the weighted sum of squares, dispersion of the residuals, standard errors of the fitted pharmacokinetic parameters, and the Akaike information criterion *(41)*. When the drug was administered on a 24-hour infusion schedule and concentrations were available for 24 hours posttreatment, the quality of the fit was as good using a two- or three-compartment model. Therefore, the two-compartment model was selected because of its simplicity. When exatecan was given as a 24-hour infusion and concentrations available for only 6 hours posttreatment, a single compartment model fit the data as well as the two- or three-compartment models, which is not surprising in view of the potential masking of the distribution phase by a 24-hour infusion schedule and the inability to adequately describe the terminal elimination phase because of the lack of plasma observations after 6 hours. In subjects treated with exatecan administered over 30 minutes and concentrations available for 24 hours posttreatment, a three-compartmental model was demonstrated to be systematically superior in fitting plasma concentrations based on the aforementioned criteria. Pharmacokinetic parameter estimates derived from these fits were then used as prior values for a population pharmacokinetic analysis, performed using an iterative two-stage methodology (IT2S) *(42–44)*. All concentrations were modeled using a weighting procedure of $Wj + 1/S_j^2$, where the variance of S_j^2 was calculated for each observation using the equation $S_j^2 = (a + b*Y)^2$, where a and b are the intercept and slope of each variance model. The slope is the residual variability associated with each concentration (i.e., sum of the intraindividual variability and the sum of all experimental errors), and the intercept is related to the limit of detection of the analytical assay. Variance parameter estimates were derived using maximum likelihood analysis (ADAPT-II Release 4; Biomedical Simulations Resource, University of Southern California, Los Angeles, CA) *(43)*. These estimates were used as beginning priors and were updated iteratively during the population pharmacokinetic analysis until a stable value was found *(43)*. The parameters derived were: the macro rate constants λ_1, λ_2, and λ_z associated with λ_1, λ_2, and λ_z (terminal) phases, respectively; λ_1–$t_{1/2}$, λ_2–$t_{1/2}$, λ_z–$t_{1/2}$, calculated as 0.693 divided by the respective macro constants; and V_{ss}, calculated as the sum of the central and peripheral volumes of distribution.

Urinary metabolites were detected using both high-performance liquid chromatography and liquid chromatographic/mass spectrometry/mass spectrophotometry methods and subsequently isolated, purified, and identified using nuclear magnetic resonance *(23,24,27)*. In the urine of rats and

humans, both UM-1 and UM-2 were identified. Mass balance studies in humans are to precisely determine the extent of metabolite formation and excretion are ongoing (C. Takimoto, personal communication, September 2003). Furthermore, Phase I and pharmacokinetic studies in patients with various grades of hepatic or renal dysfunction are also being performed (C. Takimoto, personal communication, September 2003).

6.3. Clinical Results

6.3.1. Toxicity

The principal toxicity of exatecan was similar for all schedules of administration *(25,26,29–36)*. Myelosuppression, particularly neutropenia, was the principal DLT of exatecan. In HP patients, both neutropenia and thrombocytopenia were dose-limiting. On the daily × 5 every 3-week schedule, the ANC nadir was typically experienced between days 10 and 15, treatment delays resulting from unresolved neutropenia were uncommon, and there was no evidence of a cumulative effect of exatecan on the ANC nadirs in both MP and HP patients *(32)*. However, the relationship between exatecan dose and effect on neutrophils was steep in the dosing range evaluated. The steepness of this relationship is illustrated in Fig. 3, which shows that the percent decrements in ANC sharply increased to nearly 100% as the dose of exatecan was increased above 0.4 mg/m^2/day *(32)*. Severe thrombocytopenia and anemia occurred much less frequently than neutropenia, and were usually noted concomitant with severe neutropenia. These effects were also more severe in HP patients. Anemia related to exatecan was generally mild (grade 1) or moderate (grade 2) and cumulative in that it tended to progressively worsen with repetitive dosing.

Nonhematologics; effects consisted primarily of mild to moderate gastrointestinal toxicity. Nausea and vomiting were typically mild or moderate in severity, generally noted in the peritreatment period, and appeared to be dose-related. Nausea and vomiting were generally prevented or managed successfully with prochlorperazine or serotonin 5-hydroxytryptophan receptor antagonists, but routine premedication was not instituted because most events were nausea alone, mild in severity, and sporadic. Delayed emesis was not common. Mild to moderate diarrhea was also noted in patients, most of whom had been previously treated with fluoropyrimidine- or irinotecan-based regimens. Transient and reversible elevations of serum transaminases or alkaline phosphatase were also observed infrequently, and acute pancreatitis occurred in two patients (approximately 1%) in phase I trials. Alopecia that was dose-related, typically mild, and generally cumulative was also noted. Other toxicities included stomatitis, malaise, headache, anorexia, or alkaline phosphatase, altered taste sensation, and dizziness. These effects were noted across the entire exatecan dosing range and definite temporal

OnCusp
Ex. 1002

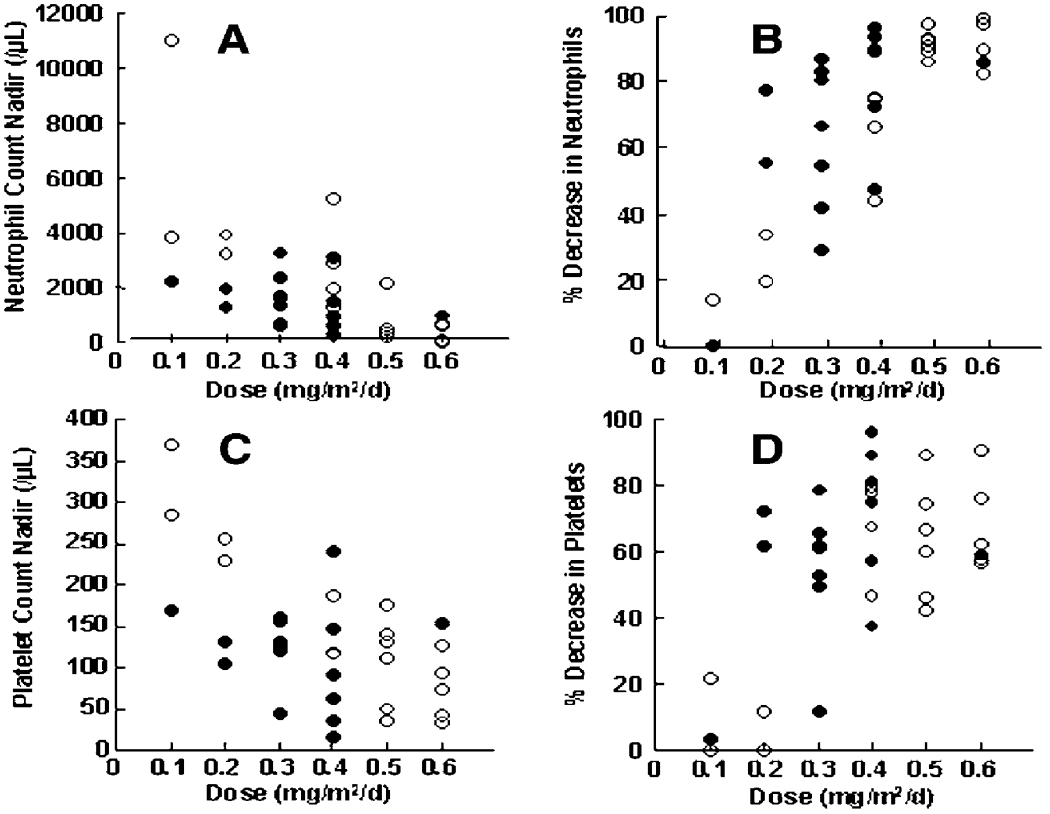


Fig. 3. Scatterplots depicting the effects of the dose of exatecan on **(A)** absolute neutrophil count (ANC) nadirs; **(B)** percentage change in the ANC; **(C)** platelet count nadirs; and **(D)** percentage change in platelet counts. The extent of prior treatment is also indicated. (●) heavily pretreated; (○) minimally pretreated.

relationships could not be discerned for any of these potential toxicities, indicating that the underlying malignant process may have contributed.

6.3.2. Maximum Tolerated Dose

The MTD and lowest doses associated with consistently intolerable toxicity (>MTD) are listed in Table 4. MP patients tolerated higher doses of exatecan than HP patients except for the single-dose, every-3-week regimen for which a single MTD was determined for HP and MP patients alike. However, this study involved only 12 patients, and the MTD was close to the starting dose. The MTDs for exatecan administered as a 30-minute iv infusion daily × 5 every 3 weeks were 0.5 and 0.3 mg/m^2/day for MP and HP patients, respectively. Representative concentration versus time curves are shown in Fig. 4. The number of dose escalation steps in each study

Table 4
Pertinent Single-Agent Phase I Clinical Trials of Exatecan

Administration schedule	*Site (reference)*	*No. of patients*	*Prior treatment*	*MTD ($mg/m^2/day$)*	*>MTD ($mg/m^2/day$)*	*Principal DLT*	*Other toxicities*
30 minutes (day 1) every 3 weeks	IGR, France *(30)*	12	MP/HP	5.33	7.1	ANC	Nausea, vomiting, fever, alopecia, asthenia, anemia
	NCCE, Japan *(29)*	15	MP/HP	NR	NR	ANC	PLT
30 minutes daily × 5 every 3 weeks	IDD, USA *(32)*	36	MP	0.5	0.6	ANC	Nausea, vomiting, diarrhea, liver finctions, anemia
			HP	0.3	0.4	ANC, PLTs	
	NCH, Japan *(29)*	28	NR	0.4	0.45	ANC, PLTs	Nausea, vomiting, diarrhea, malaise
24-hour CI every 3 weeks	MDA (USA) *(33)*	22	MP	2.4	3.0	ANC	PLTs, anemia,
			HP	<2.4	3.0	ANC	nausea, vomiting, diarrhea
24-hour weekly × 3 every 4 weeks	MSKCC (USA) *(34)*	27	MP	1.0	1.2	ANC, PLTs	Nausea, vomiting, diarrhea, anorexia, asthenia, fever,
			HP	<0.8	0.8	ANC, PLTs	stomatitis, alopecia, pancreatitis (with lipase elevation)
30 minutes weekly × every 4 weeks	Oxford/Vrije (UK/Holland) *(35)*	35	MP	2.75	3.13	ANC	Diarrhea, alopecia, mucositis
			HP	2.06	2.35	ANC	
5- to 21-day CI every 4 weeks	IDD (USA) *(36)*	31	MP	0.15	0.23	ANC	Anemia, PLTs
			HP	0.15	0.23	ANC, PLTs	

ANC, absolute neutrophil pointl CI, continuous infusion; HP, heavily pretreated; IDD, Institute for Drug Development; IGR, Institute for Gustave Roussy; MDA, M. D. Anderson Cancer Center; MP, minimally pretreated; NCCE, National Cancer Institute East; NR, noot reported; PLTS, platelets.

OnCusp
Ex. 1002

OnCusp
Ex. 1002

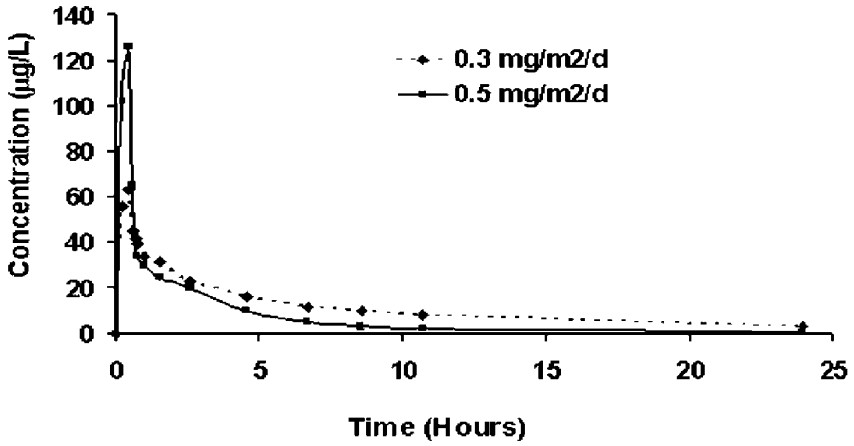


Fig. 4. Representative plasma total exatecan concentration-time profiles (day 1) in patients treated with DX-8951f at the 0.3 mg/m^2/day (◆) and 0.5 mg/m^2/day (■) dose levels.

reflected the MTD/starting dose ratios and was not related to the type of dose escalation scheme used. It was not possible to evaluate the impact of the modified continual reassessment method in these studies because of the small number of patients and early intervention of investigators in modifying the dose levels assigned by the modified continual reassessment scheme at toxic dose levels.

In a comparison of exatecan clinical and preclinical toxicokinetics, MTD/toxic dose low (TDL) ratio were similar (dog [2.0] and man [1.5–3.1]) *(45)*. On the other hand, human toxicokinetics appeared to be schedule-independent, whereas toxicokinetics in dogs were schedule-dependent, which might be explained by differences in metabolic rates between species.

6.3.3. Antitumor Activity

Major antineoplastic activity was observed in patients with several types of solid neoplasms in phase I investigations *(25,26,29–36)*. Partial responses (≥ 50% reduction in the sum of the bidimensional products of measurable tumors) were reported in previously treated patients with non–small-cell lung, extrapulmonary small cell, colorectal, and hepatocellular carcinomas and sarcoma. Disease stabilization, including minor responses (<50% reduction in the sum of the bidimensional products of measurable disease) was observed in patients with colorectal carcinoma, hepatocellular carcinoma, prostate carcinoma, and carcinoma of unknown primary type involving the peritoneum. Interestingly, antitumor activity was noted in cancers that were previously demonstrated to be resistant to other TOP-I-targeting therapeutics such as irinotecan and topotecan *(25,26,29–36)*. The 30-minute iv infusion daily × 5 every 3 week, 30-minute iv infusion weekly × 3 every 4 week,

OnCusp
Ex. 1002

Table 5
Mean Pharmacokinetic Parameters in Phase I Evaluations of Exatecan

Pharmacokinetic parameter	*Pharmacokinetic analytical method*	
	Noncompartmental	*Population compartmental*
Clearance (L/hour/m^2)	1.87 (67%)	1.63 (64%)
Urinary excretion (%)	Not applicable	9.9 (60%)
Volume of distribution (central) (L/m^2)	Not applicable	6.4 (28.7%)
Volume of distribution (steady-state) (L/m^2)	17 (39%)	17.65 (28.9%)
Terminal half-life (hours)	9.1 (54%)	12.3 (60%)

Note: Represent mean value (coefficient of variation).

and the 5- to 21-day continuous iv infusion every 3–4 week regimens appeared to be associated with greater activity than the single-dose regimen or the 24-hour intermittent regimens, however, the phase I clinical trial is not the proper setting for generating comparative data regarding scheduling. There was no relationship between the number of patients demonstrating antitumor activity and the dose intensity of the regimens used in individual studies. The 30-minute daily × 5 every 3 week regimen, which appeared to be the most active in phase I evaluations, was selected as the principal regimen in phase II studies, whereas the corresponding MTDs for MP and HP patients, 0.3 and 0.5 mg/m^2/day, were selected as phase II doses.

6.3.4. Clinical Pharmacology

The pharmacokinetics of exatecan were dose-independent within the dose range evaluated in phase I evaluations, with pharmacokinetic indices of exposure (e.g., AUC, C_{max}) proportionate to dose *(25,26,29–36)*. Similarly, both clearance and V_{ss} were dose-independent. There was no evidence of drug accumulation in the plasma over from day 1 to day 5 in most patients treated with exatecan as a 30-minute iv infusion on the daily for 5 days schedule *(32)*. Table 5 displays the mean pharmacokinetic parameters of exatecan in phase I evaluations, and plasma concentration curves for total exatecan in representative patients treated with 30-minute iv infusions are shown in Fig. 5. Both total exatecan and its lactone form were measured only in the 30-minute single iv dose every 3 week study conducted in Japan *(29)*. The AUC of the lactone was approximately 30% of the AUC of total exatecan, and the plasma AUC of UM-1 was 4% of the total exatecan AUC. Twenty-five percent of the administered dose of exatecan was recovered in the urine, and there was a 2:1 ratio between the UM-1 metabolite and unmetabolized exatecan *(25,29,31)*.

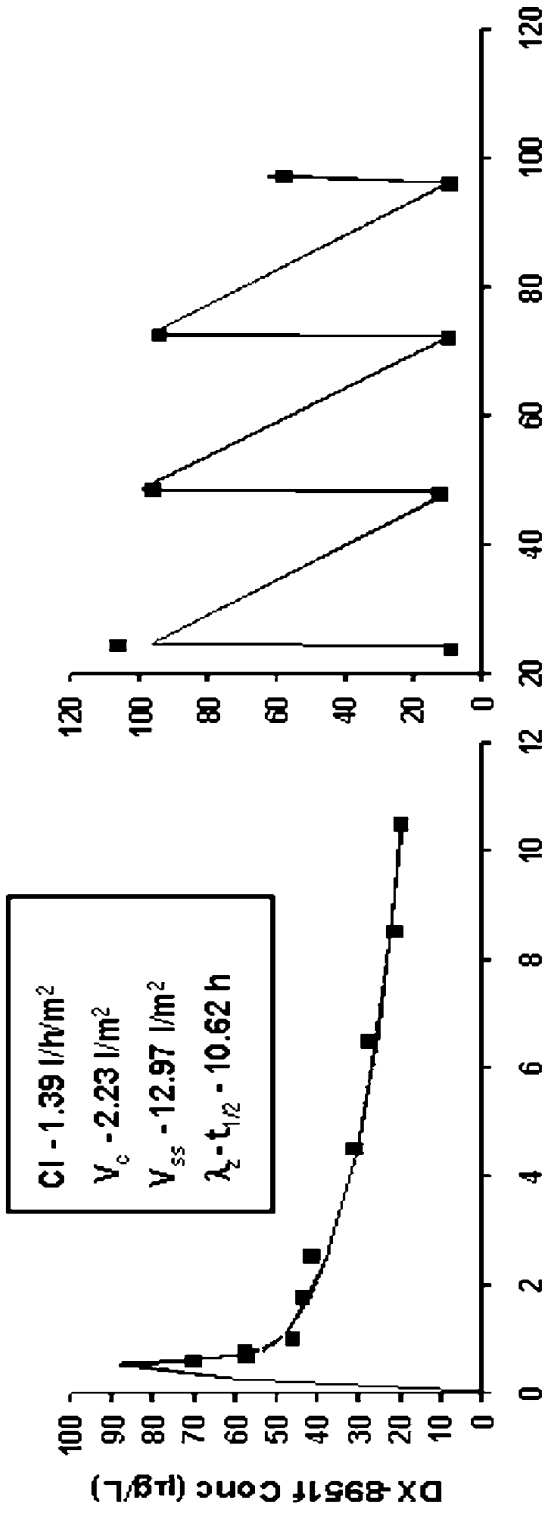


Fig. 5. Representative patient's plasma concentration data (■) fit to the population model using an IT2S approach. The patient was treated with exatecan at the 0.5 mg/m^2/day dose level. Pharmacokinetic parameter values derived from the population model are listed.

Because there was no evidence of nonlinear drug elimination, auto-induction, or inhibition of drug clearance based on visual inspection of individual plasma concentration-versus-time curves in the phase I studies, linear pharmacokinetic models were evaluated for quality of fit. The compartmental pharmacokinetic models developed in individual studies were very adequate in explaining the observed plasma concentrations and excreted urinary amounts of exatecan. In study PRT002, in which exatecan was administered as a 30-minute iv infusion on a daily × 5 every 3-week schedule, a two-compartment model consistently missed peak plasma concentrations and a three-compartment model was systematically superior in fitting all plasma concentration-time data sets for total exatecan on both days 1 and 5 *(25,32)*. Therefore, pharmacokinetic parameters derived from the triexponential model were used to develop a population pharmacokinetic model using an IT2S approach. A representative patient's plasma concentration data fit to this population model are shown in Fig. 5. Pertinent pharmacokinetic parameters for total exatecan derived from this model were nearly identical to those derived using noncompartmental methods, with mean (coefficient of variation) clearance, and terminal half-life values of 1.64 L/hour/m^2 *(57)* and 15.8 hours *(65)*, respectively. Mean values for the central and steady-state volumes of distribution, were 2.40 L/m^2 *(30)*, respectively *(25,32)*.

The relationships between the both the AUC and C_{max} values for total exatecan and the percentage decrements in neutrophils were consistently described by sigmoidal E_{max} models, as shown in Fig. 6A,B, which depicts scatterplots of individual data in study PRT002 and sigmoidal E_{max} models fitting the data *(32)*. With these models, the AUC and C_{max} values predicted to yield a 50% decrement in neutrophils (AUC_{50} and $C_{max\text{-}50}$) were 115 mg/hour/L and 31 mg/L, respectively. The relationships between pertinent pharmacokinetic parameters for total exatecan and platelet counts, as depicted in the scatterplots in Fig. 6C,D could be described adequately by neither linear nor nonlinear models. Within particular dose levels, pharmacokinetic parameters reflecting total exatecan exposure were generally greater in those patients who experienced dose-limiting myelosuppression during their first course, but the relatively small numbers of both dose-limiting events and patients at each dose level has limited the statistical power of such analyses. Such models may be very useful clinically as they may be able to predict which exatecan dosing regimens and doses would minimize decrements in blood cell counts.

7. DISEASE-DIRECTED (PHASE II–III) EVALUATIONS

Disease-directed evaluations of exatecan are currently being performed in both North America and Europe in patients with advanced carcinomas of the pancreas (first and second line), colon/rectum (second line, no prior CPT analog), ovary (relapsed after taxanes and platinum; no more than two prior

OnCusp
Ex. 1002

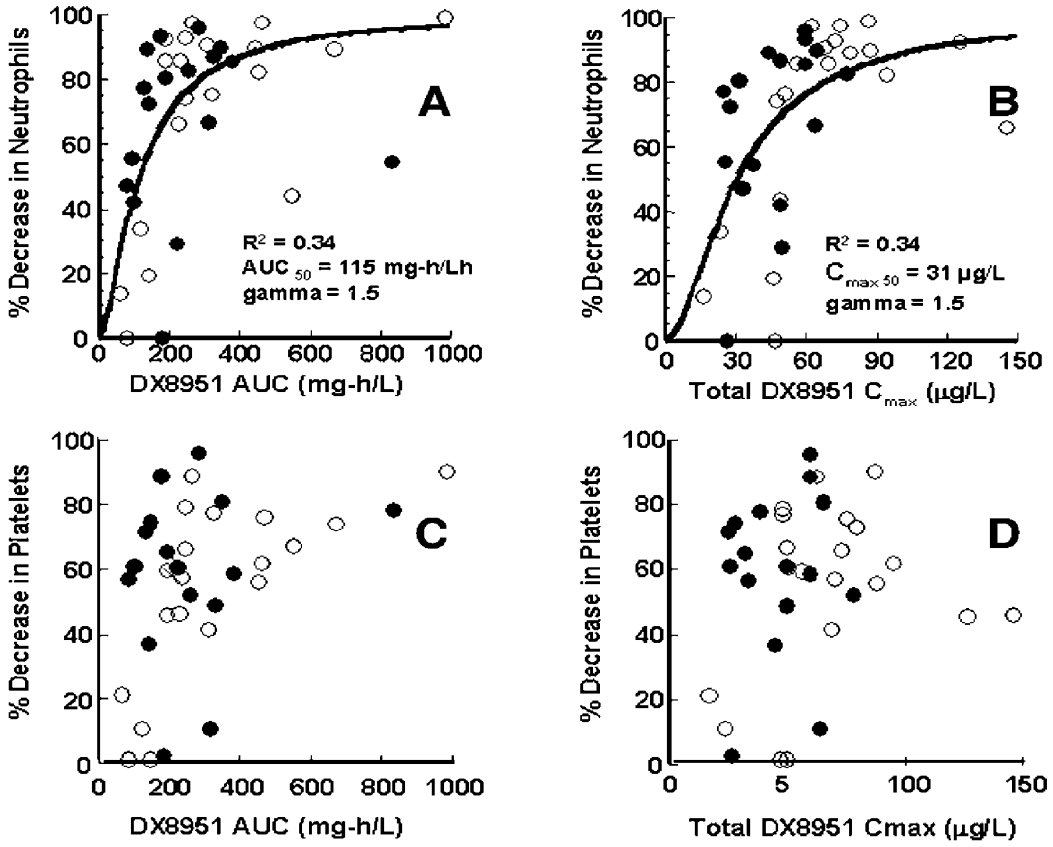


Fig. 6. Scatterplots depicting the relationships between percentage decrements in absolute neutrophil count during the first course of exatecan and total exatecan AUC **(A)** and C_{max} **(B)**, and between percentage decrements in platelets during the first course and AUC **(C)** and C_{max} **(D)**. The extent of prior treatment, as defined in the Patients and Methods section, is also indicated. (●) heavily pretreated; (?) minimally pretreated. The solid lines represent fits of sigmoidal E_{max} models to the data when appropriate.

regimens), uterine cervix (first or second line), lung (non-small cell; first line), liver (first or second line), biliary duct (first or second line), hormone-refractory prostate, head and neck (first line), and breast (relapsed after taxane and anthracycline; up to three prior regimens) *(25,46–56)*. In the majority of these trials, exatecan is being administered as a 30-minute iv infusion daily ×5 every 3 weeks. Starting doses for MP and HP patients have been 0.4–0.5 and 0.3 mg/m^2/day, respectively. To ascertain information about the relative activity of various schedules of exatecan, patients with advanced ovarian cancer are being randomized to treatment with exatecan administered iv over 30 minutes on either a daily ×5 every 3 week schedule

(starting dose, 0.3 mg/m^2/day) or weekly × 3 every 4 week schedule (starting dose, 2.1 mg/m^2/day) in a randomized phase II evaluation.

Perhaps the most intriguing and unique activity with exatecan to date has been noted in patients with advanced adenocarcinomas of the pancreas, biliary track, gallbladder, and liver *(49–53)*. At this juncture, the most advanced results are available from a Phase II study of exatecan in patients with advanced adenocarcinoma of the pancreas *(48–50)*. A single, multicenter trial of exatecan administered as a 30-minute infusion at a dose of 0.5 mg/m^2/day × 5 every 3 weeks was conducted in 39 patients with metastatic adenocarcinoma of the pancreas and a subset of 23 patients who had not received prior chemotherapy has been analyzed. Three patients (13%) had confirmed partial responses lasting 2.8, 4.3, and 10.1 months. The median survival time for the 23 previously untreated patients was 9.3 months. The 6-, 12-, and 24-month survival times were 70%, 39%, and 5%, respectively. Toxicity was primarily myelosuppression and fatigue. A phase I study of exatecan in combination with gemcitabine, conducted in patients with advanced solid malignancies, yielded phase II/III doses of exatecan of 2.0 mg/m^2 and gemcitabine 1000 mg/m^2 when both drugs were administered on a weekly × 3 every 3 week schedule *(51)*. The toxicity profile was similar to exatecan as a single-agent exatecan with the exception of apparently more severe thrombocytopenia. In the study, 7 of 31 patients with advanced pancreatic cancer who had received the regimen as additional therapy experienced major responses, including one complete and six partial responses. The median duration of response was 8 months and the median survival time was 8 months. The 6-, 12-, and 24-month survival times were 55%, 39%, and 19%, respectively. These results to two large-scale randomized trials in the North America and Europe, which have completed their accrual targets. In the North American study, a combination of exatecan and gemcitabine was compared with gemcitabine alone and in the European study, exatecan as a single-agent was compared with gemcitabine alone *(60,61)*. However, preliminary results from both studies indicate that no survival benefits were conferred.

A multicenter phase II study of exatecan 0.5 mg/m^2/day × 5 every 3 weeks has also been conducted in patients with advanced biliary and gallbladder carcinomas who received a maximum of one prior chemotherapy regimen *(52)*. Of 41 patients able to be evaluated for efficacy, 21 (50%) of whom had had prior chemotherapy, 2 (4.9%) had partial responses, 4 (9.8%) had minor responses, and 12 (29.3%) had stable disease as their best response. The median overall survival was 7.8 months and the 6- and 12-month survival rates were 61% and 32%, which will serve as the foundation for future combination studies in biliary and gallbladder carcinomas. In a phase II study involving 43 patients with hepatocellular carcinoma who had received a maximum of one prior chemotherapy regimen, exatecan was

administered at a dose of 0.5 mg/m^2/day × 5 every 3 weeks *(53)*. Two patients had partial responses, whereas 6 had minor responses, and 14 had stable disease as their best response. The median time to progression was 3.3 months and median survival time was 7.4 months, with respective 6- and 12-month survival rates of 61% and 35%. Despite its modest activity as a single-agent activity, it was felt that the results provided a sufficient foundation for the development of relatively nontoxic exatecan-based multiagent regimens for hepatocellular carcinoma.

Exatecan administered as a 30-minute iv infusion at a dose of 0.5 mg/m^2/day × 5 every 3 weeks demonstrated no significant activity in a phase II study in patients with metastatic colorectal cancer who had received no prior treatment with CPT derivatives *(48)*. Similarly, negligible activity has been reported with exatecan 0.5 mg/m^2/day for 5 days every 3 weeks in previously untreated patients with advanced non–small-cell lung cancer (54). The major response rate was 5.1% and median times to progression and survival were 88 and 262 days, respectively. Moderate activity was observed in patients with advanced breast cancer who had experienced resistance or progressive disease after chemotherapy that included anthracyclines and taxanes *(55)*. Of 39 patients able to be evaluated, 3 (7.7%) experienced partial responses and 20 (51.3% had either a minor response or stable disease. Approximately 20% of patients had stable disease for at least 6 months. To characterize the activity of exatecan in patients with advanced ovarian cancer who were either refractory to or relapsed after both platinum agents and taxanes, patients were randomized to one of two dosing schedules: (Arm A) daily × 5 every 3 weeks, starting dose 0.3 mg/m^2/day, or (Arm B) weekly × 3 every 4 weeks, starting dose 2.1 mg/m^2 weekly *(47)*. In a preliminary report involving 47 patients (Arm A, $n = 31$; and arm B, $n = 16$) and including 23 patients who were able to be evaluated for response, two patients (both on Arm A) had partial responses and five subjects had stable disease as their best response. In a study of exatecan 0.5 mg/m^2/day × 5 every 3 weeks in previously untreated patients with non-small-cell lung cancer, partial responses were reported in 3 (18%) of 16 of patients who were able to be evaluated for response and 5 patients had stable disease as their best response *(51)*. Many other disease-directed studies in a wide array of adult solid malignancies are ongoing.

The potential utility of exatecan in pediatric malignancies is also being studied, beginning with a phase I study of exatecan as a 30-minute iv infusion daily × 5 every 3 weeks in pediatric patients with solid malignancies (starting dose, 0.25 mg/m^2/day). Furthermore, evaluations of exatecan in adult acute leukemias are also under way *(56)*. In a phase I study, doses of exatecan were escalated from 0.6 to 1.35 mg/m^2/day as a 30-minutes iv infusion daily × 5 every 3 weeks. Severe stomatitis was consistently noted at the 1.35 mg/m^2/day dose level. On the 30-minute infusion daily × 5

schedule, the 1.2 mg/m^2/day dose level appears tolerable, and increasing the duration of treatment from 5 to 7 days at the 0.9 mg/m^2/day dose level has not been associated with prohibitive toxicity. Antileukemic activity, primarily reductions in circulating blasts and bone marrow cellularity, has also been consistently noted across all dose levels in HP patients.

8. DE-310, A MACROMOLECULAR CARRIER OF DX-8951

DE-310 is a novel drug construct consisting of exatecan linked to a biodegradable carrier, carboxymethyldextran poly alcohol, via a peptide spacer. This macromolecular polymer drug deliver system was designed to enhance the antitumor efficacy of exatecan. The slow release of exatecan from the carrier in the tumor provides for a sustained level of localized active agent. The relatively greater acidic environment of malignant neoplasms compared with normal tissues may hypothetically favor the presence of the active lactone species in malignant neoplasms, potentially resulting in greater specificity. The supporting rationale for the development of DE-310 is that the molecule will accumulate and be retained preferentially in tumor tissue by the enhanced permeability and retention effect. The enhanced permeability into tumor tissue is due to leaky vascular architecture of the tumor blood vessels and pathophysiological mediators such as cytokines or vascular permeability factors. The retention effect is based on the lack of effective lymphatic clearance of macromolecules in tumor tissue. Thus macromolecules such as DE-310 may readily leak into tumor tissue through more permeable tumor blood vessels and may be retained in tumor tissue for a longer period. DE-310 is designed for iv administration. The macromolecular carrier used in the drug gradually depolymerizes within the body to be excreted in the urine. The peptide spacer serves as the DE-310 enzymatic cleavage site to give a low and sustained release of exatecan into tumor tissue, without prematurely releasing the drug into the systemic circulation. As a result, the number of required dosages may be reduced significantly when compared with other CPT derivatives in current use. Two phase I and pharmacokinetic studies of DE-310 administered as a single short infusion every 4 or 6 weeks have recently begun *(5,57)*. DLT on both schedules appear to be late myelosuppression, and transaminitis has been observed at doses above the MTD (6 and 7.5 mg/m^2 in HP and MP patients, respectively). Both conjugated exatecan and free exatecan concentrations increased linearly with dose and plasma drug concentrations were sustained for several weeks. The pharmacokinetic results from both studies were similar. In the every-4-week study, the mean (CV%) C_{max} for DE-310 in the form of conjugated exatecan was 4120 (21.2) ng/mL and the apparent terminal plasma half-life ($t_{1/2}$) was 208.8 (78.9) hours. The C_{max} of free exatecan was 5.8 (53.4) ng/mL and the $t_{1/2}$ was 175.1 (9.0) hours.

OnCusp
Ex. 1002

9. CONCLUSION

Exatecan was developed to exploit physicochemical properties that may result in superior antitumor activity, less toxicity and interindividual variability, and greater clinical feasibility than TOP-I–targeting agents in current clinical use. The agent was specifically selected for clinical development because of its relatively high potency and impressive activity against a broad range of human tumor cell lines and xenografts, including malignancies resistant to other CPT analogs and other classes of anticancer agents. Furthermore, unlike topotecan, 9-aminocamptothecin, and SN-38, exatecan is not a substrate for multidrug transporter Pgp, and retains activity against both tumor cell lines and xenografts with acquired multidrug resistance conferred by Pgp overexpression. Another hypothetical advantage of exatecan is that it is an intrinsically active compound and not a prodrug, which reduces concerns about interindividual variability in prodrug activation that could increase the fundamentally large interindividual variability in the toxicologic, pharmacokinetic, and antitumor profiles of the CPT analogs. Although schedule-dependence was not as prominent with exatecan in preclinical studies as with other CPT analogs, the cumulative results of these investigations indicate that maximal antitumor activity is achieved with divided dosing schedules, and these observations have served, in part, as the rationale for broad disease-directed evaluation of exatecan on a 30-minute infusion daily × 5 every 3 week schedule. In addition, exatecan demonstrated a safe and predictable toxicity profile when administered on the daily × 5 schedule, with manageable neutropenia being the principal DLT. Thrombocytopenia and anemia may be associated with neutropenia, particularly in HP patients treated at doses that approach the MTD. Nonhematologic toxicity has been less frequent and generally moderate. Exatecan also demonstrated dose-independent and predictable pharmacokinetics in the dose range evaluated and antitumor activity was consistently observed, including that against tumors that had been previously treated with topotecan or irinotecan. Although the ultimate clinical activity of exatecan will be defined only in appropriate phase II/III trials, exatecan's specific pattern of myelotoxicity, its relative paucity of nonhematologic toxicity, and its activity against a several types of neoplasms in early clinical evaluations, warranted broad disease-directed evaluations of exatecan on this administration schedule, which are nearing completion, as well as further developmental evaluations of DE-310, particularly in exatecan-sensitive tumor types, to maximize activity and optimize the therapeutic index.

REFERENCES

1. Mitsui I, Kumazawa E, Hirota Y, et al. 1995 A new water-soluble camptothecin derivative, DX-8951f, exhibits potent antitumor activity against human tumors in vitro and in vivo. Jpn J Cancer Res 86:776–782.

2. Okamoto R, Park JS, Hanaoka H, Nishiyama M. 1999 DX-8951f, a novel camptothecin derivative: critical determinants of the action and synergistic combination against gastrointestinal cancer cells [abstract]. Proc Am Assoc Cancer Res 40:712.
3. Lawrence RA, Izbicka E, DeJager R, et al. 1999 Comparison of DX-8951f and topotecan effects on tumor colony formation from freshly explanted adult and pediatric human tumor cells. Anti-Cancer Drugs 10:655–661.
4. Kumazawa E, Jimbo T, Ochi Y, Tohgo A. 1998 Potent and broad antitumor effects of DX-8951f, a water-soluble camptothecin derivative, against various human tumors xenografted in nude mice. Cancer Chemother Pharmacol 42:210–220.
5. Kumazawa E, Tohgo A. 1998 Antitumor activity of DX-8951f: a new camptothecin derivative. Exp Opin Invest Drugs 7:625–632.
6. Gonzales P, Marty J, Stringer SD, et al. 2000 In vivo antitumor activity of DX-8951f against an intracranial sarcoma tumor model [abstract]. Proc Am Assoc Cancer Res 41:1349.
7. Takiguchi S, Kumazawa E, Shimazoe T, Tohgo A, Kono A. 1997 Antitumor effect of DX-8951, a novel campotothecin analog, on human pancreatic tumor cells and their CPT-11-resistant variants cultured in vitro and xenografted into nude mice. Jpn J Cancer Res 88:760–769.
8. Joto N, Ishii M, Minami M, et al. 1997 DX-8951f, a water-soluble camptothecin analog, exhibits potent antitumor activity against a human lung cancer cell line and its SN-38-resistant variant. Int J Cancer 72:680–686.
9. Nomoto T, Nishio K, Ishidia T, Mori M, Saijo N. 1998 Characterization of a human small-cell lung cancer cell line resistant to a new water-soluble camptothecin derivative, DX-8951f. Jpn J Cancer Res 89:1179–1186.
10. Weitman S, DeJager R, Marty J, et al. 1999 Preclinical evaluation of DX-8951f against pediatric solid tumors [abstract]. Proc Am Soc Clin Oncol 18:762.
11. Vey N, Giles FJ, Kantarjian H, et al. 2000 The topoisomerase I inhibitor DX-8951f is active in a severe combined immunodeficient mouse model of human acute myelogenous leukemia. Clin Cancer Res 6:731–736.
12. Sun FX, Tohgo A, Bouvet M, et al. 2003 Efficacy of camptothecin analog DX8951f (exatecan mesylate) human pancreatic cancer in an orthotopic metastatic model. Cancer Res 63:80–85.
13. Hendricks CB, Rowinsky EK, Grochow LB, et al. 1992 Effect of P-glycoprotein expression on the accumulation and cytotoxicity of topotecan (SK &F 104864), a new campothecin analogue. Cancer Res 52:2268–2278.
14. Chen AY, Yu C, Potmesil M, et al. 1991 Camptothecin overcomes MDR1-mediated resistance in human KB carcinoma cells. Cancer Res 51:6039–6044.
15. Tsuruo T, Matsuzaki T, Matsushita M, et al. 1988 Antitumor effect of CPT-11, a new derivative of camptothecin, against pleotropic drug resistant tumors in vitro and in vivo. Cancer Chemother Pharmacol 21:71–74.
16. Mattern MR, Hofmann GA, Polsky RM, et al. 1993 In vitro and in vivo effects of clinically important camptothecin analogues in multi-drug resistant cells. Oncol Res 5:467–474.
17. van Hattum AH, Hoogsteen IJ, Schluper HM, et al. 2002 Induction of breast cancer resistance protein by the camptothecin derivative DX-8951f is associated with minor reduction of antitumour activity. Br J Cancer 87;665–672.
18. Ishii M, Iwahana M, Mitsui I, et al. 2000 Growth inhibitory effect of a new camptothecin analog, DX-8951 on various drug resistant sublines including BCRP-mediated camptothecin derative-resistant variants derived from the human lung cancer cell line PC-6. Anticancer Drugs 11:353–362.

19. van Hattum AH, Pinedo HM, Schluper HM, Erkelens CA, Tohgo A, Bov E. 2002 The activity profile of the hexacyclic camptothecin derivative DX-8951f in experimental human colon cancer and ovarian cancer. Biochem Pharm 64:1267–1277.
20. Liu L, Desai S, Sun M, et al. 2000 Mechanism of action of topoisomerase I and its inhibitors. Ann NY Acad Sci 922:1–10.
21. Okamoto R, Takano H, Okamura T, et al. 2002 O(6)-methylguanine-DNA methyltransferase (MGMT) as a determinant of resistance to camptothecan derivatives. Jpn J Cancer Res 93:93–102.
22. Daiichi Pharmaceutical Corporation. DX-8951f for injection. Investigators Brochure. Edition No. 2. Fort Lee, New Jersey, 1998.
23. Oguma T, Ohshima Y, Nakaoka M. 2000 Sensitive and high-performance liquid chromatographic method for the determination of the lactone plus hydroxy forms of the new camptothecin derivative DX-8951 in human plasma using fluorescence detection. J Chromatogr B Biomed Sci Appl 740:237–245.
24. Oguma T, Konno T, Inaba A, Nakaoka M. 2001 Validation study of assay method for DX-8951 and its metabolite in human plasma and urine by high-performance liquid chromatography/atmospheric pressure chemical ionization tandem mass spectrometry. Biomed Chromatogr 2:108–115.
25. DeJager R, Cheverton P, Tamanoi K, et al. 2000 DX-8951f: summary of phase I clinical trials. Ann NY Acad Sci 922:260–273.
26. Verschraegen CF, Royce M, Hammond L, Rowinsky EK. 2000 Exatecan. Curr Opin End Met Invest Drugs 2:1631–1638.
27. Oguma T, Konno T, Inaba A, Nakaoka M. 2001 Validation study of assay method for DX-8951 and its metabolite in human plasma and urine by high-performance liquid chromatography/atmospheric pressure chemical ionization tandem mass spectrometry. Biomed Chromatogr 15:108–115.
28. Oguma T, Yamada M, Konno T, Inukai K, Nakaoka M. 2001 High-performance liquid chromatographic analysis of lactone, an hydroxy acid of new antitumor drug, DX-8951 (exatecan), in mouse plasma. Biol Pharm Bull 24:176–180.
29. Minami H, Fujii H, Igarashi T, et al. 2001 Phase I study and clinical pharmacology of DX-8951f, a new camptothecin derivative, infused over 30 minutes every three weeks [abstract]. Clin Cancer Res 7:3056–3064.
30. Boige V, Raymond E, Faivre S, et al. 2000 Phase I and pharmacokinetic study of the camptothecin analog DX-8951f administered as a 30-minute infusion every 3 weeks in patients with advanced cancer. J Clin Oncol 18:3986–3992.
31. Kamiya Y, Yamamoto N, Yamada Y, et al. 1999 Phase I and pharmacokinetic (PK) study of DX-8951f, a novel camptothecin analog, given as a 30 minute infusion daily x 5 days [abstract]. AACR NCI EORTC Mol Targets Cancer Ther Suppl A:327.
32. Rowinsky EK, Johnson TR, Geyer CE Jr, et al. 2000 DX-8951f , a hexacyclic camptothecin analog, on a daily-times-five schedule: a phase I and pharmacokinetic study in patients with advanced solid malignancies. J Clin Oncol 18:3151–3163.
33. Royce ME, Hoff PM, Dumas P, et al. 2001 Phase I and pharmacokinetic study of exetacan mesylate (DX-8951f): a novel campothecin analog. J Clin Oncol 19:1493–1500.
34. Sharma S, Kemeny N, Schwartz GK, et al. 2001 A phase I study of topoisomerase I inhibitor exatecan mesylate (DX-8951f) given as weekly 24-hour continuous infusions three of every four weeks. Clin Cancer Res 7:3963–3970.
35. Braybrooke JP, Boven E, Bates NP, et al. 2003 Phase I and pharmacokinetic study of the topoisomerase I inhibitor, exatecan mesylate (DX-8951f), using a weekly

30-minute intravenous infusion, in patients with advanced solid malignancies. Ann Oncol 14;913–921.
36. Garrison MA, Hammond LA, Geyer CE, et al. 2003 A phase I and pharmokinetic study of the hexacyclic camptothecin analog exatecan mesylate (DX-8951F) administered as a protracted infusion in patients with advanced solid malignancies. Clin Cancer Res 9:2527–2537.
37. Rowinsky EK, Grochow LB, Sartorius SE, et al. 1996 Phase I and pharmacologic study of high doses of the topoisomerase I inhibitor topotecan with granulocyte colony-stimulating factor in patients with solid tumors. J Clin Oncol 14:1224–1235.
38. Rowinsky EK, Kaufman SH, Baker SD, et al. 1996 Sequences of topotecan and cisplatin: phase I, pharmacologic, and in vitro studies to examine sequence dependence. J Clin Oncol 14:3074–3084.
39. Rowinsky E, Grochow L, Hendricks C, et al. 1992 Phase I and pharmacologic study of topotecan : a novel topoisomerase I inhibitor. J Clin Oncol 10:647–656.
40. Metzler CM. 1987 Extended least squares (ELS) for pharmacokinetic models. J Pharm Sci 76:565–571.
41. Yamaoka K, Nakagawa T, Uno T. 1978 Application of Akaike's information criterion (AIC) in the evaluation of linear pharmacokinetic equations. J Pharmacokinet Biopharm 6:165–175.
42. Lalonde RL. Pharmacodynamics. In: Applied pharmacokinetics: principles of therapeutic drug monitoring. 3rd ed. Evans WE, Schentag JJ, Jusko WJ, eds. Applied Therapeutics, Washington, 1992, 4-1–4-33.
43. D'Argenio DZ, Schumitzky A. ADAPT-II users manual. Biomedical Simulation Resource, University of Southern California, 1997.
44. Collins DG, Forrest A. IT2s user's guide. State University of New York Buffalo, 1995.
45. Jager RD, Oguma T, Kajimura T, et al. 1999 Comparison of DX8951f clinical and preclinical toxicokinetics (TK) [abstract]. Proc Am Soc Clin Oncol 18:178A.
46. Kudelka A, Verschraegen CF, Vincent M, et al. 2000 Phase II study of intravenous DX-8951f in patients (Pts) with advanced ovarian, tubal, or peritoneal cancer refractory to platinum, taxane, and topotecan [abstract]. Proc Am Soc Clin Oncol 19:392A.
47. Calvert P, Jayson G, Atkinson R, et al. 2000 Phase II clinical and pharmacokinetic study of exatecan mesylate (DX-8951f) in patients with advanced ovarian cancer, refractory to, or relapsed after platinum and taxane [abstract]. Ann Oncol 11(Suppl. 4):84.
48. Royce, M, Saltz L, Rowinsky E, et al. 2003 A phase II study of intravenous exatecan mesylate (DX-8951f) administered daily for five days every three weeks to patients with advanced or metastatic adenocarcinoma of the colon or rectum. Invest. New Drugs. 22:53–61.
49. D'Adamo D, Hammond L, Donehower R, et al. 2001 Final results of a phase II study of DX-8951f (exatecan mesylate, DX) in advanced pancreatic cancer [abstract] Proc Am Soc Clin Oncol 37:134a.
50. O'Reilly EM, Hammond L, Sharma S, et al. 2000 A phase II study of exetecan mesylate (DX-8951f, DX) in advanced pancreatic cancer [abstract]. Proc Am Soc Clin Oncol 19:299a.
51. Talbot DC, White S, Jones P, et al. 2000 Phase II study of exatecan mesylate (DX-8951f) in advanced NSCLC [abstract]. Proc Am Soc Clin Oncol 19:549a.

52. O'Reilly EM, Lenzi R, Mani S, et al. 2002 Phase I study of DX-8951f (exatecan mesylate, DX) and gemcitabine (gem) in advanced solid malignancies [abstract]. Proc Am Soc Clin Oncol 21:99A.
53. Abou-Alfa GL, O'Reilly EM, Rowinsky EK, et al. 2002 Final results of a phase II study of DX-8951f (DX, exatecan mesylate) in biliary tree cancers. Proc Am Soc Clin Oncol 21:561.
54. Patt YZ, Rowinsky E, O'Reilly E, et al. 2002 Phase II trial of DX-8951f (exatecan mesylate) in hepatocellular carcinoma (HCC): a final analysis [abstract]. Proc Am Soc Clin Oncol 21:139a..
55. Braybrooke JP, Ranson M, Manegold C, et al. 2003 Phase II study of exatecan mesylate (DX-8951f) as first-line therapy for advanced non-small cell lung cancer. Lung Cancer 41:215–219.
56. Eteva FJ, Rivera E, Cristofanilli M, et al. 2003 A phase II study of intravenous exatecan mesylate (DX-8951f) administered daily for 5 days every 3 weeks to patients with metastatic breast cancer. Cancer 98:900–907.
57. Giles FJ, Cortes JE, Thomas DA, et al. 2002 Phase I and pharmacokinetic study of DX-8951f (exatecan mesylate), a hexacyclic campothecin, on a daily-time-five schedule in patients with advanced leukemia. Clin Cancer Res 8:2134–2141.
58. Takimoto CHM, Forero L, Schwartz GH, et al. 2003 A phase I and pharmacokinetic study of DE-310 administered as a 3 hour infusion every 4 weeks (wks) to patients (pts) with advanced solid tumors or lymphomas [abstract]. Proc Am Soc Clin Oncol 22:130.
59. De Jonge M, Sparreboom, A, De Bruijn P, et al. 2003 Phase I and PK study of DE-310 (D) given once every 2 or 6 wks (w) in pts with solid tumors [abstract]. Proc Am Soc Clin Oncol 22:130.
60. Cheverton P, Friess H, Andras C, et al. 2004 Phase III results of exatecan (DX-8951f) versus gemcitabine (Gem) in chemotherapy-naive patients with advanced pancreatic cancer (APC). Proc Am Soc Clin Oncol 23:314s.
61. O'Reilly EM, Abou-Alfa GK, Letourneau R, et al. 2004 A randomized phase III trial of DX-8951f (exatecan mesylate; DX) and gemcitabine (GEM) vs. gemcitabine alone in advanced pancreatic cancer (APC). Proc Am Soc Clin Oncol 23:315s.

Your reference: **SHU/PD20-9009RU**
Our reference: **2403-532821RU**
Application No.: **2016143351**
Attorney Name: **Elena Nazina**

GORODISSKY

TRANSLATION

OFFICIAL ACTION

(21) Application number **2016143351/04**(**069410**)

(22) Date of filing the application **10 April 2015**

(86) PCT Application number and date **JP2015/002020** of **10 April 2015**

(71) Applicant(s) **DAIICHI SANKYO COMPANY, LIMITED, JP**

DAIICHI SANKYO EUROPE GmbH, DE

(51) IPC

A61K47/64 (2017.01) ***A61K39/395*** (2006.01)

A61K31/535 (2006.01) ***C07K16/28*** (2006.01)

A61P35/00 (2006.01)

QUESTIONS, ARGUMENTS, OBJECTIONS, PROPOSALS

Having considered the application materials, the Examiner determined that a request for supplementary materials is necessary in accordance with cl.143 of the Administrative Regulations, due to the presence of obstacles to the making positive decision.

The Applicant requests to consider the said application with 10.04.2015 date of filing and with priority according to the original application JP 2014-081454 from 10.04.2014.

A set of claims, an invention description and invention drawings submitted as of the date of filing the application have been considered.

What is claimed is a group of inventions comprising 8 subject matters: claims 1 and 16 — an antibody-drug conjugate (embodiments); claims 24, 37 — a medicine (embodiments); claim 25 — an antitumor medicine and/or anticancer medicine; claims 27, 36 — a pharmaceutical composition (embodiments); claim 29 — a method for treating a tumor and/or cancer.

According to Item 43 of the Rules, substantive examination of application documents in accordance with Article 1386 of Part 4 of the Civil Code of the Russian Federation (hereinafter referred to as the Code) includes assessment of the sufficiency of disclosure of the invention essence in the application documents stipulated by Item 2(1-4) of Article 1375 of the Code and submitted as of the date of filing the application, for implementation of the invention by those skilled in the art; carrying out the

information search concerning the claimed invention to assess the state of the art in comparison with which the industrial applicability, novelty and inventive step of the invention are going to be assessed in accordance with Items 2-4 of Article 1350 of the Code, as well as the assessment of the industrial applicability, novelty and the inventive step of the invention.

The Examiner courteously draws the Applicants attention to the fact that, according to Item 53 of the Rules, in the course of the assessment of the sufficiency of disclosure of the invention essence in the application documents stipulated by Item 2(1-4) of Article 1375 of the Code and submitted as of the date of filing the application, for implementation of the invention by those skilled in the art it is checked whether the application documents comprise data concerning the purpose of the invention, the technical result provided by the invention, whether the set of essential features necessary for achievement of the technical result stipulated by the Applicant is disclosed, as well as whether the rules of disclosure of the essence of the invention and the disclosure of the data concerning the possibility of implementation of the invention established by Items 36-43, 45-50 of the Requirements to application documents are observed.

According to Item 45 of the Requirements, the invention description section "Implementation of the invention" shall comprise data disclosing the method of implementation of the invention for realization of the invention purpose claimed by the Applicant and with confirmation of the possibility of achievement of the technical result in case of implementation of the invention through provision of a detailed description of at least one example of implementation of the invention with references to relevant drawings, if provided.

Concerning the claimed group of inventions, the Examiner respectfully draws the Applicants attention to the following.

1) Kindly be noted that claims 1 and 16 do not specify the purpose antibody-drug conjugate.

Analyzing the application materials, the Examiner observes that the purpose the inventions of claims 1 and 16 is treating tumor and/or cancer.

2) Also kindly be noted that the generic term of the independent claims 24 and 37 stipulated as "Medicine" is incompliant with the said requirement due to the causes specified below. According to Article 4 of Chapter 1 of the Federal Law from April 12, 2010 No61-FZ "On Circulation of Medicines" (Adopted by the State Duma on 24.03.2010, Approved by the Council of Federation on 31.03.2010, Published on 14.04.2010 in the Rossijskaya Gazeta, Came into force on 01.01.2010) dosage form is a condition of a medicinal product corresponding to the administration methods and use thereof, and

ensuring the required therapeutic effect. Therefore, independent claims 24 and 37 characterizing the "Medicine" have to comprise the characteristic of the therapeutic effect exerted on the patient's organism.

Analysis of the application materials showed that the therapeutic effect of the inventions of claims 24 and 37 is the therapy of cancer and tumors. Therefore, the purpose of claims 24 and 37 is the treating cancer and/or tumor.

3) Further, we respectfully draw the Applicant's attention to the absence of the purpose of the pharmaceutical composition in claims 27 and 36.

It should be noted that in the set of claims the generic term reflecting the purpose may be stipulated as "pharmaceutical composition" without the specification of the mode of administration, biological activity and destination for treating a certain disease.

In this instance it shall be controlled, whether the original invention description comprises data on the possibility of the use of the claimed agent for prophylaxis, diagnostics and/or treating of significant number of diseases of various aetiopathogenesis or its activity with respect to various targets. Data provided by the present invention description indicate that the claimed composition, for instance, exerts activity only with respect to treating cancer, and therefore such data cannot be deemed sufficient for confirmation of possibility of implementation of the purpose of the claimed invention encompassed by the broad term "pharmaceutical composition".

Herein, the description is silent on the possibility of the use of the claimed pharmaceutical composition for treating a significant number of diseases of various aetiopathogeneses. Analyzing the application materials, the Examiner observes that the purpose of the compositions of claims 27 and 36 is treating of tumor and/or cancer.

Therefore, the purpose of the claimed group of inventions of claims 1, 16, 24, 25, 27, 29, 36, 37 is treating of cancer and/or tumor.

Analyzing the realization of the purpose, the Examiner respectfully draws the Applicants attention to the fact that the set of claims implies the administration to a patient of an individual compound characterized by a structural formula representing a wide range of specific compounds. Application materials comprise the schemes of preparation of a range of compounds and their features (pages 193-229), a screening of biological activity of individual compounds in vitro (pages 230-24). Thereby it shall be observed that the application materials point out the antitumor effect only for antibody-drug

conjugates (3), (10), (13), (16a), characterized by specific structural formulas of compounds (pages 247-277).

However, neither in the prior art, nor in the application materials there are any data allowing to suppose that all the compounds specified in the tables enable to treat patients suffering the above mentioned diseases. At that, from the prior art it is known that different functional groups in case of their provision to a molecule of a compound, as well as the transformation of the compound structure itself, may change its pharmacological activity (BELIKOV V.G., Pharmaceutical Chemistry, M., "Vysshaya Shkola", 1993, pages 43-47).

Moreover, with respect to the data on the efficiency of the compounds according to in vitro analysis specified on pages 230-247, we respectfully draw the Applicant's attention to the fact that it is not possible to directly extrapolate the data on an integral organism, because it is known from the prior art that significant differences can be found between in vitro experiments and treating of a human being ("Brief Course of Molecular Pharmacology" edited by P.V. Sergeyev, M., 1975, page 10). This is attributed to the fact that a plurality of factors influences the excretion of the activity of a compound with respect to a living organism, and those factors are not taken into account in the course of an in vitro experiment. These are distribution of the compound in biological matrices of the organism, availability of the binding targets, biological transformation and the like (L.Ye. Kholodov et al, "Clinical Pharmacokinetics", M., "Meditsina", 1985, pages 83-98, 134-138, 160, 378-380). In this connection, data on the activity procured as a result of *in vitro* experiments cannot serve the confirmation of the activity of a compound in the environment of a living organism.

We respectfully remind the Applicant that, according to effective normative legal acts, for an invention implying the possibility of prophylaxis or treating of human or animal diseases, data indicating of their influence on the disease aetiopathogenesis shall be collected in the course of an experiment involving adequate models (Item 49(6) of the Requirements).

Therefore, the group of inventions of the independent claims 1, 16, 24, 25, 27, 29, 36, 37 and the claims dependent thereon is not compliant with the requirement of the sufficiency of the disclosure of the essence of the invention (Item 53 of the Rules) with the exception of the embodiments of the drug-antibody conjugates (3), (10), (13), (16a).

For the Applicant's information. On the moment of issuance of the present Official Action the Examiner could not observe in the prior art any data disclosing the availability or obviousness of applicability of drug-antibody conjugates (3), (10), (13), (16a) for treating cancer and/or tumor.

The Applicant is invited to analyze the arguments of the Examiner.

Please find a Search Report enclosed for your records, which was conducted pursuant to Item 2 of Article 1386 of the Code.

Annex: Search Report on 1 sheet

The Applicant shall submit: the Applicant's arguments concerning the above Examiner's arguments and/or the amended set of claims (in accordance with Item 96 of the Rules).

The additional materials submitted by the Applicant should not change the essence of the claimed invention (Item 2 of the Article 1378 of the Code).The additional materials will be available for studying by third parties, pursuant to Item 2 of the Article 1394 of the Code, after publication of the data about granting a patent.According to Item 6 of Article 1386 of the Code, should the Applicant provide additional materials, it is controlled, whether the said materials change the essence of the application (Article 1378). The parts of the additional materials that change the essence of the application are not taken into account when the invention application is considered.

Such materials can be provided by the Applicant as independent claims.

Federal Executive Authority on Intellectual Property informs the Applicant hereof.

Features are deemed to be claimed not only in the instance when they are comprised in the amended claims provided by the Applicant, but also when the Applicant only mentions the necessity to include the said features into the claims. Should a feature of the invention be stipulated in application documents as a generic term without the disclosure of particular forms if its implementation, provision of the said form of implementation in additional materials with its attribution to the feature incorporatable into the claims is the reason to deem the additional materials changing the essence of the application (Item 96 of the Rules).

The Examiner

Your reference: **SHU/PD20-9009RU**
Our reference: **2403-532821RU**
Application No.: **2016143351**
Attorney Name: **Elena Nazina**

GORODISSKY

Federal Service on Intellectual Property
Federal State Budgetary Enterprise "Federal Institute of Industrial Property"
(FIPS)
SEARCH REPORT

1. IDENTIFICATION OF THE APPLICATION	
Registration number	Filing date
2016143351/04(069410)	**10 April 2015**
PCT/JP2015/002020	**10 April 2015**

Priority is established on the date of:
[ ] filing the application
[ ] receipt of supplementary materials of _____ for earlier filed application No.
[ ] priority on the basis of original application No. _____ from which said application was divided
[ ] filing original application No. _____ from which said application was divided
[ ] filing earlier filed application No.
[x] filing the first application(s) in the state-member of the Paris Convention

(31) Number of the first application(s)	(32) Filing date of the first application(s)	(33) Country code
2014-081454	**April 10, 2014**	**JP**

The title of the invention (utility model) [x] as claimed [] amended (see Notes):
ANTI-HER3 ANTIBODY-DRUG CONJUGATE

Applicant:

DAIICHI SANKYO COMPANY, LIMITED **3-5-1, Nihonbashi-honcho** **Chuo-ku, Tokyo 103-8426** **Japan**	**JP**
DAIICHI SANKYO EUROPE GmbH **Zielstattstrasse 48,** **81379 Muenchen,** **Germany**	**DE**

2. UNITY OF INVENTION
[x] fulfilled [ ] not fulfilled Comments: see Notes

3. CLAIMS:	
[x] all claims were considered	
[ ] the following claims were considered	(see Notes)
[ ] amended claims were considered	(see Notes)

4. CLASSIFICATION OF the SUBJECT MATTER OF THE INVENTION (UTILITY MODEL) (IPC index, current version indicator)
A61K 47/64 (2017.01)
A61K 39/395 (2006.01)
A61K 31/535 (2006.01)
C07K 16/28 (2006.01)
A61P 35/00 (2006.01)

5. FIELD SEARCHED
5.1. The minimum of PCT documents revised (indicated by IPC indexes):
A61K 47/64, 39/395, 31/535, C07K 16/28, A61P 35/00
5.2 Other revised documents as was included into search collations:

Your reference: **SHU/PD20-9009RU**
Our reference: **2403-532821RU**
Application No.: **2016143351**
Attorney Name: **Elena Nazina**

5.3 Electronic databases used in the search: (the name of a database and search terms, if possible):
DWPI, E-Library, Google, Google Patents, PatSearch, Science Direct

6. DOCUMENTS CONSIDERED TO BE RELEVANT

Category*	Citation of document, with indication, where appropriate, of the relevant passages	Relevant to claim No.
1	2	3
A	RU 2404810 C2 (GENENTECH INC [US]), 27.11.2010, the entire document	1-38
A	WO 2012019024 A2 (IMMUNOGEN INC [US]), 09.02.2012, abstract, claims 1, 40	1-38
A	JEFFREY C KANG ET AL. Engineering multivalent antibodies to target heregulin-induced HER3 signaling in breast cancer cells, mAbs, 2014, 6:2, p. 340-353	1-38
A	SIEVERS, E. L. et al, Antibody-Drug Conjugates in Cancer Therapy. Annual Review of Medicine, 2013, 64(1), p. 15-29	1-38

*Special categories of cited documents: "A" document defining the general state of the art which is not considered to be of particular relevance "E" earlier document but published on or after the international filing date "L" document which may throw doubts on priority claim(s) or which is cited to establish the publication date of another citation or other special reason (as specified) "O" document referring to an oral disclosure, use, exhibition or other means "P" document published prior to the international filing date but later than the priority date claimed T" later document published after the International filing date or priority date and not in conflict with the application but cited to understand the principle or theory underlying the invention	"X" document of particular relevance; the claimed invention cannot be considered novel or cannot be considered to involve an inventive step when the document is taken alone "Y" document of particular relevance; the claimed invention cannot be considered to involve an inventive step when the document is combined with one or more other such documents, such combination being obvious to a person skilled in the art "&" document member of the same patent family

7. NOTES

8. FORMALITIES

The present report consists of 1 sheet.	Copy of cited references on ___ sheets in ____ copy(ies) are attached
Date of the actual completion of the search: 04.03.2019	Authorized officer (position held and signature): State Expert on Intellectual Property Chernysheva D.V.
Search Authority: **FIPS** **30-1 Berezhkovskaya nab., Moscow G-59, GSP-3, 123995** **Russian Federation** **Tel: (+8 499) 240-60-15, Fax: (+8 495) 531-63-18;** **e-mail: fips@rupto.ru**	

Федеральная служба по интеллектуальной собственности
Федеральное государственное бюджетное учреждение
«Федеральный институт промышленной собственности»
(ФИПС)
Бережковская наб., 30, корп. 1, Москва, Г-59, ГСП-3, 125993
Телефон (8-499) 240- 60- 15, Факс (8-495) 531-63-18

Форма N 10 ИЗ-2017
100,181

ООО "Юридическая фирма Городисский и Партнеры"
ул. Б.Спасская, 25, строение 3
Москва
129090

На № 2403-532821RU от 14.03.2018
Наш № 2016143351/04(069410)
При переписке просим ссылаться на номер заявки
Исходящая корреспонденция от ***05.03.2019***

З А П Р О С
экспертизы по существу

(21) Заявка № 2016143351/04(069410)

(22) Дата подачи заявки 10.04.2015

(71) Заявитель(и) ДАЙИТИ САНКИО КОМПАНИ, ЛИМИТЕД, JP, ДАЙИТИ САНКИО ЮРОП ГмбХ, DE

(51) МПК
A61K47/64 (2017.01) ***A61K31/535*** (2006.01) ***A61P35/00*** (2006.01)
A61K39/395 (2006.01) ***C07K16/28*** (2006.01)

8		044403

ВОПРОСЫ, ДОВОДЫ, ЗАМЕЧАНИЯ, ПРЕДЛОЖЕНИЯ

Рассмотрев материалы заявки, экспертиза пришла к выводу о необходимости запроса дополнительных материалов в соответствии с п. 143 Административного Регламента***, поскольку имеются препятствия для вынесения решения по заявке.

Заявитель просит рассмотреть указанную заявку с датой подачи 10.04.2015 с приоритетом по первоначальной заявке JP 2014-081454 от 10.04.2014.

Рассмотрена формула, описание и чертежи изобретения, представленные на дату подачи заявки.

Заявлена группа изобретений, состоящая из 8 объектов: п.1,16 – конъюгат антитело-лекарственное средство (варианты); п. 24, 37 - лекарственное средство (варианты); п. 25 - противоопухолевое лекарственное средство и/или противораковое лекарственное средство; п. 27,36 – фармацевтическая композиция (варианты); п. 29 – способ лечения опухоли/или рака.

Согласно п. 43 Правил**** рассмотрения документов заявки по существу в соответствии со статьей 1386 части четвертой Гражданского Кодекса РФ (далее Кодекс*) включает проверку достаточности раскрытия сущности изобретения в документах заявки, предусмотренных подпунктами 1-4 пункта 2 статьи 1375 Кодекса* и представленных на дату ее подачи, для осуществления изобретения специалистом в данной области техники; проведение информационного поиска в отношении заявленного изобретения для определения уровня техники, с учетом которого будет осуществляться проверка его соответствия условиям промышленной применимости, новизны и изобретательского уровня

• Информация о состоянии делопроизводства по заявке может быть получена по телефону 8 (499) 240 60 15;

• Сведения о состоянии делопроизводства по заявкам размещаются на сайте ФИПС по адресу «www.fips.ru» в разделе «Информационные ресурсы / Открытые реестры»;

• При изменении адреса для переписки по заявке заявитель обязан сообщить об этом незамедлительно.

---

*Гражданский кодекс Российской Федерации Часть четвёртая от 18 декабря 2006 г. N 231-ФЗ с изменениями и дополнениями.

**Положение о патентных и иных пошлинах за совершение юридически значимых действий, связанных с патентом на изобретение, полезную модель, промышленный образец, с государственной регистрацией товарного знака и знака обслуживания, с государственной регистрацией и предоставлением исключительного права на наименование места происхождения товара, а также с государственной регистрацией отчуждения исключительного права на результат интеллектуальной деятельности или средство индивидуализации, залога исключительного права, предоставления права использования такого результата или такого средства по договору, перехода исключительного права на такой результат или такое средство без договора, утвержденное постановлением Правительства Российской Федерации от 10.12.2008 N 941 с изменениями.

***Административный регламент предоставления Федеральной службой по интеллектуальной собственности государственной услуги по государственной регистрации изобретения и выдаче патента на изобретение, его дубликата утвержден приказом Минэкономразвития России от 25.05.2016 года N 315, зарегистрирован 14.07.2016, регистрационный N 42843, с изменениями.

****Правила составления, подачи и рассмотрения документов, являющихся основанием для совершения юридически значимых действий по государственной регистрации изобретений, и их формы утверждены приказом Минэкономразвития России от 25.05.2016 N 316, зарегистрированы 11.07.2016, регистрационный N 42800.

*****Требования к документам заявки на выдачу патента на изобретение утверждены приказом Минэкономразвития России от 25.05.2016 N 316, зарегистрированы 11.07.2016, регистрационный N 42800.

в соответствии с пунктами 2-4 статьи 1350 Кодекса*, а также проверку промышленной применимости, новизны и изобретательского уровня изобретения.

Внимание заявителя обращается на то, что согласно п.53 Правил**** при проверке достаточности раскрытия сущности заявленного изобретения в документах заявки, предусмотренных подпунктами 1-4 пункта 2 статьи 1375 Кодекса* и представленных на дату ее подачи, для осуществления изобретения специалистом в данной области техники проверяется, содержатся ли в документах заявки сведения о назначении изобретения, о техническом результате, обеспечиваемом изобретением, раскрыта ли совокупность существенных признаков, необходимых для достижения указанного заявителем технического результата, а также соблюдены ли установленные пунктами 36-43, 45-50 Требований***** к документам заявки правила, применяемые при раскрытии сущности изобретения и раскрытии сведений о возможности осуществления изобретения.

Согласно п. 45 Требований***** в разделе описания изобретения "Осуществление изобретения" приводятся сведения, раскрывающие, как может быть осуществлено изобретение с реализацией указанного заявителем назначения изобретения и с подтверждением возможности достижения технического результата при осуществлении изобретения путем приведения детального описания, по крайней мере, одного примера осуществления изобретения со ссылками на графические материалы, если они представлены.

Что касается назначения заявленной группы изобретений, экспертиза обращает внимание на следующее.

1) Обращаем внимание на пп. 1,16, в которых не указано назначение конъюгат антитело-лекарственное средство.

Анализируя материалы заявки, экспертиза полагает, что назначением заявленных изобретений по пп. 1,16 является лечение опухоли и/или рака.

2) Также обращаем внимание на родовое понятие независимых пп.24,37, сформулированное как: «Лекарственное средство», которое не удовлетворяет указанному требованию по причинам указанным ниже. В соответствии со статьей 4 Главы 1 Федерального закона от 12 апреля 2010 года N 61-ФЗ «Об обращении лекарственных средств» (Принят Государственной Думой 24.03.2010, Одобрен Советом Федерации 31.03.2010, Опубликован 14 апреля 2010 в Российской Газете, Вступил в силу 01.01.2010) лекарственная форма – состояние лекарственного препарата, соответствующее способам его введения и применения и обеспечивающее достижение необходимого лечебного эффекта. Следовательно, независимые пп.24,37, характеризующие «Лекарственное средство» должны содержать характеристику лечебного эффекта, оказываемого на организм пациента.

Анализируя материалы заявки, лечебных эффектом заявленных изобретений по пп.24,37 является терапия рака и опухолей. Таким образом, назначением н.п. 24,37 является лечение рака и/или опухоли.

3) Далее обращаем внимание заявителя на то, что в пп.27,36 отсутствует назначение фармацевтической композиции.

Следует отметить, что в формуле изобретения родовое понятие, отражающее назначение, может быть указано как «фармацевтическая композиция» без указания на механизм воздействия, биологической активности или предназначенности для лечения какого-либо заболевания. В таком случае проверяется, приведены ли в первоначальном описании изобретения сведения о возможности использования заявленного средства для профилактики, диагностики и/или лечения значительного количества болезней различного этиопатогенеза или его активности в отношении различных мишеней. Сведения, приведенные в этом описании изобретения, свидетельствуют, что указанная композиция, например, проявляет активность только в отношении для лечения рака, то такие сведения нельзя считать достаточными для подтверждения возможности реализации указанного в формуле изобретения назначения, охватываемого широким понятием «фармацевтическая композиция».

При этом в описании отсутствуют сведения о возможности использования заявленной фармацевтической композиции для лечения значительного количества болезней различного этиопатогенеза.

Анализируя материалы заявки, экспертиза считает, что назначением композиций по пп. 27,36 является лечения рака и/или опухоли.

Таким образом, назначением заявленной группы изобретений по пп. 1,16,24,25,27,29,36,37 является лечение рака и/или опухоли.

Анализируя реализацию назначения, экспертиза обращает внимание на то, что согласно формуле изобретения предполагается введение субъекту индивидуального соединения, охарактеризованного структурной формулой, которые представляют собой большой ряд конкретных веществ. Материалы заявки содержат схемы синтеза ряда соединений и их характеристики (с.193-229), скрининг биологической активности синтезированных индивидуальных соединений in vitro (с.230-247). При этом, необходимо отметить, что в материалах заявках противоопухолевый эффект показан лишь для конъюгатов антитело-лекарственное средство (3), (10), (13), (16а), которые характеризуются конкретными структурными формулами соединений (с. 247-277). Однако ни в уровне техники, ни в материалах заявки нет никаких сведений, позволяющих предположить, что все указанные в таблицах вещества позволят осуществить лечение пациентов, страдающих

указанными выше заболеваниями. При этом из уровня техники известно, что различные функциональные группы при их введении в молекулу вещества, а также изменение самой структуры вещества, могут изменять его фармакологическую активность (БЕЛИКОВ В.Г., Фармацевтическая химия, М., Высшая школа, 1993, с. 43-47).

Кроме того, в отношении сведений об эффективности соединений по результатам in vitro анализа, указанных на с.230-247, обращаем внимание на то, что напрямую экстраполировать эти данные на целостный организм не представляется возможным, поскольку из уровня техники известно, что между экспериментами in vitro и лечением человека могут быть выявлены существенные различия («Краткий курс молекулярной фармакологии» под ред. П.В.Сергеева, М., 1975, с.10). Связано это с тем, что на проявление активности вещества в условиях живого организма оказывает влияние множество факторов, действие которых эксперимент in vitro не учитывает: распределение вещества в биологических средах организма, доступность для мишеней действия, биотрансформация и т.д. (Л.Е.Холодов и др. «Клиническая фармакокинетика», М., «Медицина», 1985, с. 83-98, 134-138, 160, 378-380). В связи с этим данные об активности, полученные в результате экспериментов in vitro, не могут служить подтверждением активности вещества в условиях живого организма.

Напоминаем заявителю о том, что согласно действующим нормативным правовым актам, для изобретения, относящегося к возможности профилактики и/или лечения и заболеваний людей или животных, приводятся данные, свидетельствующие о влиянии на этиопатогенеза заболевания, полученные в эксперименте на адекватных моделях (п. 49(6) Требований*****).

Таким образом, группа изобретений по независимым пп. 1,16,24,25,27,29,36,37 и зависимым от них пунктам не соответствуют требование достаточности раскрытия сущности заявленного изобретения (п.53 Правил****) за исключением вариантов конъюгатов антитело-лекарственное средство (3), (10), (13), (16а).

К сведению заявителя. На момент направления данного запроса экспертизе не удалось обнаружить в уровне техники сведений, раскрывающих известность или очевидность конъюгатов антитело-лекарственное средство (3), (10), (13), (16а) для лечения рака и/или опухоли.

Заявителю предлагается проанализировать доводы экспертизы.

Направляем Вам для сведения отчет об информационном поиске, проведенном в соответствии с п.2 ст.1386 Кодекса*.

Приложение: отчет об информационном поиске на 1 л. в 1 экз.

Заявителю необходимо представить:

свои доводы в отношении вышеизложенных доводов экспертизы, и/или скорректированную формулу (в соответствии с п. 96 Правил****).

Если заявитель **в трёхмесячный срок со дня направления запроса** не представит запрашиваемые материалы или не подаст ходатайство о продлении этого срока, заявка будет признана отозванной. Срок представления запрошенных материалов может быть продлен, но не более чем на десять месяцев (*общий срок продления не должен превышать десять месяцев*) (п. 6 ст. 1386 Кодекса*)

Продление срока ответа на запрос экспертизы осуществляется при условии уплаты соответствующей патентной пошлины в установленном порядке.

Дополнительные материалы, поданные заявителем, не должны изменять заявку на изобретение по существу (п. 2 ст. 1378 Кодекса*).

Дополнительные материалы представляются на ознакомление третьим лицам в соответствии с п. 2 ст. 1394 Кодекса* после публикации сведений о выдаче патента.

Согласно п.6 ст. 1386 Кодекса* в случае, если заявителем представлены дополнительные материалы, проверяется, не изменяют ли они заявку по существу (статья 1378). Дополнительные материалы в части, изменяющей заявку по существу, при рассмотрении заявки на изобретение во внимание не принимаются. Такие материалы могут быть представлены заявителем в качестве самостоятельной заявки. Федеральный орган исполнительной власти по интеллектуальной собственности уведомляет об этом заявителя.

Признаки считаются подлежащими включению в формулу изобретения не только в том случае, когда они содержатся в представленной заявителем уточненной формуле изобретения, но и когда заявитель лишь указывает на необходимость включения в формулу изобретения таких признаков.

Если на дату подачи заявки признак изобретения был выражен в документах заявки общим понятием без раскрытия частных форм его выполнения, то представление такой формы выполнения в дополнительных материалах с отнесением ее к признаку, подлежащему

включению в формулу изобретения, является основанием для признания дополнительных материалов изменяющими заявку по существу (п.96 Правил****).

Главный государственный эксперт по интеллектуальной собственности отдела органической химии и фармацевтики ФИПС

Документ подписан электронной подписью
Сведения о сертификате ЭП
Сертификат
25155CA55794E992E8116EC84ABB5397
Владелец Рубайло
Дарья Петровна
Срок действия с 05.10.2018 по 08.02.2027

Д. П. Рубайло
8(499)240-61-58

Чернышева Д.В.

8 (499) 240-50-17

Форма № 18 ИЗ,ПМ-2011

Федеральная служба по интеллектуальной собственности
Федеральное государственное бюджетное учреждение
«Федеральный институт промышленной собственности»
(ФИПС)

ОТЧЕТ О ПОИСКЕ

1. **ИДЕНТИФИКАЦИЯ ЗАЯВКИ**

Регистрационный номер	Дата подачи
2016143351/04(069410)	10.04.2015
PCT/JP2015/002020	10.04.2015

Приоритет установлен по дате:
[ ] подачи заявки
[ ] поступления дополнительных материалов от к ранее поданной заявке №
[ ] приоритета по первоначальной заявке № из которой данная заявка выделена
[ ] подачи первоначальной заявки № из которой данная заявка выделена
[ ] подачи ранее поданной заявки №

[X] подачи первой(ых) заявки(ок) в государстве-участнике Парижской конвенции

(31) Номер первой(ых) заявки(ок)	(32) Дата подачи первой(ых) заявки(ок)	(33) Код страны
1. 2014-081454	10.04.2014	JP

Название изобретения (полезной модели): [X] - как заявлено; [ ] - уточненное (см. Примечания)
КОНЪЮГАТ АНТИ-HER3 АНТИТЕЛО-ЛЕКАРСТВЕННОЕ СРЕДСТВО

Заявитель: ДАЙИТИ САНКИО КОМПАНИ, ЛИМИТЕД, JP, ДАЙИТИ САНКИО ЮРОП ГмбХ, DE

2. **ЕДИНСТВО ИЗОБРЕТЕНИЯ**
[X] соблюдено [ ] не соблюдено. Пояснения: см. Примечания

3. **ФОРМУЛА ИЗОБРЕТЕНИЯ:**
[X] приняты во внимание все пункты (см. Примечания)
[ ] приняты во внимание следующие пункты:
[ ] принята во внимание измененная формула изобретения (см. Примечания)

4. **КЛАССИФИКАЦИЯ ОБЪЕКТА ИЗОБРЕТЕНИЯ (ПОЛЕЗНОЙ МОДЕЛИ)** (Указываются индексы МПК и индикатор текущей версии)

A61K 47/64 (2017.01)
A61K 39/395 (2006.01)
A61K 31/535 (2006.01)
C07K 16/28 (2006.01)
A61P 35/00 (2006.01)

5. **ОБЛАСТЬ ПОИСКА**
5.1 Проверенный минимум документации PCT (указывается индексами МПК)
A61K 47/64, 39/395, 31/535, C07K 16/28, A61P 35/00
5.2 Другая проверенная документация в той мере, в какой она включена в поисковые подборки:

5.3 Электронные базы данных, использованные при поиске (название базы, и если, возможно, поисковые термины):
DWPI, E-Library, Google, Google Patents, PatSearch, Science Direct

6. **ДОКУМЕНТЫ, ОТНОСЯЩИЕСЯ К ПРЕДМЕТУ ПОИСКА**

Категория*	Наименование документа с указанием (где необходимо) частей, относящихся к предмету поиска	Относится к пункту формулы №

(см. на обороте)

1	2	3
A	RU 2404810 C2 (GENENTECH INC [US]), 27.11.2010, весь документ	1-38
A	WO 2012019024 A2 (IMMUNOGEN INC [US]), 09.02.2012, abstract, claim 1,40	1-38
A	JEFFREY C KANG ET AL. Engineering multivalent antibodies to target heregulin-induced HER3 signaling in breast cancer cells, mAbs, 2014, 6:2, p. 340-353.	1-38
A	SIEVERS, E. L. et al, Antibody-Drug Conjugates in Cancer Therapy. Annual Review of Medicine, 2013, 64(1), p. 15-29.	1-38

*Особые категории ссылочных документов:

«A» документ, определяющий общий уровень техники и не считающийся особо релевантным

«E» более ранний документ, но опубликованный на дату международной подачи или после нее

«L» документ, подвергающий сомнению притязание(я) на приоритет, или который приводится с целью установления даты публикации другого ссылочного документа, а также в других целях (как указано)

«O» документ, относящийся к устному раскрытию, использованию, экспонированию и т.д.

«P» документ, опубликованный до даты международной подачи, но после даты испрашиваемого приоритета

«T» более поздний документ, опубликованный после даты международной подачи или даты приоритета и не порочащий заявку, но приведенный для понимания принципа или теории, на которых основывается изобретение

«X» документ, имеющий наиболее близкое отношение к предмету поиска: заявленное изобретение не обладает новизной или изобретательским уровнем в сравнении с документом, взятым в отдельности

«Y» документ, имеющий наиболее близкое отношение к предмету поиска; заявленное изобретение не обладает изобретательским уровнем, когда документ взят в сочетании с одним или несколькими документами той же категории, такая комбинация документов очевидна для специалиста

«&» документ, являющийся патентом-аналогом

7. **ПРИМЕЧАНИЯ:**

8. **УДОСТОВЕРЕНИЕ ОТЧЕТА**

Настоящий отчет состоит из 1 л.	К отчету приложены копии ссылок на - л. в - экз.
Дата действительного завершения поиска: 04.03.2019	Должность и подпись уполномоченного лица:
Поисковый орган: **ФИПС** **Бережковская наб., 30, корп. 1, Москва, Г-59, ГСП-3, 125993** **Телефон (8-499) 240- 60- 15. Факс (8-495) 531- 63- 18;** **e-mail: fips@rupto.ru**	ГЭ по ИС 2 к. Чернышева Д.В.

Your reference: **SHU/PD20-9008RU**
Our reference: **2403-533625RU**
Application No.: **2016123597**
Attorney Name: **Elena Nazina**

GORODISSKY

TRANSLATION

OFFICIAL ACTION

(21) Application number **2016123597/10(036880)**.

(22) Date of filing the application **28 January 2015**.

(71) Applicant(s) **DAIICHI SANKYO COMPANY, LIMITED, JP**

(51) IPC **A61K 31/4745, A61K 39/395, A61P 35/00**

QUESTIONS, ARGUMENTS, OBJECTIONS, PROPOSALS

Having studied the application materials, the Examiner arrives at the conclusion about necessity to request additional information, since there are bars to making a decision regarding the application.

The Applicant claims the convention priority on 31 January 2014 according to first applications No. 2014-017777 filed with the Japan Patent Office.

To be examined are the original claims consisting of 27 claims and comprising 6 subjects.

We kindly point out the following violations as related to the drafting of the claims.

Pursuant to Section 24.4(3) of the Administrative Regulations, it shall be established, if there is a possibility for a person skilled in the art to understand the substantial content of a feature based on the prior art.

The feature of claim 3 "-КДGGFG-" does not provide for the possibility of understanding it, since there is a Russian letter "Д" in the single-letter spelling of the amino acid sequence.

Therefore, the Applicant may amend the claims, taking into consideration said violations.

The Examiner kindly points out that if it is established that a feature is characterized in violation of the condition set forth in sub-section (4), Section 10.8 of the Administrative Regulations, but the Applicant refuses to amend the claims, the application will be considered to have been withdrawn.

Pursuant to Section 10.8.1.5(3) of the Administrative Regulations, a dependent claim shall not be presented in such a way that a replacement or elimination of the features of the invention takes place, such invention characterized in that claim to which the dependent claim is subordinate.

Claim 16 depends on claim 15 and comprises a feature "n^3 is 2" and "L^2 is a single bond". This replaces the features of claim 15, wherein "n^3 is 5" and "L^2 is a single bond".



Claim 17 depends on claim 15 and comprises features "n^3 is 5, L^2 is -NH-$(CH_2CH_2-O)n^4$-CH_2CH_2-C(=O)-, and n^4 is 4". This replaces the features of claim 15, wherein "n^3 is 2, L^2 is -NH-$(CH_2CH_2-O)n^4$-CH_2CH_2-C(=O)-, and n^4 is 2".

Therefore, the Applicant may amend the claims, taking into consideration said violations.

Pursuant to Section 10.8.1.3(1) of the Administrative Regulations, a claim shall comprise the features of the invention, including a generic term showing the purpose, which opens the presentation of the claims.

And in independent claims 1 and 14, the purpose of the "antibody-drug conjugate" is not indicated.

Therefore, the Applicant may amend claims 1 and 14, taking into consideration said violation.

Pursuant to Section 10.8.1.4(2) of the Administrative Regulations, an independent claim shall relate to one invention only.

Independent claims 23 and 27 relate (each) to two inventions, since the set of features contained therein (in particular, an antitumor drug, an anticancer drug, a method for treating tumor, and a method for treating cancer) comprises the characteristic of inventions related to a set of means, and each has its own purpose, without the implementation of a common purpose by said set of means.

Therefore, the Applicant may amend claims 23 and 27, taking into consideration said violation, for example, by making several independent claims, based on each of claims 23 and 27.

With regard to independent claims 1, 14, 23 and 27, we kindly advise the following.

In case of correction of the violation as related to the drafting of said claims, they may be recognized compliant with the patentability conditions.

With regard to independent claims 22 and 25 defining a drug or a pharmaceutical composition, we kindly advise the following.

Pursuant to Section 24.5.1(2) of the Administrative Regulations, one shall make sure that the implementation of the purpose indicated by the Applicant is really possible in case of the carrying out of the invention according to any claim.

If mere experimental data can evidence the possibility to carry out the invention and to implement the indicated purpose, then it shall be checked if the description of the invention contains the examples of embodiment thereof with the indication of relevant data, and it shall be established if such examples are sufficient for the conclusion on the compliance with said requirement to apply to

various particular embodiments of the feature, such particular embodiments falling within the notion indicated by the Applicant in the claims.

In the claims, the generic term showing the purpose may be indicated as "a pharmaceutical composition" (or "a drug"), without a reference to a mode of action, biological activity or specificity to treat a disease. In this case, one should check if the description of the invention contains information on the possibility to use the claimed composition for preventing, diagnosing and/or treating a significant number of diseases of various etiopathogeneses or activity thereof in relation to various targets.

If the information presented in the description evidences that said composition exhibits activity, for example, only in relation to a certain type of subjects, such information may not be considered sufficient for the confirmation of possibility to implement the purpose indicated in the claims, such purpose covered by the broad notion "pharmaceutical composition".

The information presented in the description evidences that the claimed composition (and the drug) exhibits activity only in relation to a certain type of subjects – treating cancer (examples). Thus, such information may not be considered sufficient for the confirmation of possibility to implement the purpose indicated in the claims, such purpose covered by the broad notion "pharmaceutical composition" (or "drug").

Thus, the inventions according to claims 22 and 25 are incompliant with the industrial applicability patentability condition, since the implementation of the purpose is not confirmed in the entire scope of the claims (Section 24.5.1(2) of the Administrative Regulations).

The Applicant may indicate the purpose in claims 22 and 25 as "a pharmaceutical composition for treating cancer" and "a drug for treating cancer", respectively, and should consider that amended claim 22 does not copy claim 23.

Attached, please, find a single copy of the Search Report on one sheet.

* Administrative Regulations for the performance by the Federal Service for Intellectual Property, Patents and Trademarks of the public function related to the arrangement of the acceptance of applications for inventions and the consideration and examination thereof, and proper issue of patents of the Russian Federation, passed by Order No. 327 of the Russian Ministry of Education and Science on October 29, 2008, and registered by the Russian Ministry of Justice on February 20, 2009, No. 13413 (Bulletin of Federal Agency Regulations, 2009, No.21).

If the Applicant does not furnish requested materials **within three months from the date of dispatch of this Office Action** or does not submit a request to prolong this term, the application will be considered to have been withdrawn. The term established for submission of requested materials may be extended, but for no more than for ten months (total extension term may not exceed ten months) (Section 6 Art. 1386 of the Code).

Extension of the term for reply to the Examiner's Office Action shall be effected subject to the payment of a relevant patent fee as applicable.

Supplementary materials submitted by the Applicant shall not alter the substance of the application (Section 2 Art. 1378 of the Code).

The supplementary materials may be made available to third parties pursuant to Section 2, Art. 1394 of the Code after the information on the issue of a patent is published.

Your reference: SHU/PD20-9008RU
Our reference: 2403-533625RU
Application No.: 2016123597
Attorney Name: Elena Nazina

GORODISSKY

Federal Service on Intellectual Property
Federal State Budgetary Enterprise "Federal Institute of Industrial Property"
(FIPS)
SEARCH REPORT

1. IDENTIFICATION OF THE APPLICATION

Registration number	Filing date
2016123597/10(036880)	28 January 2015
PCT/JP2015/000355	28 January 2015

Priority is established on the date of:
[ ] filing the application
[ ] receipt of supplementary materials of _____ for earlier filed application No.
[ ] priority on the basis of original application No. _____ from which said application was divided
[ ] filing original application No. _____ from which said application was divided
[ ] filing earlier filed application No.
[x] filing the first application(s) in the state-member of the Paris Convention

	(31) Number of the first application(s)	(32) Filing date of the first application(s)	(33) Country code
1.	2014-017777	31 January 2014	JP
2.	2014-168944	22 August 2014	JP
3.	2014-227886	10 November 2014	JP

The title of the invention (utility model) [x] as claimed [] amended (see Notes):
ANTI-HER2 ANTIBODY-DRUG CONJUGATE

Applicant:
DAIICHI SANKYO COMPANY, LIMITED JP

2. UNITY OF INVENTION
[x] fulfilled [ ] not fulfilled Comments: see Notes

3. CLAIMS:
[x] all claims were considered
[ ] the following claims were considered (see Notes)
[ ] amended claims were considered (see Notes)

4. CLASSIFICATION OF the SUBJECT MATTER OF THE INVENTION (UTILITY MODEL) (IPC index, current version indicator)
A61K 31/4745 (2006.01)
A61K 39/395 (2006.01)
A61P 35/00 (2006.01)

5. FIELD SEARCHED
5.1. The minimum of PCT documents revised (indicated by IPC indexes):
A61K 31/4745
A61K 39/395
A61P 35/00
5.2 Other revised documents as was included into search collations:
5.3 Electronic databases used in the search: (the name of a database and search terms, if possible):
DWPI, Espacenet, Google, PatSearch, PubMed, RUPTO, USPTO, Yandex

6. DOCUMENTS CONSIDERED TO BE RELEVANT

Category*	Citation of document, with indication, where appropriate, of the relevant passages	Relevant to claim No.
1	2	3

Your reference: **SHU/PD20-9008RU**
Our reference: **2403-533625RU**
Application No.: **2016123597**
Attorney Name: **Elena Nazina**

A	US 20030171262 A1 (DAIICHI PHARMACEUTICAL CO., LTD [JP]) 11.09.2003, abstract, [0002], [0042], table 1, claims 1-26	1-27
A	BAROK M., et al., Trastuzumab-DM1 is highly effective in preclinical models of HER2-positive gastric cancer.Cancer Lett. 2011 Jul 28;306(2):171-9. doi: 10.1016/j.canlet.2011.03.002. Epub 2011 Apr 1., abstract	1-27
A	WENTE MN., et al., DE-310, a macromolecular prodrug of the topoisomerase-I-inhibitor exatecan (DX-8951), in patients with operable solid tumors.Invest New Drugs. 2005 Aug;23(4):339-47., abstract	1-27
A	OGUMA T., et al., Validation study of a method for assaying DE-310, a macromolecular carrier conjugate containing an anti-tumor camptothecin derivative, and the free drug in tumor tissue by high performance liquid chromatography/atmospheric pressure chemical ionization tandem mass spectrometry.Biomed Chromatogr. 2005 Jan;19(1):19-26., abstract	1-27

*Special categories of cited documents: "A" document defining the general state of the art which is not considered to be of particular relevance "E" earlier document but published on or after the international "L" document which may throw doubts on priority claim(s) or which is cited to establish the publication date of another citation or other special reason (as specified) "O" document referring to an oral disclosure, use, exhibition or other means "P" document published prior to the international filing date but later than the priority date claimed T" later document published after the international tiling date or priority date and not in conflict with the application but cited to understand the principle or theory underlying the invention	"X" document of particular relevance; the claimed invention cannot be considered novel or cannot be considered to involve an inventive step when the document is taken alone "Y" document of particular relevance; the claimed invention cannot be considered to involve an inventive step when the document is combined with one or more other such documents, such combination being obvious to a person skilled in the art "&" document member of the same patent family

7. NOTES

8. FORMALITIES

The present report consists of 1 sheet.	Copy of cited references on ___ sheets in ____ copy(ies) are attached
Date of the actual completion of the search:	Authorized officer (position held and signature):
Search Authority: **FIPS** **30-1 Berezhkovskaya nab., Moscow G-59, GSP-3, 123995** **Russian Federation** **Tel: (+8 499) 240-60-15, Fax: (+8 495) 531-63-18;** **e-mail: fips@rupto.ru**	State Expert on Intellectual Property N

Федеральная служба по интеллектуальной собственности
Федеральное государственное бюджетное учреждение
«Федеральный институт промышленной собственности»
(ФИПС)
Бережковская наб., 30, корп. 1, Москва, Г-59, ГСП-3, 125993
Телефон (8-499) 240- 60- 15. Факс (8-495) 531-63-18

Форма N 18 ИЗ-2017
100,181

ООО 'Юридическая фирма Городисский и Партнеры' ул. Большая Спасская, д.25, строение 3 Москва 129090
129090

На № 2403-533625RU от -
Наш № 2016123597/04(036880)
При переписке просим ссылаться на номер заявки и сообщить дату получения настоящей корреспонденции от *11.10.2018*

ЗАПРОС
экспертизы по существу

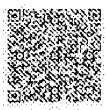
(21) Заявка № 2016123597/04(036880)

(22) Дата подачи заявки 28.01.2015

(71) Заявитель(и) ДАЙИТИ САНКИО КОМПАНИ, ЛИМИТЕД, JP

(51) МПК
A61K31/4745 (2006.01) ***A61K39/395*** (2006.01) ***A61P35/00*** (2006.01)

6		042610



ВОПРОСЫ, ДОВОДЫ, ЗАМЕЧАНИЯ, ПРЕДЛОЖЕНИЯ

Рассмотрев материалы заявки, экспертиза пришла к заключению о необходимости запроса дополнительных сведений, поскольку имеются препятствия для вынесения решения по заявке.

Заявитель просит установить конвенционный приоритет согласно первой заявке 2014-017777 от 31.01.2014, поданной в патентное ведомство JP.

К рассмотрению предложена первоначальная формула изобретения, состоящая из 27 пунктов и содержащая 6 объектов.

Обращаем внимание на нарушения в части составления формулы.

Согласно п.24.4.(3) Административного регламента****** устанавливается, имеется ли возможность понимания специалистом на основании уровня техники смыслового содержания признака.

Признак п.3 "-КДGGFG-" не обеспечивают возможность понимания, поскольку в однобуквенном написании аминокислотной последовательности присутствует русская буква "Д".

В связи с чем заявитель вправе скорректировать формулу с учетом указанных нарушений.

Экспертиза отмечает, что если установлено, что признак охарактеризован с нарушением условия, приведенного в подпункте (4) пункта 10.8 Административного регламента, но заявитель отказывается скорректировать формулу изобретения, заявка признается отозванной.

• Информация о состоянии делопроизводства по заявке может быть получена по телефону 8 (499) 240 60 15;

• Сведения о состоянии делопроизводства по заявкам размещаются на сайте ФИПС по адресу «www.fips.ru» в разделе «Информационные ресурсы / Открытые реестры»;

• При изменении адреса для переписки по заявке заявитель обязан сообщить об этом незамедлительно.

---

*Гражданский кодекс Российской Федерации Часть четвёртая от 18 декабря 2006 г. N 231-ФЗ с изменениями и дополнениями.

**Положение о патентных и иных пошлинах за совершение юридически значимых действий, связанных с патентом на изобретение, полезную модель, промышленный образец, с государственной регистрацией товарного знака и знака обслуживания, с государственной регистрацией и предоставлением исключительного права на наименование места происхождения товара, а также с государственной регистрацией отчуждения исключительного права на результат интеллектуальной деятельности или средство индивидуализации, залога исключительного права, предоставления права использования такого результата или такого средства по договору, перехода исключительного права на такой результат или такое средство без договора, утвержденное постановлением Правительства Российской Федерации от 10.12.2008 N 941 с изменениями.

***Административный регламент предоставления Федеральной службой по интеллектуальной собственности государственной услуги по государственной регистрации изобретения и выдаче патента на изобретение, его дубликата утвержден приказом Минэкономразвития России от 25.05.2016 года N 315, зарегистрирован 14.07.2016, регистрационный N 42843, с изменениями.

****Правила составления, подачи и рассмотрения документов, являющихся основанием для совершения юридически значимых действий по государственной регистрации изобретений, и их формы утверждены приказом Минэкономразвития России от 25.05.2016 N 316, зарегистрированы 11.07.2016, регистрационный N 42800.

*****Требования к документам заявки на выдачу патента на изобретение утверждены приказом Минэкономразвития России от 25.05.2016 N 316, зарегистрированы 11.07.2016, регистрационный N 42800.

Согласно п.10.8.1.5.(3) Административного регламента****** не следует излагать зависимый пункт формулы изобретения таким образом, что при этом происходит замена или исключение признаков изобретения, охарактеризованного в том пункте формулы, которому он подчинен.

Пункт 16 зависит от п.15 и включает признак "n^3 равно 2" и "L^2 является одинарной связью". Что заменяет признаки п.15, где "n^3 равно 5" и "L^2 является одинарной связью".

Пункт 17 зависит от п.15 и включает признаки "n^3 равно 5, L^2 является -NH-(CH_2CH_2-O)n^4-CH_2CH_2-C(=O)- и n^4 равно 4". Что заменяет признаки п.15, где "n^3 равно 2, L^2 является -NH-(CH_2CH_2-O)n^4-CH_2CH_2-C(=O)- и n^4 равно 2".

В связи с чем заявитель вправе скорректировать формулу с учетом указанных нарушений.

Согласно п.10.8.1.3.(1) Административного регламента****** пункт формулы включает признаки изобретения, в том числе родовое понятие, отражающее назначение, с которого начинается изложение формулы.

При этом в независимых п.п. 1, 14 не указано назначение "Конъюгата антитела с лекарственным средством ".

В связи с чем заявитель вправе скорректировать п.п. 1, 14 с учетом указанного нарушения.

Согласно п.10.8.1.4.(2) Административного регламента****** независимый пункт формулы изобретения должен относиться только к одному изобретению.

Независимые пункты 23, 27 относятся (каждый) к двум изобретениям, поскольку содержащаяся в них совокупность признаков (в частности: противоопухолевое лекарственное средство; противораковое лекарственное средство; способ лечения опухоли; способ лечения рака) включает характеристику изобретений, относящихся к совокупности средств, каждое из которых имеет собственное назначение, без реализации указанной совокупностью средств общего назначения.

В связи с чем заявитель вправе скорректировать п.п. 23, 27 с учетом указанного нарушения, например, путем создания нескольких независимых пунктов на основе каждого из п.п. 23, 27.

Относительно независимых п.п. 1, 14, 23, 27 сообщаем следующее.

В случае устранения нарушения в части составления формулы для указанных пунктов, они могут быть признаны соответствующими условиям патентоспособности.

Относительно независимых п.п. 22, 25, характеризующих лекарственное средство или фармацевтическую композицию, сообщаем следующее.

Согласно п. 24.5.1. (2) Административного регламента******, следует убедиться в том, что в случае осуществления изобретения по любому из пунктов формулы действительно возможна реализация указанного заявителем назначения.

Если о возможности осуществления изобретения и реализации им указанного назначения могут свидетельствовать лишь экспериментальные данные, проверяется наличие в описании изобретения примеров его осуществления с приведением соответствующих данных, а также устанавливается, являются ли приведенные примеры достаточными, чтобы вывод о соблюдении указанного требования распространялся на разные частные формы реализации признака, охватываемые понятием, приведенным заявителем в формуле изобретения.

В формуле изобретения родовое понятие, отражающее назначение, может быть указано как "фармацевтическая композиция" (или "лекарственное средство") без указания на механизм воздействия, биологической активности или предназначенности для лечения какого-либо заболевания. В этом случае следует проверить, приведены ли в описании изобретения сведения о возможности использования заявленной композиции для профилактики, диагностики и/или лечения значительного количества болезней различного этиопатогенеза или ее активности в отношении различных мишеней.

Если сведения, приведенные в описании изобретения, свидетельствуют, что указанная композиция, например, проявляет активность только в отношении определенного вида объектов, то такие сведения нельзя считать достаточными для подтверждения возможности реализации указанного в формуле изобретения назначения, охватываемого широким понятием "фармацевтическая композиция".

Сведения, приведенные в описании изобретения, свидетельствуют, что заявленная композиция (и лекарственное средство) проявляет активность только в отношении определенного вида объектов – лечения рака (примеры). Т.о такие сведения нельзя считать достаточными для подтверждения возможности реализации указанного в формуле изобретения назначения, охватываемого широким понятием "фармацевтическая композиция" (или "лекарственное средство").

Т.о. изобретения по п.п. 22, 25 не соответствуют условию патентоспособности "промышленная применимость", поскольку не подтверждена реализация назначения во всей широте заявленных притязаний (п. 24.5.1. (2) Административного регламента******).

Заявитель вправе указать назначение в п.п. 22, 25 в виде "фармацевтическая композиция для лечения рака" и "лекарственное средство для лечения рака", соответственно. При этом учесть, чтобы измененный п.22 не дублировал п.23.

Направляем Вам в приложении отчет о поиске на 1 л в 1 экз.

******Административный регламент исполнения Федеральной службой по интеллектуальной собственности, патентам и товарным знакам государственной функции по организации приема заявок на изобретение и их рассмотрения, экспертизы и выдачи в установленном порядке патентов Российской Федерации на изобретение утвержден приказом Министерства образования и науки Российской Федерации от 29 октября 2008 г. N 327, зарегистрированным Министерством юстиции Российской Федерации 20 февраля 2009 г. N 13413 (Бюллетень нормативных актов федеральных органов исполнительной власти, 2009, N 21).

Если заявитель **в трёхмесячный срок со дня направления запроса** не представит запрашиваемые материалы или не подаст ходатайство о продлении этого срока, заявка будет признана отозванной. Срок представления запрошенных материалов может быть продлен, но не более чем на десять месяцев (*общий срок продления не должен превышать десять месяцев*) (п. 6 ст. 1386 Кодекса*)

Продление срока ответа на запрос экспертизы осуществляется при условии уплаты соответствующей патентной пошлины в установленном порядке.

Дополнительные материалы, поданные заявителем, не должны изменять заявку на изобретение по существу (п. 2 ст. 1378 Кодекса*).

Дополнительные материалы представляются на ознакомление третьим лицам в соответствии с п. 2 ст. 1394 Кодекса* после публикации сведений о выдаче патента.

Главный государственный эксперт по интеллектуальной собственности отдела органической химии и фармацевтики ФИПС

Документ подписан электронной подписью
Сведения о сертификате ЭП
Сертификат 25155CA55794E992E81159CCEBFD784F
Владелец Орлова Татьяна Петровна
Срок действия с 10.10.2018 по 08.02.2027

Т. П. Орлова
8(499)240-61-58

Игумнов Д.Ю. 8(499)240-50-92

Форма № 18 ИЗ,ПМ-2011

Федеральная служба по интеллектуальной собственности
Федеральное государственное бюджетное учреждение
«Федеральный институт промышленной собственности»
(ФИПС)

ОТЧЕТ О ПОИСКЕ

1. ИДЕНТИФИКАЦИЯ ЗАЯВКИ

Регистрационный номер	Дата подачи
2016123597/04(036880)	28.01.2015
PCT/JP2015/000355	28.01.2015

Приоритет устанавлен по дате:
[ ] подачи заявки
[ ] поступления дополнительных материалов от к ранее поданной заявке №
[ ] приоритета по первоначальной заявке № из которой данная заявка выделена
[ ] подачи первоначальной заявки № из которой данная заявка выделена
[ ] подачи ранее поданной заявки №
[X] подачи первой(ых) заявки(ок) в государстве-участнике Парижской конвенции

(31) Номер первой(ых) заявки(ок)	(32) Дата подачи первой(ых) заявки(ок)	(33) Код страны
1. 2014-017777	31.01.2014	JP
2. 2014-168944	22.08.2014	JP
3. 2014-227886	10.11.2014	JP

Название изобретения (полезной модели): [X] - как заявлено; [ ] - уточненное (см. Примечания)
АНТИ-HER2 КОНЪЮГАТ АНТИТЕЛА С ЛЕКАРСТВЕННЫМ СРЕДСТВОМ

Заявитель: ДАЙИТИ САНКИО КОМПАНИ, ЛИМИТЕД, JP

2. ЕДИНСТВО ИЗОБРЕТЕНИЯ
[X] соблюдено [ ] не соблюдено. Пояснения: см. Примечания

3. ФОРМУЛА ИЗОБРЕТЕНИЯ:
[X] приняты во внимание все пункты
[ ] приняты во внимание следующие пункты: (см. Примечания)
[ ] принята во внимание измененная формула изобретения (см. Примечания)

4. КЛАССИФИКАЦИЯ ОБЪЕКТА ИЗОБРЕТЕНИЯ (ПОЛЕЗНОЙ МОДЕЛИ) (Указываются индексы МПК и индикатор текущей версии)

A61K 31/4745 (2006.01)
A61K 39/395 (2006.01)
A61P 35/00 (2006.01)

5. ОБЛАСТЬ ПОИСКА
5.1 Проверенный минимум документации PCT (указывается индексами МПК)
A61K 31/4745
A61K 39/395
A61P 35/00
5.2 Другая проверенная документация в той мере, в какой она включена в поисковые подборки:

5.3 Электронные базы данных, использованные при поиске (название базы, и если, возможно, поисковые термины):
DWPI, Espacenet, Google, PatSearch, PubMed, RUPTO, USPTO, Yandex

6. ДОКУМЕНТЫ, ОТНОСЯЩИЕСЯ К ПРЕДМЕТУ ПОИСКА

Кате-	Наименование документа с указанием (где необходимо) частей,	Относится к

(см. на обороте)

гория*	относящихся к предмету поиска	пункту формулы №
1	2	3
A	US 20030171262 A1 (DAIICHI PHARMACEUTICAL CO., LTD [JP]) 11.09.2003, реферат, [0002], [0042], таблица 1, пункты 1-26 формулы изобретения	1-27
A	BAROK M., et al., Trastuzumab-DM1 is highly effective in preclinical models of HER2-positive gastric cancer.Cancer Lett. 2011 Jul 28;306(2):171-9. doi: 10.1016/j.canlet.2011.03.002. Epub 2011 Apr 1., реферат	1-27
A	WENTE MN., et al., DE-310, a macromolecular prodrug of the topoisomerase-I-inhibitor exatecan (DX-8951), in patients with operable solid tumors.Invest New Drugs. 2005 Aug;23(4):339-47., реферат	1-27
A	OGUMA T., et al., Validation study of a method for assaying DE-310, a macromolecular carrier conjugate containing an anti-tumor camptothecin derivative, and the free drug in tumor tissue by high performance liquid chromatography/atmospheric pressure chemical ionization tandem mass spectrometry.Biomed Chromatogr. 2005 Jan;19(1):19-26., реферат	1-27

*Особые категории ссылочных документов:

«A» документ, определяющий общий уровень техники и не считающийся особо релевантным

«E» более ранний документ, но опубликованный на дату международной подачи или после нее

«L» документ, подвергающий сомнению притязание(я) на приоритет, или который приводится с целью установления даты публикации другого ссылочного документа, а также в других целях (как указано)

«O» документ, относящийся к устному раскрытию, использованию, экспонированию и т.д.

«P» документ, опубликованный до даты международной подачи, но после даты испрашиваемого приоритета

«T» более поздний документ, опубликованный после даты международной подачи или даты приоритета и не порочащий заявку, но приведенный для понимания принципа или теории, на которых основывается изобретение

«X» документ, имеющий наиболее близкое отношение к предмету поиска; заявленное изобретение не обладает новизной или изобретательским уровнем в сравнении с документом, взятым в отдельности

«Y» документ, имеющий наиболее близкое отношение к предмету поиска; заявленное изобретение не обладает изобретательским уровнем, когда документ взят в сочетании с одним или несколькими документами той же категории, такая комбинация документов очевидна для специалиста

«&» документ, являющийся патентом-аналогом

7. **ПРИМЕЧАНИЯ:**

8. **УДОСТОВЕРЕНИЕ ОТЧЕТА**

Настоящий отчет состоит из 1 л.

К отчету приложены копии ссылок на л. в экз.

Дата действительного завершения поиска: 08.10.2018

Должность и подпись уполномоченного лица:

ВГЭ по ИС. Игумнов Д.Ю.

Поисковый орган:
ФИПС
Бережковская наб., 30, корп. 1, Москва, Г-59, ГСП-3, 125993
Телефон (8-499) 240- 60- 15. Факс (8-495) 531- 63- 18;
e-mail: fips@rupto.ru

nature biotechnology

PERSPECTIVE

The discovery and development of brentuximab vedotin for use in relapsed Hodgkin lymphoma and systemic anaplastic large cell lymphoma

Peter D Senter & Eric L Sievers

Progress has been made recently in developing antibody-drug conjugates (ADCs) that can selectively deliver cancer drugs to tumor cells. In principle, the idea is simple: by attaching drugs to tumor-seeking antibodies, target cells will be killed and nontarget cells will be spared. In practice, many parameters needed to be addressed to develop safe and effective ADCs, including the expression profiles of tumor versus normal tissues, the potency of the drug, the linker attaching the drug and placement of the drug on the antibody, and the pharmacokinetic and stability profiles of the resulting ADC. All these issues had been taken into account in developing brentuximab vedotin (Adcetris), an ADC that recently received accelerated approval by the US Food and Drug Administration for the treatment of relapsed Hodgkin lymphoma and systemic anaplastic large cell lymphoma (ALCL). Research is under way to extend the applications of brentuximab vedotin and to advance the field by developing other ADCs with new linker and conjugation strategies.

The concept of targeting cancer cells with ADCs has roots that can be traced back more than a century, when the German immunologist Paul Ehrlich (Fig. 1) proposed that if toxic molecules could be selectively delivered to disease-causing cells, it would be possible to develop therapeutic modalities with specificities that were otherwise unattainable[1]. For treating cancer, this would require a targeting agent that selectively binds to tumor cell surface antigens, coupled with a cytotoxic drug that could kill the cells once delivered. Antibodies that have been selected to distinguish between tumor and non-tumor cells are ideally suited for this purpose because they are readily available, biologically compatible, minimally immunogenic and may circulate in the body for extended periods of time. The adaptation of antibodies to Ehrlich's vision is schematically represented in Figure 2, which shows how ADCs can elicit specific tumor cell killing either through receptor-mediated endocytosis[2–4] or extracellular drug release[5]. Target cells are killed if sufficient drug is selectively delivered, ideally sparing normal tissues from chemotherapeutic damage.

Whereas early ADC research was undertaken with available targeting reagents such as polyclonal antibodies to human tumor antigens[6], it was not until the development of monoclonal antibody (mAb) technology by Kohler and Milstein (Fig. 1) in 1975 (ref. 7) that tumor targeting became technologically feasible. Soon afterward, several pharmaceutical and biotech companies actively developed ADC programs for treating cancer, with an emphasis on proof-of-principle experiments using conventional anticancer drugs targeted to tumor types for which the drugs had been already approved. Unfortunately, advanced agents from this work, such as KS1/4–desacetylvinblastine hydrazide[8] (Eli Lilly; Indianapolis) in patients with metastatic adenocarcinomas, and BR96–doxorubicin (Adriamycin)[9] (Bristol-Myers Squibb; New York) in patients with metastatic breast cancer proved to be clinically unsuccessful. Shortcomings became evident, stemming from conjugate immunogenicity, low drug potency, antigen expression on normal tissues and instability of the linkers that joined the drugs to the mAbs.

Attention then turned to ADCs that contained highly potent cytotoxic drugs that were likely to be too toxic for use in an untargeted setting. The reasoning was that the limitations of intratumoral macromolecular uptake[10] could be overcome if very few drug molecules were required to kill the target cell. Higher drug potency necessitated both choosing target antigens judiciously as well as addressing the immunogenic properties of the mAb carrier to avoid high ADC and immune complex concentrations in normal tissues. With these parameters in mind, gemtuzumab ozogamicin (Mylotarg) was developed by Wyeth (now part of Pfizer, New York) and Celltech (now part of UCB, Brussels) for the treatment of acute myeloid leukemia (AML)[11]. The drug consisted of an anti-CD33 mAb conjugated with a derivative of calicheamicin, a highly potent enediyne antibiotic. Despite encouraging clinical results that led to accelerated approval of gemtuzumab ozogamicin in 2000, a subsequent phase 3 confirmatory trial raised new concerns about the product's safety and failure to demonstrate clinical benefit[12,13]. In 2010, Pfizer voluntarily withdrew the drug from the US market. Subsequent findings in three additional randomized trials comparing standard induction chemotherapy with and without gemtuzumab ozogamicin in newly diagnosed AML patients stood in contrast to the phase 3 confirmatory study and suggested clinical benefit among certain patients—those whose AML was characterized by either 'good' or 'intermediate' risk cytogenetics[14–16]. The impact that the different phase 3 trials might have on the future development of gemtuzumab ozogamicin as a drug remains for global regulatory bodies to determine.

Several lessons can be taken from the gemtuzumab ozogamicin development program. Calicheamicin is hydrophobic, and only a few drugs can be conjugated before high levels of aggregated protein are obtained. Consequently, the manufacturing process used at the time gemtuzumab

Seattle Genetics, Bothell, Washington, USA. Correspondence should be addressed to P.D.S. (psenter@seagen.com).

Published online 10 July 2012; doi:10.1038/nbt.2289

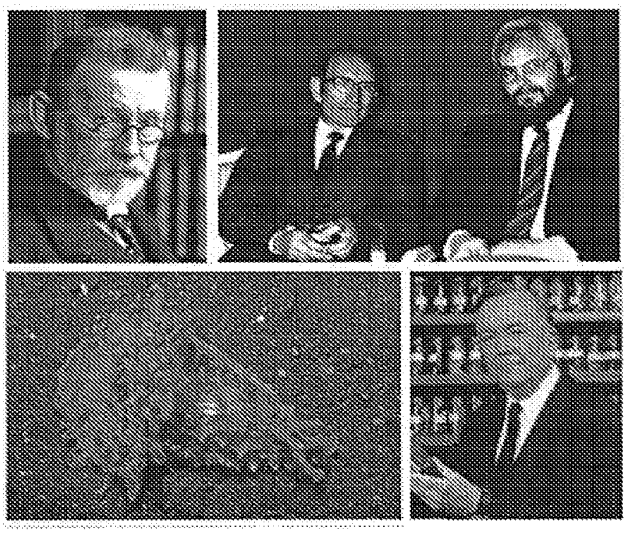


Figure 1 Some of the key players that helped advance ADC technology. Paul Ehrlich proposed the concept of 'magic bullets' in the early 1900s (top left). In 1975, César Milstein and George Köhler described how mAbs with exquisite specificities could be produced (top right). George Pettit extracted highly potent cytotoxins from natural sources (bottom right), such as the Indian Ocean sea hare (*Dolabela auricularia*, bottom left), that eventually led us to the discovery and development of the drug component of brentuximab vedotin.

ozogamicin was developed yielded 50% unconjugated mAb in the final drug product[17,18]. The linker between calicheamicin and the mAb released 50% of bound drug in 48 h[19]. Finally, the drug component was derived from a soil microorganism, which restricted the ability to design new forms to circumvent these limitations.

Here we describe how each of these issues was addressed in the design and development of brentuximab vedotin, a clinically effective ADC for the treatment of Hodgkin lymphoma and systemic ALCL.

Selecting the right drug-linker

In developing the ADC platform technology described here, we took a lesson from the Indian Ocean sea hare, *Dolabela auricularia* (Fig. 1), which has been known for more than 2,000 years to harbor highly toxic extractable substances to protect itself from being eaten. George Pettit (Fig. 1) and co-workers characterized several toxic components from the sea hare that exhibited activities against cancer cell lines and elucidated the structure and mechanism of dolastatin 10 (Fig. 3), one of the most potent antimitotic agents ever described[20]. Several related molecules have been produced through total synthesis[21], establishing that the drug class, now known as the auristatins, could be prepared in large quantities. Like the vinca alkaloids, the auristatins exert anticancer activity by inhibiting tubulin polymerization. A phase 2 clinical trial with dolastatin 10 in patients with advanced breast cancer confirmed the drug's high toxicity[22]. Although minimal clinical benefit was obtained at the optimal dose of 0.4 mg m^{-2}, this did not diminish our interest in the class because we established combinatorial routes to the synthesis of thousands of auristatins that allowed us to fully explore linker technologies, and the effects of hydrophilicity, stability and potency on ADC activity. This work led to monomethyl auristatin E (MMAE; Fig. 3), a synthetic analog of dolastatin 10 that had high potency, water solubility and stability under physiological conditions, together with a built-in functionality for stable linker attachment. These were qualities in the cytotoxic component of the ADC that we deemed to be highly important for optimal activity[23].

We considered several linker technologies, including acid-labile hydrazones such as those present on gemtuzumab ozogamicin and BR96–doxorubicin, and disulfides that had been used for maytansinoid-containing ADCs[24]. After exploring possibilities along these lines, our attention was drawn to protease-cleavable linkers because protease activity is abundant in lysosomes, where ADCs commonly traffic, and is almost absent outside cells because of modulation by secreted protease inhibitors[25]. We could readily attach MMAE to suitable peptides through the N-terminal amine via a self-immolative spacer, *p*-aminobenzyloxycarbonyl (PABC). The purpose of the spacer is to situate the cleavable peptide away from the drug to allow facile proteolysis. Upon peptide cleavage, the PABC group rapidly fragments, leading to the release of MMAE in chemically unmodified form. The dipeptide we selected from among many was valine-citrulline (Val-Cit), which is stable in the plasma but is very rapidly hydrolyzed by lysosomal enzymes, such as cathepsin B[23,25]. We used a maleimide functionality to attach the spacer to mAb cysteine residues. In the mouse, the *in vivo* half-life of the linker we used to bind the drug to the mAb was in the range of a week[26], which was a major advancement over many of the previously reported technologies for generating ADCs. The structure of the resulting mAb-Val-Cit-PABC-MMAE is shown in Figure 3.

Establishing appropriate conjugation technology

The number of molecules of the drug and where they reside on the mAb carrier can impact ADC pharmacokinetics, tumor exposure and stability in the circulation[27,28]. Because of this, we and others have focused considerable attention on conjugation technology, which has resulted in a variety of methods that provide different drug configurations and different degrees of product heterogeneity (Fig. 4). The greatest number of species is obtained when drugs are linked through mAb lysine residues, which was the case with gemtuzumab ozogamicin[17] and the breast cancer drug trastuzumab emtansine (T-DM1; Herceptin conjugated to a derivative of maytansine; Genentech, South, San Francisco, CA, USA)[29]. This is due to a small number of drugs, on average four, distributed among the large number of lysines scattered throughout the antibody structure. In contrast, less heterogeneity is obtained by either reacting all IgG interchain cysteines with the drug[23]

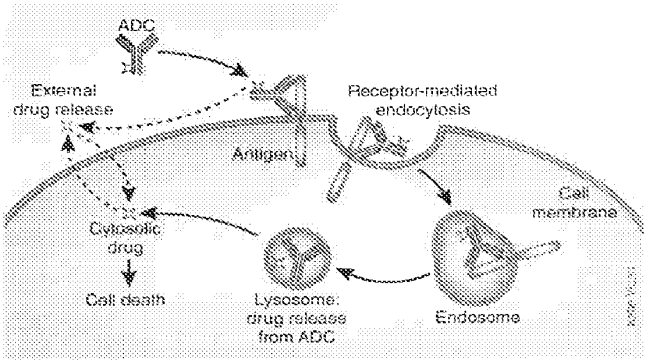


Figure 2 Mechanisms of drug delivery mediated by ADCs. Upon binding to tumor cell surface antigens, a drug conjugated to a mAb is internalized by a process known as receptor-mediated endocytosis, which can lead to drug release inside the target cell[2–4]. Alternatively, if the mAb remains bound to the antigen on the cell surface, extracellular drug release may take place, depending on the antigen that is targeted and the mode of drug attachment[5].

or using recombinant technologies that define particular cysteines for conjugation[28,30,31]. Between these extremes lies partial substitution of interchain disulfides, the method we eventually adopted.

IgGs contain reducible disulfide bonds that covalently link the heavy and light chains together. Initially, our group[23] produced highly uniform ADCs with eight drugs per antibody molecule, using all available cysteine residues generated upon mAb reduction. The resulting ADCs remained intact in the absence of the disulfides, consistent with previous reports that mAbs devoid of any interchain disulfide bonds are fully active[32]. Because the drugs were distal to the antigen-binding sites, antigen binding was not affected. However, subsequent studies demonstrated that such heavily loaded antibodies were rapidly cleared from the circulation, most likely due to differences in overall ADC hydrophobicity, and had reduced therapeutic windows compared with similarly prepared conjugates having an average of four auristatin drugs per antibody[27]. Reproducible technologies were therefore established to generate ADCs with an average of four drugs per mAb, and analytical methodologies, including liquid chromatography–mass spectrometry and hydrophobic interaction chromatography were developed to characterize the products present in the conjugation mixture[27,33]. The resulting ADCs contained primarily two, four and six molecules of drug per mAb, with four drugs per mAb being predominant. Small amounts of ADCs with 0 and 8 drugs per mAb (~8% each) were also obtained. All of the conjugated drugs resided among the heavy-heavy chain and heavy-light chain reduced disulfides. Notably, the use of partial reduction conjugation technology to generate four-loaded auristatin ADCs was applicable to nearly all IgGs tested and could be performed at scales ranging from micrograms to kilograms[34]. The yields were in the range of 95%, binding affinity was preserved and purified ADCs with minimal (<2%) aggregation levels were obtained in less than a day.

The target is critical

In choosing an appropriate antigen for the application of auristatin-based ADCs, we selected targets that were highly expressed on tumor cells, with minimal expression on normal tissues. This was motivated by the extreme potency (~10–100 pM) of four MMAE–containing ADCs[27] and information obtained from previous clinical trials with agents such as BR96-doxorubicin[9] and anti-CD44v6-DM1 (ref. 35), where target-related dose-limiting toxicities had been observed. Thus, although several target antigens have been successfully used in preclinical ADCs that contain peptide-linked auristatins[2–4], we focused on those that provided the highest levels of tumor selectivity.

CD30 is an ideal target for selective drug delivery. The antigen is highly expressed in Hodgkin lymphoma, ALCL, cutaneous T-cell lymphoma and other selected lymphoid tumors, as well as in some nonlymphoid malignancies including germ cell cancers[36]. Cross-reactivity of CD30 on normal tissues is very low, with some expression on activated, but not resting, T and B cells. CD30 is a tumor necrosis factor receptor (TNFR) superfamily member, which stimulates apoptosis[37] via TNFR-associated factor 2 degradation[38]. Because of its expression profile and its role in the regulation of cell survival, considerable interest has surrounded CD30 as a target both for anti-CD30 mAbs and for ADCs.

Hodgkin lymphoma and systemic ALCL represent substantial unmet medical needs.

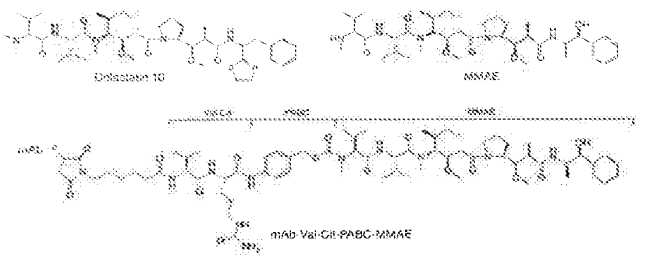


Figure 3 Structures of highly potent antimitotic drugs. Dolastatin 10 was isolated from *D. auricularia*, whereas MMAE was derived from total synthesis. MMAE is released from the mAb conjugate by proteolysis of the Val-Cit dipeptide, followed by elimination of the PABC group.

Although front-line Hodgkin lymphoma therapy with ABVD (doxorubicin (Adriamycin), bleomycin (Blenoxane), vinblastine and dacarbazine (DTIC)) and BEACOPP (bleomycin, etoposide (Vepesid), doxorubicin (Adriamycin), cyclophosphamide (Cytoxan), vincristine (Oncovin), procarbazine (Matulane) and prednisone) results in high remission rates, up to 20% of the patients are refractory and advanced-stage patients often relapse[39]. CHOP (cyclophosphamide, doxorubicin, vincristine and prednisone) therapy is used in front-line systemic ALCL treatment, but in ~40–65% of patients, the disease recurs[40]. We envisioned that targeted drug delivery through the CD30 antigen on Hodgkin lymphoma and systemic ALCL could be a novel approach to the treatment of these malignancies.

Clinical trials have been reported for unconjugated anti-CD30 mAbs. MDX-060, a fully human mAb, has been tested in a phase 1/2 trial in patients with Hodgkin lymphoma, ALCL and cutaneous T-cell lymphoma[41]. The unconjugated antibody was well tolerated and provided some evidence of clinical activity, with overall response rates (ORRs) that included complete and partial responses of 6% in Hodgkin lymphoma (4 of 63 patients) and 29% in ALCL (2 of 7 patients, both complete responses). Similar results were obtained with SGN-30, a chimeric mAb also known as cAC10 (ref. 37). Patients with Hodgkin lymphoma and ALCL were given high doses (6 or 12 mg kg^{-1}) SGN-30 weekly in a phase 2 clinical trial[42]. There were no objective responses in Hodgkin lymphoma patients, although 29% of these patients experienced stable

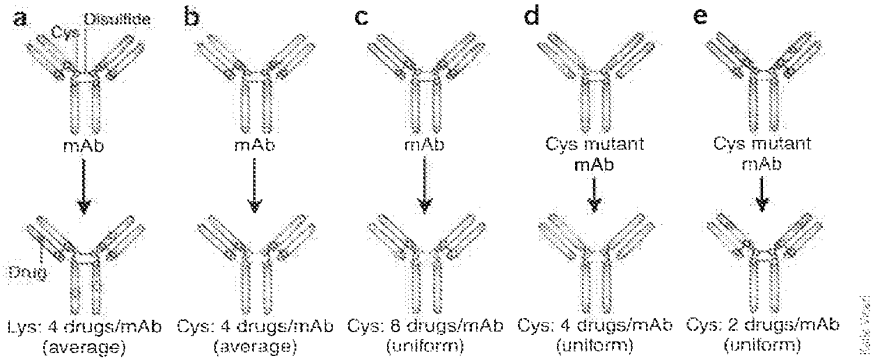


Figure 4 Drug-conjugation strategies. (a,b) Random distribution of the drugs on the mAb lysine groups (a)[18,24] leads to the higher levels of heterogeneity than attachment of the drugs to cysteine residues generated upon mAb reduction (b)[23]. (c–e) The least amount of heterogeneity is obtained by reacting all the interchain disulfides with drug[23] (c) and using engineered mAbs that have defined sites for available cysteine reactivity (d,e).

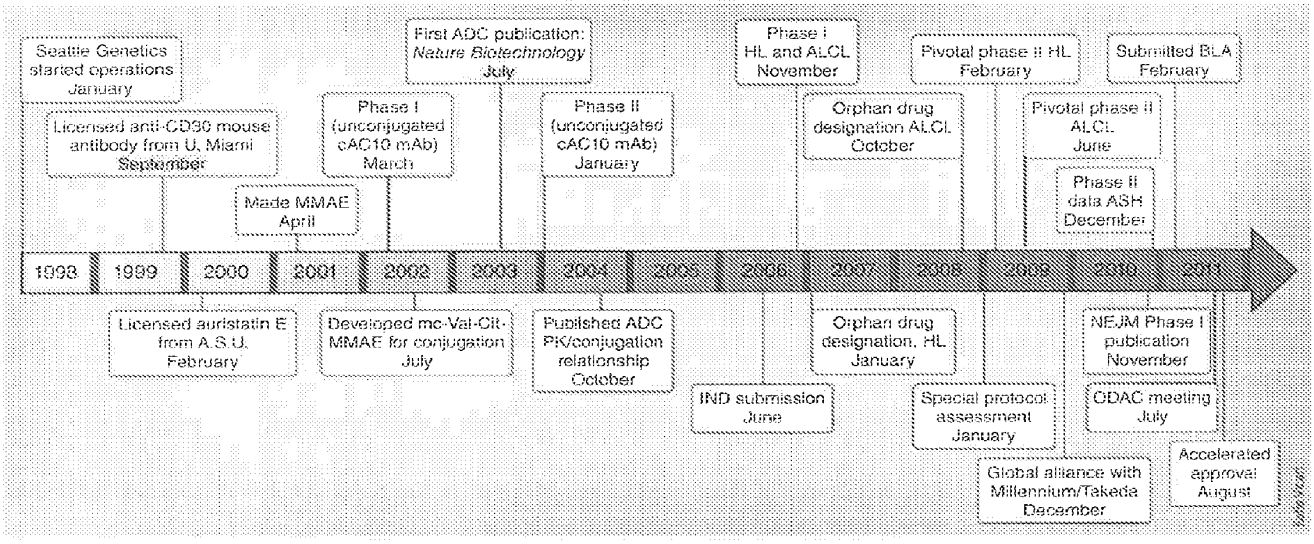


Figure 5 Some important milestones that led to accelerated approval of brentuximab vedotin. The initial work (1998–2004) surrounded the development of the mAb (cAC10), drug (MMAE) and linker (mc-Val-Cit) components, conjugation technology and preclinical activities. Clinical work with brentuximab vedotin commenced in November 2006, leading to accelerated approval on 19 August 2011. ASH, American Society of Hematology; ASU, Arizona State University; IND, investigational new drug; BLA, biologics license application; NEJM, New England Journal of Medicine; ODAC, Oncology Drugs Advisory Committee.

disease while on drug. Among ALCL patients, 5% (2 of 41 patients) achieved complete responses and 12% (5 of 41 patients) had partial responses. The response rate in a phase 1 Hodgkin lymphoma trial with an anti-CD30–ricin A chain conjugate was also quite modest[43]. Thus, although these agents were not promising enough to warrant clinical development, the data obtained, together with the antigen expression profile, supported development of an optimized and highly potent anti-CD30 ADC for the treatment of CD30-positive malignancies.

Development of brentuximab vedotin

We applied the technology described using the highly potent auristatin derivative MMAE, a protease-cleavable dipeptide linker, and a reproducible and robust method for generating active ADCs to the cAC10 mAb (chimeric IgG1), the same antibody that had been used in an unconjugated form in the Hodgkin lymphoma/ALCL phase 2 clinical trial just described. cAC10-Val-Cit-PABC-MMAE, now known as brentuximab vedotin, comprising on average four molecules of MMAE attached to cAC10 interchain cysteine residues through the protease-cleavable Val-Cit-PABC linker. The timeline for the development of this molecule from its constitutive components to accelerated approval on 19 August 2011 is illustrated in Figure 5.

Typical preparations of brentuximab vedotin contained less than 2% aggregated protein and bound to CD30 with unaltered affinity (3 nM) compared with the nonconjugated antibody[27,44]. The conjugate was highly potent against CD30$^+$ Hodgkin lymphoma and ALCL tumor cells *in vitro*, with half-maximal inhibitory concentration (IC_{50}) values of 3–50 pM (0.5–8 ng ml^{-1}). The effects were antigen-selective because non–CD30-expressing cells were ~1,000 times less sensitive to the effects of the ADC.

In vivo therapy studies in immunodeficient mice established that single-dose brentuximab vedotin regressed and cured established human Hodgkin lymphoma[30] and ALCL[27] tumor xenografts at doses of 1–3 mg kg^{-1}. With a maximum tolerated dose (MTD) of ~100 mg kg^{-1} in mice, the therapeutic window was pronounced[27]. Also favorable was the half-life of brentuximab vedotin, which was 14 d in mice compared with 16.7 d for the unconjugated antibody[27]. Finally, the ADC could be combined with chemotherapeutic agents used in treating Hodgkin lymphoma[45]. These studies provided the rationale for putting brentuximab vedotin into the clinic.

A phase 1 dose-escalation trial for brentuximab vedotin was initiated in 2006 in patients with CD30$^+$ malignancies[46]. Treatment was every three weeks at doses ranging from 0.1 mg kg^{-1} to 3.6 mg kg^{-1} delivered intravenously. The trial was designed to determine the MTD of the drug, with secondary objectives that included characterization of pharmacokinetics and antitumor activities. At 1.8 mg kg^{-1} every three weeks (the MTD), objective responses were obtained, including complete responses (4 of 12 patients) and partial responses (2 of 12 patients). The ORR (complete and partial responses) among all 45 patients in the trial was 38%, which included a 24% complete-response rate. During the study, low titers of antitherapeutic antibody were found in two of 40 patients tested. A second phase 1 trial of brentuximab vedotin was carried out to test its effects when administered weekly[47]. The dosing range was 0.4–1.4 mg kg^{-1}, the MTD was 1.2 mg kg^{-1} and the ORR was 59%, with 34% complete responses. The most common adverse events in both trials were peripheral sensory neuropathy, neutropenia, fatigue, nausea and diarrhea.

Encouraging data from the phase 1 trials served as a foundation for paired prospective, single-arm pivotal phase 2 trials that enrolled patients with relapsed or refractory Hodgkin lymphoma or systemic ALCL, respectively. The primary endpoint of both trials was ORR by independent radiographic review. In the Hodgkin lymphoma trial, patients were required to have had lymphoma that was progressive or recurrent after prior autologous stem cell transplant[48]. Tumor reductions were observed in 94% of the 102 enrolled Hodgkin lymphoma patients (Fig. 6) and the ORR was 75%. Complete responses were achieved in 34% of patients; the median duration of these responses was 20.5 months at the time of publication[48]. Similarly, among 58 patients with relapsed or refractory systemic ALCL, the ORR was 86%, and

57% of the patients experienced complete responses with a median duration of 13.2 months[40]. The most common adverse events in these paired pivotal trials were peripheral sensory neuropathy, nausea, fatigue, neutropenia and diarrhea. In August 2011, the US Food and Drug Administration (FDA; Rockville, MD, USA) granted accelerated approval for the use of brentuximab vedotin in relapsed Hodgkin lymphoma and relapsed systemic ALCL. Brentuximab vedotin is the only ADC currently approved for use, and it is the first approved drug for treating Hodgkin lymphoma in 30 years.

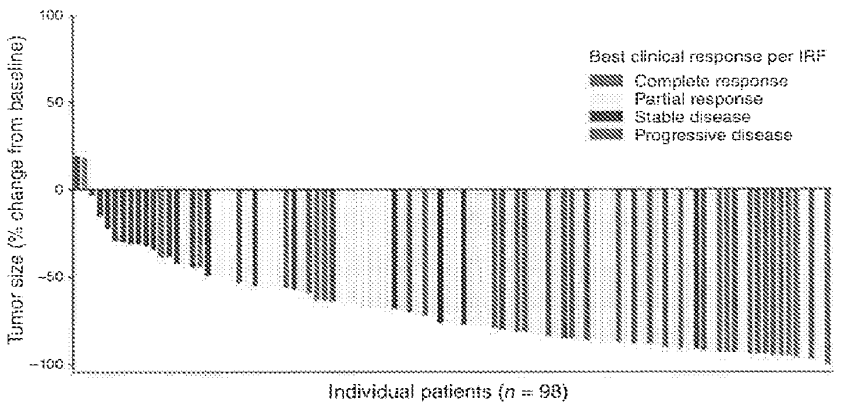


Figure 6 Maximum percentage reduction in the sum of the product of tumor diameters in individual patients (n = 98) per Cheson *et al.*[65]. Tumor size reductions were observed in 96 (94%) of 102 patients in the pivotal phase II Hodgkin lymphoma clinical trial[48]. Reprinted with permission from ref. 48. IRF, Independent review facility.

Prospects for the future

The power of ADC technology is evident by comparing the clinical activities of advanced conjugates with those of unconjugated antibodies that bind the same antigens. A phase 2 clinical trial with unconjugated cAC10 provided 0% ORR in Hodgkin lymphoma and 17% ORR in ALCL[42], in stark contrast to the results obtained with brentuximab vedotin: a 75% ORR for Hodgkin lymphoma[48] and 86% ORR in ALCL[40]. Consequently, several studies are ongoing with brentuximab vedotin and other auristatin-based ADCs. A randomized, placebo-controlled phase 3 trial (the AETHERA trial) is under way in Hodgkin lymphoma patients at high risk of progression after autologous stem cell transplant. Phase 2 trials are ongoing in patients with CD30$^+$ B- and T-cell lymphoma and non-lymphomatous malignancies. Phase 1 trials have also been initiated to explore the activities of brentuximab vedotin in combination with chemotherapy for the treatment of front line Hodgkin lymphoma and CD30$^+$ mature T-cell lymphomas. We and our collaborators are exploring the applicability of the ADC technology for other antigen targets in more than 15 active clinical trials. These include a phase 2 trial of CDX-011 (anti-glycoprotein nonmetastatic melanoma protein B mAb-Val-Cit-MMAE ADC) for the treatment of breast cancer and melanoma[49] and phase 1 trials in many other hematologic malignancies and solid tumors. In the next two years, we expect that a tremendous amount of new data will be available on how the auristatin technology applies to other cancer indications and other antigen targets.

New data will also be emerging for other ADCs in advanced clinical development. These include T-DM1, an ADC comprising the anti-HER2 mAb trastuzumab conjugated with an antimitotic maytansinoid anticancer drug for the treatment of HER2-positive breast cancer[29]. Trastuzumab is typically used in combination chemotherapy but has single-agent activity ranging from 15% to 26%[50–52]. T-DM1 is not only more active with ORRs of 25–64%, but offers an improved safety profile compared with traditional chemotherapy in phase 2 clinical trials[29,53–56]. The drug is currently in two randomized phase 3 clinical trials. The EMILIA trial is investigating T-DM1 activity against the lapatinib and capecitabine combination in patients who failed prior trastuzumab-based therapies for metastatic breast cancer. The MARIANNE trial is a randomized study comparing the effects of single-agent T-DM1, T-DM1 plus pertuzumab and trastuzumab drug combinations in front-line therapy for advanced metastatic breast cancer.

Another ADC of interest is inotuzumab ozogamicin, an anti-CD22–calicheamicin conjugate in a phase 3 clinical trial for the treatment of acute lymphocytic leukemia (ALL[57]). As with gemtuzumab ozogamicin, the cytotoxic component kills cells by binding to the minor groove of DNA and inducing double-strand breaks. In phase 1/2 clinical trials, the anti-CD22 mAb epratuzumab gave 18% ORR in indolent non-Hodgkin lymphoma[58]. A recently reported phase 2 clinical trial of inotuzumab ozogamicin in patients with relapsed ALL demonstrated a 57% ORR, with 18% (9 of 49 patients) having complete responses. This highly potent ADC (phase 2 dose 1.8 mg m^{-2}) has promising indications for the treatment of refractory and relapsed ALL.

Whereas much of the focus on ADCs is on how they perform clinically, the field is rapidly advancing and expanding owing to substantial technological advancements in conjugate design and composition. Beyond the auristatin, maytansinoid and calicheamicin drug components described here, new highly potent drugs for ADCs are emerging with distinct mechanisms of activity. These include duocarmycins[59] and pyrrolobenzodiazepine dimers[60], both of which alkylate DNA after binding to the minor groove, the RNA polymerase inhibitor amanitin[61] and many others.

Great strides have also been made in conjugation technology. As noted above, lysine and native mAb cysteine modification lead to multiple ADC species that differ in potency and pharmacokinetics. Site-specific introduction of cysteine residues into the antibody structure has been used to make highly uniform ADCs that not only have pronounced activities[31], but may also provide levels of stability beyond what can be achieved normally[28]. Research is under way to exploit these findings and to extend them by introducing unnatural or modified amino acids into antibody structures for the purposes of specific drug attachment[62,63]. New scaffolds for drug delivery that differ from mAbs in substantial ways are also under investigation, and studies with them should provide insights into the effects of size, clearance and distribution on therapeutic efficacy[64].

Thus, the approval of brentuximab vedotin represents not only an advancement for the treatment of relapsed Hodgkin lymphoma and systemic ALCL but also a major milestone for ADCs as a whole. This biologic drug evolved over many years, as insights had been made into the structure-activity relationship of the auristatins, new linker technologies and conjugation protocols were developed, and the merits of targeting the CD30 antigen became apparent. The role of ADCs in chemotherapy of cancer is likely to grow in the near future, as existing

molecules advance toward approval and technological innovations, such as those reported here, are put into practice.

ACKNOWLEDGMENTS

We are grateful for meaningful and enduring contributions by our colleagues at Seattle Genetics and various international cancer centers, our corporate partner, Millennium, the Takeda Oncology Company and to patients with life-threatening lymphoma, who collectively participated in clinical trials of brentuximab vedotin —ultimately leading to its approval by the FDA.

COMPETING FINANCIAL INTERESTS

The authors declare competing financial interests: details are available in the online version of the paper.

Published online at http://www.nature.com/doifinder/10.1038/nbt.2289.
Reprints and permissions information is available online at http://www.nature.com/reprints/index.html.

1. Schwartz, R.S. Paul Ehrlich's magic bullets. *N. Engl. J. Med.* **350**, 1079–1080 (2004).
2. Senter, P.D. Potent antibody drug conjugates for cancer therapy. *Curr. Opin. Chem. Biol.* **13**, 235–244 (2009).
3. Carter, P.J. & Senter, P.D. Antibody-drug conjugates for cancer therapy. *Cancer J.* **14**, 154–169 (2008).
4. Wu, A.M. & Senter, P.D. Arming antibodies: prospects and challenges for immunoconjugates. *Nat. Biotechnol.* **23**, 1137–1146 (2005).
5. Bernardes, G.J. *et al.* A traceless vascular-targeting antibody-drug conjugate for cancer therapy. *Angew. Chem. Int. Edn Engl.* **51**, 941–944 (2012).
6. Arnon, R. & Sela, M. In vitro and in vivo efficacy of conjugates of daunomycin with anti-tumor antibodies. *Immunol. Rev.* **62**, 5–27 (1982).
7. Köhler, G. & Milstein, C. Continuous cultures of fused cells secreting antibody of predefined specificity. *Nature* **256**, 495–497 (1975).
8. Petersen, B.H., DeHerdt, S.V., Schneck, D.W. & Burnol, T.F. The human immune response to KS1/4-desacetylvinblastine (LY256787) and KS1/4-desacetylvinblastine hydrazide (LY203728) in single and multiple dose clinical studies. *Cancer Res.* **51**, 2286–2290 (1991).
9. Tolcher, A.W. *et al.* Randomized phase II study of BR96-doxorubicin conjugate in patients with metastatic breast cancer. *J. Clin. Oncol.* **17**, 478–484 (1999).
10. Jain, R.K. Tumor physiology and antibody delivery. *Front. Radiat. Ther. Oncol.* **24**, 32–46 (1990).
11. Sievers, E.L. & Linenberger, M. Mylotarg: antibody-targeted chemotherapy comes of age. *Curr. Opin. Oncol.* **13**, 522–527 (2001).
12. Petersdorf, S. et al. Preliminary results of Southwest Oncology Group Study SO106: an international intergroup phase 3 randomized trial comparing the addition of gemtuzumab ozogamicin to standard induction therapy versus standard induction therapy followed by a second randomization to post-consolidation gemtuzumab ozogamicin versus no additional therapy for previously untreated acute myeloid leukemia. *Blood* **114**, abstract 790 (2009). Paper presented at the American Society of Hematology National Meeting, New Orleans, December 5–9, 2009.
13. Ravandi, F. Gemtuzumab ozogamicin: one size does not fit all—the case for personalized therapy. *J. Clin. Oncol.* **29**, 349–351 (2011).
14. Burnett, A.K. *et al.* Identification of patients with acute myeloblastic leukemia who benefit from the addition of gemtuzumab ozogamicin: results of the MRC AML15 trial. *J. Clin. Oncol.* **29**, 369–377 (2011).
15. Castaigne, S. *et al.* Effect of gemtuzumab ozogamicin on survival of adult patients with de novo acute myeloid leukaemia (ALFA-0701): a randomised, open-label, phase 3 study. *Lancet* **379**, 1508–1516 (2012).
16. Walter, R.B., Appelbaum, F.R., Estey, E.H. & Bernstein, I.D. Acute myeloid leukemia stem cells and CD33-targeted immunotherapy. *Blood* advance online publication, doi:10.1182/blood-2011-11-325050 (27 January 2012).
17. Bross, P.F. *et al.* Approval summary: gemtuzumab ozogamicin in relapsed acute myeloid leukemia. *Clin. Cancer Res.* **7**, 1490–1496 (2001).
18. Hollander, I., Kunz, A. & Hamann, P.R. Selection of reaction additives used in the preparation of monomeric antibody-calicheamicin conjugates. *Bioconjug. Chem.* **19**, 358–361 (2008).
19. Boghaert, E.R. *et al.* Determination of pharmacokinetic values of calicheamicin-antibody conjugates in mice by plasmon resonance analysis of small (5 microl) blood samples. *Cancer Chemother. Pharmacol.* **61**, 1027–1035 (2008).
20. Pettit, G.R. *et al.* The isolation and structure of a remarkable marine animal antineoplastic constituent: dolastatin 10. *J. Am. Chem. Soc.* **109**, 6883–6885 (1987).
21. Pettit, G.R. *et al.* Antineoplastic agents 365. Dolastatin 10 SAR probes. *Anticancer Drug Des.* **13**, 243–277 (1998).
22. Perez, E.A. *et al.* Phase II trial of dolastatin-10 in patients with advanced breast cancer. *Invest. New Drugs* **23**, 257–261 (2005).
23. Doronina, S.O. *et al.* Development of potent monoclonal antibody auristatin conjugates for cancer therapy. *Nat. Biotechnol.* **21**, 778–784 (2003).
24. Chari, R.V. Targeted cancer therapy: conferring specificity to cytotoxic drugs. *Acc. Chem. Res.* **41**, 98–107 (2008).
25. Dubowchik, G.M., Mosure, K., Knipe, J.O. & Firestone, R.A. Cathepsin B-sensitive dipeptide prodrugs. 2. Models of anticancer drugs paclitaxel (Taxol), mitomycin C and doxorubicin. *Bioorg. Med. Chem. Lett.* **8**, 3347–3352 (1998).
26. Alley, S.C. *et al.* Contribution of linker stability to the activities of anticancer immunoconjugates. *Bioconjug. Chem.* **19**, 759–765 (2008).
27. Hamblett, K.J. *et al.* Effects of drug loading on the antitumor activity of a monoclonal antibody drug conjugate. *Clin. Cancer Res.* **10**, 7063–7070 (2004).
28. Shen, B.Q. *et al.* Conjugation site modulates the *in vivo* stability and therapeutic activity of antibody-drug conjugates. *Nat. Biotechnol.* **30**, 184–189 (2012).
29. LoRusso, P.M., Weiss, D., Guardino, E., Girish, S. & Sliwkowski, M.X. Trastuzumab emtansine: a unique antibody-drug conjugate in development for human epidermal growth factor receptor 2-positive cancer. *Clin. Cancer Res.* **17**, 6437–6447 (2011).
30. McDonagh, C.F. *et al.* Engineered antibody-drug conjugates with defined sites and stoichiometries of drug attachment. *Protein Eng. Des. Sel.* **19**, 299–307 (2006).
31. Junutula, J.R. *et al.* Site-specific conjugation of a cytotoxic drug to an antibody improves the therapeutic index. *Nat. Biotechnol.* **26**, 925–932 (2008).
32. Andersen, D.C. & Reilly, D.E. Production technologies for monoclonal antibodies and their fragments. *Curr. Opin. Biotechnol.* **15**, 456–462 (2004).
33. Sun, M.M. *et al.* Reduction-alkylation strategies for the modification of specific monoclonal antibody disulfides. *Bioconjug. Chem.* **16**, 1282–1290 (2005).
34. Lyon, R.P., Meyer, D.L., Setter, J.R. & Senter, P.D. Conjugation of anticancer drugs through endogenous monoclonal antibody cysteine residues. *Methods Enzymol.* **502**, 123–138 (2012).
35. Tijink, B.M. *et al.* A phase I dose escalation study with anti-CD44v6 bivatuzumab mertansine in patients with incurable squamous cell carcinoma of the head and neck or esophagus. *Clin. Cancer Res.* **12**, 6064–6072 (2006).
36. Deutsch, Y.E., Tadmor, T., Podack, E.R. & Rosenblatt, J.D. CD30: an important new target in hematologic malignancies. *Leuk. Lymphoma* **52**, 1641–1654 (2011).
37. Wahl, A.F. *et al.* The anti-CD30 monoclonal antibody SGN-30 promotes growth arrest and DNA fragmentation in vitro and affects antitumor activity in models of Hodgkin's disease. *Cancer Res.* **62**, 3736–3742 (2002).
38. Duckett, C.S. & Thompson, C.B. CD30-dependent degradation of TRAF2: implications for negative regulation of TRAF signaling and the control of cell survival. *Genes Dev.* **11**, 2810–2821 (1997).
39. Connors, J.M. State-of-the-art therapeutics: Hodgkin's lymphoma. *J. Clin. Oncol.* **23**, 6400–6408 (2005).
40. Pro, B. *et al.* Brentuximab vedotin (SGN-35) in patients with relapsed or refractory systemic anaplastic large cell lymphoma: results of a phase 2 study. *J. Clin. Oncol.* advance online publication doi:10.1200/JCO.2011.38.0402 (21 May 2012).
41. Ansell, S.M. *et al.* Phase I/II study of an anti-CD30 monoclonal antibody (MDX-060) in Hodgkin's lymphoma and anaplastic large-cell lymphoma. *J. Clin. Oncol.* **25**, 2754–2763 (2007).
42. Forero-Torres, A. *et al.* A phase II study of SGN-30 (anti-CD30 mAb) in Hodgkin lymphoma or systemic anaplastic large cell lymphoma. *Br. J. Haematol.* **146**, 171–179 (2009).
43. Schnell, R. *et al.* A Phase I study with an anti-CD30 ricin A-chain immunotoxin (Ki-4.dgA) in patients with refractory CD30+ Hodgkin's and non-Hodgkin's lymphoma. *Clin. Cancer Res.* **8**, 1779–1786 (2002).
44. Kim, K.M. *et al.* Anti-CD30 diabody-drug conjugates with potent antitumor activity. *Mol. Cancer Ther.* **7**, 2486–2497 (2008).
45. Oflazoglu, E., Kissler, K.M., Sievers, E.L., Grewal, I.S. & Gerber, H.P. Combination of the anti-CD30-auristatin-E antibody-drug conjugate (SGN-35) with chemotherapy improves antitumour activity in Hodgkin lymphoma. *Br. J. Haematol.* **142**, 69–73 (2008).
46. Younes, A. *et al.* Brentuximab vedotin (SGN-35) for relapsed CD30-positive lymphomas. *N. Engl. J. Med.* **363**, 1812–1821 (2010).
47. Fanale, M.A. *et al.* A phase I weekly dosing study of brentuximab vedotin in patients with relapsed/refractory CD30-positive hematologic malignancies. *Clin. Cancer Res.* **18**, 248–255 (2012).
48. Younes, A. *et al.* Results of a pivotal phase II study of brentuximab vedotin for patients with relapsed or refractory Hodgkin's lymphoma. *J. Clin. Oncol.* advance online publication, doi:10.1200/JCO.2011.38.0410 (29 May 2012).
49. Keir, C.H. & Vahdat, L.T. The use of an antibody drug conjugate, glembatumumab vedotin (CDX-011), for the treatment of breast cancer. *Expert Opin. Biol. Ther.* **12**, 259–263 (2012).
50. Baselga, J. *et al.* Phase II study of efficacy, safety, and pharmacokinetics of trastuzumab monotherapy administered on a 3-weekly schedule. *J. Clin. Oncol.* **23**, 2162–2171 (2005).
51. Cobleigh, M.A. *et al.* Multinational study of the efficacy and safety of humanized anti-HER2 monoclonal antibody in women who have HER2-overexpressing metastatic breast cancer that has progressed after chemotherapy for metastatic disease. *J. Clin. Oncol.* **17**, 2639–2648 (1999).
52. Vogel, C.L. *et al.* Efficacy and safety of trastuzumab as a single agent in first-line treatment of HER2-overexpressing metastatic breast cancer. *J. Clin. Oncol.* **20**, 719–726 (2002).
53. Burris, H.A. III *et al.* Phase II study of the antibody drug conjugate trastuzumab-DM1 for the treatment of human epidermal growth factor receptor 2 (HER2)-positive breast cancer after prior HER2-directed therapy. *J. Clin. Oncol.* **29**, 398–405 (2011).
54. Hurvitz, S.A., Hu, Y., O'Brien, N. & Finn, R.S. Current approaches and future directions in the treatment of HER2-positive breast cancer. *Cancer Treat. Rev.* advance online publication, doi:10.1016/j.ctrv.2012.04.008 (4 June 2012).
55. Krop, I.E. *et al.* Phase I study of trastuzumab-DM1, an HER2 antibody-drug conjugate, given every 3 weeks to patients with HER2-positive metastatic breast cancer. *J. Clin. Oncol.* **28**, 2698–2704 (2010).
56. Krop, I.E. *et al.* A phase II study of trastuzumab emtansine in patients with

human epidermal growth factor receptor 2-positive metastatic breast cancer who were previously treated with trastuzumab, lapatinib, an anthracycline, a taxane, and capecitabine. *J. Clin. Oncol.* advance online publication, doi: 10.1200/JCO.2011.40.5902 (29 May 2012).
57. Kantarjian, H. *et al.* Inotuzumab ozogamicin, an anti-CD22-calecheamicin conjugate, for refractory and relapsed acute lymphocytic leukaemia: a phase 2 study. *Lancet Oncol.* **13**, 403–411 (2012).
58. Leonard, J.P. *et al.* Phase I/II trial of epratuzumab (humanized anti-CD22 antibody) in indolent non-Hodgkin's lymphoma. *J. Clin. Oncol.* **21**, 3051–3059 (2003).
59. Beck, A., Senter, P. & Chari, R. World Antibody Drug Conjugate Summit Europe: February 21-23 2011, Frankfurt, Germany *MAbs* **3**, 331–337 paper presented at the World Antibody Drug Conjugate Summit Europe, Frankfurt, Germany, February 21–23, 2011.
60. Hartley, J.A. *et al.* SG2285, a novel C2-aryl-substituted pyrrolobenzodiazepine dimer prodrug that cross-links DNA and exerts highly potent antitumor activity. *Cancer Res.* **70**, 6849–6858 (2010).
61. Moldenhauer, G. *et al.* Therapeutic potential of amanitin-conjugated anti-epithelial cell adhesion molecule monoclonal antibody against pancreatic carcinoma. *J. Natl. Cancer Inst.* **104**, 622–634 (2012).
62. Liu, C.C. & Schultz, P.G. Adding new chemistries to the genetic code. *Annu. Rev. Biochem.* **79**, 413–444 (2010).
63. Wu, P. *et al.* Site-specific chemical modification of recombinant proteins produced in mammalian cells by using the genetically encoded aldehyde tag. *Proc. Natl. Acad. Sci. USA* **106**, 3000–3005 (2009).
64. Friedman, M. & Stahl, S. Engineered affinity proteins for tumour-targeting applications. *Biotechnol. Appl. Biochem.* **53**, 1–29 (2009).
65. Cheson, B.D. *et al.* Revised response criteria for malignant lymphoma. *J. Clin. Oncol.* **25**, 579–586 (2007).

Letter | Published: 22 January 2012

Conjugation site modulates the *in vivo* stability and therapeutic activity of antibody-drug conjugates

Ben-Quan Shen, Keyang Xu [...] Jagath R Junutula

Nature Biotechnology 30, 184–189 (2012) | Download Citation

Abstract

The reactive thiol in cysteine is used for coupling maleimide linkers in the generation of antibody conjugates. To assess the impact of the conjugation site, we engineered cysteines into a therapeutic HER2/neu antibody at three sites differing in solvent accessibility and local charge. The highly solvent-accessible site rapidly lost conjugated thiol-reactive linkers in plasma owing to maleimide exchange with reactive thiols in albumin, free cysteine or glutathione. In contrast, a partially accessible site with a positively charged environment promoted hydrolysis of the succinimide ring in the linker, thereby preventing this exchange reaction. The site with partial solvent-accessibility and neutral charge displayed both properties. In a mouse mammary tumor model, the stability and therapeutic activity of the antibody conjugate were affected positively by succinimide ring hydrolysis and negatively by maleimide exchange with thiol-reactive constituents in plasma. Thus, the chemical and structural dynamics of the conjugation site can influence antibody conjugate performance by modulating the stability of the antibody-linker interface.

Access options

Rent or Buy article

Get unlimited, online access to 1 article for 48 hours.

from $8.99

Rent or Buy

All prices are NET prices.

Subscribe to Journal

Get full journal access for 1 year.

59,00 €

only 4,92 € per issue

Subscribe

All prices are NET prices.
VAT will be added later in the checkout.

Additional access options:

Log in | OpenAthens | Shibboleth

References

1. Carter, P.J. & Senter, P.D. Antibody-drug conjugates for cancer therapy. *Cancer J.* **14**, 154–169 (2008).

2. Polakis, P. Arming antibodies for cancer therapy. *Curr. Opin. Pharmacol.* **5**, 382–387 (2005).

3. Kreitman, R.J. & Pastan, I. Immunotoxins for targeted cancer therapy. *Adv. Drug Deliv. Rev.* **31**, 53–88 (1998).

4. Marik, J. & Junutula, J.R. Emerging role of immunoPET in receptor targeted cancer therapy. *Curr. Drug Deliv.* **8**, 70–78 (2011).

5. Ryan, S.M., Mantovani, G., Wang, X., Haddleton, D.M. & Brayden, D.J. Advances in PEGylation of important biotech molecules: delivery aspects. *Expert Opin. Drug Deliv.* **5**, 371–383 (2008).

6. McCarron, P.A. *et al.* Antibody conjugates and therapeutic strategies. *Mol. Interv.* **5**, 368–380 (2005).

7. Medintz, I.L., Uyeda, H.T., Goldman, E.R. & Mattoussi, H. Quantum dot bioconjugates for imaging, labelling and sensing. *Nat. Mater.* **4**, 435–446 (2005).

8. Hamblett, K.J. *et al.* Effects of drug loading on the antitumor activity of a monoclonal antibody drug conjugate. *Clin. Cancer Res.* **10**, 7063–7070 (2004).

9. Polson, A.G. *et al.* Antibody-drug conjugates for the treatment of non-Hodgkin's lymphoma: target and linker-drug selection. *Cancer Res.* **69**, 2358–2364 (2009).

10. Chapman, A.P. *et al.* Therapeutic antibody fragments with prolonged in vivo half-lives. *Nat. Biotechnol.* **17**, 780–783 (1999).

11. Junutula, J.R. *et al.* Site-specific conjugation of a cytotoxic drug to an antibody improves the therapeutic index. *Nat. Biotechnol.* **26**, 925–932 (2008).

12. Lewis Phillips, G.D. *et al.* Targeting HER2-positive breast cancer with trastuzumab-DM1, an antibody-cytotoxic drug conjugate. *Cancer Res.* **68**, 9280–9290 (2008).

13. Doronina, S.O. *et al.* Development of potent monoclonal antibody auristatin conjugates for cancer therapy. *Nat. Biotechnol.* **21**, 778–784 (2003).

14. Chari, R.V.J. Targeted cancer therapy: conferring specificity to cytotoxic drugs. *Acc. Chem. Res.* **41**, 98–107 (2008).

15. Wu, A.M. & Senter, P.D. Arming antibodies: prospects and challenges for immunoconjugates. *Nat. Biotechnol.* **23**, 1137–1146 (2005).

16. Junutula, J.R. *et al.* Engineered thio-trastuzumab-DM1 conjugate with an improved therapeutic index to target human epidermal growth factor receptor 2-positive breast cancer. *Clin. Cancer Res.* **16**, 4769–4778 (2010).

17. Xu, K. *et al.* Characterization of intact antibody-drug conjugates from plasma/serum in vivo by affinity capture capillary liquid chromatography-mass

spectrometry. *Anal. Biochem.* **412**, 56–66 (2011).

18. Alley, S.C. *et al.* Contribution of linker stability to the activities of anticancer immunoconjugates. *Bioconjug. Chem.* **19**, 759–765 (2008).

19. Lin, D., Saleh, S. & Liebler, D.C. Reversibility of covalent electrophile-protein adducts and chemical toxicity. *Chem. Res. Toxicol.* **21**, 2361–2369 (2008).

20. Knight, P. Hydrolysis of p-NN′-phenylenebismaleimide and its adducts with cysteine. Implications for cross-linking of proteins. *Biochem. J.* **179**, 191–197 (1979).

21. Khan, M.N. Kinetics and mechanism of the alkaline hydrolysis of maleimide. *J. Pharm. Sci.* **73**, 1767–1771 (1984).

22. Kalia, J. & Raines, R.T. Catalysis of imido group hydrolysis in a maleimide conjugate. *Bioorg. Med. Chem. Lett.* **17**, 6286–6289 (2007).

23. Austin, C.D. *et al.* Endocytosis and sorting of ErbB2 and the site of action of cancer therapeutics trastuzumab and geldanamycin. *Mol. Biol. Cell* **15**, 5268–5282 (2004).

24. Chen, Y. *et al.* Armed antibodies targeting the mucin repeats of the ovarian cancer antigen, MUC16, are highly efficacious in animal tumor models. *Cancer Res.* **67**, 4924–4932 (2007).

Acknowledgements

We thank our Genentech colleagues: J. Speer and E. Wu for reagent generation and inventory; D. Bumbaca for plasma stability study; J. Lau and I. Inigo for ADC efficacy studies; P. Carter and S. Panowski for critical review of the manuscript; H.B. Lowman, S. Kenkare-Mitra and I. Mellman for their insightful discussions. Anti-MMAE mouse monoclonal antibodies were a generous gift from Seattle Genetics.

Author information

Ben-Quan Shen & Keyang Xu
These authors contributed equally to this work.

Affiliations

Genentech Inc., 1 DNA *Way*, S. *San Francisco*, *California*, USA.
Ben-Quan Shen, Keyang Xu, Luna Liu, Helga Raab, Sunil Bhakta, Margaret Kenrick, Kathryn L Parsons-Reponte, Janet Tien, Shang-Fan Yu, Elaine Mai, Dongwei Li, Jay Tibbitts, Jakub Baudys, Ola M Saad, Suzie J Scales, Paul J McDonald, Philip E Hass, Charles Eigenbrot, Trung Nguyen, Willy A Solis, Reina N Fuji, Kelly M Flagella, Darshana Patel, Susan D Spencer, Leslie A Khawli, Allen Ebens, Wai Lee Wong, Richard Vandlen, Surinder Kaur, Mark X Sliwkowski, Richard H Scheller, Paul Polakis & Jagath R Junutula

Contributions

B.-Q.S. and K.X. designed experiments developed the methodology, performed plasma stability studies and wrote the manuscript. L.L. and M.K. performed plasma stability and LC-MS analyses. H.R. conducted ADC conjugations and S.B. generated THIOMAB constructs and performed *in vitro* potency studies. K.L.P.-R., J.T. and S.-F.Y. performed *in vivo* efficacy studies. E.M., D.L. and J.T. conducted pharmacokinetic studies. J.B. and O.M.S. quantified free MMAE levels in the plasma. S.J.S. performed internalization studies. P.J.M. and P.E.H. purified antibodies. C.E. performed antibody structural analysis. T.N., W.A.S., R.N.F. and K.M.F. designed and conducted preclinical safety studies. D.P. and S.D.S. provided project management support. L.A.K., A.E., W.L.W., R.V., S.K., M.X.S. and R.H.S. provided direction and guidance. P.P. provided direction, guidance and assisted in writing the manuscript. J.R.J. led the overall conjugation site-dependent antibody conjugate program, generated trastuzumab THIOMAB constructs, designed experiments and wrote the manuscript.

Competing interests

All authors were employees of Genentech/Roche at the time this work was conducted.

Corresponding author

Correspondence to Jagath R Junutula.

Supplementary information

PDF files

1. Supplementary Text and Figures
   Supplementary Tables 1 and 2 and Supplementary Figures 1–18

Rights and permissions

To obtain permission to re-use content from this article visit RightsLink.

About this article

Publication history

Received	Accepted	Published
08 July 2011	20 December 2011	22 January 2012

DOI

https://doi.org/10.1038/nbt.2108

Subjects

Breast cancer Molecular engineering Molecularly targeted therapy

Nature Biotechnology ISSN 1546-1696 (online)

SPRINGER NATURE

© 2018 Springer Nature Limited. All rights reserved.

OnCusp
Ex. 1002

Bioconjugate Chem. **2009**, *20*, 60–70

Systematic Research of Peptide Spacers Controlling Drug Release from Macromolecular Prodrug System, Carboxymethyldextran Polyalcohol–Peptide–Drug Conjugates

Yoshinobu Shiose,*,§ Hiroshi Kuga,† Hitoshi Ohki,‡ Masahiro Ikeda,‡ Fumiyoshi Yamashita,|| and Mitsuru Hashida||

Biological Research Laboratories IV and Medicinal Chemistry Research Laboratories II, Daiichi Sankyo Co. Ltd., Kasai R&D Center, Kita-Kasai 1-16-13, Edogawa-Ku, Tokyo 134-8630, Japan and Department of Drug Delivery Research, Graduate School of Pharmaceutical Sciences, Kyoto University, Kyoto 606-8501, Japan. Received June 13, 2008; Revised Manuscript Received October 9, 2008

The primary purpose of this study was to comprehensively delineate specificity of the peptide spacer sequence to tumor-expressed proteases for the design of macromolecular carrier–peptide spacer–drug conjugate system. 225 conjugates of carboxymethyldextran polyalcohol (CM-Dex-PA) as water-soluble carrier and a dansyl derivative (*N*-(4-aminobutyl)-5-(dimethylamino)-1-naphthalenesulfonamide, DNS) as the model drug linked with different tetrapeptide spacers (Gly-Gly-P_2–P_1, P_2, P_1: Ala, Asn, Gly, Cit, Gln, Ile, Leu, Met, Phe, Pro, Ser, Thr, Trp, Tyr, and Val) were combinatorially synthesized. First, the drug release assay of all of the fluorogenic model conjugates was performed in murine Meth A solid tumor homogenates. The drug release rate was higher with conjugates having hydrophobic amino acids at P_2. It was also found that conjugates with Asn release the drug rapidly and, in contrast, those with Pro does not. Second, we selected three peptide spacers (Gly-Gly-Phe-Gly, Gly-Gly-Ile-Gly, Gly-Gly-Pro-Leu), which release only DNS at different rates, and applied them to doxorubicin (DXR) conjugates. These three DXR conjugates were used for investigating relationships with drug release, pharmacokinetics, and antitumor activity against Meth A bearing mice of these conjugates. The release of DXR from the conjugates corresponded well with that of DNS conjugates in tumor homogenates. CM-Dex-PA-Gly-Gly-Phe-Gly-DXR and CM-Dex-PA-Gly-Gly-Ile-Gly-DXR indicated strong antitumor activity, with the comparable pharmacokinetic profile of released DXR in tumor. Taken with the fact that the drug release rate in tumor homogenates was ~10-fold different between these two DXR conjugates, it is likely that cellular uptake of the conjugate would be rate-limiting, rather than the drug release process under the in vivo situation. However, much weaker antitumor activity was observed with CM-Dex-PA-Gly-Gly-Pro-Leu-DXR, of which the drug release was extremely slow.

INTRODUCTION

Development of macromolecular prodrugs, which alter the pharmacokinetic profile of an aimed drug through conjugation with macromolecules, is a promising approach to increasing therapeutic efficacy and reducing adverse effect of the drug. Coupling of low-molecular-weight drugs to water-soluble macromolecular carrier can involve the following: (1) the improvement of drug movement in the body, prolonging its residence time in the blood circulation; (2) sustained release of the drug from the carrier by chemical or enzymatic hydrolysis; (3) site-specific delivery of drug due to moieties recognizing target cells (*1*). In solid tumors, macromolecules are known to accumulate preferentially, due to the "enhanced permeability and retention (EPR)" effect, i.e., leakiness of tumor angiogenic blood vessels and lack of effective lymphatic drainage (*2*). Exploitation of such mechanisms for tumor targeting has been successfully proven with various anticancer drugs, including doxorubicin, paclitaxel, camptothecin, and their analogues (*3*–*6*).

In addition to the efficiency of delivery to target tissue, the stability of the drug–polymer linkage is an important factor in determining therapeutic potentials. Prodrugs intended for tumorotropic delivery are required to release the drug using proteolytic cleavage of the polymer–drug linker by overexpressed enzymes in the tumor tissue, including thiol protease cathepsin B, metalloproteases such as collagenases and stromelysins, and serine proteases like plasminogen activator and plasmin. Acid-activated cleavage of the polymer–drug bond can also be used since the polymeric drug encounters endosomal/lysosomal acidification in tumor cells. The works of Duncan et al. on poly-*N*-(2-hydroxypropyl)methacrylamide (HPMA)-*p*-nitroaniline conjugates linked with peptidyl spacers have suggested that of all the lysosomal proteases the thiol protease cathepsin B was primarily responsible for the cleavage of the drug–polymer linkage (*7*–*9*). In addition, the rate of release of the *p*-nitroaniline was found to be dependent on the specificity of the peptide spacer sequence to cathepsin B, with the fastest rates of hydrolysis being observed for Gly-Phe-Leu-Gly among nine tetrapeptide spacers tested (*10*).

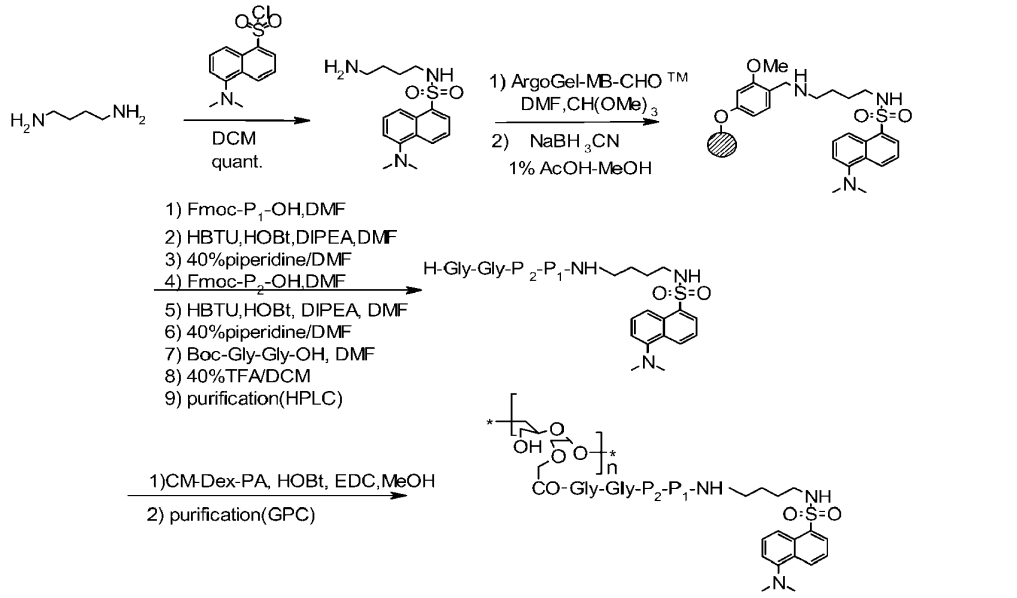
Being aware that there have been a limited number of studies (*10*–*13*) on sequence specificity of peptide spacers in tumorotropic macromolecular prodrugs, we initiated this study to comprehensively delineate specificity of the peptide spacer sequence to tumor-expressed proteases in a similar manner to that reported by Schmid et al. (*14*). 225 conjugates of carboxymethyl dextran polyalcohol (CM-Dex-PA) and a dansyl derivative (*N*-(4-aminobutyl)-5-(dimethylamino)-1-naphthalenesulfona-

* To whom correspondence should be addressed. Phone: +81-3-5696-3915. Fax: +81-3-5696-4264. E-mail:shiose.yoshinobu.gn@daiichisankyo.co.jp.
§ Biological Research Laboratories IV.
|| Kyoto University.
† Present address: Development Research Department, Daiichi Sankyo Inc., 389 Thornall Street, Edison, NJ 08837, USA.
‡ Medicinal Chemistry Research Laboratories II.

10.1021/bc800238f CCC: $40.75 © 2009 American Chemical Society
Published on Web 12/18/2008

OnCusp
Ex. 1002

Scheme 1. Synthesis of the CM-Dex-PA-Tetrapeptide-DNS Conjugates



P_1,P_2 = Ala, Asn, Cit, Gln, Gly ,Ile, Leu, Met, Phe, Pro, Ser, Thr, Trp, Tyr ,Val

mide, DNS) linked with different tetrapeptide spacers were combinatorially synthesized, and the rate of release of DNS from the conjugates was measured using murine Meth A solid tumor homogenates. Effectiveness of CM-Dex-PA as a backbone of tumorotropic macromolecular prodrugs has been demonstrated in our previous studies (*6*). On the basis of the in vitro studies, conjugates of CM-Dex-PA and DXR[1] linked with different peptide spacers (Gly-Gly-Phe-Gly, Gly-Gly-Ile-Gly, and Gly-Gly-Pro-Leu) were designed. The in vitro drug release, pharmacokinetics, and in vivo antitumor activity of the carboxymethyldextran polyalcohol−doxorubicin conjugates were investigated to demonstrate the importance of peptide spacers in the design of macromolecular prodrugs.

EXPERIMENTAL PROCEDURES

Reagents. Fifteen fluoren-9-ylmethyloxycarbonyl (Fmoc)-protected amino acids were purchased from Bachem America Inc. (Torrance, CA). Doxorubicin (DXR) was obtained from Kyowa Hakko Co., Ltd. (Tokyo, Japan). Other chemicals were of reagent grade and used without further purification.

Synthesis of *N*-(4-Aminobutyl)-5-(dimethylamino)-1-naphthalenesulfonamide (DNS). After 1,4-butanediamine (33.0 g, 371 mmol) was dissolved in dichloromethane (100 mL), dansyl chloride (5.0 g, 18.5 mmol) in dichloromethane (100 mL) was added dropwise to the solution for 30 min on ice. The reaction mixture was stirred at room temperature for 20 h. After the solvent was evaporated, the residue was dissolved in ethyl acetate, washed with saturated sodium bicarbonate and NaCl, and then dried with sodium sulfate. After the solvent was evaporated, DNS (5.99 g) was yielded as oil. ^{1}H NMR ($CDCl_3$) δ: 1.28−1.37 (m, 2 H, CH_2), 1.43−1.49 (m, 2 H, CH_2), 2.57 (t, 2 H, J = 6.4 Hz, CH_2), 2.84−2.89 (m, 8 H, Me_2, CH_2), 7.18 (d, 1 H, J = 7.6 Hz, H-6 of Dansyl), 7.51, 7.55 (2d, 2 H, J = 8.3 Hz, 8.8 Hz, H-3, H-7 of Dansyl), 8.25 (d, 1 H, J = 7.0 Hz, H-2 of Dansyl), 8.33 (d, 1 H, J = 8.8 Hz, H-8 of Dansyl), 8.53 (d, 1 H, J = 8.3 Hz, H-6 of Dansyl).

Succinic acid (66 mg) was added to the solution of DNS (90 mg) in methanol (20 mL). The solvent was evaporated, and diethyl ether was added to the residue for solidification. The residue was washed with diethylether and dried to yield 130 mg of DNS salt (0.5 succinic acid 0.7 hydrate). Anal. Calcd for $C_{16}H_{23}N_3O_2S \cdot 0.5$ succinic acid$\cdot 0.7\ H_2O$: C, 55.00; H, 7.03; N, 10.69; S, 8.16. Found: C, 55.10; H, 6.80; N, 10.46; S, 8.16. DNS was dissolved in 50% acetonitrile solution and prepared to 3.57 mg/mL. Furthermore, the solution was diluted to adequate concentration as HPLC standard sample.

Combinatorial Synthesis of CM-Dex-PA-Tetrapeptide-DNS Conjugates (Scheme 1). *a. Transduction to MB-CHO Resin of DNS.* DNS succinic salt (5.96 g, 18.54 mmol) in *N*,*N*-dimethylformamide (DMF, 30 mL) was added to trimethyl ester (30 mL) suspended with ArgoGelTM-MB CHO resin (6.9 g, 0.40 mmol/g). After shaking for 16 h, the solvent was removed, and the resin was washed with methanol and dried. To the resin, 1% acetic acid in methanol (100 mL) and 1 N $NaBH_3CN$ in tetrahydrofuran (THF, 20 mL) were added, and the solution was shaken for 2 days. The resin was isolated, washed with methanol and chloroform, and dried overnight to yield DNS-resin (19.7 g).

b. Synthesis of H-Gly-Gly-P_2-P_1-DNS by ACT496. Using DNS-resin (25 mg, 0.01 mmol), 225 kinds of crude H-Gly-Gly-P_2-P_1-DNS (15 × 15 amino acids) were synthesized by

[1]Abbreviations: Ala, L-alanine; Asn, L-asparagine; Cit, L-citrulline; DCC, *N*,*N*′-dicyclohexylcarbodiimide; DIPEA, diisopropylethylamine; DMF, *N*,*N*-dimethylformamide; DNS, *N*-(4-aminobutyl)-5-(dimethylamino)-1-naphthalenesulfonamide; DXR, Doxorubicin; EDC, 1-ethyl-3-(3-dimethylaminopropyl)carbodiimide; EDTA, ethylenediaminetetraacetic acid; Fmoc, fluoren-9-ylmethyloxycarbonyl; Gln, L-glutamine; Gly, L-glycine; GPC, gel permeation chromatography; HBTU, 2-(1*H*-benzotriazole-1-yl)-1,1,3,3-tetramethyluronium hexafluorophosphate; HOBt, 1-hydroxybenzotriazole; HPLC, high-performance liquid chromatography; Ile, L-isoleucine; LC/MS, liquid chromatography−mass spectrometry; Leu, L-leucine; MMPs, matrix metalloproteases; MES, 2-(*N*-morpholino)ethanesulfonic acid; Met, L-methionine; Phe, L-phenylalanine; Pro, L-Proline; Ser, L-serine; THF, tetrahydrofuran; Thr, L-Threonine; Tos, toluenesulfonyl; Trp, L-tryptophan; Trt, triphenylmethyl; Tyr, L-Tyrosine; Val, L-valine.

ACT496 (Advanced Chem. Tech., KY). P_2 and P_1 amino acids were Ala, Asn, Cit, Gln, Gly, Ile, Leu, Met, Phe, Pro, Ser, Thr, Trp, Tyr, and Val. The DNS resin was placed in the reaction vessel of the synthesizer and washed with DMF. The DMF was removed by filtration. To bond P_1 amino acid to DNS, a 0.1 M solution of Fmoc-protected amino acids in DMF (0.5 mL) was added, followed by 1-hydroxybenzotriazole (HOBt, 0.1 mL of 0.5 M solution in DMF), diisopropylethylamine (DIPEA, 0.2 mL of 0.5 M solution in DMF), and 2-(1*H*-benzotriazole-1-yl)-1,1,3,3-tetramethyluronium hexafluorophosphate (HBTU, 0.2 mL of 0.25 M solution in DMF). The mixture was shaken for 2 h at room temperature. Then, DMF was removed by filtration. The procedure was performed once again. The resin was washed three times with 1 mL DMF. To remove the Fmoc group, piperidine in DMF was added and the mixture shaken for 1 min. The resin was washed with DMF (3 times). The bonding of P_2 amino acid to P_1-DNS, the removal of Fmoc, and the bonding of Boc-Gly-Gly to P_2-P_1-DNS were performed following the same protocol as that for P_1 amino acid. After the reaction was completed, the resin was washed twice with 1 mL DMF, twice with 1 mL THF, once with 1 mL MeOH, and three times with 1 mL CH_2Cl_2. To remove the Boc group and isolate H-Gly-Gly-P_2-P_1-DNS from the resin, CH_2Cl_2 solution including 50% trifluoroacetic acid (1 mL) was added and incubated for 2 h. The crude H-Gly-Gly-P_2-P_1-DNS was collected by filtration and dried.

c. HPLC Purification of Crude H-Gly-Gly-P_2-P_1-DNS. The crude H-Gly-Gly-P_2-P_1-DNS, which was synthesized by the solid phase method, was dissolved in methanol (500 μL), transferred to Eppendorf tube, and evaporated. Then, these were dissolved in 10% methanol (100−200 μL) and purified by HPLC. The HPLC separation was performed on a 15 × 250 mm reversed-phase column packed with Capcell Pak C18 UG 120 (Shiseido, Tokyo, Japan) with 8 mL/min flow rate. The detector was set at 260 nm (UV-8020, Tosoh, Tokyo, Japan). The mobile phase consisted of methanol/acetonitrile (1:2) and 0.1 M trifluoroacetic acid, of which the proportion ranged from 20% to 45% according to the elution property of H-Gly-Gly-P_2-P_1-DNS. All samples were confirmed by LC/MS and HPLC purity (260 nm) >95%.

d. Synthesis of CM-Dex-PA. Carboxymethyl dextran polyalcohol (CM-Dex-PA) was synthesized from dextran (molecular weight 500 kDa, Pharmacia). Dextran (50 g) was dissolved in 0.1 M acetic acid buffer (pH 5.5, 5 L). A sodium periodic acid (165.0 g) was dissolved in distilled water (5 L) and added to the solution of dextran. The mixture was stirred under shade at 4 °C for ten days. Then, ethylene glycol (35 mL) was added and the mixture stirred overnight. The reaction mixture was adjusted to pH 7.5 using 8 M sodium hydroxide solution. Then, sodium borohydride (70 g) was added, and the mixture was stirred overnight. The solution was adjusted to pH 5.5 with acetic acid on ice, and ultrafiltration was performed using a Biomax 50 (size exclusion 50 kDa, Millipore). The filtration was freeze−dried to yield dextran polyalcohol (Dex-PA, 27.1 g). Dex-PA was dissolved in 14% sodium hydroxide solution (150 mL), and monochloroacetic acid (30 g) was added under cooling with ice and stirred at room temperature overnight. The reaction mixture was treated by ultrafiltration using Biomax 50 after having adjusted to pH 8 with acetic acid. A macromolecular fraction was freeze−dried, and Na salt (5.6 g) of CM-Dex-PA was obtained. The molecular weight of CM-Dex-PA was approximately 263 000 using pullulan standard by GPC and has a polydispersity index of 1.6 (M_w/M_n). The decrease in molecular weight of dextran following periodic acid oxidation has also been observed by Ahmad et al. (*15*), presumably due to structural changes associated with C2−C3 bond cleavage and increased molecular flexibility. The carrier was shelf-stable for over three months. On the other hand, the degrees of substitution of the CM groups in the carrier were determined by titration (ca. 0.0027 mol CM equiv per gram of CM-Dex-PA).

e. Synthesis of CM-Dex-PA-Gly-Gly-P_2-P_1-DNS. CM-Dex-PA was dissolved in collidine buffer (pH 7.0) containing 50% methanol to yield a concentration of 15 mg/mL. A 36 μL aliquot of 10 mg/mL 1-ethyl-3-(3-dimethylaminopropyl)carbodiimide (EDC) and 10 μL of 10 mg/mL HOBt in methanol was added to 200 μL of the CM-Dex-PA solution. H-Gly-Gly-P_2-P_1-DNS was dissolved in 42 μL of methanol, added to the reaction mixture, and then stirred for 3 h. 36 μL of the 10 mg/mL EDC solution was added and the mixture stirred for another 3 h, to yield CM-Dex-PA-Gly-Gly-P_2-P_1-DNS.

f. Purification of CM-Dex-PA-Gly-Gly-P_2-P_1-DNS. The reaction mixture of CM-Dex-PA-Gly-Gly-P_2-P_1-DNS was diluted with 600 μL of distilled water and subjected to GPC for purification. The conjugates were eluted with 0.1 M sodium acetate buffer (pH 5.0) containing 20% of acetonitrile using TSK GEL PW-6000XL column (Tosoh, Tokyo, Japan). The flow rate was 1 mL/min and detected at 254 nm (SPD-10A, Shimazu, Tokyo, Japan). The fraction eluting between 8.5 and 11.5 min, which corresponded to the molecular weight of 100 to 400 kDa, was collected.

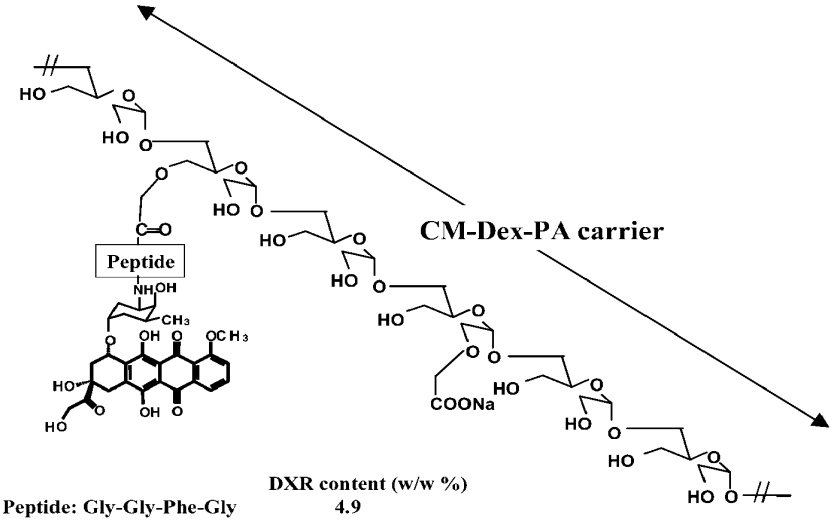
g. Determination of DNS Contents in CM-Dex-PA-Gly-Gly-P_2-P_1-DNS. The eluate fraction was diluted 10 times with distilled water. The content of DNS associated with CM-Dex-PA-Gly-Gly-P_2-P_1-DNS was determined by the GPC system equipped with a fluorescence detector (RF-10A, Shimazu, Tokyo, Japan) set at excitation and emission wavelength of 335 and 530 nm, respectively. Other conditions were the same as mentioned above. The DNS content was calculated by the calibration curve of DNS. The DNS content of the conjugates ranged from 3% to 6% (w/w).

Synthesis of CM-Dex-PA-tetrapeptide-DXR Conjugates. CM-Dex-PA-Gly-Gly-Phe-Gly-DXR, CM-Dex-PA-Gly-Gly-Ile-Gly-DXR, and CM-Dex-PA-Gly-Gly-Pro-Leu-DXR were synthesized by Research Laboratory of Daiichi Pharmaceutical Co., Ltd. (Tokyo, Japan).

a. Synthesis of H-Gly-Gly-Phe-Gly-DXR. A mixture of H-Phe-Gly-OH (10 g, 44.0 mmol) and toluenesulfonyl (Tos) OH (8.36 g, 44.0 mmol) and benzylalcohol (10 mL) was suspended and refluxed through a Dean−Stark system for 16 h. A reaction mixture was concentrated, and ether was added to give Tos OH·H-Phe-Gly-OBzl (20 g, 94%). Triphenylmethyl (Trt) -Gly-Gly-OH·Et_3N (1.40 g, 3.0 mmol) and TosOH·H-Phe-Gly-OBzl (1.46 g, 3.0 mmol) and HOBT (490 mg, 3.6 mmol) and (*N*,*N*′-dicyclohexylcarbodiimide DCC, 740 mg, 3.6 mmol) were dissolved in DMF (10 mL) and the mixture stirred overnight. The mixture was concentrated, diluted with ethyl acetate, and washed with 5% aqueous citric acid, a saturated sodium bicarbonate solution, saturation solution of salt, and distilled water in this order. Then, it was dried with $MgSO_4$ and filtered, and the filtrate was concentrated. Trt-Gly-Gly-Phe-Gly-OBzl was obtained by column chromatography (CH_2Cl_2/MeOH = 50:1) to yield 1.5 g. Trt-Gly-Gly-Phe-Gly-OBzl (500 mg) and $HCOONH_4$ (150 mg) were dissolved in DMF (5 mL), followed by the addition of 5% Pd−C (500 mg) and agitation for 2 h. Pd−C was removed by filtration, and the filtrate was purified by column chromatography (CH_2Cl_2/MeOH = 50:1) to give Trt-Gly-Gly-Phe-Gly-OH (330 mg, 78%). ^{1}H NMR (CD_3OD): δ 7.18−7.45 (m, 20H), 4.64 (dd, 1H, J = 8.8, 5.6 Hz), 3.94 (d, 1H, J = 16.5 Hz), 3.80 (d, 1H, J = 16.5 Hz), 3.78 (d, 1H, J = 17.5 Hz), 3.64 (d, 1H, J = 17.5 Hz), 3.23 (dd, 1H, J = 14.2, 5.6 Hz), 2.90 (dd, 1H, J = 14.2, 8.8 Hz), 2.90 (s, 1H).

Trt-Gly-Gly-Phe-Gly-OH (330 mg, 0.57 mmol), DCC (141 mg, 0.68 mmol), and HOBt (92 mg, 0.68 mmol) were dissolved in DMF (120 mL), and DMF solution containing of HCl/DXR

OnCusp
Ex. 1002



	DXR content (w/w %)
Peptide: Gly-Gly-Phe-Gly	4.9
Gly-Gly-Leu-Gly	4.1
Gly-Gly-Pro-Leu	5.2

Figure 1. Partial structure of DXR conjugates.

(331 mg, 0.57 mmol) and triethylamine (0.063 mL, 0.57 mmol) were added and the mixture stirred for 16 h. Then, Trt-Gly-Gly-Phe-Gly-DXR was purified by column chromatogrphy (CH_2Cl_2/MeOH = 10/1) to yield 400 mg. ^{1}H NMR (CD_3OD): δ 7.91 (d, 1H, J = 7.6 Hz), 7.80 (t, 1H), 7.54 (d, 1H, J = 8.3 Hz), 7.16−7.26 (m, 5H), 5.43 (d, 1H, J = 3.9 Hz), 5.13 (br, 1H), 4.73 (s, 2H), 4.43 (dd, 1H, J = 8.4, 6.6 Hz), 4.30 (q, 1H, J = 6.6 Hz), 4.16 (m, 1H), 4.03 (d, 1H, J = 17.0 Hz), 4.02 (s, 3H), 3.86 (d, 1H, J = 16.9 Hz), 3.83 (d, 1H, J = 17.0 Hz), 3.77 (d, 1H, J = 15.9 Hz), 3.73 (d, 1H, J = 15.9 Hz), 3.62 (d, 1H, J = 1.5 Hz), 3.59 (d, 1H, J = 16.9 Hz), 3.13 (dd, 1H, J = 13.9, 6.6 Hz), 3.10 (d, 1H, J = 18.6 Hz), 3.00 (d, 1H, J = 18.6 Hz), 2.94 (dd, 1H, J = 13.9, 8.4 Hz), 2.38 (d, 1H, J = 14.7 Hz), 2.19 (dd, 1H, J = 14.7, 5.1 Hz), 1.98 (ddd, 1H, J = 12.7, 12.7, 3.9 Hz), 1.71 (dd, 1H, J = 12.7, 4.6 Hz), 1.28 (d, 3H, J = 6.6 Hz).

Trt-Gly-Gly-Phe-Gly-DXR (350 mg, 0.32 mmol) was dissolved in 75% AcOH (2 mL) and stirred for 1 h. Distilled water (10 mL) was added, and the solution was filtered and dried in vacuo. The resulting red solid product was collected by treatment of Dowex 1 × 8 ion-exchange resin (CL-form) and dried in vacuo to give HCl·H-Gly-Gly-Phe-Gly-DXR (180 mg).

b. Synthesis of CM-Dex-PA-Gly-Gly-Phe-Gly-DXR. CM-Dex-PA (750 mg) was dissolved in 50% MeOH/0.02 M Tris-maleate buffer (pH 7.0) (50 mL). HCl·H-Gly-Gly-Phe-Gly-DXR (100 mg) in MeOH (10 mL) and EDC·HCl (80 mg) in MeOH (4 mL) were added and the mixture stirred for 4.5 h. A solution of EDC·HCl (40 mg) in MeOH (4 mL) was added twice at 1.5 and 3 h. To stop the reaction, 3 M NaCl (50 mL) was added, and the mixture was filtered using a MW 50 kDa cutoff membrane. The product was dried in vacuo, redissolved in 3 M NaCl, and precipitated by dropping into EtOH (40 mL). The precipitate was collected, treated by ultrafiltration, and purified through a 0.22 μM filter, to give the product (740 mg). CM-Dex-PA-Gly-Gly-Ile-Gly-DXR and CM-Dex-PA-Gly-Gly-Pro-Leu-DXR were synthesized by the same method. The contents of DXR in the DXR conjugates ranged from 4% to 6% w/w, and contamination of free DXR was less than 0.01% DXR equiv. The partial structure of these conjugates was indicated in Figure 1.

Inoculation of Tumor Cells. Meth A (murine fibrosarcoma) was kindly obtained from Dr. Ichiro Azuma (Institute of Immunological Science, School of Medicine, Hokkaido University, Japan). Meth A tumors were propagated in vivo by subcutaneous inoculation of cells (1 × 10^6 cells/0.1 mL) into the left flank of syngenic male BALB/c mice (6 weeks of age). Murine histiocytoma M5076 cells were obtained from Japanese Foundation for Cancer Research (Tokyo, Japan). The cells were cultured in RPMI 1640 medium supplemented with 17% horse serum (Hyclone Laboratories, Logan, UT). M5076 solid tumors were propagated in vivo by subcutaneous inoculation of cells (1 × 10^6 cells/0.1 mL) into the left flank of syngenic male C57BL/6 mice (6 weeks of age).

Preparation of Tumor Homogenate from Meth A Solid Tumor in Mice. Meth A solid tumor homogenates were prepared according to the method of Rozhin et al. (*16*). On 21 days post-subcutaneous inoculation of Meth A tumor cells, the mice were sacrificed under anesthesia to excise the tumor tissue. A pool of the tumor tissues with a total weight of 27 g was washed three times with 20 mL of ice−cold MES buffer (250 mM sucrose, 25 mM MES, 1 mM EDTA, pH 6.5), and then placed in 35 mL of the fresh MES buffer. The tumor homogenization was performed at 4 °C for 5 min. The homogenate was centrifuged at 500 × g for 11 min, and the supernatant was collected and centrifuged again at the same condition. Furthermore, the supernatant was centrifuged at 15 000 × g for 19 min to yield a mitochondrial lysosomal pellet. The pellet was resuspended in citrate buffer (pH 5.5), quickly frozen, and stored at −80 °C. M5076 tumor homogenates were prepared by the same method.

Drug Release Assay of DNS Conjugates and DXR Conjugates in Tumor Homogenate. The enzyme reaction mixture consisted of 80 μL of Britton Robinson buffer (pH 4.5), 5 μL of 200 mM cysteine, 5 μL of 0.1% Brij 35, and 5 μL of the tumor homogenate. Five microliter of the DNS conjugate or DXR conjugate solution was added to the mixture and incubated at 40 °C for given time period (DNS conjugates, 2 or 20 h; DXR conjugates, 4, 8, 24 h). Then, acetonitrile (100 μL) was added to stop the reaction. Following centrifugation of the solution at 15 000 × g for 10 min, the amount of the liberated drug contained in the supernatant was determined by HPLC.

OnCusp
Ex. 1002

Release of DXR from the Conjugates in M5076 Cell Culture. Two milliliters of M5076 cell suspension (5×10^6 cells/mL) was seeded onto a 60 mm dish, and cultured in RPMI 1640 medium supplemented with 17% horse serum medium for 2 h. 100 μL of DXR conjugate solution (2 mg DXR equiv/mL) was added to the cell culture dish, and incubated at 37 °C in a humidified atmosphere of 5% CO_2 (v/v) in air. 24 h later, 1 M HCl containing 90% acetonitrile (2 mL) was added, and the lysate was taken and centrifuged for 10 min at 10 000 × *g*. The amount of DXR released from the conjugates was determined by HPLC.

Antitumor Activity of DXR Conjugates against Meth A Bearing Mice. After inoculation of Meth A cells (day 0), DXR conjugate (5, 20, or 40 mg DXR equiv/kg) or DXR (5, 10, or 20 mg/kg) were intravenously administered on day 9. On day 14, mice were sacrificed to excise and weigh tumor masses. The growth inhibition rate (IR) on the basis of tumor weight was calculated using the following formula: IR = (1 − TWt/TWc) × 100 (%), where TWt and TWc represent the mean tumor weight for treated and nontreated groups, respectively. The statistical significance of differences between the nontreated and treated groups was evaluated using Dunnett's test. The body weight of mice (BWt) was measured every day and compared to that on day 0 (BWc). The rate of body weight loss (BWL) was calculated on the basis of the following formula: BWL (%) = (1 − BWt/BWc) × 100. BWLmax indicates the maximum value of BWL.

Distribution of DXR in Tumor, Liver, and Serum after Administration of DXR Conjugates. Meth A bearing mice were intravenously administered with DXR conjugates or DXR at 20 mg DXR equiv/kg. In order to examine the release of DXR from macromolecular conjugates in detail, distribution of DXR following injection of the conjugates was measured on the same time scale as the case of DXR, which is rapidly distributed to and eliminated from tissues. That is, at 2, 4, 8, 24, and 48 h after injection, mice were anesthetized with dimethyl ether, and blood, liver, and tumor were collected. The blood were left to clot for 10 min and then centrifuged (10 000 × *g*, 10 min at 4 °C) to collect serum. The samples (serum, liver, and tumor) were stored at −30 °C until analysis. 100 μL of the serum was mixed with 100 μL of 1 M HCl containing 90% acetonitrile (v/v) and then centrifuged at 10 000 × *g* for 10 min at 4 °C. The supernatant was injected into the HPLC system. To liver and tumor 0.5 M HCl containing 50% acetonitrile (v/v) were added (1 mL solvent per 0.25 g tissue), homogenized on ice by the handy micro-homogenizer NS-310F (Microtec Co., LTD, Chiba, Japan), and centrifuged at 10 000 × *g* for 10 min at 4 °C. The supernatant was injected into the HPLC system. A preliminary experiment indicated that the procedure provided more than 95% recovery of DXR from tissues.

HPLC Condition. LC/MS was performed with an HP 1100 HPLC system with API 150Ex mass spectrometer on a Develosil Combi-RP-5 column (4.6 × 50 mm, Nomura Chemical Co., Ltd. Aichi, Japan). The mobile phase consisted of A, 0.1% HCOOH/H_2O (v/v), and B, 0.1% HCOOH/acetonitrile (v/v), with a linear gradient from 0% to 100% of B for 3.6 min (flow rate 2.5 mL/min). Determination of DNS and its peptide conjugates released was performed with a HPLC system on a Symmetry Shield RP18 column (4.6 × 100 mm, Waters Co., Milford, MA) and a fluorimetric detector (excitation 335 nm, emission 530 nm); the mobile phase consisted of acetonitrile and methanol (2:1) and 0.1 M sodium acetic acid, with a linear gradient from 30% to 90% for 15 min (flow rate 1 mL/min). Determination of DXR was performed on a Symmetry Shield RP18 column (4.6 × 100 mm) and a fluorimetric detector (excitation 480 nm, emission 590 nm); the mobile phase consisted of acetonitrile, methanol, and 0.1 M sodium acetic acid buffer (23.4/11.6/65.0, v/v/v, flow rate 1 mL/min).

RESULTS

Drug Release Assay of DNS Conjugates by Meth A Homogenate. Considering the pH dependence on the cathepsin activities associated with Meth A tumor homogenate (*17*), the drug release assay of the conjugates was performed at pH 4.5. When CM-Dex-PA-Gly-Gly-P_2-P_1-DNS was incubated, not only DNS but its peptide conjugate (P_1-DNS and P_2-P_1-DNS) were detected by HPLC. Figure 2 is a $P_2 \times P_1$ combination of pie charts, of which the diameter represents the total release rate. The red, blue, and yellow colors indicate DNS, P_1-DNS, and P_2-P_1-DNS. In the case of Pro at P_1, the release of DNS and its peptide conjugates was very slow (small chart) for any amino acids at P_2, while in the case of Asn at P_1, DNS (red color) was rapidly released. On the other hand, when P_2 was Val, Tyr, Trp, Phe, Met, Leu, or Ile, DNS was rapidly released. By contrast, Thr, Ser, Pro, Gly, Gln, Cit, and Ala at P_2 retarded the release of DNS and its peptide conjugates. Interestingly, when Asn was at P_2, P_1-DNS (blue color) was largely released. Taken together with the result of Asn at P_1, peptidases associated with Meth A tumor homogenates preferentially cleaved the carboxy side of Asn. In the case of Pro at P_1 and P_2, P_2-P_1-DNS (yellow color) and DNS tended to be mainly released, respectively, indicating that both the amino and carboxy sides of Pro are extremely resistant against the peptidases.

With regard to the conjugates which released DNS completely within 20 h, drug release for the shorter time (2 h) was also measured (Figure 3). When P_2 was Tyr, Phe, or Leu, and P_1 was Met, Leu, Gln, or Cit, the release of DNS were extremely high.

As well as Meth A homogenates, M5076 tumor homogenates were subjected to DNS release assays of the conjugates. When drug release in M5076 tumor homogenate was investigated with nine voluntarily selected conjugates (peptide: Gly-Gly-Leu-Met, Gly-Gly-Met-Asn, Gly-Gly-Gly-Asn, Gly-Gly-Phe-Gly, Gly-Gly-Ile-Cit, Gly-Gly-Ile-Leu, Gly-Gly-Pro-Gln, Gly-Gly-Pro-Ala, Gly-Gly-Met-Pro), it was highly correlated with that of Meth A tumor homogenate (Figure 4).

Comparison of Drug Release between DNS Conjugates and DXR Conjugates in Meth A Homogenates. As well as the DNS-bearing model conjugates, the release of DXR from DXR conjugates was investigated in Meth A homogenates. The conjugates, which have three typical peptide spacers (i.e., Gly-Gly-Phe-Gly, Gly-Gly-Ile-Gly, or Gly-Gly-Pro-Leu), were selected. Although the amount of DXR released within 20 h was less than that of DNS, the rank order of three types of conjugates was the same in both DXR- and DNS conjugates: that is, the release of the drugs was highest with conjugates having Gly-Gly-Phe-Gly, followed by Gly-Gly-Ile-Gly and Gly-Gly-Pro-Leu (Table 1).

Drug Release Assay of DXR Conjugates in M5076 Tumor Homogenates and in Vitro Cultured M5076 Cells. As well as Meth A homogenates, the M5076 tumor homogenates were subjected to drug release assays of DXR conjugates. DXR conjugates, for which the spacer varied in the rate of hydrolysis (Gly-Gly-Phe-Gly, Gly-Gly-Ile-Gly, Gly-Gly-Pro-Leu), were selected. The release rate constants of DXR from CM-Dex-PA-Gly-Gly-Phe-Gly-DXR, CM-Dex-PA-Gly-Gly-Ile-Gly-DXR, and CM-Dex-PA-Gly-Gly-Pro-Leu-DXR were 0.064 h^{-1}, 0.0066 h^{-1}, and 0.00013 h^{-1}, respectively (see Supporting Information). It indicated that, as well as in the case of DNS conjugates, the rank order of the DXR conjugates was the same in both Meth A and M5076 tumor homogenates.

In addition, the release of DXR from the conjugates was also evaluated in the in vitro cultured M5076 cells. Figure 5

OnCusp
Ex. 1002

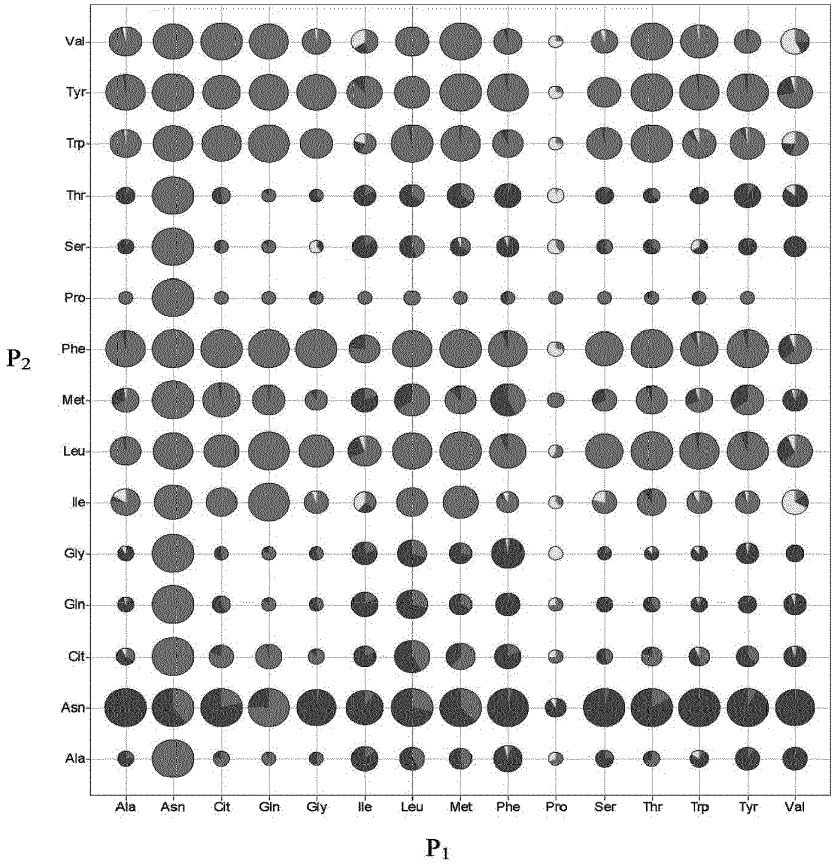


Figure 2. Characterization of DNS and its derivatives released from DNS conjugates in Meth A homogenate at 37 °C for 20 h. The vertical axis indicates the P_2 residure, and the horizontal axis indicates the P_1 residure. The total amounts of drug release are indicated by the size of circle, and the ratio of DNS, P_1-DNS, and P_2-P_1-DNS are indicated as red, blue, and yellow, respectively.

represents a plot of the amount released within 24 h in the cultured M5076 cells against the release rate constant evaluated in the homogenates. Although the rank order of drug release was the same in both cultured cells and tumor homogenates, the difference between CM-Dex-PA-Gly-Gly-Phe-Gly-DXR and CM-Dex-PA-Gly-Gly-Ile-Gly-DXR was not so remarkable in the cultured cells (ca. 1% for both) as expected from the tumor homogenates (~10-fold difference). It is likely that cellular uptake of the DXR conjugates is the rate-limiting step, and therefore the difference in the intracellular hydrolysis rate minimally affects the appearance of DXR from the conjugates.

Antitumor Activity of DXR Conjugates against Meth A Bearing Mice. Antitumor activity of CM-Dex-PA-Gly-Gly-Phe-Gly-DXR, CM-Dex-PA-Gly-Gly-Ile-Gly-DXR, and CM-Dex-PA-Gly-Gly-Pro-Leu-DXR was investigated in Meth A bearing mice. As shown in Table 2, intravenous injection of 5−40 mg/kg CM-Dex-PA-Gly-Gly-Phe-Gly-DXR remarkably decreased the tumor weight, although the loss of body weight (>20%) was observed at the highest dose. CM-Dex-PA-Gly-Gly-Ile-Gly-DXR, in spite of giving slower in vitro drug release than CM-Dex-PA-Gly-Gly-Phe-Gly-DXR, exhibited comparable antitumor activity to CM-Dex-PA-Gly-Gly-Phe-Gly-DXR, although two mice died at 40 mg/kg. On the other hand, antitumor effect of CM-Dex-PA-Gly-Gly-Pro-Leu-DXR was much less than the other two DXR conjugates. It clearly indicated that the rate of drug release is important in the antitumor activity. When DXR itself was administered at 20 mg/kg, four of six mice died, and antitumor activity was moderate. At 10 mg/kg, on the other hand, the antitumor activity and body weight loss were not observed. Thus, macromolecular prodrugs exhibiting a fast drug release due to tumor proteases, e.g., CM-Dex-PA-Gly-Gly-Phe-Gly-DXR and CM-Dex-PA-Gly-Gly-Ile-Gly-DXR, greatly improved therapeutic potential of DXR.

Distribution of DXR in Tumor and Liver after Administration of DXR Conjugates. The serum, hepatic, and tumoral levels of free DXR after intravenous injection of DXR conjugates were determined. When DXR was administered, the serum level of DXR was decreased rapidly in the early phase and gradually in the late phase. When the conjugates were injected intravenously, the serum level of free DXR was extremely low (Figure 6A).

As for administration of DXR, its tumoral level reached a maximum at 4 h and gradually decayed thereafter. In contrast, when CM-Dex-PA-Gly-Gly-Phe-Gly-DXR or CM-Dex-PA-Gly-Gly-Ile-Gly-DXR was administered, the tumoral level of free DXR released from the conjugates was gradually increased and remained high for a long time. The tumoral level of free DXR from the conjugates at 48 h was about 3-fold higher than the level following administration of DXR itself. In the case of CM-Dex-PA-Gly-Gly-Pro-Leu-DXR, the level of free DXR was minimally detected (Figure 6B).

DXR was highly distributed into the liver immediately after intravenous injection. In the case of CM-Dex-PA-Gly-Gly-Phe-Gly-DXR or CM-Dex-PA-Gly-Gly-Ile-Gly-DXR, the hepatic level of free DXR was kept low. The Cmax values for the conjugates were 5-fold lower than that for DXR. In the case of

OnCusp
Ex. 1002

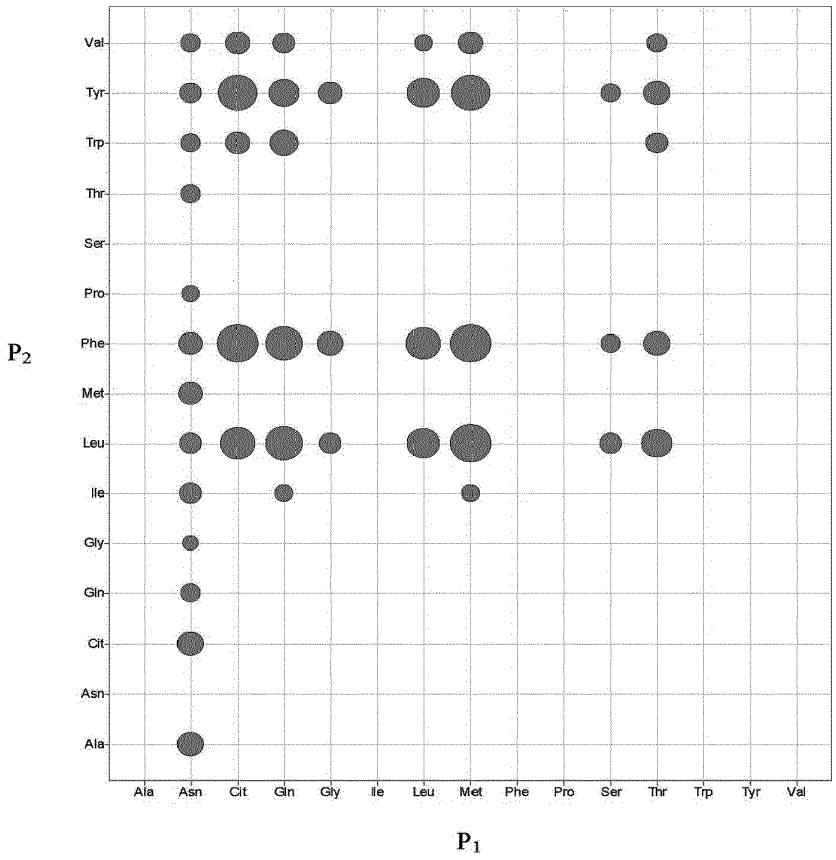


Figure 3. Released DNS for 2 h from DNS conjugates, which released DNS to 70% for 20 h. The vertical axis indicates the P_2 residure, and the horizontal axis indicates the P_1 residue. The amounts of drug released are indicated by the size of circle.

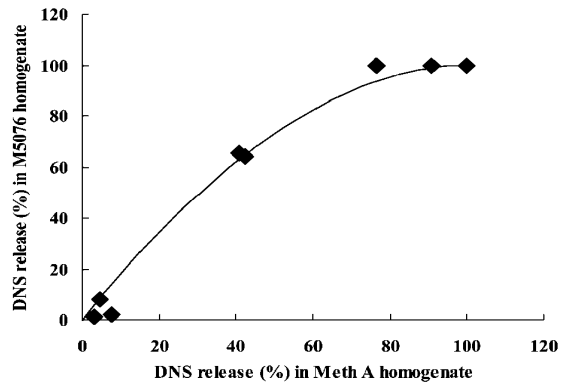


Figure 4. The relationship of released DNS from DNS conjugates between Meth A and M5076 homogenate. Several kinds of DNS conjugates were incubated in Meth A or M5076 homogenate for 20 h, and released DNS were determined by HPLC.

CM-Dex-PA-Gly-Gly-Pro-Leu-DXR, DXR was hardly detected in the liver as well as the tumor (Figure 6C).

DISCUSSION

Tumorotropic macromolecular prodrugs with peptide spacers promise to improve the efficacy and reduce the toxicity of the cancer chemotherapy. It is generally believed that the prodrugs

Table 1. Drug Release from DNS Conjugates and DXR Conjugates in 20 h Incubation with Meth A Homogenates

	drug release (%)	
peptide	DNS conjugate	DXR conjugate
Gly-Gly-Phe-Gly	100	100
Gly-Gly-Ile-Gly	41	8
Gly-Gly-Pro-Leu	15	0.3

that reached tumor tissues are taken up by tumor cells and release drug by lysosomal cysteine protease, cathepsins (*9, 10, 18*). Substrate specificity of cathepsins has been investigated over a few decades (*19*−*21*), including high-throughput profiling of serine and cysteine proteases using a microarray technique (*22*−*24*). However, taking into account that a polymer backbone sterically limits acceess of proteases to the peptide bond (*11, 25*−*27*), systematic studies specialized to macromolecular prodrugs have been required. In this context, we combinatorially synthesized 225 fluorogenic macromolecular prodrugs with a CM-Dex-PA backbone and evaluated sequence dependence of amino acid spacers on the rate of drug release by tumor-associated proteases. We intended to evaluate structure−activity relationship of drug release under rather physiologically relevant conditions (i.e., tumor cell homogenates) than by individual cathepsins, since it was obvious that multiple proteases including cathepsins B and L are responsible for hydrolysis of the same type of macromolecular prodrugs (*17*).

Several investigations have already found that dipeptide having hydrophobic amino acid at P_2, such as Phe, Val, Leu, Ile, and Trp, and basic amino acid as Lys, or hydrogen bond

OnCusp
Ex. 1002

Table 2. Antitumor Activity of DXR Conjugates against Meth A Bearing Mice[a]

compound	schedule	dose[b] (mg/kg)	tumor weight mean ± SE (g)	IR (%)	BWLmax[c]	D/U[d]
control			1.823 ± 0.446	0	<0	0/6
CM-Dex-PA-Gly-Gly-Phe-Gly-DXR	qdx1	40	0.207 ± 0.061***	89	21.6	0/6
	qdx1	20	0.260 ± 0.051***	86	6.7	0/6
	qdx1	10	0.389 ± 0.091***	79	2.5	0/6
	qdx1	5	0.759 ± 0.136**	58	1.7	0/6
CM-Dex-PA-Gly-Gly-Ile-Gly-DXR	qdx1	40	0.291 ± 0.115**	84	23.9	2/6
	qdx1	20	0.286 ± 0.089***	84	3.4	0/6
	qdx1	10	0.444 ± 0.038**	76	1.5	0/6
	qdx1	5	0.753 ± 0.167*	59	0.5	0/6
CM-Dex-PA-Gly-Gly-Pro-Leu-DXR	qdx1	40	1.094 ± 0.213	40	6.1	0/6
	qdx1	20	1.296 ± 0.166	29	<0	0/6
	qdx1	10	1.092 ± 0.300	40	<0	0/6
	qdx1	5	1.196 ± 0.185	34	<0	0/6
DXR	qdx1	20	0.738 ± 0.500	60	13	4/6
	qdx1	10	1.360 ± 0.282	25	3.7	0/6
	qdx1	5	1.571 ± 0.415	14	1.1	0/6

[a] Meth A cells were inoculated s.c. into BALB/c mice (Day 0). After 9 days, mice received a single (qd×1) administration of DXR conjugates and DXR (Day 9). Tumor weight was assessed on day 21. Asterisks indicate significant differences from the untreated control by Dunnett*s test. [b] Dose levels of compounds were expressed as those of DXR. [c] Maximum rate (%) of body weight loss, with numbers in parentheses denoting the day. <0 indicates no body weight loss. [d] Number of mice that died of toxicity/number of mice used. Death days were as follows. CM-Dex-PA-GGIG-DXR 40 mg/kg: day 16 and 17. DXR 20 mg/kg: days 17, 20, 20, and 20. *** $P < 0.001$. ** $P < 0.01$. * $P < 0.05$.

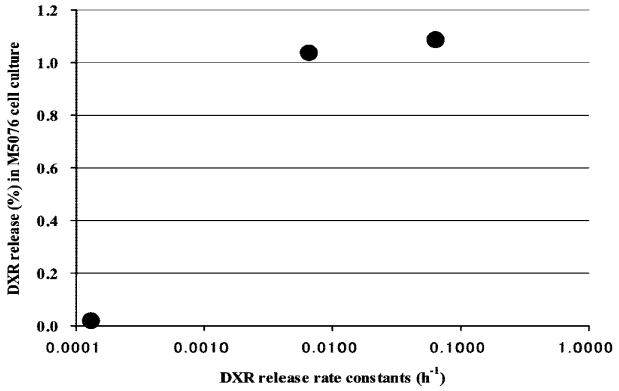


Figure 5. Relationship of released DXR from DXR conjugates between tumor homogenate and M5076 cell culture. CM-Dex-PA-Gly-Gly-Phe-Gly-DXR, CM-Dex-PA-Gly-Gly-Ile-Gly-DXR, and CM-Dex-PA-Gly-Gly-Pro-Leu-DXR were incubated with M5076 homogenate or M5076 cells for 24 h; released DXR were determined by HPLC (see Supporting Information).

amino acid as Cit at P_1, is able to be the substrate to cathepsin B (*28*). As shown in Figure 2, the release of DNS from prodrugs was rapid in the case of Val, Tyr, Trp, Phe, Met, Leu, and Ile at the P_2 position but slow in the case of Thr, Ser, Pro, Gly, Gln, Cit, and Ala. Thus, hydrophobicity of amino acids at P_2 would undoubtedly be important. When the P_1 position was a hydrophobic amino acid (Ile, Leu, Met, Phe, Tyr, Val), the cleavage appeared to occur even for spacers showing some resistance due to hydrophilic characters at P_2. It suggests that the proteases might simply recognize hydrophobic moieties and have a moderate sequence specificity. In addition, it should be noted that the P_1-DNS form tended to be released. From the viewpoint of molecular design, such hydrophobic amino acids should not be selected for P_1 to avoid the undesirable release of amino acid-conjugated drug.

In addition, when Asn was at P_1 or P_2, DNS and P_1-DNS, respectively, was released. It suggested that proteases associated with Meth A homogenate preferentially cleave the peptide bond at the C-terminal of Asn. On the other hand, the drug release rate became extremely low, when Pro was at P_1 or P_2. Pro, due to its distinctive cyclic structure in the side chain, exhibits steric hindrance and electrostatic repulsion and protects biologically active peptides against enzymatic degradation (*29*). Proteases associated with tumor cells would not be exceptional.

As mentioned above, it is desirable to design a macromolecular conjugate that does not release any conjugates with amino acids or peptides but only a native drug. On the basis of the examinations using fluorogenic macromolecular prodrugs, we selected three peptide spacers (Gly-Gly-Phe-Gly, Gly-Gly-Ile-Gly, Gly-Gly-Pro-Leu) that release only DNS at different rates and applied the spacers to the design of DXR conjugates. The rank order of the release of DXR from the conjugates was the same as that of DNS conjugates in both Meth A and M5076 tumor homogenates. Thus, examinations using fluorogenic macromolecular prodrugs undoubtedly gave useful information on the design of DXR conjugates. When CM-Dex-PA-Gly-Gly-Pro-Leu-DXR was administered to Meth A tumor-bearing mice, the tissue concentration of free DXR and antitumor activity was observed only minimally. This was quite reasonable, since the release of DXR from CM-Dex-PA-Gly-Gly-Pro-Leu-DXR was extremely slow in tumor homogenates. On the other hand, CM-Dex-PA-Gly-Gly-Phe-Gly-DXR and CM-Dex-PA-Gly-Gly-Ile-Gly-DXR, in spite of the fact that the release rate was ~10-fold different in tumor homogenates, exhibited similar pharmacokinetics and antitumor activity. The release of DXR from the conjugates would be determined not only by enzymatic activity but also by cellular uptake. It should be reiterated that water-soluble macromolecules hardly permeate plasma membranes. In the in vitro experiments using M5076 cells, the release of DXR was similar between CM-Dex-PA-Gly-Gly-Phe-Gly-DXR and CM-Dex-PA-Gly-Gly-Ile-Gly-DXR, being as slow as 1% of DXR per 24 h. Along with the fact that more than 15% of DXR could be released from these conjugates within 24 h, it is most likely that cellular uptake of the DXR conjugates is the rate-limiting step in vitro. As for DXR conjugates with the carboxymethyl—pullulan (CMPul) backbone (*12, 30, 31*), it has been reported that CMPul-Gly-Gly-Phe-Gly-DXR, which releases DXR rapidly in tumor homogenates, showed the highest antitumor activity, while CMPul-Gly-Gly-Gly-Gly-DXR, which releases DXR slowly, showed weaker activity than DXR in walker-256 and Yoshida sarcoma-bearing rat models. Our present investigation also revealed that the Gly-Gly-Gly-Gly spacer gave much slower release of DXR as compared to Gly-Gly-Phe-Gly and Gly-Gly-Ile-Gly spacers. Although the past (*12, 30, 31*) and present studies were different in terms of tumor models and polymer backbones, they presented an

OnCusp
Ex. 1002

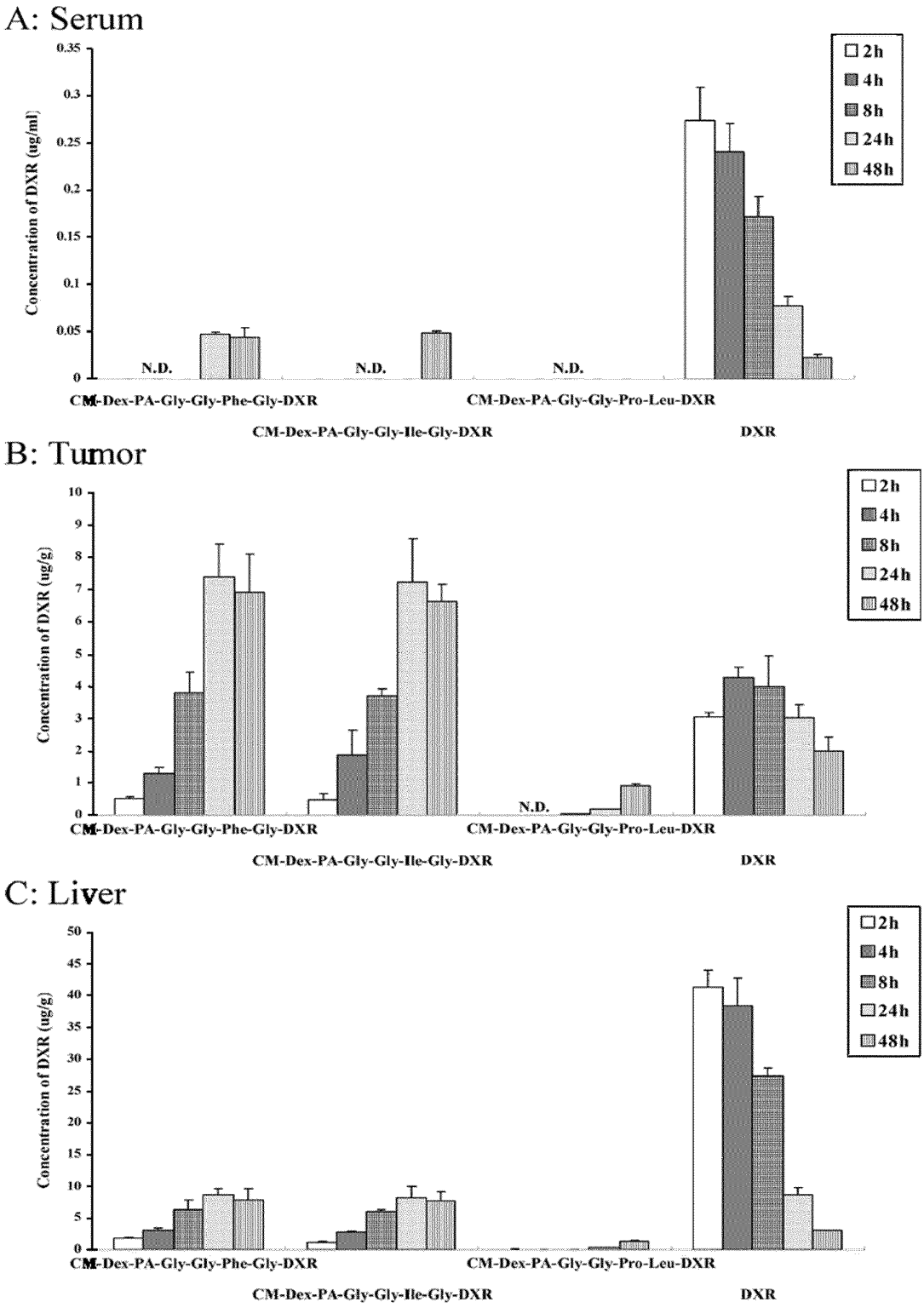


Figure 6. Pharmacokinetic profiles of free DXR after i.v. administration of DXR-conjugates or DXR to Meth A bearing mice at a dose equivalent to 20 mg/kg. Each point represents the mean for three mice; bars, SD. Parts A, B, and C indicate DXR concentration of serum, tumor, and liver, respectively. N.D.: Not detected.

essentially similar tendency. It might be concluded that the faster release of DXR provides greater antitumor activity, but the trend is saturated since cellular uptake of conjugates is smaller than the release of DXR based on the in vitro observations.

It is well-known that matrix metalloproteases (MMPs) are highly expressed in the tumor tissues. Macromolecular drug conjugates releasing active ingredients with MMPs have also been developed (*32, 33*). These conjugates were designed on the basis of earlier studies on substrate specificity of MMPs demonstrating a consensus motif of Pro-X-X-X_{Hy} where X_{Hy} is a hydrophobic amino acid residue (*34*−*36*). It is also known that peptides having Leu and Ile instead of Pro in the sequence can be substrates for MMP-2 (*34*). Since our macromolecular prodrugs have quite different amino acid sequences, i.e., Gly-Gly-X-X, from MMP substrates and showed a fairly good in vitro/in vivo correlation of drug release, it is unlikely that MMPs are responsible for the release of DXR from the conjugates. At this moment, however, involvement of MMPs has yet to be ruled out.

In summary, we systematically investigated the properties of peptide spacers controlling the drug release from conjugates and found representative peptide spacers, which release only parent drug with different rates. With regard to DXR conjugates, the conjugates showing a faster drug release rate provided greater antitumor activity in tumor-bearing mice. Considering that antitumor drugs are classified into time−concentration product (AUC)-dependent and time-dependent drugs (*37, 38*), however, the release rate of drugs needed to be controlled properly. We believe the present study provides useful information on the design of macromolecular prodrugs intended for antitumor chemotherapy.

ACKNOWLEDGMENT

The support of Dr. Kazuhiro Inoue is gratefully acknowledged. We thank Satoru Ohsuki for supporting the synthesis of the conjugates, and Setsuko Fukutake for carrying out the antitumor activity experiments.

Supporting Information Available: Additional table. This material is available free of charge via the Internet at http://pubs.acs.org.

LITERATURE CITED

(1) Kopecek, J., Kopeckova, P., Minko, T., Lu, Z.-R., and Peterson, C. M. (2001) Water soluble polymers in tumor targeted delivery. *J. Controlled Release 74*, 147–158.

(2) Maeda, H. (2001) The enhanced permeability and retention (EPR) effect in tumor vasculature: the key role of tumor-selective macromolecular drug targeting. *Adv. Enzyme Regul. 41*, 189–207.

(3) Vasey, P. A., Kaye, S. B., Morrison, R., Twelves, C., Wilson, P., Duncan, R., Thomson, A. H., Murray, L. S., Hilditch, T. E., Murray, T., Burtles, S., Fraier, D., Frigerio, E., and Cassidy, J. (1999) Phase I clinical and pharmacokinetic study of PK1 [N-(2-hydroxypropyl)methacrylamide copolymer doxorubicin]: first member of a new class of chemotherapeutic agents-drug-polymer conjugates. *Clin. Cancer Res. 5*, 83–94.

(4) Singer, J. W. (2005) Paclitaxel poliglumex (XYOTAX, CT-2103): a macromolecular taxane. *J. Controlled Release 109*, 120–126.

(5) Posey, J. A. III, Saif, M. W., Carlisle, R., Goetz, A., Rizzo, J., Stevenson, S., Rudoltz, M. S., Kwiatek, J., Simmons, P., Rowinsky, E. K., Takimoto, C. H., and Tolcher, A. W. (2005) Phase 1 study of weekly polyethylene glycol-camptothecin in patients with advanced solid tumors and lymphomas. *Clin. Cancer Res. 11*, 7866–7871.

(6) Inoue, K., Kumazawa, E., Kuga, H., Susaki, H., Masubuchi, N., and Kajimura, T. (2003) CM-dextran-polyalcohol-camptothecin conjugate: DE-310 with a novel carrier system and its preclinical data. *Adv. Exp. Med. Biol. 519*, 145–153.

(7) Duncan, R., Rejmanova, P., Kopecek, J., and Lloyd, J. B. (1981) Pinocytic uptake and intracellular degradation of N-(2-hydroxypropyl)methacrylamide copolymers. A potential drug delivery system. *Biochim. Biophys. Acta 678*, 143–150.

(8) Duncan, R., Lloyd, J. B., and Kopecek, J. (1980) Degradation of side chains of N-(2-hydroxypropyl) methacrylamide copolymers by lysosomal enzymes. *Biochem. Biophys. Res. Commun. 94*, 284–290.

(9) Duncan, R., Cable, H. C., Lloyd, J. B., Rejmanova, P., and Kopecek, J. (1982) Degradation of side-chains of N-(2-hydroxypropyl)methcrylamide copolymers by lysosomal thiol-proteinases. *Biosci. Rep. 12*, 1041–1046.

(10) Duncan, R., Cable, H. C., Lloyd, J. B., Rejmanova, P., and Kopecek, J. (1983) Polymers containing enzymatically degradable bond, 7. Design of oligopeptide side chains in poly N-(2-hydroxypropyl)methacrylamide copolymers to promote degradation by lysosomal enzymes. *Makromol. Chem. 184*, 1997–2008.

(11) Trouet, A., Masquelier, M., Baurain, R., and Deprez-De Campeneere, D. (1982) A covalent linkage between daunorubicin and proteins that is stable in serum and reversible by lysosomal hydrolases, as required for a lysosomotropic drug-carrier conjugate: in vitro and in vivo studies. *Proc. Natl. Acad. Sci. U.S.A. 79*, 626–629.

(12) Nogusa, H., Yano, T., Kashima, N., Yamamoto, K., Okuno, S., and Hamana, H. (2000) Structure-activity relationships of carboxymethylpullulan-peptide-doxorubicin conjugates-systematic modification of peptide spacers. *Bioorg. Med. Chem. Lett. 10*, 227–230.

(13) Veronese, F. M., Schiavon, O., Pasut, G., Mendichi, R., Andersson, L., Tsirk, A., Ford, J., Wu, G., Kneller, S., Davies, J., and Duncan, R. (2005) PEG-doxorubicin conjugates: influence of polymer structure on drug release, in vitro cytotoxicity, biodistribution, and antitumor activity. *Bioconjugate Chem. 16*, 775–784.

(14) Schmid, B., Warnecke, A., Fichtner, I., Jung, M., and Kratz, F. (2007) Development of albumin-binding camptothecin prodrugs using a peptide positional scanning library. *Bioconjugate Chem. 18*, 1786–1799.

(15) Ahmad, S., Tester, R. F., Corbett, A., and Karkalas, J. (2006) Dextran and 5-aminosalicylic acid (5-ASA) conjugates: synthesis, characterization and enzymic hydrolysis. *Carbohydr. Res. 341*, 2694–2701.

(16) Rozhin, J., Robinson, D., Stevens, M. A., Lah, T. T., Honn, K. V., Ryan, R. E., and Sloan, B. F. (1987) Properties of plasma membrane-associated cathepsin B-like cysteinase in metastatic B16 melanoma variants. *Cancer Res. 47*, 6620–6628.

(17) Shiose, Y., Ochi, Y., Kuga, H., Yamashita, F., and Hashida, M. (2007) Relationship between drug release of DE-310, macromolecular prodrug of DX-8951f, and cathepsins activity in several tumors. *Biol. Pharm. Bull. 30*, 2365–2370.

(18) Rejmanova, P., Pohl, J., Baudys, M., Kostka, V., and Kopecek, J. (1983) Polymers containing enzymatically degradable bond, 8. Degradation of oligopeptide sequences in N-(2-hydroxypropyl)methacrylamide copolymers by bovine spleen cathepsin B. *Makromol. Chem. 184*, 2009–2020.

(19) Barrett, A. J. (1980) Fluorimetric assays for cathepsin B and cathepsin H with methylcoumarylamide substrates. *Biochem. J. 187*, 909–912.

(20) Maciewicz, R. A., and Etherington, D. J. (1988) A comparison of four cathepsins (B, L, N and S) with collagenolytic activity from rabbit spleen. *Biochem. J. 256*, 433–440.

(21) Hasnain, D., Hirama, T., Huber, C. P., Mason, P., and Mort, J. S. (1993) Characterization of cathepsin B specificity by site-directed mutagenesis. Importance of Glu^{245} in the S2-P2 specificity for arginine and its role in transition state stabilization. *J. Biol. Chem. 268*, 235–240.

OnCusp
Ex. 1002

(22) Gosalia, D. N., and Diamond, S. L. (2003) Printing chemical libraries on microarray for fluid phase nanoliter reactions. *Proc. Natl. Acad. Sci. U.S.A. 100*, 8721–8726.

(23) Gosalia, D. N., Salisbury, C. M., Maly, D. J., Ellman, J. A., and Diamond, S. L. (2005) Profiling serine protease substrate specificity with solution phase fluorogenic peptide microarrays. *Proteomics 5*, 1292–1298.

(24) Gosalia, D. N., Salisbury, C. M., Maly, D. J., Ellman, J. A., and Diamond, S. L. (2005) High throughput substrate specificity profiling of serine and cysteine proteases using solution-phase fluorogenic peptide microarrays. *Mol. Cell. Proteomics 4*, 626–636.

(25) D'Souza, A. J. M., Topp, E. M. (2004) Release from polymeric prodrugs: linkages and their degradation. *J. Pharm. Sci. 93*, 1962−1979.

(26) Conover, C. D., Greenwald, R. B., Pendri, A., and Shum, K. L. (1999) Camptothecin delivery systems: the utility of amino acid spacers for the conjugation of camptothecin with polyethylene glycol to create prodrugs. *Anti-Cancer Drug Des. 14*, 499–506.

(27) Etrych, T., Jelinkova, M., Rihova, B., and Ulbrich, K. (2001) New HPMA copolymers containing doxorubicin bound via pH-sensitive linkage: synthesis and preliminary in vitro and in vivo biological properties. *J. Controlled Release 73*, 89–102.

(28) Dubowchik, G. M., Firestone, R. A., Padilla, L., Willner, D., Hofstead, S. J., Mosure, K., Knipe, J. O., Lasch, S. J., and Trail, P. A. (2002) Cathepsin B-labile dipeptide linkers for lysosomal release of doxorubicin from internalizing immunoconjugates: model studies of enzymatic drug release and antigen-specific in vitro antitumor activity. *Bioconjugate Chem. 13*, 858–869.

(29) Cunningham, D. F., and O'Connor, B. (1997) Proline specific peptidases. *Biochim. Biophs. Acta 1343*, 160–186.

(30) Nogusa, H., Yano, T., Kajiki, M., Gonsho, A., Hamana, H., and Okuno, S. (1997) Antitumor effects and toxicities of carboxymethylpullulan-peptide-doxorubicin conjugates. *Biol. Pharm. Bull. 20*, 1061–1065.

(31) Nogusa, H., Yano, T., Kajiki, M., Gonsho, A., Hamana, H., and Okuno, S. (2000) Distribution characteristics of carboxymethylpullulan-peptide-doxorubicin conjugates in tumor-bearing rats: different sequence of peptide spacers and DXR contents. *Biol. Pharm. Bull. 23*, 621–626.

(32) Lee, G. Y., Park, K., Kim, S. Y., and Byun, Y. (2007) MMPs-specific PEGylated peptide-DOX conjugate micelles that can contain free doxorubicin. *Eur. J. Pharm. Biopharm. 67*, 646–654.

(33) Chau, Y., Dang, N. M., Tan, F. E., and Langer, R. (2006) Investigation of targeting mechanism of new dextran-peptide-methotrexate conjugates using biodistribution study in matrix-metalloproteinase-overexpressing tumor xenograft model. *J. Pharm. Sci. 95*, 542–551.

(34) Chen, E. I., Kridel, S. J., Howard, E. W., Li, W., Godzik, A., and Smith, J. W. (2002) A unique substrate recognition profile for matrix metalloproteinase-2. *J. Biol. Chem. 277*, 4485–4491.

(35) Netzel-Artnett, S., Sang, Q. X., Moore, W. G., Navre, M., Birkedal-Hansen, H., and Van Wart, H. E. (1993) Comparative sequence specificities of human 72- and 92-kDa gelatinase (type IV collagenases) and PUMP (matrilysin). *Biochemistry 32*, 6427–6432.

(36) Seltzer, J. L., Akers, K. T., Weingarten, H., Grant, G. A., McCourt, D. W., and Eisen, A. Z. (1990) Cleavage specificity of human skin type IV collagenase (gelatinase). Identification of cleavage sites in type I gelatin, with confirmation using synthetic peptides. *J. Biol. Chem. 265*, 20409–20413.

(37) Shimoyama, M. (1975) The quantitative measurement of cytocidal actions of alkylating agents and anticancer antibiotics against in vitro cultured yoshida ascites sarcoma. *J. Jpn. Soc. Cancer Ther. 10*, 63–72.

(38) Shimoyama, M. (1975) The quantitative measurement of cytocidal actions of antimetabolites, vinca alkaloids and L-asparaginase against in vitro cultured yoshida ascites sarcoma. *J. Jpn. Soc. Cancer Ther. 10*, 195–201.

BC800238F

OnCusp
Ex. 1002

December 2007 Biol. Pharm. Bull. 30(12) 2365—2370 (2007) 2365

Relationship between Drug Release of DE-310, Macromolecular Prodrug of DX-8951f, and Cathepsins Activity in Several Tumors

Yoshinobu SHIOSE,*[,a] Yusuke OCHI,[b] Hiroshi KUGA,[c] Fumiyoshi YAMASHITA,[d] and Mitsuru HASHIDA[d]

[a] *Biological Research Laboratories IV, Daiichi Sankyo Co., Ltd., Kasai R&D Center; 1–16–13 Kita-Kasai, Edogawa-ku, Tokyo 134–8630, Japan:* [b] *R&D Planning Department, Planning Group, Daiichi Sankyo Co., Ltd., 1–2–58 Hiromachi, Shinagawa-ku, Tokyo 140–8710, Japan:* [c] *Development Research Department, Daiichi Sankyo Inc.; 389 Thornall Street, Edison, NJ08837, U.S.A.: and* [d] *Department of Drug Delivery Research, Graduate School of Pharmaceutical Sciences, Kyoto University; Kyoto 606–8501, Japan.*

Received May 23, 2007; accepted September 20, 2007; published online September 25, 2007

DE-310 is composed of the topoisomerase-I inhibitor DX-8951 (exatecan) and carboxymethyldextran polyalcohol (CM-Dex-PA) carrier, which are covalently linked *via* peptidyl spacer (Gly-Gly-Phe-Gly). In this study, we investigated relationship between the cathepsin activity and the drug release of DE-310 by use of human liver origin cathepsin (B, L and H) and tumor cells (murine tumor cells (Meth A and M5076), and human tumor cells (HCT116, A549, PC-12, T98G, and HL-60)). Preliminary studies indicated that human liver cathepsin B produced Glycyl DX-8951 (G-DX-8951) from DE-310 more preferentially than DX-8951, whereas human liver cathepsin L produced DX-8951 preferentially. Release of drugs from DE-310 and cathepsin activities were measured in tumor cell types. The release of both DX-8951 and G-DX-8951 from DE-310 correlated well with cathepsin B activity of tumor cells. The release of DX-8951 was weakly, but not significantly, correlated with cathepsin L activity. In M5076 (high cathepsin activity) or Meth A (low cathepsin activity) xenograft models, the levels of DX-8951 and G-DX-8951 in M5076 were higher than in Meth A after single intravenous administration of DE-310. Our findings suggest that cathepsin B is primarily responsible for drug release from DE-310 in tumor.

Key words macromolecular prodrug; DE-310; camptothecin; cathepsin B; cathepsine L

Utilization of drug delivery systems is an attractive approach to improving efficacy and safety of anticancer drugs. Long-circulating macromolecular or particulate carriers are known to preferentially accumulate in solid tumors, due to the "enhanced permeability and retention (EPR)" effect,[1] *i.e.*, leakiness of tumor angiogenic blood vessels and lack of effective lymphatic drainage. SMANCS (neocartinostatin polymer conjugate), Doxil (doxorubicin liposome), and Daunozome (daunorubicin liposome)[2,3] that exploit the EPR effect have already been launched in the market. Besides, PK1 (doxorubicin-HPMA polymer),[4] XYOTAX (paclitaxel-polyglutamate),[5] and NK911 (doxorubicin micelle)[6] are under clinical investigation.

DE-310 is a novel macromolecular prodrug of the topoisomerase-I inhibitor (1*S*,9*S*)-1-amino-9-ethyl-5-fluoro-1,2,3,9,12,15-hexahydro-9-hydroxy-4-methyl-10*H*,13*H*-benzo[de]-pyrano)[3′,4′:6,7]indolizino[1,2-*b*]quinoline-10,13-dione (DX-8951).[7] DX-8951 is covalently linked with carboxymethyl dextran polyalcohol (CM-Dex-PA) *via* the Gly-Leu-Phe-Gly (GGFG) tetrapeptide spacer (Fig. 1).[7] It has been demonstrated that a single dose of 11.4 mg/kg DE-310 exhibited stronger anti-tumor activity in mice than repeated doses (10 mg/kg daily for 5 d) of DX-8951f (exatecan; DX-8951 monomethansulfonate salt).[8] Taking into account that DX-8951f belongs to time-dependent anti-cancer drugs,[9] slow release of DX-8951 from DE-310 in addition to long-term retention in tumor tissues would have been beneficial in exhibiting such an effective anti-tumor activity.

The peptide spacer of DE-310 was designed to be cleaved by cysteine protease, cathepsins. Expression of cathepsins B, H, and L in tumor tissues and their involvement in tumor progression have been indicated.[10] Cathepsin B is expressed more highly in malignant tumors[11] and is responsible for destruction of basal membranes, processing of matrix proteases, and inactivation of protein inhibitors.[12] On the other hand, cathepsin H is highly expressed in colon cancer cells,[13] and cathepsin L is secreted in metastatic bone marrow tumor.[14] It is likely that the level of cathepsin species in tumor tissues would be one of the factors determining anti-tumor activity of DE-310.

In this study, we examined the drug release from DE-310 by cathepsins B, H, and L obtained from human liver to identify the products of hydrolysis and determine the rate of hydrolysis for each cathepsin species. Then, we examined *in vitro* drug release from DE-310 in different murine or human tumor cell types, in addition to the activity or expression of cathepsins B, H and L in the cells. Correlation between the drug release and cathepsin levels was analyzed to quantitatively delineate the mechanism of drug release from DE-310. In addition, tumor tissue distribution of DE-310 was investi-

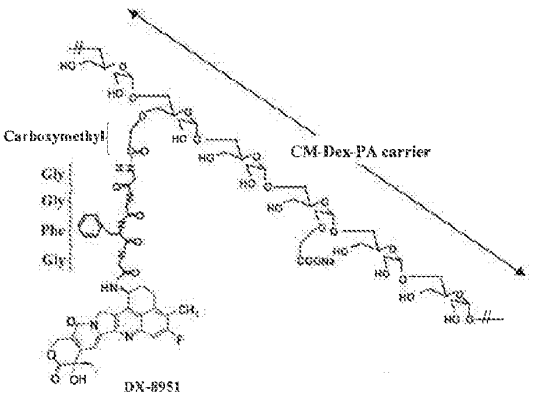


Fig. 1. Structure of DE-310

* To whom correspondence should be addressed. e-mail: shiose.yoshinobu.gn@daiichisankyo.co.jp

© 2007 Pharmaceutical Society of Japan

OnCusp
Ex. 1002

gated in two types of solid tumor bearing mice, *i.e.*, Meth A and M5076, which were different in cathepsin activity.

MATERIALS AND METHODS

Materials DE-310 is composed of carboxymethylated polyalcohol carrier, tetrapeptidyl spacer (Gly-Gly-Phe-Gly), and camptothecin analog DX-8951. DX-8951f is [(1*S*,9*S*)-1-amino-9-ethyl-5-fluoro-1,2,3,9,12,15-hexahydro-9-hydroxy-4-methyl-10*H*,13*H*-benzo[de]pyrano[3',4':6,7]indolizino-[1,2-*b*]quinoline-10,13-dione] monomethanesulfonate (salt) dehydrate. These were synthesized by Daiichi Pharmaceutical Co., Ltd. (Tokyo, Japan). DE-310 contained 5—7%w/w DX-8951 and its molecular weight (MW) was *ca.* 340000 with a narrow polydisperaity (weight average MW/number-average MW<1.3). For use, DE-310 was dissolved in pyrogen-free distilled water (Otsuka Pharmaceutical Company, Tokyo, Japan) and stored 4 °C overnight. Benzyloxycarbonyl-arginylarginine-4-methyl-7-coumarylamide (Z-Arg-Arg-MCA) and l-arginine-4-methyl-7-coumarylamide (Arg-MCA), which are specific substrates for cathepsin B and cathepsin H, respectively,[15] were purchased from Peptide Institute, Inc. (Osaka, Japan). Cathepsin B (human liver, 3175 units/ml solution) was purchased from Sigma (St. Louis, MO, U.S.A.). Cathpsin L (human liver, 41.7 mU/ml solution) and Cathepsin H (human liver, 1330 mU/mg protein; 893.76 mU/ml solution) were purchased from Calbiochem (La Jolla, CA, U.S.A.). Cathepsin H was diluted to 446.88 mU/ml with 20 mM acetate buffer (pH 5.0) containing 1 mM of EDTA and 0.1% Brij 35. Cathepsin C (Bovine Spleen, 5.4 units/mg solid) was purchased from Sigma (St. Louis, MO, U.S.A.), diluted to 10.26 units/ml with 20 mM acetate buffer (pH 5.5) containing 1 mM of EDTA and 0.1% Brij 35.

Meth A (murine fibrosarcoma) was kindly obtained from Dr. Ichiro Azuma (Institute of Immunological Science, School of Medicine, Hokkaido University, Japan). HCT116 (human colon cancer) and T98G (human glioma) were obtained from American Type Culture Collection (VA, U.S.A.). A549 (human lung carcinoma) and PC-12 (human lung carcinoma expressed *p*-glycoprotein) were obtained from Toray Industries (Shizuoka, Japan). All of the cells were cultured in RPMI 1640 (Gibco-BRL, NY, U.S.A.) medium supplemented with 10% fetal bovine serum (FBS; Hyclone Laboratries, Logan, UT, U.S.A.). M5076 (murine ovarian sarcoma) was obtained from the Japanese Foundation for Cancer Research (Tokyo, Japan), and cultured in RPMI 1640 medium supplemented with 17% horse serum (HS; Hyclone Laboratries, Logan, UT, U.S.A.).

***In Vitro* Drug Release from DE-310 with Human Cathepsins** A 10 μl aliquot of 41.7 mU/ml human cathepsin solution was added to 180 μl of Britton–Robinson buffer (pH 4.5, 5.5 or 6.5) containing 1 mM of EDTA and 10 mM of cysteine and 0.1% Brij 35. Then a 10 μl aliquot of DE-310 solution was added to give a final concentration of 5 nmol/ml (DX-8951 equivalents). These reactions were done at 40 °C for 20 h and stopped by the addition of 200 μl of CH_3CN : 0.1 N HCl = 1 : 1 solution to the mixture. The amount of DX-8951 and G-DX-8951 in the reaction mixture was measured by HPLC.

***In Vitro* Drug Release from DE-310 with Tumor Cells** Meth A, M5076, HCT116, T98G, A549, HL-60 and PC-12 were plated in non-coated 60 mm dishes (1×10^7 cells/4 ml/dish) and then DE-310 solution was added to give a final concentration of 20 μg/ml (DX-8951 equivalents). These dishes were incubated at 37 °C for 24 h in air containing 5% CO_2. In the case of Meth A, M5076, and HL-60, the dishes were shaken with a micomixer (Model No. MX-5, Sanko Junyaku Company, Tokyo, Japan). At the end of incubation, the cells were centrifuged at 1000 *g* for 10 min, and 500 μl of the supernatant was taken for the HPLC assay. The cells were rinsed with saline 3 times and treated with 300 μl of the 1 : 1 (v/v) mixture of 0.5 M HCl and acetonitrile. In the case of HCT116, A549, PC-12 and T98G, which are adherent cells, the culture medium was aspirated off and then the cells were rinsed with saline 3 times and lysed with 1 ml of the 1 : 1 (v/v) mixture of 0.5 M HCl and acetonitrile. In both cases, the cell lysate was centrifuged at 10000 *g* for 10 min and the supernatant were analyzed by HPLC. Furthermore, release drugs in culture medium were determined. The culture media were collected, and added to same volume of 0.5 M HCl containing 50% (v/v) acetonitrile solution. The solutions were centrifuged at 10000 *g* for 10 min, and the supernatants were analyzed by HPLC.

Cathepsins Activities in Tumor Cells The cell suspensions (1×10^7 cells/ml) were homogenized by the handy micro homogenizer NS-310F (MICROTEC, Co., Ltd., Chiba, Japan) and then centrifuged (12000 *g*, 4 °C, 10 min) to yield the supernatant. The content of proteins leaked in the supernatant was determined by Bio-Rad protein assay dye reagent (Japan Bio-Rad Laboratories, Inc., Tokyo, Japan), using bovine serum albumin as a reference. The activities of cathepsins B and H in the supernatant were measured using the substrates Z-Arg-Arg-MCA and Arg-MCA, respectively, in a similar manner to the method of Barrett.[15] Briefly, to 2 μl of the solution, 125 μl of 400 mM phosphate buffer (352 mM KH_2PO_4, 48 mM Na_2HPO_4, 4 mM EDTA, pH 6.0), 365 μl of 0.1% Brij 35 and 4 μl of freshly prepared 1 M cysteine were added and preincubated for 5 min at 40 °C. The reaction was started by the addition of 1 μl of 10 mM substrate (Z-Arg-Arg-MCA or Arg-MCA) solution. Ten minutes later, 500 μl of the solution containing 100 mM sodium chloroacetate, 30 mM sodium acetate and 70 mM acetic acid was added to stop the reaction. The amount of 7-amino-4-methyl-coumarin (AMC) liberated was measured by HPLC. Enzyme activities were calculated using a calibration curve established with AMC standard. One unit of enzyme activity was defined as the amount of enzyme required to liberate 1 μmol of AMC per minute from the substrates at 40 °C. Expression of cathepsin L in the tumor cell was determined by a commercially available ELISA kit (RD laboratories, Diessen, Germany). The level of cathepsin L was expressed in mU of analyte per milligram of tissue protein.

Tumor Tissue Distribution of DE-310 in Meth A and M5076 Xenograft Models Meth A cells (1×10^6 cells/0.1 ml/mouse) and M5076 cells (2×10^6 cells/0.1 ml/mouse) were inoculated subcutaneously into the right flank of syngeneic BALB/c and C57BL/6 mice (Japan SLC, Inc., Shizuoka, Tokyo), respectively. When estimated tumor volume reached to approximately 500 mm^3 after transplantation, the mice were injected intravenously with DE-310 at 11.4 mg/kg (DX-8951 equivalents, n=3). At 24, 48, and 72 h

OnCusp
Ex. 1002

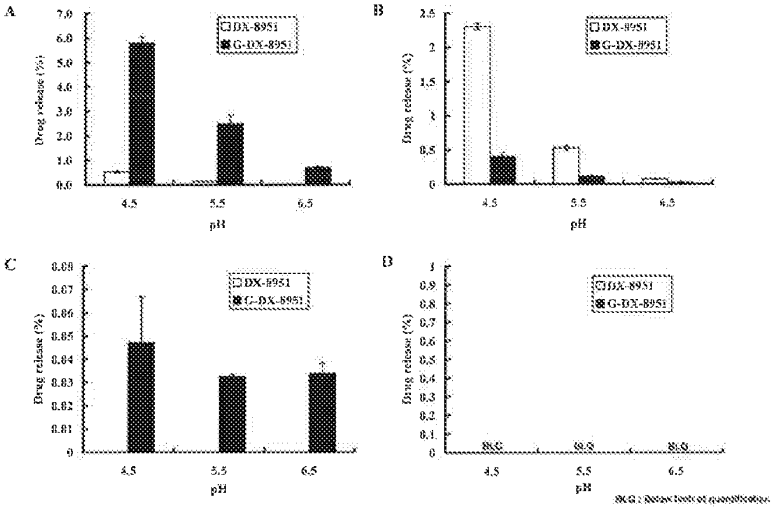


Fig. 2. Release of DX-8951 and Glycyl DX-8951 from DE-310 Incubated with Cathepsin B (A), Cathepsin L (B), Cathepsin H (C), and without Any Enzymes (D) at 37 °C for 20 h

after administration of DE-310, tumor tissue was removed and weighed. Samples were stored at −30 °C until analysis. The samples were mixed with CH_3CN : 0.5 N HCl=1 : 1 solution at 4-fold volume (v/w) per tissue weight, and homogenized on ice using handy micro homogenizer to extract DX-8951, G-DX-8951 and conjugated-DX-8951. The homogenates were centrifuged (15000 *g*, 10 min), and the supernatant was analyzed to determine the amount of DX-8951 and G-DX-8951 by HPLC. Furthermore, for determining the amount of conjugated DX-8951, 5 μl of the supernatant was added to 95 μl of α-chymotrypsin (2 mg/ml) dissolved by Britton–Robinson buffer (pH 6.0), and incubated at 40 °C for 2 h. After that, the reaction was stopped by adding 100 μl of CH_3CN : 0.5 N HCl=1 : 1 solution and centrifuged (15000 *g*, 10 min). The supernatant was analyzed to determine the amount of total G-DX-8951 by HPLC, conjugated-DX-8951 calculated by deduction of G-DX-8951 from total amount of G-DX-8951.[16]

HPLC Analysis The concentrations of DX-8951 and G-DX-8951 in the medium and cell extracts were determined by reversed-phase HPLC (CCPM-II pump, Tosoh, Tokyo, Japan) at 40 °C implementing Symmetry Shield RP18 (4.6×100 mm; Waters, Milford, MA, U.S.A.). The mobile phase was a mixture of 36.5% of acetonitrile/methanol (2/1, v/v) and 64.5% of 0.1% trifluoroacetic acid at Symmetry Shield RP18 column, flowed at 1.0 ml/min. Detection was performed using the Waters 474 fluorescence detector (Waters, Milford, MA, U.S.A.) with excitation and emission wavelength of 375 nm and 445 nm, respectively. The peak area was calculated using a Millenium chromatography manager system (Waters, Milford, MA, U.S.A.). Measurement of AMC in cathepsins assay samples were also carried out with the same HPLC system, where excitation and emission wavelengths were set at 346 nm and 437 nm, respectively. The mobile phase of AMC was a mixture of 27% of acetonitrile/methanol (2/1, v/v) and 73% of distilled water.

RESULTS

***In Vitro* Drug Release from DE-310 with Human Cathepsins** Preliminary studies were carried out with cathepsins isolated from human liver. Figure 2 shows the release of DX-8951 and G-DX-8951 from DE-310 incubated with human cathepsins. For all cathepsins, the quantity of drug release decreased with increasing pH within the pH range tested. In cathepsin B, the release of G-DX-8951 was 10-fold higher than that of DX-8951 at pH 4.5 (Fig. 2A). On the contrary, cathepsin L catabolized the release of DX-8951 more preferentially (approximately 6-fold higher) than that of G-DX-8951 (Fig. 2B). As for cathepsin H, no DX-8951 was detected while only a small amount of G-DX-8951 was detected (<0.05 %) (Fig. 2C). When DE-310 was incubated in the absence of any enzymes, the drugs were not released at all (Fig. 2D).

***In Vitro* Drug Release from DE-310 with Murine and Human Cells** In order to investigate relationship between drug release from DE-310 and cathepsin activity, first, drug release from DE-310 was investigated in different tumor cells, *i.e.*, two types of murine (Meth A and M5076) and 5 types of human (T98G, A549, HL-60, PC-12, and HCT116) tumors cells. The release of both DX-8951 and G-DX-8951 were detected in all cell lines, where the total amount of DX-8951 and G-DX-8951 released varied 3.77—51.27 pmol/10^7 cells/24 h and 15.53—467.63 pmol/10^7 cells/24 h, respectively (Table 1). Here, most of the drugs released were detected in the incubation medium. The release of DX-8951 was the highest in M5076 cells, followed by T98G> A549≈Meth A>HL-60>PC-12≈HCT116. Although the release of G-DX-8951 was also highest in M5076 cells, it was remarkably low in A549 cells that exhibited a high activity towards the release of DX-8951. The release of the drugs did not occur when DE-310 was incubated with the cell-conditioned medium (data not shown).

Cathepsins Activity in Tumor Cells To delineate vari-

ability of the release of drugs from DE-310 in different tumor cells, the levels of cathepsins B, H and L were investigated (Table 2). Cathepsin B activity was much more variable than that of cathepsin H. The activity of cathepsin B was the highest in T98G cells followed by M5076>A549>PC-12>HCT116>Meth A>HL-60. Expression of cathepsin L in human tumor cells was evaluated by ELISA involving human cathepsin L antibody, protein expression of cathepsin L per total amount of protein was determined in human tumor cells, except for murine tumors. Expression of cathepsin L per cellular proteins ranged from 0.90 to 2.89 mU/mg protein, which was the highest in T98G cells followed by A549>HCT116>PC-12>HL-60. On the other hand, cathepsin H activity ranged from 0.03 to 0.08, which was much lower than other cathepsins.

Table 1. The Drug Release from DE-310 with Several Tumor Cells *in Vitro*

Origin	Cell line	Source	DX-8951 (pmol/10^7 cells)	G-DX-8951 (pmol/10^7 cells)
Murine	Meth A	Cell lysate	0.32±0.09	1.28±0.24
		Medium	15.01±3.11	38.93±3.64
		Total	15.33±3.04	40.22±3.88
	M5076	Cell lysate	1.11±0.26	14.74±0.16
		Medium	50.17±7.86	452.89±16.11
		Total	51.27±7.66	467.63±16.26
Human	HCT116	Cell lysate	0.44±0.07	3.65±0.51
		Medium	3.33±1.04	31.6±1.91
		Total	3.77±1.01	35.25±1.89
	A549	Cell lysate	0.47±0.10	1.65±0.18
		Medium	17.17±4.33	13.87±5.49
		Total	17.64±4.23	15.53±5.37
	PC-12	Cell lysate	0.34±0.07	1.25±0.11
		Medium	5.14±1.17	50.53±0.93
		Total	5.49±1.24	51.76±0.84
	T98G	Cell lysate	1.99±0.40	16.21±0.90
		Medium	30.28±7.25	115.95±5.54
		Total	32.27±7.10	132.16±4.66
	HL-60	Cell lysate	BLQ	2.28±0.24
		Medium	5.60±0.73	42.38±6.15
		Total	5.60±0.73	44.66±0.32

DE-310 (20 μg/ml) were incubated with several tumors (1×10^7 cells/dish) at 37 °C for 24 h (n=3). The release drugs were determined by HPLC (mean±S.D.). BLQ: Below limit of quantification.

Table 2. Cathepsin Activities in Various Tumor Cells[a]

Origin	Cell line	Cathepsin B (mU/mg protein)	Cathepsin H (mU/mg protein)	Cathepsin L (mU/mg protein)
Murine	Meth A	0.89±0.14	0.03±0.004	N.D.[b]
	M5076	5.36±0.61	0.08±0.011	N.D.[b]
Human	HCT116	1.30±0.16	0.04±0.005	2.08±0.03
	A549	4.25±0.50	0.04±0.007	2.26±0.15
	PC-12	3.67±0.64	0.03±0.003	1.11±0.08
	T98G	11.88±1.60	0.05±0.009	2.89±0.03
	HL-60	0.42±0.17	0.05±0.011	0.90±0.02

a) Cell suspensions (1×10^7 cells/ml) were homogenized, and centrifuged to yield the supernatant. The content of protein in the supernatant was determined by Bio-Rad protein assay dye reagent. The activities of cathepsins B and H in the supernatant were determined using the substrates Z-Arg-Arg-MCA and Arg-MCA, respectively, while that of cathepsin L was determined by ELISA kit. *b*) Not determined.

Correlation Analysis The relationship between activity of cathepsins and drug release using murine and human tumor cells was statistically investigated in Table 3. Here, cathepsin activity represents the total amount of the liberated drug detected in both incubation medium and cell lysate. The release of DX-8951 from DE-310 was highly correlated with cathepsin B activitiy in human tumor cells (r=0.9421, p=0.0166). The release of G-DX-8951 was also correlated with cathepsin B activity and released G-DX-8951 (r=0.8494, p=0.0685). As for cathepsin L, there was a positive association between expression and released DX-8951, though it was not statistically significant (r=0.8047, p=0.1005). Between the level of cathepsin L expression and released G-DX-8951, there was not a significant correlation. Furthermore, when we did similar analysis with added two murine tumor cells, the correlation coefficient between cathepsin B and released DX-8951 or G-DX-8951 decreased to 0.6110, 0.3430, respectively (data not shown). As a result, though there were a few examples, it suggested that species differences with murine and human existed in the correlation with cathepsin B and drug release.

Tumor Tissue Distribution of DE-310 Distribution of conjugated DX-8951, DX-8951, and G-DX-8951 in Meth A or M5076 tumor tissues was evaluated at 24, 48, and 72 h post intravenous injection of DE-310 (Table 4). At all time points, concentration of DX-8951 and G-DX-8951 was higher in M5076 xenograft models than in Meth A xenograft

Table 3. Correlations between Drug Release and Cathepsin Activity in Tumor Cells

Drug release *vs.* cathepsin activity	Correlation coefficient (r)	p value
DX-8951 *vs.* cathepsin B	0.9421	0.0166
G-DX-8951 *vs.* cathepsin B	0.8494	0.0685
DX-8951+G-DX-8951 *vs.* cathepsin B	0.9114	0.0312
DX-8951 *vs.* cathepsin L	0.8047	0.1005
G-DX-8951 *vs.* cathepsin L	0.4838	0.4098
DX-8951+G-DX-8951 *vs.* cathepsin L	0.5785	0.3069

Table 4. Tumor Distribution of Conjugated and Released DX-8951 in Meth A and M5076 Xenograft Models after Intravenous Injection of DE-310[a]

Tumor	Time (h)	DX-8951 (nmol/g)	G-DX-8951 (nmol/g)	Conjugated DX-8951 (nmol/g)	Percent released[b]	
					DX-8951	G-DX-8951
Meth A	24	0.25±0.04	0.71±0.14	45.58±9.89	0.55	1.56
	48	0.11±0.02	0.27±0.04	28.06±2.45	0.39	0.96
	72	0.08±0.02	0.19±0.05	18.95±4.60	0.42	1.00
M5076	24	1.64±0.24	14.82±1.52	146.91±20.33	1.12	10.09
	48	0.57±0.06	4.52±0.64	76.64±12.18	0.74	5.90
	72	0.49±0.09	3.24±0.69	74.07±21.46	0.66	4.37

a) DE-310 (11.4 mg DX-8951 equivalent/kg) was intravenously administered in Meth A or M5076 bearing mice. Tumor tissue was excised at 24, 48, and 72 h post injection, and DX-8951 species in tumor tissues were determined. *b*) Percent released means the ratio of released drugs to conjugated DX-8951.

5541 of 14295

OnCusp
Ex. 1002

models. Even when the level of DX-8951 and G-DX-8951 was standardized with that of conjugated DX-8951, the level of both forms DX-8951, especially G-DX-8951, was greater in M5076 xenograft models.

DISCUSSION

DE-310 has a GGFG tetrapeptide spacer for linking DX-8951 with CM-Dex-PA. It was believed that the GGFG sequence was a substrate of lysosomal enzymes,[17—19] as well as GFLG[20,21] or some others.[22—25] Nogusa *et al.*[17—19] examined effect of peptide spacers on the release and anti-tumor activity of the drug, doxorubicin (DXR), conjugated with carboxymethyl-pullulan (CMPul). CMPul-GGFG-DXR showed the highest release of the drug, followed by CMPul-GFGG-DXR and CMPul-GGGG-DXR, when the conjugates were incubated with lysosomes for 24 h.[17] Among the three conjugates, CMPul-GGFG-DXR indicated the strongest anti-tumor effect against rat bearing Walker-256, and Yoshida sarcoma.[18] Their research group subsequently reported that anti-tumor activity of CMPul-GGFG-DXR was equivalent to that of CMPul-GFLG-DXR,[19] which has a well-known GFLG spacer.[20,21]

Our previous studies have shown that DE-310 elicits significant anti-tumor activity in various tumor models, whereas the activity occurred at lower doses and with a more profound effect than DX-8951 alone.[8] High levels and prolonged retention of conjugated DX-8951, DX-8951, and G-DX-8951 have been observed in tumor tissues after intravenous injection of DE-310 in Meth A tumor-bearing mice.[26] Thus, liberated DX-8951s are believed to exhibit a cytotoxic effect in tumor tissues. Preclinical data indicated that the inhibitory activity of DX-8951 on topoisomerase-I activity is comparable to G-DX-8951 and that the *in vitro* cytotoxicity of DX-8951 is about 20—190 times more potent than G-DX-8951 (unpublished results). A clinical study demonstrated that G-DX-8951 concentration in tumor tissues are approximately ten fold greater than DX-8951, suggesting that G-DX-8951 might partially contribute to the cytotoxic activity of DE-310.[27]

Structural requirements for drug release from macromolecular prodrugs have been discussed by Soyez *et al.*[28] who concluded that, whereas general trends could be found, the type of carrier and drug used greatly influences the degradation rate and pattern due to specificities of substrate-enzyme reactions. Taking into account the difference in cytotoxic effects between DX-8951 and G-DX-8951, the present study was initiated to investigate how these two forms appear from DE-310 hydrolysis.

Our previous investigation demonstrated that the release of the parent drugs from DE-310 were completely inhibited by a representative cysteine protease inhibitor E-64[29] in Meth A cell homogenate, indicating the involvement of cathepsins in this process. *In vitro* studies revealed (a) that cathepsin B produces both DX-8951 and G-DX-8951 while cathepsin L produces DX-8951 preferentially, (b) that the activity of cathepsins in tumor cells varies widely, and (c) that the release of G-DX-8951 from DE-310 showed a high correlation with cathepsin B activity in tumor cells, while that of DX-8951 did with cathepsins B and L. Thus, variablity of cathepsins activity in cell types would affect the release rate of DX-8951 or G-DX-8951 from DE-310 in the *in vivo* conditions. When Meth A and M5076 xenograft models were compared, tumor tissue concentration ratio of liberated drugs, especially G-DX-8951, was greater in M5076 xenograft model (Table 4). The *in vivo* result is reasonable, given that cathepsin B activity of M5076 cells was much greater than that of Meth A cells.

In the hydrolysis of HPMA-GFLG-nitroanilide,[21] PK1,[30] and CMPul-GGFG-DXR[17—19] by cathepsin B, glycylated forms were not produced from macromolecular prodrugs. When norfloxacin was coupled with chloroformate-activated dextran *via* GFLG spacer, on the other hand, G-norfloxacin was released in the presence of cathepsin B. Cathepsin B is a lysosomal thiol protease that has been found in the cells of many species. Besides endopeptidase activity, cathepsin B has also carboxydipeptidase activity.[31] Soyez *et al.*[28] reported that NAP was released from HPMA-GFLG-NAP while F-NAP was released first from HPMA-GFLGF-NAP. Thus, the pattern of release appears to depend on the kind of drugs and spacers, relating to steric or electrostatic effect of their molecular structures.

The present study demonstrated that the release of drug from DE-310 depends on expression of cathepsins in tumor. Since the rate of drug release determines concentration–time course of liberated drug, it might be an important factor determining anti-tumor activity. The release of drug does not appear to be rate-limiting, since the tumor tissue concentration–time profiles of free DX-8951 and G-DX-8951 were parallel to that of conjugated DX-8951 (Table 4). When anti-tumor activity of DE-310 was concerned, however, appearance of G-DX-8951 would not be desirable. To avoid this problem, further design of spacer will be needed. Dubowchik *et al.*[32] indicated that cathepsine B-mediated drug release was increased when self-immolative *p*-aminobenzylcarbonyl (PABC) spacer was inserted between DXR and lysosomal protease-sensitive peptides. In our on-going studies, PABC was inserted between DX-8951 and GGFG in DE-310, demonstrating that the release of free DX-8951 from the conjugate was more than 100 times greater than DE-310 in homogenates prepared from murine Meth A solid tumor. The experimental results will be reported elsewhere.

Acknowledgements The authors wish to thank Dr. Eiji Kumazawa and Dr. Kazuhiro Inoue for their advice concerning study.

REFERENCES

1) Maeda H., *Adv. Enzyme Regul.*, **41**, 189—207 (2001).
2) Matsumura Y., Maeda H., *Cancer Res.*, **46**, 6387—6392 (1986).
3) Jankneqi R., *Support Care Cancer*, **4**, 298—304 (1996).
4) Vasey P., Kaye S. B., Morrison R., Twelves C., Wilson P., Duncan R., Thomson A. H., Murray L. S., Hilditch T. E., Murray T., Burtles S., Fraier D., Frigerio E., Cassidy J., *Clin. Cancer Res.*, **5**, 83—94 (1999).
5) Singer J. W., *J. Control. Release*, **109**, 120—126 (2005).
6) Nakanishi T., Fukushima S., Okamoto K., Suzuki M., Matsumura Y., Yokoyama M., Okano T., Sakurai Y., Kataoka K., *J. Control. Release*, **74**, 295—302 (2001).
7) Inoue K., Kumazawa E., Kuga H., Susaki H., Masubuchi N., Kajimura T., *Adv. Exp. Med. Biol.*, **519**, 145—153 (2003).
8) Kumazawa E., Ochi Y., *Cancer Sci.*, **95**, 168—175 (2004).
9) Kumazawa E., Tohgo A., *Expert Opin. Invest. Drugs*, **7**, 625—632 (1998).
10) Staak A., Tolic D., Kristiansen G., Schnorr D., Loening S. A., Jung K.,

Urology, **63**, 1089—1094 (2004).
11) Troy A. M., Sheahan K., Mulcahy H. E., Duffy M. J., Hyland J. M. P., O'Donoghue D. P., *Eur. J. Cancer*, **40**, 1610—1616 (2004).
12) Sloane B. F., Moin K., Lah T. T., "Biochemical and Molecular Aspects of Selected Cancers," Vol 2, ed. by Pretlow T. G., Pretlow T. P., Academic Press, San Diego, 1994, pp. 411—466.
13) Schweiger A., Christensen I. J., Nielsen H. J., Sorensen S., Brunner N., Kos J., *Int. J. Biol. Markers*, **19**, 289—294 (2004).
14) Katunuma N., Tsuge H., Nukatsuka M., Asao T., Fukushima M., *Arch. Biochem. Biophys.*, **397**, 305—311 (2002).
15) Barrett A. J., *Biochem. J.*, **187**, 909—912 (1980).
16) Shiose Y., Kuga H., Yamashita F., Hashida M., *J. Pharm. Biomed. Anal.*, **43**, 1290—1296 (2007).
17) Nogusa H., Yano T., Okuno S., Hamada H., Inoue K., *Chem. Pharm. Bull.*, **43**, 1931—1936 (1995).
18) Nogusa H., Yano T., Kajiki M., Gensho A., Hamana H., Okuno S., *Biol. Pharm. Bull.*, **20**, 1061—1065 (1997).
19) Nogusa H., Yano T., Kashima N., Yamamoto K., Okuno S., Hamana H., *Bioorg. Med. Chem. Lett.*, **10**, 227—230 (2000).
20) Duncan R., Kopeckova R. P., Strohalm J., Hume I., Cable H. C., Pohl J., Lloyd J. B., Kopecek J., *Br. J. Cancer*, **55**, 165—174 (1987).
21) Rejmanova P., Kopecek J., Pohl J., Baudys M., Kostka V., *Makromol. Chem.*, **184**, 2009—2020 (1983).
22) Caiolfa V. R., Zamai M., Fiorino A., Frigerio E., Pellizzoni C., d'Argy R., Ghiglieri A., Castelli M. G., Farao M., Pesenti E., Gigli M., Arqchucci F., Suarato A., *J. Control. Release*, **65**, 105—119 (2000).
23) Conover C. D., Greenwald R. B., Pendri A., Gilbert C. W., Shum K. L., *Cancer Chemother. Pharmacol.*, **42**, 407—414 (1998).
24) Zou Y., Wu Q. P., Tansey W., Chow D., Hang M. C., Charmsaqavej C., Wallace S., Li C., *Int. J. Oncol.*, **18**, 331—336 (2001).
25) Okuno S., Harada M., Yano T., Yano S., Kiuchi S., Tsuda N., Sakamura Y., Imai J., Kawaguchi T., Tsujihara K., *Cancer Res.*, **60**, 2988—2995 (2000).
26) Masubuchi N., *Pharmazie*, **59**, 374—377 (2004).
27) Wente M. N., Kleeff J., Buchler M. W., Wanders J., Cheverton P., Langman S., Friess H., *Investigational New Drugs*, **23**, 339—347 (2005).
28) Soyez H., Schacht E., Vanderkerken S., *Adv. Drug Deliv. Rev.*, **21**, 81—106 (1996).
29) Ochi Y., Shiose Y., Kuga H., Kumazawa E., *Cancer Chemother. Pharmacol.*, **55**, 323—332 (2005).
30) Duncan R., Rejmanova P., Kopecek J., Lloyd J. B., *Biochem. Biophys. Acta*, **678**, 143—150 (1981).
31) Barrett A. J., Kirschke H., *Methods Enzymol.*, **80**, 535—561 (1981).
32) Dubowchik G. M., Firestone R. A., *Bioorg. Med. Chem. Lett.*, **8**, 3341—3346 (1998).

by Stanford University - Main Campus - Lane Medical Library on 03/18/15. For personal use only.

Antibody-Drug Conjugates in Cancer Therapy

Eric L. Sievers and Peter D. Senter

Seattle Genetics, Bothell, Washington 98021; email: esievers@seagen.com, psenter@seagen.com

Annu. Rev. Med. 2013. 64:15–29

First published online as a Review in Advance on October 3, 2012

The *Annual Review of Medicine* is online at med.annualreviews.org

This article's doi: 10.1146/annurev-med-050311-201823

Copyright © 2013 by Annual Reviews. All rights reserved

Keywords

immunotherapy, chemotherapeutic, monoclonal antibody, tumor, drug delivery, targeting

Abstract

An antibody-drug conjugate (ADC) provides the possibility of selectively ablating cancer cells by combining the specificity of a monoclonal antibody (mAb) for a target antigen with the delivery of a highly potent cytotoxic agent. ADC target antigens are typically highly expressed on the surface of cancer cells compared to normal cells. The tumor target, the cytotoxic agent, and the manner in which the agent is attached to the antibody are key determinants of clinical activity and tolerability. Recently, several clinical trials have demonstrated that ADCs achieve higher clinical response rates than unconjugated mAbs targeting the same cell surface antigen. Brentuximab vedotin represents one such ADC that has recently been approved for the treatment of relapsed Hodgkin and systemic anaplastic large cell lymphomas—both characterized by high expression of the target antigen, CD30, on the surface of malignant cells. This review summarizes key characteristics of current, clinically active ADCs and highlights recent clinical data illustrating the benefit of antibody-targeted delivery of cytotoxic agents to cancer cells.

by Stanford University - Main Campus - Lane Medical Library on 05/18/15. For personal use only.

INTRODUCTION

HL: Hodgkin lymphoma

ALCL: anaplastic large-cell lymphoma

Clinically useful, unconjugated monoclonal antibodies (mAbs) selectively recognize antigens that are preferentially expressed on or near tumor cells and exert their cytotoxic effects through mechanisms such as cell signaling, antibody-dependent cellular cytotoxicity, antibody-dependent cellular phagocytosis, and complement-dependent cytotoxicity (1). However, the majority of these mAbs are used in combination with chemotherapy, and many others have demonstrated insufficient clinical activity. Therefore, significant effort has been devoted to empowering mAbs through various modifications (2). One approach by which the activities of these mAbs have been enhanced is through conjugation with cytotoxic drugs, generating antibody-drug conjugates (ADCs) capable of antigen-specific delivery of highly potent cytotoxic drugs to tumor cells.

DESIGN PRINCIPLES

In order to improve efficacy without compromising safety, an ADC must preferentially deliver the cytotoxic payload to tumor cells expressing the target antigen rather than to healthy tissue. This is accomplished by exploiting the specificity of a mAb targeting an antigen that is highly expressed on the surface of malignant cells. After binding the target antigen, the ADC-antigen complex is typically internalized and transported to intracellular organelles where release of the attached drug can occur. Upon release, the cytotoxic drug can interfere with various cellular mechanisms, leading to cell death (**Figure 1**). The development of ADCs has relied on several key areas of research including the choice of an appropriate antigen target, development of novel highly potent cytotoxic drugs, development of stable linkers that can release the cytotoxic payload upon internalization, and conjugation technology. This review discusses recent advances in these areas of research along with the application of these technologies to ADCs currently in the clinic.

Select an Appropriate Target

Target selection is arguably the most important contributor to the antitumor activity and tolerability of an ADC. As a general rule, cancer cells do not display novel immunogenic antigens because such behavior would lead to rapid clearance by the immune system. However, cancer cells occasionally express normal cell surface antigens at levels that are distinguishable from their healthy normal cellular counterparts. Ideally, the target antigen should be expressed with substantially higher copy numbers on tumor cells, as the efficacy and tolerability of an ADC appear to depend, in part, on its relative expression on normal tissue compared to tumor cells (3, 4). Two ADCs that have shown pronounced clinical activity at tolerated doses, brentuximab vedotin (ADCETRIS®) and trastuzumab emtansine (T-DM1), target antigens with preferential expression on tumor cells. The normal cell surface antigen targeted by brentuximab vedotin, CD30, is strongly expressed on the Reed-Sternberg cells of Hodgkin lymphoma (HL) and on systemic anaplastic large-cell lymphoma (ALCL) tumor cells (5). CD30 expression is otherwise thought to be largely limited to activated T and B cells in the physiologic state (6, 7). Similarly, the HER2 antigen, targeted by T-DM1, is highly overexpressed on some metastatic breast cancer tumors compared to normal tissue (8–10). Both of these ADCs have shown meaningful clinical activities with manageable safety profiles (11–13).

Upon binding of the ADC, many antigens undergo rapid internalization along with the bound ADC through receptor-mediated endocytosis (**Figure 1**). The efficiency of internalization can vary between an ADC and the unconjugated antibody; in some cases both species internalize at the same rate, whereas in other cases the ADC internalizes more efficiently (14, 15). The rate and extent of internalization are important because it influences uptake of the drug as well as release of the drug in tumor and normal cells (16, 17).

The expression level of the target antigen appears to be another important factor

by Stanford University - Main Campus - Lane Medical Library on 05/18/13. For personal use only.

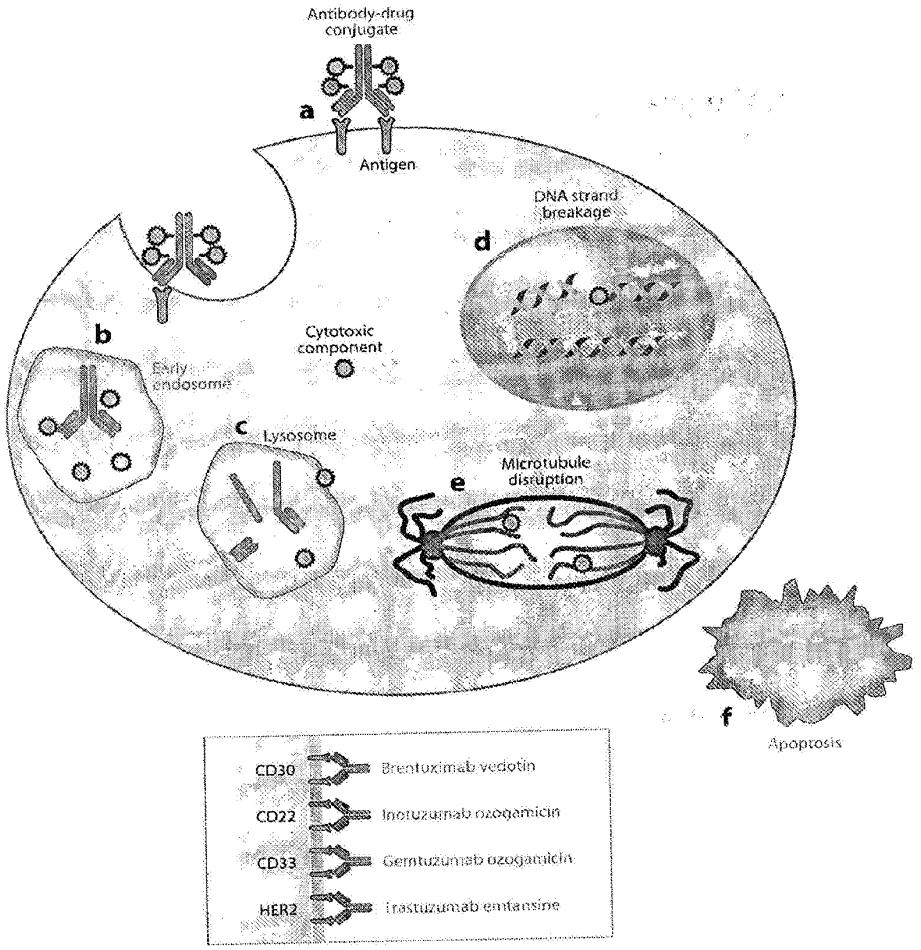


Figure 1

Generalized mechanism of action of antibody-drug conjugates (ADCs). (*a*) The ADC binds to the antigen on the target cell. (*b*) The antigen-ADC complex is internalized through receptor-mediated endocytosis and, in most cases, is transported from early endosomes to lysosomes. (*c*) In the lysosome, internal conditions may destabilize the linker or mAb backbone, causing the cytotoxic component to dissociate and circulate freely in the cytoplasm. Most cytotoxic components of current ADCs either bind to the minor groove of DNA and induce strand breakage (*d*) or bind to tubulin, resulting in microtubule disruption (*e*). (*f*) Both processes lead to apoptosis. *Inset*: Four advanced-stage ADCs are brentuximab vedotin, inotuzumab ozogamicin, gemtuzumab ozogamicin, and trastuzumab emtansine. The antigen targets for each ADC are shown.

in targeting tumors with ADCs; however, ADCs have shown efficacy over a wide range of antigen expression levels. For example, while CD33-positive acute myelogenous leukemia tumors express relatively low levels of target antigen (5,000–10,000 receptors per cell), meaningful clinical responses have been observed with gemtuzumab ozogamicin

by Stanford University - Main Campus - Lane Medical Library on 05/18/13. For personal use only.

(Mylotarg®, GO), an ADC that targets the CD33 antigen (18, 19). Effective treatment of tumors with such low antigen expression levels requires an ADC with a highly potent cytotoxic component, such as calicheamicin in GO. Conversely, HER2 can be expressed on metastatic breast cancer tumor cells with very high copy numbers (in some cases, >3 million copies per cell) in some patients (20). Significant clinical activity against HER2-positive metastatic breast cancer has been reported for T-DM1, an ADC composed of trastuzumab conjugated to a cytotoxic maytansinoid, mertansine (DM1) (10, 21). These and other ADCs are effective over a wide range of antigen expression levels, although preclinical studies have shown that higher antigen expression levels do in fact predict greater ADC potency in cell culture (22). Taken together, these observations suggest that although expression level is an important factor in determining ADC potency, even antigen targets with lower copy numbers can be effectively targeted with a sufficiently potent ADC.

Minimize Systemic Drug Release

The linker that connects the cytotoxic drug to the mAb is a key determinant of ADC activity. These linkers covalently couple the cytotoxic drug to the antibody, producing an ADC that should be relatively stable in circulation (3). Stability of the linker is important because it prevents damage to nontarget tissue through spontaneous release of the cytotoxic drug while maximizing tumor drug exposure (3). Upon internalization, however, the linkers should facilitate efficient drug release. Intracellular conditions such as the low-pH environment in lysosomes or the reducing environment of the cytosol can destabilize acid-labile hydrazone linkers or disulfide-based linkers, respectively, resulting in drug release (**Figure 1**) (23). For example, the ADC GO contains an acid-labile hydrazone linking the calicheamicin-derived cytotoxic component to the CD33 mAb (24). However, both acid-labile hydrazone linkers and disulfide-based linkers are relatively unstable in plasma, with half-lives in plasma of approximately 48–72 hours and 1 day, respectively (2, 25).

Dipeptide linkers and thioether linkers have also been used in ADC development. Dipeptide linkers such as citrulline-valine linkers are predominantly cleaved by specific lysosomal proteases, imparting greater stability in plasma and increased exposure to the conjugated drug after intravenous delivery (26). Brentuximab vedotin is an ADC that uses a cleavable citrulline-valine dipeptide linker to facilitate release of the cytotoxic agent, monomethylauristatin E (MMAE) (27). There are also noncleavable thioether linkers that depend on degradation of the mAb component in the lysosome. Antibody degradation leads to the release of the cytotoxic drug still bound to the linker and the amino acid residue of the antibody to which it was attached (28, 29). T-DM1 is an ADC that uses this type of linker to tether the maytansinoid cytotoxic component to the mAb (21).

Tailor Conjugation Technology to Optimize Drug Effect

The specific method of attachment of the cytotoxic drug and linker to the mAb has been shown to play a key role in ADC activity and tolerability. The most common methods of antibody-drug conjugation are alkylation of reduced interchain disulfides, acylation of lysine residues, and alkylation of genetically engineered cysteine residues. The number of drugs per mAb and drug position have been shown to influence ADC aggregation, antigen binding, clearance from the circulation, potency, and tolerability (2, 30). Underconjugation can decrease potency of the ADC mixture, whereas the conjugation of too many drugs per mAb can lead to decreased circulation half-life, reduced tolerability, and impaired antigen binding (2, 30). The ideal number of drug molecules per antibody for most current ADCs appears to be about four. This ratio minimizes the presence of unconjugated antibody, limits the circulation half-life to that of the unmodified

by Stanford University - Main Campus - Lane Medical Library on 03/18/13. For personal use only.

Table 1 Antibody-drug conjugates in clinical development

Drug	Status	Therapeutic area	Target	Cytotoxic class
brentuximab vedotin	approved	HL, ALCL	CD30	auristatin
gemtuzumab ozogamicin	withdrawn	AML	CD33	calicheamicin
inotuzumab ozogamicin	phase III	NHL, ALL	CD22	calicheamicin
trastuzumab emtansine	phase III	MBC	HER2	maytansinoid
BT062	phase II	multiple myeloma	CD138	maytansinoid
CDX-011	phase II	breast, melanoma	GPNMB	auristatin
milatuzumab-dox	phase II	multiple myeloma	CD74	anthracycline (doxorubicin)
SAR3419	phase II	DLBCL, ALL	CD19	maytansinoid
AGS-16M8F	phase I	RCC	AGS-16	auristatin
ASG-22ME	phase I	solid tumors	nectin-4	auristatin
ASG-5ME	phase I	prostate, pancreatic	SLC44A4	auristatin
BAY 79-4620	phase I	solid tumors	carbonic anhydrase 9	auristatin
BAY 94-9343	phase I	solid tumors	mesothelin	maytansinoid
BIIB015	phase I	solid tumors	cripto	maytansinoid
IMGN529	phase I	NHL, CLL	CD37	maytansinoid
IMMU-130	phase I	colorectal	CEACAM5	camptothecin analog (SN-38)
lorvotuzumab mertansine	phase I	SCLC, multiple myeloma	CD56	maytansinoid
MDX-1203	phase I	NHL, RCC	CD70	alkylating agent (duocarmycin)
PSMA ADC	phase I	prostate	PSMA	auristatin
RG7593	phase I	hematologic malignancies	CD22	auristatin
SAR566658	phase I	solid tumors	CA6	maytansinoid
SGN-75	phase I	NHL, RCC	CD70	auristatin

Abbreviations: ALCL, anaplastic large-cell lymphoma; ALL, acute lymphocytic leukemia; AML, acute myeloid leukemia; CLL, chronic lymphocytic leukemia; DLBCL, diffuse large B-cell lymphoma; HL, Hodgkin lymphoma; MBC, metastatic breast cancer; NHL, non-Hodgkin lymphoma; RCC, renal cell carcinoma; SCLC, small-cell lung cancer.

antibody, and does not significantly disrupt antigen binding (2).

Employ Highly Potent Cytotoxic Agents

Early ADC development focused on the use of readily available, clinically approved drugs such as doxorubicin, methotrexate, mitomycin, flurouracil, and vinca alkaloids (2). These drugs have relatively low potencies, so access to solid tumors by macromolecules was inefficient and accumulation of the cytotoxic drug in target cells was poor. The low clinical activity exhibited by these early ADCs prompted the development of ADCs employing much more potent cytotoxic drugs, which, though too toxic to use in an untargeted manner, have sufficient potency to be used in a more targeted manner (2).

The majority of highly potent cytotoxic agents used in current ADCs are auristatins, maytansinoids, or calicheamicins (**Table 1**). The cytotoxicities of auristatins and maytansinoids arise from binding to tubulin and the inhibition of polymerization, causing cell cycle arrest and subsequent apoptosis of the target cell (**Figure 1**) (2, 31, 32). MMAE is an auristatin that is used in several ADCs,

by Stanford University - Main Campus - Lane Medical Library on 05/18/15. For personal use only.

conjugated directly to native cysteine residues using maleimide for conjugation and a dipeptide linker (valine and citrulline—vcMMAE) to facilitate drug release (33). MMAE is the cytotoxic component of the only ADC that is currently commercially available, brentuximab vedotin. The most advanced clinical ADC containing a maytansinoid derivative is T-DM1.

DNA-binding cytotoxic agents used in ADCs include duocarmycin and calicheamicin analogs. These agents exert their cytotoxic effects by binding to DNA in the double-helix minor groove (3). For example, binding of calicheamicin analogs induces double-strand breaks in DNA, resulting in cell death (**Figure 1**) (34). These molecules are very potent, but their lack of selectivity has prevented their use as single-agent therapeutics (3). Calicheamicins in particular have been integrated into inotuzumab ozogamicin, an ADC in late-stage clinical development, as well as the previously commercially available ADC GO, which has been voluntarily withdrawn from the market.

CLINICAL DEVELOPMENT

Considerable attention to the selection of (*a*) optimal tumor targets, (*b*) highly potent cytotoxic payloads, and (*c*) stabilizing linker technologies has yielded promising new treatment options for cancer patients. ADCs consistently demonstrate better response rates than unconjugated mAbs that target the same cell surface antigen and have been clinically evaluated in similar advanced cancer patient populations. **Table 2** presents a selection of tumor antigens that have been targeted by both unconjugated antibodies and ADCs in the context of the objective response rates observed in similar patient populations. For all antigen targets, more robust antitumor activity was observed in clinical trials incorporating treatment with a single-agent ADC. The patient populations compared were relatively similar and all studies examined single-agent therapy, but it is important to note that none of the reported studies directly compared an ADC with its unconjugated mAb counterpart. In addition, in the case of CD22, CD33, and one of the unconjugated HER2 antibodies, the unconjugated mAb and the conjugated mAb recognize different epitopes of the target antigen. Despite these differences, the clinical trial data support the hypothesis that antibodies can be successfully employed to deliver potent cytotoxic agents to cancer cells, resulting in clinically meaningful activity exceeding that of unconjugated mAbs with manageable toxicity. This section of the review focuses on ADCs that are or have been commercially available and those in late-stage development. Earlier-stage compounds are also briefly discussed. **Table 1** lists some of these ADCs.

Brentuximab Vedotin

Brentuximab vedotin is a next-generation ADC that is approved for use in the United States and is the first drug approved for HL in more than 30 years. It is composed of the chimeric mAb cAC10, which is specific for human CD30, as mentioned above, and the auristatin MMAE, a cytotoxic agent. The antibody is covalently attached to an average of four MMAE molecules per mAb through a protease-cleavable dipeptide linker. The ADC binds to the CD30 antigen and undergoes rapid internalization and proteolysis, leading to the efficient release of MMAE inside the target cells (35). Brentuximab vedotin embodies the important ADC design principles mentioned above: (*a*) an internalizing tumor-associated antigen that is minimally expressed on normal tissues, (*b*) a linker that minimizes systemic drug release, (*c*) a conjugation technology that preserves the pharmacokinetic properties of the mAb carrier, and (*d*) a potent cytotoxic component that is rapidly released upon exposure to intracellular proteases.

In 2011, brentuximab vedotin received accelerated approval from the US Food and Drug Administration (FDA) for the treatment of HL after failure of autologous stem cell transplant or after at least two prior multi-agent chemotherapy regimens in patients who are not autologous stem cell transplant candidates.

Table 2 Clinical efficacy of unconjugated antibodies and related antibody-drug conjugates

Target (indication)	Unconjugated antibody			Conjugated antibody		
	Species	ORR (%)	Reference	Species	ORR (%)	Reference
CD22 (NHL)	epratuzumab[a]	18	68[b]	inotuzumab ozogamicin[a]	39–53	52,[b] 69[b]
CD30 (HL)	cAC10	0	70[b]	brentuximab vedotin	75	11[b]
CD30 (ALCL)	cAC10	17	70[b]	brentuximab vedotin	86	12[b]
CD33 (AML)	lintuzumab[a]	15	71[c]	gemtuzumab ozogamicin[a]	26–30	42,[d] 72,[d]
HER2 (MBC)	trastuzumab	15–26	73,[b] 74,[e] 75[e]	trastuzumab emtansine	26–64	13,[b] 39,[e] 76,[b] 77,[b]
	pertuzumab[a]	7	78[b]			

Abbreviations: ALCL, anaplastic large-cell lymphoma; AML, acute myeloid leukemia; HL, Hodgkin lymphoma; MBC, metastatic breast cancer; NHL, non-Hodgkin lymphoma; ORR, objective response rate.

[a]Unconjugated and conjugated antibodies recognize the same antigen target but different epitopes.

[b]Relapsed or refractory disease.

[c]Previously untreated (or treated with palliative therapy) or in relapse after standard induction chemotherapy.

[d]Untreated first recurrence.

[e]Previously untreated disease.

by Stanford University - Main Campus - Lane Medical Library on 03/18/15. For personal use only.

Accelerated approval was also granted for the treatment of systemic ALCL after failure of at least one prior multi-agent chemotherapy regimen. The approved dose of brentuximab vedotin is 1.8 mg/kg intravenously once every three weeks for up to 16 treatment cycles. In a pivotal single-arm phase II trial in relapsed or refractory HL patients, brentuximab vedotin demonstrated an objective response rate of 75% and a durable complete remission rate of 34% (11). In the subset of patients who obtained a complete remission, the median progression-free survival was 29.0 months (36). Similarly, in a pivotal single-arm phase II trial in relapsed or refractory systemic ALCL patients, brentuximab vedotin demonstrated an objective response rate of 86% and a durable complete remission rate of 57%. Patients who obtained a best response of complete remission experienced a median progression-free survival of 14.6 months (12). The robust clinical efficacy of the ADC brentuximab vedotin in patients with relapsed or refractory HL or systemic ALCL contrasts with the modest clinical activity exhibited by the unconjugated antibody in clinical trials (**Table 2**), highlighting the observation that ADCs can greatly enhance the activity of the parent antibody. In both studies, adverse events were generally grade 1 or 2 in severity and were largely manageable with either supportive care or dose reductions and/or delays. Adverse events of grade 3 or higher in both studies included peripheral sensory neuropathy, neutropenia, thrombocytopenia, and anemia. Peripheral sensory neuropathy was the most common adverse event in both studies, occurring in more than half of patients who received brentuximab vedotin (11, 12).

A total of four randomized phase III registrational trials will evaluate the potential efficacy of brentuximab vedotin in a variety of clinical settings, including earlier lines of treatment for HL and systemic ALCL as well as new indications such as cutaneous T cell lymphoma (CTCL) and other mature T cell lymphomas that express the CD30 target antigen. One unmet clinical need is represented by those patients with HL whose lymphoma recurs after autologous stem cell transplant. This typically young patient population has a median survival of only 2.4 years (37). To address this pronounced unmet need, a randomized placebo-controlled phase III trial is testing the hypothesis that post-transplant administration of brentuximab vedotin will prevent disease progression and improve outcomes (AETHERA trial; NCT01100502). To

by Stanford University - Main Campus - Lane Medical Library on 03/18/15. For personal use only.

improve long-term outcomes in patients with newly diagnosed CD30-positive lymphomas, two planned international randomized phase III trials will evaluate the inclusion of brentuximab vedotin in the multi-agent treatment of newly diagnosed advanced-stage HL and mature T cell lymphoma. Additionally, a fourth randomized phase III trial is under way comparing the clinical activity of brentuximab vedotin with methotrexate or bexarotene (physician's choice) in patients with CD30-positive CTCL (NCT0158499).

Trastuzumab Emtansine

Trastuzumab emtansine (T-DM1), as described above, is an ADC formed by the conjugation of the maytansinoid DM1 with the anti-HER2 mAb trastuzumab through a noncleavable linker. Currently, T-DM1 is the only ADC in late-stage clinical development for metastatic breast cancer that overexpresses the HER2 antigen (38). The unconjugated antibody trastuzumab, available commercially as Herceptin®, was originally developed for the treatment of the 15%–25% of breast cancer cases that exhibit protein overexpression of HER2. Typically, trastuzumab is used in combination with conventional chemotherapy for first-line treatment of these breast cancers. However, trastuzumab has also been used as a single agent in the treatment of HER2-positive metastatic breast cancer, demonstrating objective response rates ranging from 15% to 26%. Conjugation of the cytotoxic agent DM1 to trastuzumab offered improvements in objective response rates, with single-agent efficacy in HER2-positive metastatic breast cancer ranging from 26% to 64% (**Table 2**). It is important to note that in these trials, T-DM1 was active against metastatic breast cancer that was previously resistant to trastuzumab-based therapy, highlighting the importance of the cytotoxic DM1 component.

In addition to improved efficacy, the targeting of chemotoxic agents using a mAb in ADCs should provide an improved safety profile compared to traditional chemotherapy. A head-to-head randomized phase II study was conducted in previously untreated metastatic breast cancer patients comparing the safety and efficacy of single-agent T-DM1 with trastuzumab in combination with the chemotherapeutic agent docetaxel, the standard of care in the front-line setting. Preliminary topline results from this study demonstrated a somewhat higher objective response rate (64% versus 58%) and median progression-free survival (14.2 months versus 9.2 months) in the single-agent T-DM1 group, but a lower rate of grade 3 or 4 adverse events (46.4% versus 89.4%) and treatment discontinuations due to adverse events (7.2% versus 28.8%). Furthermore, many side effects associated with conventional chemotherapy, such as diarrhea, neutropenia, rash, neuropathy, and alopecia, were less prominent in patients treated with single-agent T-DM1 compared with trastuzumab in combination with conventional chemotherapy (39). This study illustrates how antigen binding in ADCs may help improve the therapeutic index by focusing exposure to the cytotoxic agent on tumor cells.

Building on results from phase I and phase II clinical trials, EMILIA, a randomized open-label phase III trial, explored the safety and efficacy of single-agent T-DM1 in patients with HER2-positive locally advanced or metastatic breast cancer. Either single-agent T-DM1 or a combination of capecitabine and lapatinib was administered to 978 patients. The primary endpoints were progression-free survival, overall survival, and safety. Patients treated with T-DM1 showed significantly improved progression-free survival compared to those treated with lapatinib plus capecitabine (9.6 months versus 6.4 months; $p < 0.0001$). Median overall survival was not reached in the T-DM1 arm, but the one-year and two-year overall survival rates showed a trend to be higher in the T-DM1 arm (one-year: 84.7% versus 77.0%; two-year: 65.4% versus 47.5%). Single-agent T-DM1 was well tolerated, and the most common adverse events with severity of at least grade 3 were thrombocytopenia (12.9%), increased aspartate amino transferase levels (4.3%), and increased alanine amino

by Stanford University - Main Campus - Lane Medical Library on 03/18/15. For personal use only.

transferase levels (2.9%) (40). Two other phase III studies are currently under way: MARIANNE (NCT01120184), which compares the safety and efficacy of single-agent T-DM1 with trastuzumab/pertuzumab or trastuzumab/taxane combination therapy in the first-line setting, and TH3RESA (NCT01419197), which compares T-DM1 with treatment of the physician's choice in metastatic breast cancer patients who have already received two prior regimens of HER2-directed therapy.

Gemtuzumab Ozogamicin

Gemtuzumab ozogamicin (CMA-676; GO) is an ADC composed of a DNA-binding calicheamicin derivative coupled to a humanized IgG4 mAb directed against CD33, a normal myeloid cell surface antigen that is present on leukemia tumors in ~90% of patients with acute myeloid leukemia (AML) (41). It was the first ADC to receive marketing authorization in the United States, receiving accelerated approval from the FDA in 2000 (see above) for the treatment of patients with CD33-positive AML in first relapse who are 60 years of age or older and who are not considered candidates for other cytotoxic chemotherapy (18). Approval was granted on the basis of results from three open-label single-arm phase II trials in a total of 142 patients in which 30% of patients obtained complete remission or complete remission with incomplete platelet recovery (42). However, clinically meaningful GO-related hepatotoxicity was reported in some patients (43, 44). This toxic effect led to the addition of a boxed warning for hepatotoxicity in the US label for GO in 2001.

In association with the accelerated approval, the sponsor and FDA agreed to the design and execution of a randomized phase III trial (SWOG 106) in order to confirm evidence of clinical benefit. This study compared GO-containing induction therapy (45 mg/m^2 daunorubicin, cytarabine, and GO) with standard induction therapy (60 mg/m^2 daunorubicin and cytarabine) in first-line AML patients under the age of 61. Unfortunately, no apparent benefit of GO was observed with regard to achievement of complete remission (GO-containing arm: 66%; control arm: 69%) or relapse-free survival (hazard ratio = 1.00, p = 0.50). Additionally, patients in the GO-containing arm experienced a higher induction death rate (GO-containing arm: 5.8%; control arm: 0.8%; p = 0.002) (45). Critics of the study point out that the dose of daunorubicin was lower in patients in the GO-containing arm, which may have masked further benefit of GO in induction. In addition, the induction death rate in the control arm (0.8%) was much lower than the rate seen in other chemotherapy trials of patients under age 61, suggesting that the trial's findings might not represent a realistic picture of the clinical benefit or risks of GO (46, 47). Despite these uncertainties raised in the medical literature, Pfizer voluntarily withdrew GO from the market at the request of the FDA in June 2010.

Results of recent phase III trials suggest GO may confer meaningful clinical benefit for certain patient subpopulations. Together, the open-label trials AML15 and AML16 randomized 2,228 patients to receive induction therapy with or without 3 mg/m^2 GO. In both trials, induction therapy containing GO was well tolerated without unacceptable increases in toxicity. The AML15 trial showed a significant survival benefit for GO-containing induction therapy in younger AML patients with favorable-risk cytogenetics (five-year overall survival: 79% with GO, 51% without GO; odds ratio = 0.32) (46). AML16 showed a significant survival benefit in older AML patients regardless of cytogenetic status (two-year overall survival: 35% with GO, 29% without GO; p = 0.04) (48). The phase III open-label ALFA-0701 trial investigated induction therapy with or without lower, fractionated doses of GO (3 mg/m^2 on days 1, 4, and 7). The rationale for the lower 3 mg/m^2 dose was based on the responses to lower doses of GO in the initial phase I studies, and dose fractionation is supported by the rapid re-expression of CD33 molecules observed after first exposure. This approach

NHL: non-Hodgkin lymphoma(s)

ALL: acute lymphocytic leukemia(s)

DLBCL: diffuse large B cell lymphoma

by Stanford University - Main Campus - Lane Medical Library on 03/18/15. For personal use only.

was remarkably successful. Time-to-endpoint assessments including event-free survival (15.6 months versus 9.7 months), relapse-free survival (28.1 months versus 11.4 months), and overall survival (34.0 months versus 19.2 months) were significantly more favorable for patients in the GO-containing arm (49). The significant survival benefits observed in these phase III studies suggest that induction regimens containing GO may have an important future role in the treatment of patients with good- or intermediate-risk AML (47).

Inotuzumab Ozogamicin

Inotuzumab ozogamicin (CMC-544) consists of a humanized anti-CD22 IgG4 mAb conjugated to a calicheamicin derivative by an acetyl butyrate linker that targets the normal B cell surface antigen CD22, which is expressed on the majority of non-Hodgkin lymphomas (NHL) and acute lymphocytic leukemias (ALL) of B cell derivation (41, 50, 51). Akin to the relatively restricted maturational expression of the normal myeloid antigen CD33, the B cell antigen CD22 does not appear to be meaningfully expressed by either lymphocyte progenitors or memory B cells—possibly resulting in lower chronic immunosuppression than might be observed in the context of comprehensive B cell ablation obtained by other agents (52, 53).

Promising preliminary evidence of inotuzumab ozogamicin antitumor activity was observed in several single-arm trials. In the first dose-escalation trial, inotuzumab ozogamicin was administered to 79 patients with multiple-relapsed or treatment-refractory B cell lymphomas as an intravenous infusion every three or four weeks at doses ranging from 0.4 to 2.4 mg/m^2. Thrombocytopenia and neutropenia were observed more commonly at higher dose levels, and the maximum tolerated dose was defined as 1.8 mg/m^2 delivered every three weeks. Thrombocytopenia not associated with clinically meaningful episodes of hemorrhage was the most notable recurrent adverse event. With the intention of allowing greater time for platelet recovery, an expansion cohort increased the dosing interval to four weeks. The overall response rate was 39% across various lymphoma subtypes and dose levels (52). Similarly, a 57% overall response rate was observed in an exploratory phase II trial in 49 adults and children with relapsed ALL (54). Because allogeneic hematopoietic stem cell transplantation is particularly useful as a means of securing long-term leukemia control among patients with relapsed ALL who achieve remission, it is also notable that a strategy employing inotuzumab ozogamicin consolidated by allograft was reasonably well tolerated and appeared to enable a proportion of patients to achieve and maintain durable remissions (55).

On the basis of these collective findings, multiple randomized trials in diffuse large B cell lymphoma (DLBCL) and ALL are likely to help define the utility of this novel ADC (NCT01232556 and NCT01564784). Data from these randomized trials should enable regulators and clinicians to determine if inotuzumab ozogamicin provides greater clinical benefit than existing treatment approaches in patients with relapsed or refractory B cell cancers.

Early-Stage ADCs

In addition to the later-stage and commercially used ADCs discussed above, many ADCs are in early-stage clinical testing (**Table 1**). CDX-011 (glembatumumab vedotin) is an ADC in phase II testing that consists of the auristatin MMAE conjugated to a mAb that recognizes GPNMB, a novel glycoprotein often expressed at higher levels in melanoma and breast tumors relative to normal tissue. In a phase I/II trial in patients with unresectable late-stage melanoma, CDX-011 showed overall response rates ranging from 14% to 19% depending on dosing frequency and GPNMB expression levels (56, 57). In breast cancer, GPNMB expression is associated with poor outcomes including reduced progression-free survival and overall survival. This is consistent with results in a clinical trial of heavily pretreated breast cancer patients, which showed an association

by Stanford University - Main Campus - Lane Medical Library on 03/18/13. For personal use only.

between GPNMB expression and improved outcomes following CDX-011 treatment, with an objective response rate of 29% in GPNMB-positive patients and 0% in GPNMB-negative patients (56, 58). A randomized phase II study is currently under way in advanced breast cancer patients comparing the safety and efficacy of chemotherapy of the investigator's choice to CDX-011 (NCT01156753).

Another ADC in early-stage clinical testing is SAR3419, a maytansinoid-based ADC targeting CD19 in B cell malignancies. In a phase I/II study in patients with relapsed or refractory CD19-expressing B cell NHL, including follicular lymphoma and DLBCL, 32% of patients achieved an objective response, including six complete remissions. SAR3419 exhibited a manageable safety profile with no evidence of myelosuppression (59). SAR3419 is currently being tested in phase II trials in patients with relapsed or refractory DLBCL (NCT01472887) and ALL (NCT01440179).

FUTURE DEVELOPMENTS

The use of ADCs as therapeutics is a new field driven by innovation at all levels of development. At the preclinical level, novel antigen targets for drug delivery are being discovered (2, 32). These include antigens found on both hematologic and solid tumors. A great deal of research is also under way to define new highly potent drugs that are appropriate for ADC applications. These include the DNA-alkylating agents duocarmycins and pyrrolobenzodiazepine dimers, as well as the RNA polymerase inhibitor amanitin (60–62). These drugs may complement the activities of the auristatins and other drugs that are currently in advanced clinical trials. Other advancements being made in the field include site-directed mAb mutations with both natural and unnatural amino acids that permit specific drug attachment and more uniform production of ADCs with specific drug/mAb ratios (63, 64). Besides having more predictable pharmacokinetics, such conjugates may provide advantages in terms of tolerability (63) and stability (65). Finally, a considerable amount of research has been directed toward antibody alternatives that might penetrate solid tumors more efficiently than mAbs (66). Localization studies with an antibody fragment–drug conjugate derived from a diabody (molecular mass 26 kDa) demonstrated tumor localization. The disadvantages of this construct were higher-than-normal tissue exposure and rapid blood clearance. Despite these shortcomings, the diabody-based ADC showed antitumor activity at tolerated doses in preclinical models (67). Further studies are needed to establish the potential of non-IgG scaffolds for ADC drug delivery.

The use of ADCs has ushered in a new era of immune-based treatments for cancer. The coupling of novel highly potent cytotoxic agents with carefully engineered antibodies has provided meaningful improvements in clinical activity over unconjugated antibodies. The design of novel linkers and new conjugation technologies have enabled further improvements in stability and tolerability. Further honing of ADC technology along with active clinical development programs will likely provide new treatments for patients with previously unmet needs.

DISCLOSURE STATEMENT

The authors are employees of Seattle Genetics, Inc., and receive salary- and equity-based remuneration.

ACKNOWLEDGMENTS

The authors acknowledge the medical writing assistance of J. Christian Hesketh, employed by Seattle Genetics, Inc.

by Stanford University - Main Campus - Lane Medical Library on 03/18/15. For personal use only.

LITERATURE CITED

1. Reichert JM, Rosensweig CJ, Faden LB, et al. 2005. Monoclonal antibody successes in the clinic. *Nat. Biotechnol.* 23:1073–78
2. Senter PD. 2009. Potent antibody drug conjugates for cancer therapy. *Curr. Opin. Chem. Biol.* 13:235–44
3. Teicher BA, Chari RV. 2011. Antibody conjugate therapeutics: challenges and potential. *Clin. Cancer Res.* 17:6389–97
4. Chari RV. 2008. Targeted cancer therapy: conferring specificity to cytotoxic drugs. *Acc. Chem. Res.* 41:98–107
5. Wahl AF, Klussman K, Thompson JD, et al. 2002. The anti-CD30 monoclonal antibody SGN-30 promotes growth arrest and DNA fragmentation in vitro and affects antitumor activity in models of Hodgkin's disease. *Cancer Res.* 62:3736–42
6. Stein H, Foss HD, Durkop H, et al. 2000. CD30$^+$ anaplastic large cell lymphoma: a review of its histopathologic, genetic, and clinical features. *Blood* 96:3681–95
7. Falini B, Pileri S, Pizzolo G, et al. 1995. CD30 (Ki-1) molecule: a new cytokine receptor of the tumor necrosis factor receptor superfamily as a tool for diagnosis and immunotherapy. *Blood* 85:1–14
8. Francisco JA, Cerveny CG, Meyer DL, et al. 2003. cAC10-vcMMAE, an anti-CD30-monomethyl auristatin E conjugate with potent and selective antitumor activity. *Blood* 102:1458–65
9. Oflazoglu E, Kissler KM, Sievers EL, et al. 2008. Combination of the anti-CD30-auristatin-E antibody-drug conjugate (SGN-35) with chemotherapy improves antitumour activity in Hodgkin lymphoma. *Br. J. Haematol.* 142:69–73
10. Lewis Phillips GD, Li G, Dugger DL, et al. 2008. Targeting HER2-positive breast cancer with trastuzumab-DM1, an antibody-cytotoxic drug conjugate. *Cancer Res.* 68:9280–90
11. Younes A, Gopal AK, Smith SE, et al. 2012. Results of a pivotal phase II study of brentuximab vedotin for patients with relapsed or refractory Hodgkin's lymphoma. *J. Clin. Oncol.* 30:2183–89
12. Pro B, Advani R, Brice P, et al. 2012. Brentuximab vedotin (SGN-35) in patients with relapsed or refractory systemic anaplastic large cell lymphoma: results of a phase 2 study. *J. Clin. Oncol.* 30:2190–96
13. Krop IE, Beeram M, Modi S, et al. 2010. Phase I study of trastuzumab-DM1, an HER2 antibody-drug conjugate, given every 3 weeks to patients with HER2-positive metastatic breast cancer. *J. Clin. Oncol.* 28:2698–704
14. Law CL, Cerveny CG, Gordon KA, et al. 2004. Efficient elimination of B-lineage lymphomas by anti-CD20-auristatin conjugates. *Clin. Cancer Res.* 10:7842–51
15. Smith LM, Nesterova A, Alley SC, et al. 2006. Potent cytotoxicity of an auristatin-containing antibody-drug conjugate targeting melanoma cells expressing melanotransferrin/p97. *Mol. Cancer Ther.* 5:1474–82
16. Alley SC, Zhang X, Okeley NM, et al. 2009. The pharmacologic basis for antibody-auristatin conjugate activity. *J. Pharmacol. Exp. Ther.* 330:932–38
17. Thurber GM, Schmidt MM, Wittrup KD. 2008. Antibody tumor penetration: transport opposed by systemic and antigen-mediated clearance. *Adv. Drug Deliv. Rev.* 60:1421–34
18. Bross PF, Beitz J, Chen G, et al. 2001. Approval summary: gemtuzumab ozogamicin in relapsed acute myeloid leukemia. *Clin. Cancer Res.* 7:1490–96
19. Sievers EL. 2003. Antibody-targeted chemotherapy of acute myeloid leukemia using gemtuzumab ozogamicin (Mylotarg). *Blood Cells Mol. Dis.* 31:7–10
20. Slamon DJ, Leyland-Jones B, Shak S, et al. 2001. Use of chemotherapy plus a monoclonal antibody against HER2 for metastatic breast cancer that overexpresses HER2. *N. Engl. J. Med.* 344:783–92
21. Junttila TT, Li G, Parsons K, et al. 2010. Trastuzumab-DM1 (T-DM1) retains all the mechanisms of action of trastuzumab and efficiently inhibits growth of lapatinib insensitive breast cancer. *Breast Cancer Res. Treat.* 128:347–56
22. Mao W, Luis E, Ross S, et al. 2004. EphB2 as a therapeutic antibody drug target for the treatment of colorectal cancer. *Cancer Res.* 64:781–88
23. Erickson HK, Widdison WC, Mayo MF, et al. 2010. Tumor delivery and in vivo processing of disulfide-linked and thioether-linked antibody-maytansinoid conjugates. *Bioconjug. Chem.* 21:84–92
24. Hamann PR, Hinman LM, Hollander I, et al. 2002. Gemtuzumab ozogamicin, a potent and selective anti-CD33 antibody-calicheamicin conjugate for treatment of acute myeloid leukemia. *Bioconjug. Chem.* 13:47–58

by Stanford University - Main Campus - Lane Medical Library on 03/18/13. For personal use only.

25. Boghaert ER, Khandke KM, Sridharan L, et al. 2008. Determination of pharmacokinetic values of calicheamicin-antibody conjugates in mice by plasmon resonance analysis of small (5 microl) blood samples. *Cancer Chemother. Pharmacol.* 61:1027–35
26. Sanderson RJ, Hering MA, James SF, et al. 2005. In vivo drug-linker stability of an anti-CD30 dipeptide-linked auristatin immunoconjugate. *Clin. Cancer Res.* 11:843–52
27. Senter P, Sievers EL. 2012. The discovery and development of brentuximab vedotin for use in relapsed Hodgkin lymphoma and systemic anaplastic large cell lymphoma. *Nat. Biotechnol.* 30:631–37
28. Erickson HK, Park PU, Widdison WC, et al. 2006. Antibody-maytansinoid conjugates are activated in targeted cancer cells by lysosomal degradation and linker-dependent intracellular processing. *Cancer Res.* 66:4426–33
29. Doronina SO, Mendelsohn BA, Bovee TD, et al. 2006. Enhanced activity of monomethylauristatin F through monoclonal antibody delivery: effects of linker technology on efficacy and toxicity. *Bioconjug. Chem.* 17:114–24
30. Hamblett KJ, Senter PD, Chace DF, et al. 2004. Effects of drug loading on the antitumor activity of a monoclonal antibody drug conjugate. *Clin. Cancer Res.* 10:7063–70
31. Carter D. 2008. The neuroendocrine tumors of the lung, 1926–1998: some historical observations. *Semin. Diagn. Pathol.* 25:154–65
32. Alley SC, Okeley NM, Senter PD. 2010. Antibody-drug conjugates: targeted drug delivery for cancer. *Curr. Opin. Chem. Biol.* 14:529–37
33. Doronina SO, Toki BE, Torgov MY, et al. 2003. Development of potent monoclonal antibody auristatin conjugates for cancer therapy. *Nat. Biotechnol.* 21:778–84
34. Thorson JS, Sievers EL, Ahlert J, et al. 2000. Understanding and exploiting nature's chemical arsenal: the past, present and future of calicheamicin research. *Curr. Pharm. Des.* 6:1841–79
35. Katz J, Janik JE, Younes A. 2011. Brentuximab vedotin (SGN-35). *Clin. Cancer Res.* 17:6428–36
36. Smith S, Chen R, Gopal A, et al. 2012. Long-term follow-up results of an ongoing pivotal study of brentuximab vedotin in patients with relapsed or refractory Hodgkin lymphoma (HL). *Eur. Hematol. Assoc. Annu. Meet. Abstr.*, Abstr. 1109
37. Horning S, Fanale M, deVos S, et al. 2008. Defining a population of Hodgkin lymphoma patients for novel therapeutics: an international effort. *Ann. Oncol.* 19:118
38. LoRusso PM, Weiss D, Guardino E, et al. 2011. Trastuzumab emtansine: a unique antibody-drug conjugate in development for human epidermal growth factor receptor 2-positive cancer. *Clin. Cancer Res.* 17:6437–47
39. Hurvitz S, Dirix L, Kocsis J, et al. 2011. ORAL trastuzumab emtansine (T-DM1) vs trastuzumab plus docetaxel (H+T) in previously-untreated HER2-positive metastatic breast cancer (MBC): primary results of a randomized, multicenter, open-label phase II study (TDM4450g/BO21976). *Eur. Multidiscip. Cancer Congr.*, Abstr. 5001
40. Blackwell KL, Miles D, Gianni L, et al. 2012. Primary results from EMILIA, a phase III study of trastuzumab emtansine (T-DM1) versus capecitabine (X) and lapatinib (L) in HER2-positive locally advanced or metastatic breast cancer (MBC) previously treated with trastuzumab (T) and taxane. *J. Clin. Oncol. Meet. Abstr.*, Abstr. LBA1
41. Ricart AD. 2011. Antibody-drug conjugates of calicheamicin derivative: gemtuzumab ozogamicin and inotuzumab ozogamicin. *Clin. Cancer Res.* 17:6417–27
42. Sievers EL, Larson RA, Stadtmauer EA, et al. 2001. Efficacy and safety of gemtuzumab ozogamicin in patients with CD33-positive acute myeloid leukemia in first relapse. *J. Clin. Oncol.* 19:3244–54
43. Giles FJ, Kantarjian HM, Kornblau SM, et al. 2001. Mylotarg (gemtuzumab ozogamicin) therapy is associated with hepatic venoocclusive disease in patients who have not received stem cell transplantation. *Cancer* 92:406–13
44. Rajvanshi P, Shulman HM, Sievers EL, et al. 2002. Hepatic sinusoidal obstruction after gemtuzumab ozogamicin (Mylotarg) therapy. *Blood* 99:2310–14
45. Petersdorf S, Kopecky K, Stuart RK, et al. 2009. Preliminary results of Southwest Oncology Group Study S0106: an international intergroup phase 3 randomized trial comparing the addition of gemtuzumab

by Stanford University - Main Campus - Lane Medical Library on 03/18/13. For personal use only.

ozogamicin to standard induction therapy versus standard induction therapy followed by a second randomization to post-consolidation gemtuzumab ozogamicin versus no additional therapy for previously untreated acute myeloid leukemia. *Am. Soc. Hematol. Annu. Meet. Abstr.*, Abstr. 790

46. Burnett AK, Hills RK, Milligan D, et al. 2011. Identification of patients with acute myeloblastic leukemia who benefit from the addition of gemtuzumab ozogamicin: results of the MRC AML15 trial. *J. Clin. Oncol.* 29:369–77
47. Ravandi F. 2011. Gemtuzumab ozogamicin: one size does not fit all—the case for personalized therapy. *J. Clin. Oncol.* 29:349–51
48. Burnett AK, Hills RK, Hunter AE, et al. 2011. The addition of gemtuzumab ozogamicin to intensive chemotherapy in older patients with AML produces a significant improvement in overall survival: results of the UK NCRI AML16 randomized trial. *Am. Soc. Hematol. Annu. Meet. Abstr.*, Abstr. 582
49. Castaigne S, Pautas C, Terré C, et al. 2012. Effect of gemtuzumab ozogamicin on survival of adult patients with de-novo acute myeloid leukaemia (ALFA-0701): a randomised, open-label, phase 3 study. *Lancet* 379:1508–16
50. Mason DY, Stein H, Gerdes J, et al. 1987. Value of monoclonal anti-CD22 (p135) antibodies for the detection of normal and neoplastic B lymphoid cells. *Blood* 69:836–40
51. Olejniczak SH, Stewart CC, Donohue K, et al. 2006. A quantitative exploration of surface antigen expression in common B-cell malignancies using flow cytometry. *Immunol. Invest.* 35:93–114
52. Advani A, Coiffier B, Czuczman MS, et al. 2010. Safety, pharmacokinetics, and preliminary clinical activity of inotuzumab ozogamicin, a novel immunoconjugate for the treatment of B-cell non-Hodgkin's lymphoma: results of a phase I study. *J. Clin. Oncol.* 28:2085–93
53. Vaickus L, Ball ED, Foon KA. 1991. Immune markers in hematologic malignancies. *Crit. Rev. Oncol. Hematol.* 11:267–97
54. Kantarjian H, Thomas D, Jorgensen J, et al. 2012. Inotuzumab ozogamicin, an anti-CD22-calecheamicin conjugate, for refractory and relapsed acute lymphocytic leukaemia: a phase 2 study. *Lancet Oncol.* 13:403–11
55. Kebriaei P, Wilhelm K, Ravandi F, et al. 2011. Inotuzumab ozogamicin (IO) is an effective salvage therapy that allows for allogeneic hematopoietic stem cell transplantation (HSCT) in remission in patients with advanced acute lymphoblastic leukemia (ALL). *Am. Soc. Hematol. Annu. Meet. Abstr.*, Abstr. 3102
56. Rose AA, Grosset AA, Dong Z, et al. 2010. Glycoprotein nonmetastatic B is an independent prognostic indicator of recurrence and a novel therapeutic target in breast cancer. *Clin. Cancer Res.* 16:2147–56
57. Hamid O, Sznol M, Pavlick AC, et al. 2010. Frequent dosing and GPNMB expression with CDX-011 (CR011-vcMMAE), an antibody-drug conjugate (ADC), in patients with advanced melanoma. *Am. Soc. Clin. Oncol. Meet. Abstr.*, Abstr. 8525
58. Saleh MN, Bendell JC, Rose A, et al. 2010. Correlation of GPNMB expression with outcome in breast cancer (BC) patients treated with the antibody-drug conjugate (ADC), CDX-011 (CR011-vcMMAE). *Am. Soc. Clin. Oncol. Meet. Abstr.*, Abstr. 1095
59. Coiffier B, Ribrag V, Dupuis J, et al. 2011. Phase I/II study of the anti-CD19 maytansinoid immunoconjugate SAR3419 administered weekly to patients (pts) with relapsed/refractory B-cell non-Hodgkin lymphoma (NHL). *Am. Soc. Clin. Oncol. Meet. Abstr.*, Abstr. 8017
60. Beck A, Senter P, Chari R. 2011. World Antibody Drug Conjugate Summit Europe: February 21–23, 2011; Frankfurt, Germany. *MAbs* 3:331–37
61. Hartley JA, Hamaguchi A, Coffils M, et al. 2010. SG2285, a novel C2-aryl-substituted pyrrolobenzodiazepine dimer prodrug that cross-links DNA and exerts highly potent antitumor activity. *Cancer Res.* 70:6849–58
62. Moldenhauer G, Salnikov AV, Luttgau S, et al. 2012. Therapeutic potential of amanitin-conjugated anti-epithelial cell adhesion molecule monoclonal antibody against pancreatic carcinoma. *J. Natl. Cancer Inst.* 104:622–34
63. Junutula JR, Raab H, Clark S, et al. 2008. Site-specific conjugation of a cytotoxic drug to an antibody improves the therapeutic index. *Nat. Biotechnol.* 26:925–32
64. Carter PJ, Senter PD. 2008. Antibody-drug conjugates for cancer therapy. *Cancer J.* 14:154–69
65. Shen BQ, Xu K, Liu L, et al. 2012. Conjugation site modulates the in vivo stability and therapeutic activity of antibody-drug conjugates. *Nat. Biotechnol.* 30:184–89

by Stanford University - Main Campus - Lane Medical Library on 05/18/15. For personal use only.

66. Friedman M, Nordberg E, Höidén-Guthenberg I, et al. 2007. Phage display selection of Affibody molecules with specific binding to the extracellular domain of the epidermal growth factor receptor. *Protein Eng. Des. Sel.* 20:189–99
67. Kim KM, McDonagh CF, Westendorf L, et al. 2008. Anti-CD30 diabody-drug conjugates with potent antitumor activity. *Mol. Cancer Ther.* 7:2486–97
68. Leonard JP, Coleman M, Ketas JC, et al. 2003. Phase I/II trial of epratuzumab (humanized anti-CD22 antibody) in indolent non-Hodgkin's lymphoma. *J. Clin. Oncol.* 21:3051–59
69. Goy A, Leach J, Ehmann WC, et al. 2010. Inotuzumab ozogamicin (CMC-544) in patients with indolent B-cell NHL that is refractory to rituximab alone, rituximab and chemotherapy, or radioimmunotherapy: preliminary safety and efficacy from a phase 2 trial. *Am. Soc. Hematol. Annu. Meet. Abstr.*, Abstr. 430
70. Forero-Torres A, Leonard JP, Younes A, et al. 2009. A phase II study of SGN-30 (anti-CD30 mAb) in Hodgkin lymphoma or systemic anaplastic large cell lymphoma. *Br. J. Haematol.* 146:171–79
71. Raza A, Jurcic JG, Feldman EJ, et al. 2009. Prolonged exposure to lintuzumab monotherapy in acute myeloid leukemia and myelodysplastic syndromes—results of a phase 1 trial. *Eur. Hematol. Assoc. Annu. Meet. Abstr.*, Abstr. 833
72. Larson RA, Sievers EL, Stadtmauer EA, et al. 2005. Final report of the efficacy and safety of gemtuzumab ozogamicin (Mylotarg) in patients with CD33-positive acute myeloid leukemia in first recurrence. *Cancer* 104:1442–52
73. Cobleigh MA, Vogel CL, Tripathy D, et al. 1999. Multinational study of the efficacy and safety of humanized anti-HER2 monoclonal antibody in women who have HER2-overexpressing metastatic breast cancer that has progressed after chemotherapy for metastatic disease. *J. Clin. Oncol.* 17:2639–48
74. Baselga J, Carbonell X, Castaneda-Soto NJ, et al. 2005. Phase II study of efficacy, safety, and pharmacokinetics of trastuzumab monotherapy administered on a 3-weekly schedule. *J. Clin. Oncol.* 23:2162–71
75. Vogel CL, Cobleigh MA, Tripathy D, et al. 2002. Efficacy and safety of trastuzumab as a single agent in first-line treatment of HER2-overexpressing metastatic breast cancer. *J. Clin. Oncol.* 20:719–26
76. Burris HA 3rd, Rugo HS, Vukelja SJ, et al. 2011. Phase II study of the antibody drug conjugate trastuzumab-DM1 for the treatment of human epidermal growth factor receptor 2 (HER2)-positive breast cancer after prior HER2-directed therapy. *J. Clin. Oncol.* 29:398–405
77. Krop I, Lorusso P, Miller K, et al. 2010. A phase 2 study of the HER2 antibody-drug conjugate trastuzumab-DM1 in patients with HER2-positive metastatic breast cancer previously treated with trastuzumab, lapatinib, and chemotherapy. *Eur. Soc. Med. Oncol. Meet. Abstr.*, Abstr. 5082
78. Cortes J, Baselga J, Petrella T, et al. 2009. Pertuzumab monotherapy following trastuzumab-based treatment: activity and tolerability in patients with advanced HER2-positive breast cancer. *Am. Soc. Clin. Oncol. Meet. Abstr.*, Abstr. 1022

Annual Review of Medicine

Volume 64, 2013

Contents

Abiraterone and Novel Antiandrogens: Overcoming Castration Resistance in Prostate Cancer
R. Ferraldeschi, C. Pezaro, V. Karavasilis, and J. de Bono 1

Antibody-Drug Conjugates in Cancer Therapy
Eric L. Sievers and Peter D. Senter 15

Circulating Tumor Cells: From Bench to Bedside
Marija Balic, Anthony Williams, Henry Lin, Ram Datar, and Richard J. Cote 31

Cytokines, Obesity, and Cancer: New Insights on Mechanisms Linking Obesity to Cancer Risk and Progression
Candace A. Gilbert and Joyce M. Slingerland 45

Glioblastoma: Molecular Analysis and Clinical Implications
Jason T. Huse, Eric Holland, and Lisa M. DeAngelis 59

Harnessing the Power of the Immune System to Target Cancer
Gregory Lizée, Willem W. Overwijk, Laszlo Radvanyi, Jianjun Gao, Padmanee Sharma, and Patrick Hwu 71

Human Papillomavirus Vaccines Six Years After Approval
Alan R. Shaw 91

Reduced-Intensity Hematopoietic Stem Cell Transplants for Malignancies: Harnessing the Graft-Versus-Tumor Effect
Saar Gill and David L. Porter 101

The Need for Lymph Node Dissection in Nonmetastatic Breast Cancer
Catherine Pesce and Monica Morrow 119

The Role of Anti-Inflammatory Drugs in Colorectal Cancer
Dingzhi Wang and Raymond N. DuBois 131

The Human Microbiome: From Symbiosis to Pathogenesis
Emiley A. Eloe-Fadrosh and David A. Rasko 145

The Rotavirus Saga Revisited
Alan R. Shaw 165

by Stanford University - Main Campus - Lane Medical Library on 03/18/13. For personal use only.

by Stanford University - Main Campus - Lane Medical Library on 03/18/13. For personal use only.

Staphylococcal Infections: Mechanisms of Biofilm Maturation and Detachment as Critical Determinants of Pathogenicity
Michael Otto 175

Toward a Universal Influenza Virus Vaccine: Prospects and Challenges
Natalie Pica and Peter Palese 189

Host Genetics of HIV Acquisition and Viral Control
Patrick R. Shea, Kevin V. Shianna, Mary Carrington, and David B. Goldstein 203

Systemic and Topical Drugs for the Prevention of HIV Infection: Antiretroviral Pre-exposure Prophylaxis
Jared Baeten and Connie Celum 219

Hyperaldosteronism as a Common Cause of Resistant Hypertension
David A. Calhoun 233

Mechanisms of Premature Atherosclerosis in Rheumatoid Arthritis and Lupus
J. Michelle Kahlenberg and Mariana J. Kaplan 249

Molecular Mechanisms in Progressive Idiopathic Pulmonary Fibrosis
Mark P. Steele and David A. Schwartz 265

Reprogrammed Cells for Disease Modeling and Regenerative Medicine
Anne B.C. Cherry and George Q. Daley 277

Application of Metabolomics to Diagnosis of Insulin Resistance
Michael V. Milburn and Kay A. Lawton 291

Defective Complement Inhibitory Function Predisposes to Renal Disease
Anuja Java, John Atkinson, and Jane Salmon 307

New Therapies for Gout
Daria B. Crittenden and Michael H. Pillinger 325

Pathogenesis of Immunoglobulin A Nephropathy: Recent Insight from Genetic Studies
Krzysztof Kiryluk, Jan Novak, and Ali G. Gharavi 339

Podocyte Biology and Pathogenesis of Kidney Disease
Jochen Reiser and Sanja Sever 357

Toward the Treatment and Prevention of Alzheimer's Disease: Rational Strategies and Recent Progress
Sam Gandy and Steven T. DeKosky 367

Psychiatry's Integration with Medicine: The Role of DSM-5
David J. Kupfer, Emily A. Kuhl, Lawson Wulsin 385

Update on Typical and Atypical Antipsychotic Drugs
Herbert Y. Meltzer 393

Ataluren as an Agent for Therapeutic Nonsense Suppression
Stuart W. Peltz, Manal Morsy, Ellen M. Welch, and Allan Jacobson 407

Treating the Developing Brain: Implications from Human Imaging and Mouse Genetics
B.J. Casey, Siobhan S. Pattwell, Charles E. Glatt, and Francis S. Lee 427

Genetic Basis of Intellectual Disability
Jay W. Ellison, Jill A. Rosenfeld, and Lisa G. Shaffer 441

Sickle Cell Disease, Vasculopathy, and Therapeutics
Adetola A. Kassim and Michael R. DeBaun 451

Duty-Hour Limits and Patient Care and Resident Outcomes: Can High-Quality Studies Offer Insight into Complex Relationships?
Ingrid Philibert, Thomas Nasca, Timothy Brigham, and Jane Shapiro 467

Quality Measurement in Healthcare
Eliot J. Lazar, Peter Fleischut, and Brian K. Regan 485

Indexes

Cumulative Index of Contributing Authors, Volumes 60–64 497

Article Titles, Volumes 60–64 501

Errata

An online log of corrections to *Annual Review of Medicine* articles may be found at http://med.annualreviews.org/errata.shtml

by Stanford University - Main Campus - Lane Medical Library on 03/18/13. For personal use only.

OnCusp
Ex. 1002

Human Breast Cancer: Correlation of Relapse and Survival with Amplification of the HER-2/*neu* Oncogene

DENNIS J. SLAMON,* GARY M. CLARK, STEVEN G. WONG, WENDY J. LEVIN, AXEL ULLRICH, WILLIAM L. MCGUIRE

The HER-2/*neu* oncogene is a member of the *erbB*–like oncogene family, and is related to, but distinct from, the epidermal growth factor receptor. This gene has been shown to be amplified in human breast cancer cell lines. In the current study, alterations of the gene in 189 primary human breast cancers were investigated. HER-2/*neu* was found to be amplified from 2- to greater than 20-fold in 30% of the tumors. Correlation of gene amplification with several disease parameters was evaluated. Amplification of the HER-2/*neu* gene was a significant predictor of both overall survival and time to relapse in patients with breast cancer. It retained its significance even when adjustments were made for other known prognostic factors. Moreover, HER-2/*neu* amplification had greater prognostic value than most currently used prognostic factors, including hormonal-receptor status, in lymph node–positive disease. These data indicate that this gene may play a role in the biologic behavior and/or pathogenesis of human breast cancer.

THE EVIDENCE LINKING PROTO-ONCOGENES TO THE INDUCtion or maintenance of human malignancies is largely circumstantial, but has become increasingly compelling. This circumstantial evidence is derived from studies of animal models, tumor cell lines, and actual human tumors. Data from animal models and cell lines include: (i) sequence homology between human proto-oncogenes and the viral oncogenes of transforming retroviruses that are known to be tumorigenic in some species (*1, 2*); (ii) transfection studies showing the transforming potential of proto-oncogenes in NIH 3T3 cells and primary embryo fibroblasts (*3–5*); and (iii) the central role of certain proto-oncogenes in tumorigenesis by chronic transforming retroviruses such as avian leukosis virus (*6*). Data from human tumors include: (i) increased expression of specific proto-oncogenes in some human malignancies (*7, 8*); (ii) localization of proto-oncogenes at or near the site of specific, tumor-associated chromosomal translocations (*9*); and (iii) amplification of proto-oncogenes in some human tumors (*10, 11*).

Additional data linking proto-oncogenes to cell growth is their expression in response to certain proliferation signals (*12, 13*) and their expression during embryonic development (*14, 15*). More direct evidence comes from the fact that, of the 20 known proto-oncogenes, three are related to a growth factor or a growth factor receptor. These genes include c-*sis*, which is homologous to the transforming gene of the simian sarcoma virus and is the β chain of platelet-derived growth factor (PDGF) (*16, 17*); c-*fms*, which is homologous to the transforming gene of the feline sarcoma virus and is closely related to the macrophage colony-stimulating factor receptor (CSF-1R) (*18*); and c-*erbB*, which encodes the EGF receptor (EGFR) and is highly homologous to the transforming gene of the avian erythroblastosis virus (*19*). The two receptor-related proto-oncogenes, c-*fms* and c-*erbB*, are members of the tyrosine-specific protein kinase family to which many proto-oncogenes belong.

Recently, a novel transforming gene was identified as a result of transfection studies with DNA from chemically induced rat neuroglioblastomas (*20*). This gene, called *neu*, was shown to be related to, but distinct from, the c-*erbB* proto-oncogene (*21*). By means of v-*erbB* and human EGFR as probes to screen human genomic and complementary DNA (cDNA) libraries, two other groups independently isolated human *erbB*–related genes that they called HER-2 (*22*) and c-*erbB*-2 (*23*). Subsequent sequence analysis and chromosomal mapping studies revealed all three genes (*neu*, c-*erbB*-2, and HER-2) to be the same (*22, 24, 25*). A fourth group, also using v-*erbB* as a probe, identified the same gene in a mammary carcinoma cell line, MAC 117, where it was found to be amplified five- to ten-fold (*26*).

This gene, which we will call HER-2/*neu*, encodes a new member of the tyrosine kinase family; and is closely related to, but distinct from, the EGFR gene (*22*). HER-2/*neu* differs from EGFR in that it is found on band q21 of chromosome 17 (*22, 24, 25*), as compared to band p11–p13 of chromosome 7, where the EGFR gene is located (*27*). Also, the HER-2/*neu* gene generates a messenger RNA (mRNA) of 4.8 kb (*22*), which differs from the 5.8- and 10-kb transcripts for the EGFR gene (*28*). Finally, the protein encoded by the HER-2/*neu* gene is 185,000 daltons (*21*), as compared to the 170,000-dalton protein encoded by the EGFR gene. Conversely, on the basis of sequence data, HER-2/*neu* is more closely related to the EGFR gene than to other members of the tyrosine kinase family (*22*). Like the EGFR protein, HER-2/*neu* has an extracellular domain, a transmembrane domain that includes two cysteine-rich repeat clusters, and an intracellular kinase domain (*21*), indicating

D. J. Slamon, S. G. Wong, and W. J. Levin are in the Division of Hematology-Oncology, Department of Medicine and Jonsson Comprehensive Cancer Center, UCLA School of Medicine, Los Angeles, CA 90024. G. M. Clark and W. L. McGuire are in the Division of Oncology, Department of Medicine, University of Texas Health Science Center at San Antonio, San Antonio, TX 78284. A. Ullrich is in the Department of Molecular Biology, Genentech, Inc., South San Francisco, CA 94080.

*To whom correspondence should be addressed.

that it too is likely to be a cellular receptor for an as yet unidentified ligand.

As a result of the published data showing amplification of HER-2/*neu* in a human mammary carcinoma cell line, and as part of an ongoing survey in our laboratory of proto-oncogene abnormalities in human tumors, we evaluated alterations of the HER-2/*neu* gene in a large series of human primary breast cancers. Our results show that amplification of this gene occurs relatively frequently in breast cancer, and that it is associated with disease relapse and overall patient survival.

Factors that are known to be important in the prognosis of breast malignancies in individual patients include: size of the primary tumor, stage of disease at diagnosis, hormonal receptor status, and number of axillary lymph nodes involved with disease (positive nodes) (*29*). The current study, which was conducted in two parts, involved the evaluation of tissue from 189 separate breast malignancies that were part of a breast cancer study ongoing at the University of Texas, San Antonio. This cohort of tumors was of interest because considerable information was available on the majority of the specimens including size of the primary tumor, estrogen receptor status, progesterone receptor status, age of patient, disease stage, and status of the axillary lymph nodes.

In the initial survey, tissue from 103 primary breast cancers was evaluated for alterations in the HER-2/*neu* gene. DNA from individual tumors was prepared as described (*30*), digested with Eco RI, and subjected to Southern blot analysis with a ^{32}P-labeled HER-2/*neu*-1 probe, which is known to detect a 13-kb hybridizing band in human DNA (*22*). Examples of tumors from the initial survey are shown in Fig. 1. Of the 103 samples examined, 19 (18%) showed evidence of HER-2/*neu* gene amplification. The degree of amplification in individual cases was determined by dilution analysis (Fig. 2A), as well as soft laser densitometry scanning. To determine that the amount of DNA loaded in each lane was equivalent, all filters were washed and rehybridized with a ^{32}P-labeled arginase gene probe (*31*). This probe identifies a 15-kb hybridizing band on Eco RI–digested human DNA, and was selected as a control because it more appropriately assesses the relative amount and transfer of high molecular weight species than a probe hybridizing with low molecular weight species, which transfer more readily on Southern blotting. All lanes were shown to contain equivalent amounts of high molecular weight DNA (Fig. 2B). Individual tumors were assigned to groups containing a single copy, 2 to 5 copies, 5 to 20 copies, and greater than 20 copies of the HER-2/*neu* gene (Fig. 1). Assignment of tumors to the various groups was done

Table 1. Association between HER-2/*neu* amplification and disease parameters in 103 breast tumors.

Factor*	Number of tumors					P†
	Single copy	2 to 5 copies	5 to 20 copies	>20 copies	Total	
Hormonal receptor status						
ER+	53	2	9	1	65	0.99
ER–	31	1	2	4	38	
PgR+	42	2	6	2	52	0.85
PgR–	42	1	5	3	51	
Tumor size (centimeters)						
≤2	13	1	1	0	15	0.82
2–5	34	1	5	1	41	
>5	17	1	2	2	22	
Unknown	20	0	3	2	25	
Age at diagnosis (years)						
≤50	21	1	2	1	25	0.83
>50	52	2	7	4	65	
Unknown	11	0	2	0	13	
Number of positive lymph nodes						
0	30	0	3	1	34	0.11
1–3	20	0	1	1	22	
>3	17	2	4	2	25	
Unknown	17	1	3	1	22	

*Receptor status was analyzed as described (*30*). ER, estrogen receptor: + and – refer to the presence or absence of ≥3 fmol of receptor per milligram of protein. PgR, progesterone receptor: + and – refers to the presence or absence of ≥5 fmol of receptor per milligram of protein. †Statistical analyses for correlation of HER-2/*neu* amplification with disease parameters were performed by the χ^2 test. *P* values were computed after combining the cases with 5 to 20 and >20 copies.

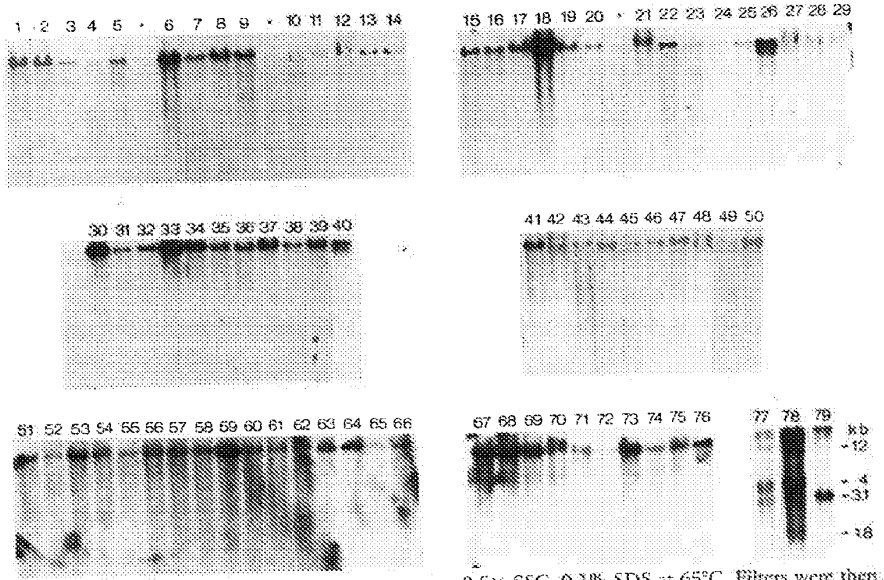


Fig. 1. Analysis of alterations of the HER-2/*neu* gene in human breast cancer. Shown are 79 of the 189 breast tumors used in this analysis. Tumors with a single copy of HER-2/*neu*: 3, 4, 10 to 15, 20, 23 to 25, 27 to 29, 31, 38, 42 to 46, 48, 49, 52, 55, 61, 65, 66, 71, 72, and 74. Tumors with two to five copies of HER-2/*neu*: 1, 2, 5, 7, 9, 16, 17, 19, 21, 22, 32, 35, 36, 47, 50, 54, 56 to 58, 60, 62, 70, and 75 to 77. Tumors with 5 to 20 copies of HER-2/*neu*: 6, 8, 26, 34, 37, 39 to 41, 51, 53, 63, 64, 67, 69, 73, and 79. Tumors with more than 20 copies of HER-2/*neu*: 18, 30, 33, 59, 68, and 78. Examples of tumors 77 to 79 have rearrangements in the HER-2/*neu* gene. DNA was extracted from tissues and digested with Eco RI as described (*30*). A total of 12 μg of Eco RI–digested DNA was loaded onto 0.8% agarose gels, separated by electrophoresis, and transferred onto nylon filter papers (Biodyne) (*30*). All filters were baked in a vacuum oven for 3 hours at 80°C, prehybridized in 6× SSC (standard saline citrate) containing 50% formamide, 10% dextran sulfate, 0.1% SDS, denatured salmon sperm DNA (1 mg/ml), and 4× Denhardts solution for 12 hours, then hybridized in the same solution containing ^{32}P-labeled nick-translated HER-2 probe (*21*) specific activity of 1×10^8 cpm per microgram of DNA; 2×10^6 cpm/ml. Hybridization occurred at 42°C for 48 hours, followed by washing of filters under the following conditions in succession: 2× SSC for 20 minutes at room temperature; two washes of 30 minutes each in 2× SSC, 0.1% SDS at 65°C; one wash of 30 minutes in 0.5× SSC, 0.1% SDS at 65°C. Filters were then exposed to XAR-5 x-ray film (Kodak) for autoradiography.

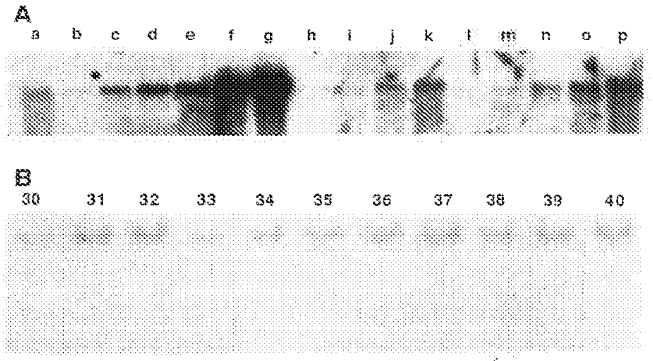


Fig. 2. (**A**) Example of dilutional analysis to assess degree of HER-2/*neu* gene amplification. Lanes a, g, k, and p were loaded with 12 μg of Eco RI–digested breast tumor DNA. Lane a is DNA from tumor 31 (Fig. 1), which represents a tumor with a single copy of the HER/2-*neu* gene. Lane g is DNA from tumor 33, which represents a tumor with >20 copies of the HER-2/*neu* gene. Lanes b to f are serial dilutions (1:100, 1:20, 1:10, 1:5, and 1:2, respectively) of the DNA sample in lane g. Lane k is DNA from tumor 35 (Fig. 1), which represents a tumor containing two to five copies of the HER-2/*neu* gene. Lanes h to j are serial dilutions (1:10, 1:5, and 1:2, respectively) of the DNA sample in lane k. Lane p is DNA from tumor 34 (Fig. 1), which represents a tumor with 5 to 20 copies of the HER-2/*neu* gene. Lanes l to o are serial dilutions (1:20, 1:10, 1:5, and 1:2, respectively) of the DNA sample in lane p. The filter was prepared and hybridized with a ^{32}P-labeled HER-2 probe as in Fig. 1. (**B**) Example of arginase probe hybridization to demonstrate that equivalent amounts of tumor DNA were loaded into each lane. Rehybridization of filter containing lanes 30 to 40 (Fig. 1). The filter was first stripped of label by washing in a buffer made up of 50% formamide, 3× SSC, and 0.1% SDS at 65°C for 20 minutes, following by three successive washes of 5 minutes each in 0.1× SSC at room temperature. Filters were exposed overnight on XAR-5 film (Kodak) to ensure removal of all radioactive probe, then rehybridized as in Fig. 1 with a ^{32}P-labeled human arginase gene probe (*31*).

in a blinded fashion, in that they were made without knowledge of disease parameters. Analysis of the data for association between gene amplification and a number of disease parameters was then performed.

Of 103 tumors evaluated in the initial survey, there was essentially no correlation between gene amplification and estrogen receptor status, progesterone receptor status, size of tumors, or age at diagnosis (Table 1). However, when analysis was performed for association between HER-2/*neu* amplification and number of positive lymph nodes, a trend was noted. This analysis showed that 4/34 (11%) of patients with no involved nodes, 2/20 (10%) with 1 to 3 involved nodes, and 8/25 (32%) with >3 involved nodes had gene amplification ($P = 0.11$). If these data were examined by comparing 0 to 3 positive nodes versus >3 positive nodes, the correlation with gene amplification became more significant ($P < 0.05$). Thus, there was a significant increase in incidence of HER-2/*neu* gene amplification in patients with >3 axillary lymph nodes involved with disease. A multivariate regression analysis to correlate HER-2/*neu* amplification with various disease parameters identified the number of positive nodes as the only significant factor, either alone or in combination, to correlate with amplification.

This initial study indicated that it might be possible to discriminate among node-positive patients on the basis of HER-2/*neu* gene amplification. It is well known that the number of positive nodes is the best prognostic factor for disease recurrence and survival in patients with breast cancer (*29*). Given the correlation between number of nodes positive and HER-2/*neu* amplification, one might predict that amplification of this gene might also have some prognostic value. No long-term follow-up data, however, were available on the 103 patients analyzed in the initial study. For this reason, a second study was conducted on 100 breast cancer samples from patients with positive axillary lymph nodes. All of the information available for the first group of 103 patients was available for these patients. In addition, relapse and survival information was available, since these cases had a median follow-up of 46 months (range 24 to 86 months). Of these 100 samples, 86 yielded sufficient DNA for study. Amplification of the HER-2/*neu* gene was measured as in the initial survey, and examples of tumors from this study are shown (Fig. 1). Amplification was found in 34/86 (40%) of these patients. For this larger sample of node-positive patients, several statistically significant or nearly significant relationships were observed. In agreement with the preliminary survey, there was an association between number of involved lymph nodes and HER-2/*neu* amplification (Table 2). In addition, the presence of gene amplification was correlated with estrogen receptor status and size of primary tumor (Table 2). Together, these two surveys yielded data on 189 patients and the association of HER-2/*neu* amplification with various disease parameters in the combined group is shown in Table 3.

While these correlations were of interest, the strong relationship

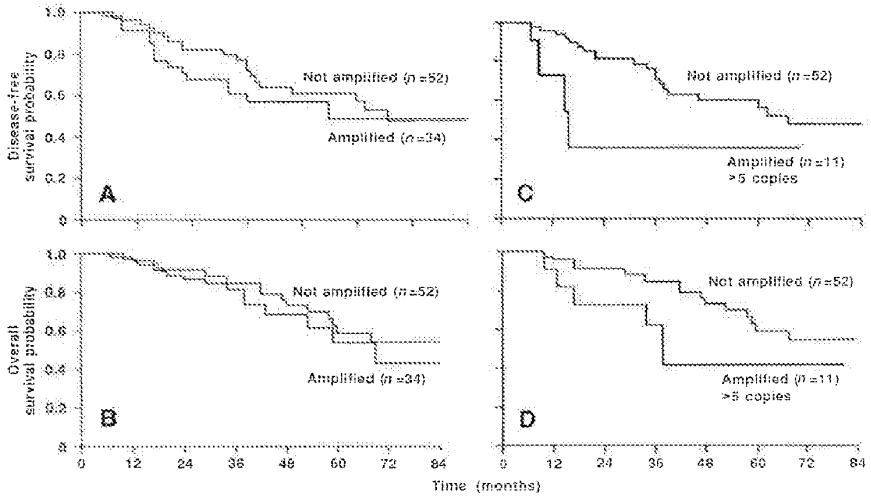


Fig. 3. Actuarial curve for relapse in (**A**) node-positive patients with no amplification versus node-positive patients with any amplification (>2 copies) of HER-2/*neu* and (**C**) node-positive patients with no amplification versus node-positive patients with greater than 5 copies of HER-2/*neu*. Actuarial curve for overall survival in (**B**) node-positive patients with no amplification versus node-positive patients with any amplification (>2 copies) of HER-2/*neu* and (**D**) node-positive patients with no amplification versus node-positive patients with greater than 5 copies of HER-2/*neu*. Actuarial curves for both relapse and overall survival were compared by the method of Kaplan and Meier (*41*) and compared by the log rank test (*42–44*).

between HER-2/*neu* amplification and nodal status ($P = 0.002$) indicated that information on amplification of this gene may correlate with disease behavior; that is, recurrences and survival. To test this, univariate survival analyses were performed in which amplification was compared to relapse and survival in this patient group. A total of 35 patients had a recurrence of the disease, and 29 had died at the time of the analyses. Median times to relapse and death were 62 months and 69 months, respectively. The median follow-up time for patients still alive was 47 months, ranging from 24 to 86 months. A total of 71 of the 86 patients (83%) received some form of therapy after mastectomy: adjuvant systemic therapy alone, 47%; adjuvant systemic therapy plus local radiation, 19%; and local radiation alone, 17%. A strong and highly statistically significant correlation was found between the degree of gene amplification and both time to disease relapse ($P = <0.0001$) and survival ($P = 0.0011$) (Table 4). Moreover, when compared in univariate analyses to other parameters, amplification of HER-2/*neu* was found to be superior to all other prognostic factors, with the exception of the number of positive nodes (which it equaled) in predicting time to relapse and overall survival in human breast cancer (Table 4). The association between HER-2/*neu* amplification and relapse and survival can be illustrated graphically in actuarial survival curves (Fig. 3, A to D). While there was a somewhat shortened time to relapse and shorter overall survival in patients having any amplification of the HER-2/*neu* gene in their tumors (Fig. 3, A and B), the greatest differences were found when comparing patients with >5 copies of the gene to those without amplification (single copy) (Fig. 3, C and D). Patients with greater than five copies of HER-2/*neu* had even shorter disease-free survival times ($P = 0.015$) and overall survival times ($P = 0.06$) when compared to patients with no amplification. The phenomenon of greater gene copy number correlating with a worse prognosis has also been seen in evaluations of N-*myc* gene amplification in human neuroblastomas (*32*).

To determine if amplification of HER-2/*neu* was independent of other known prognostic factors in predicting disease behavior, multivariate survival analyses were performed on the 86 node-positive cases. Amplification of the gene continued to be a strong prognostic factor, providing additional and independent predictive information on both time to relapse and overall survival in these patients, even when other prognostic factors were taken into account (Table 4).

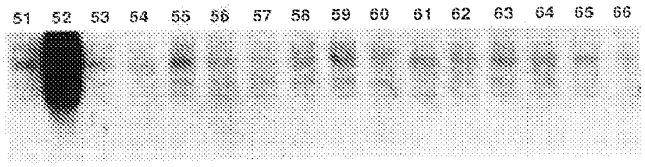


Fig. 4. Example of rehybridization of filter with human EGFR probe. Filters were stripped as in Fig. 2B, and hybridized with ^{32}P-labeled human EGFR probe (*28*), as in Fig. 1. Shown are the lower molecular weight bands hybridized with ^{32}P-labeled EGFR probe in filter-containing lanes 51 to 66 (Fig. 1). The bands from top to bottom are 2.8, 2.2, and 1.8 kb, respectively. Lane 52 is an example of a tumor showing marked amplification (>50 copies) of the EGFR gene.

Rearrangement of the HER-2/*neu* gene was rare. Of the total 189 tumors evaluated, three showed evidence of rearrangement, and in two of the three cases, the rearrangement was identical (Fig. 1, cases 77 to 79). Also, two of the rearranged HER-2/*neu* loci were amplified (Fig. 1, cases 78 and 79). The incidence of HER-2/*neu* rearrangement as determined by Eco RI digestion was too small to attempt statistical correlations.

To determine whether the phenomenon of amplification of HER-2/*neu* in breast cancer extended to related growth factor receptors, all filters were analyzed with the EGFR probe (Fig. 4). Amplification of the EGFR gene was found in 4/189 (2%) of the cases, and rearrangement of the EGFR gene was found in one of those four cases. The incidence of EGFR amplification and rearrangement was too small to attempt statistical correlation. Comparison of HER-2/*neu* amplification (53/189 or 28%) with that of the EGFR gene reveals the incidence of the former to be 14 times greater than that of the latter, indicating that the phenomenon of gene amplification is not a general one for a related tyrosine kinase–specific receptor in human breast cancer. Moreover, studies examining alterations of two other tyrosine kinase–specific proto-oncogenes, *abl* and *fes*, in breast cancer did not show amplification of these genes (*33*). Alterations of non–tyrosine kinase–related proto-oncogenes in these

Table 2. Association between HER-2/*neu* amplification and disease parameters in 86 breast tumors from node-positive patients.

Factor*	Single copy	2 to 5 copies	5 to 20 copies	>20 copies	Total	P†
Hormonal receptor status						
ER+	38	21	5	1	65	0.05
ER−	14	2	4	1	21	
PgR+	31	18	4	1	54	0.14
PgR−	21	5	5	1	32	
Tumor size (centimeters)						
≤2	18	8	3	0	29	0.09
2–5	28	12	2	1	43	
>5	6	3	4	1	14	
Age at diagnosis (years)						
≤50	16	12	6	1	35	0.06
>50	36	11	3	1	51	
Number of positive lymph nodes						
1–3	31	7	5	0	43	0.06
>3	21	16	4	2	43	

*ER and PgR are as described in Table 1. †Statistical analyses for correlation of HER-2/*neu* amplification with various disease parameters were performed by the χ^2 test. *P* values were computed after combining the 5 to 20 and >20 cases, since there were so few samples in the >20 group.

Table 3. Association between HER-2/*neu* amplification and disease parameters in combined surveys (189 patients).

Factor*	Single copy	2 to 5 copies	5 to 20 copies	>20 copies	Total	P†
Hormonal receptor status						
ER+	91	23	14	2	130	0.05
ER−	45	3	6	5	59	
PgR+	73	20	10	3	106	0.06
PgR−	63	6	10	4	83	
Tumor size (centimeters)						
≤2	31	9	4	0	44	0.19
2–5	62	13	7	2	84	
>5	23	4	6	3	36	
Unknown	20	0	3	2	25	
Age at diagnosis (years)						
≤50	37	13	8	2	60	0.11
>50	88	13	10	5	116	
Unknown	11	0	2	0	13	
Number of positive lymph nodes						
0	30	0	3	1	34	0.002
1–3	51	7	6	1	65	
>3	38	18	8	4	68	
Unknown	17	1	3	1	22	

*ER and PgR are as described in Table 1. †Statistical analyses for correlation of HER-2/*neu* amplification with various disease parameters were performed by the χ^2 test. *P* values were computed after combining the cases with 5 to 20 and >20 copies.

Table 4. Univariate and multivariate analyses comparing disease-free survival (relapse) and overall survival to prognostic factors in node-positive patients.

Factor	Univariate (*P*)		Multivariate*	
	Survival	Relapse	Survival	Relapse
Number of positive nodes	0.0001	0.0002	0.0003 (0.0938 ± 0.0256)	0.001 (0.0849 ± 0.0266)
HER-2/*neu*	0.0011	<0.0001	0.02 (0.0872 ± 0.0388)	0.001 (0.1378 ± 0.0425)
Log (PgR)	0.05	0.05		
Tumor size	0.06	0.06		
Log (ER)	0.15	0.10	0.03 (−0.5158 ± 0.2414)	
Age	0.22	0.61		

*Cox's partially nonparametric regression model was used to evaluate the predictive power of various combinations and interactions of prognostic factors in a multivariate manner (*43–44*). Results are shown as *P* (regression coefficient ± SE).

tumors have been examined. In a survey of 121 primary breast malignancies, amplification of the c-*myc* gene was found in 38 (32%) (*34*). Attempts to correlate c-*myc* gene amplification with stage of disease, hormonal receptor status, histopathologic grade, or axillary node metastases showed no association. There was a statistically significant association between c-*myc* amplification and age at diagnosis >50 years in a group of 95 of these patients (*34*). Data on relapse and survival were not presented in this study; however, there was no correlation between c-*myc* amplification and nodal status to indicate an association with disease behavior.

The exact role of various proto-oncogenes in the pathogenesis of human malignancies remains unclear. One line of evidence implicating abnormalities of these genes in human disease is association of their amplification with tumor progression in specific cancers. The N-*myc* gene is frequently amplified in human neuroblastomas and neuroblastoma cell lines (*35, 36*). Studies on the N-*myc* proto-oncogene were the first to show a direct association between abnormalities in a proto-oncogene and clinical behavior of a human tumor. N-*myc* amplification and expression correlate both with stage of disease and overall survival in patients with neuroblastoma (*10, 32, 37*). Moreover the greater the N-*myc* gene copy number, the worse the patient prognosis for all stages of the disease (*32*). Taken together, these data indicate a role for the N-*myc* gene in the pathogenesis of neuroblastoma (*32*).

Neuroblastoma is a relatively rare disease with an incidence of one per 125,000 children. Carcinoma of the breast, however, is a common malignancy affecting one of every 13 women in the United States. There are 119,000 new cases per year, and approximately 40,000 women will die of the disease in 1986 (*38*). Current treatment decisions for individual patients are frequently based on specific prognostic parameters. The major prognostic factors for breast cancer include presence or absence of tumor in the axillary nodes, size of the primary tumor, and presence or absence of hormonal receptors (*29*). The current study indicates that amplification of the HER-2/*neu* gene is a significant predictor of both overall survival and time to relapse in node-positive patients with breast cancer. Amplification of the gene retains its prognostic significance in multivariate analysis, even when adjustments are made for other known prognostic factors. Moreover, amplification of HER-2/*neu* has greater prognostic value than most currently used prognostic factors, including progesterone and estrogen receptors, and is equivalent to and independent of the best known prognosticator—number of positive lymph nodes. Finally, the degree of HER-2/*neu* amplification appears to have an effect on survival, with greater copy number being associated with a worse prognosis (Fig. 3, C and D). A similar phenomenon has been observed for N-*myc* gene amplification in human neuroblastoma (*32*).

The potential role of HER-2/*neu* in the pathogenesis of breast cancer is unknown. Like N-*myc*, the correlation of HER-2/*neu* amplification with disease progression indicates it may be an important gene in the disease process. The role of other cell receptors in the biology of breast cancer is well established (*29, 39, 40*). It is easy to speculate that a gene encoding a putative growth factor receptor, when expressed in inappropriate amounts, may give a growth advantage to the cells expressing it. Alternatively, alteration in the gene product itself may lead to a critical change in the receptor protein. A single point mutation in the transmembrane domain of the protein encoded by the rat *neu* oncogene appears to be all that is necessary for the gene to gain transforming ability (*41*). Whether this or a similar alteration is found in the amplified HER-2/*neu* gene in human breast cancer will require sequence analysis of the homologous region in the amplified human gene. In addition, studies evaluating the expression of this gene at the RNA and/or protein level will prove important in determining if HER-2/*neu* amplification results in an expected increased gene expression. The question of amplification of HER-2/*neu* in metastatic as compared to primary lesions in a given patient is important. The current study utilized only primary breast tumors for analyses. It would be of interest to determine if HER-2/*neu* copy number is altered as the tumor metastasizes. A recent study evaluating N-*myc* copy number in human small cell carcinoma of the lung showed no difference between primary and metastatic lesions (*11*).

The initial survey from the current study showed that 15% of breast cancer patients with stage I disease (node-negative) have HER-2/*neu* amplification. Unfortunately, no long-term follow-up data were available for these patients. This stage I setting may be an additional group in which HER-2/*neu* measurements will have an impact in predicting biologic behavior of the tumor, and as a result, in design of treatment strategy. Finally, if the HER-2/*neu* gene product functions as a growth factor receptor that plays a role in the pathogenesis of breast cancer, identification of its ligand and development of specific antagonists could have important therapeutic implications.

REFERENCES AND NOTES

1. J. M. Bishop, *Annu. Rev. Biochem.* 52, 301 (1983).
2. H. E. Varmus, *Annu. Rev. Genet.* 18, 553 (1984).
3. H. Land, L. F. Parada, R. A. Weinberg, *Nature (London)* 304, 596 (1983).
4. H. E. Ruley, *ibid.*, p. 602.
5. M. Schwab, H. E. Varmus, J. M. Bishop, *ibid.* 316, 160 (1985).
6. W. S. Hayward, B. G. Neel, S. M. Astrin, *ibid.* 290, 475 (1981).
7. D. J. Slamon *et al.*, *Science* 224, 256 (1984).
8. M. D. Erisman *et al.*, *Mol. Cell. Biol.* 5, 1969 (1985).
9. C. M. Croce and G. Klein, *Sci. Am.* 252, 54 (March 1985).
10. G. M. Brodeur *et al.*, *Science* 224, 1121 (1984).
11. A. J. Wong *et al.*, *ibid.* 233, 461 (1986).
12. J. Campisi *et al.*, *Cell* 36, 357 (1983).
13. M. E. Greenberg and E. B. Ziff, *Nature (London)* 311, 433 (1984).
14. R. Mulles *et al.*, *ibid.* 299, 640 (1982).
15. D. J. Slamon and M. J. Cline, *Proc. Natl. Acad. Sci. U.S.A.* 81, 7141 (1984).
16. M. D. Waterfield *et al.*, *Nature (London)* 304, 35 (1983).
17. R. F. Doolittle, M. W. Hunkapiller, L. E. Hood, *Science* 221, 275 (1983).
18. C. J. Sherr *et al.*, *Cell* 41, 665 (1985).
19. J. Downward *et al.*, *Nature (London)* 307, 521 (1984).
20. C. Shih, L. Padhy, M. Murray, R. A. Weinberg, *ibid.* 290, 261 (1981).
21. A. L. Schechter *et al.*, *ibid.* 312, 513 (1984).
22. L. Coussens *et al.*, *Science* 230, 1132 (1985).
23. K. Semba, N. Kamata, K. Toyoshima, T. Yamamoto, *Proc. Natl. Acad. Sci. U.S.A.* 82, 6497 (1985).

24. A. L. Schechter *et al.*, *Science* 229, 976 (1985).
25. S. I. Fukushige *et al.*, *Mol. Cell. Biol.* 6, 955 (1986).
26. C. R. King, M. H. Kraus, S. A. Aaronson, *Science* 229, 974 (1985).
27. D. Meerabkan and M. Smith, *Cytogenet. Cell. Genet.* 37, 71 (1984).
28. A. Ullrich *et al.*, *Nature (London)* 309, 418 (1984).
29. G. M. Clark *et al.*, *N. Engl. J. Med.* 309, 1343 (1983).
30. T. Maniatis, E. F. Fritsch, J. Sambrook, *Molecular Cloning: A Laboratory Manual*, (Cold Spring Harbor Laboratory, Cold Spring Harbor, NY, 1982), pp. 282–285.
31. G. J. Dezikes, W. W. Grody, R. M. Kern, S. D. Cederbaum, *Biochem. Biophys. Res. Commun.*, in press.
32. R. C. Seeger *et al.*, *N. Engl. J. Med.* 313, 1111 (1985).
33. T. Yokota *et al.*, *Science* 231, 261 (1986).
34. C. Escot *et al.*, *Proc. Natl. Acad. Sci. U.S.A.* 83, 4834 (1986).
35. M. Schwab *et al.*, *Nature (London)* 305, 245 (1983).
36. N. E. Kohl *et al.*, *Cell* 35, 359 (1984).
37. R. C. Seeger and D. Slamon, unpublished data.
38. E. Silverberg and J. Lubera, *CA Cancer J. Clin.* 36, 9 (1986).
39. K. B. Horwitz, W. L. McGuire, O. H. Pearson, A. Segaloff, *Science* 189, 726 (1975).
40. W. L. McGuire, *Semin. Oncol.* 5, 428 (1978).
41. C. I. Bargmann, M. C. Hung, R. A. Weinberg, *Cell* 45, 649 (1986).
42. D. R. Cox, *J. R. Stat. Soc.* 34, 187 (1972).
43. N. E. Breslow, *Int. Stat. Rev.* 43, 45 (1975).
44. E. L. Kaplan and P. Meier, *J. Am. Stat. Assoc.* 53, 457 (1958).
45. Supported by U.S. Public Health Service grants CA 36827 and CA 30195 and a grant from Triton Biosciences, Inc. We thank D. Keith, L. Gordon, and W. Alt for their technical assistance and Dr. S. Cederbaum for providing the human arginase probe.

Research Articles

The Atomic Structure of Mengo Virus at 3.0 Å Resolution

MING LUO, GERRIT VRIEND*, GREG KAMER, IWONA MINOR, EDWARD ARNOLD, MICHAEL G. ROSSMANN, ULRIKE BOEGE, DOUGLAS G. SCRABA, GREG M. DUKE, ANN C. PALMENBERG

The structure of Mengo virus, a representative member of the cardio picornaviruses, is substantially different from the structures of rhino- and polioviruses. The structure of Mengo virus was solved with the use of human rhinovirus 14 as an 8 Å resolution structural approximation. Phase information was then extended to 3 Å resolution by use of the icosahedral symmetry. This procedure gives promise that many other virus structures also can be determined without the use of the isomorphous replacement technique. Although the organization of the major capsid proteins VP1, VP2, and VP3 of Mengo virus is essentially the same as in rhino- and polioviruses, large insertions and deletions, mostly in VP1, radically alter the surface features. In particular, the putative receptor binding "canyon" of human rhinovirus 14 becomes a deep "pit" in Mengo virus because of polypeptide insertions in VP1 that fill part of the canyon. The minor capsid peptide, VP4, is completely internal in Mengo virus, but its association with the other capsid proteins is substantially different from that in rhino- or poliovirus. However, its carboxyl terminus is located at a position similar to that in human rhinovirus 14 and poliovirus, suggesting the same autocatalytic cleavage of VP0 to VP4 and VP2 takes place during assembly in all these picornaviruses.

PICORNAVIRUSES (*1*) COMPRISE A LARGE FAMILY OF SINGLE-stranded RNA-containing animal viruses. They have been classified into four genera on the basis of physical properties of the virions: (i) cardioviruses, such as encephalomyocarditis virus (EMCV), Theiler's murine encephalitis virus, and Mengo virus; (ii) enteroviruses, such as poliovirus, hepatitis A virus, and Coxsackie virus; (iii) aphthoviruses, such as foot-and-mouth disease viruses (FMDV); and (iv) rhinoviruses, of which there are about 100 serotypes. The physiological consequences of picornavirus infection are highly variable because of differing tissue tropism, differing viral stability in acid environment, and differing responses by infected host cells. Among the murine cardioviruses (*2*), for example, Mengo virus can produce fatal encephalitis, a strain of EMCV can cause diabetes, and a strain of Theiler's virus can cause chronic demyelinating disease.

Picornavirions have relative molecular mass of about 8.5×10^6 daltons, of which about 30 percent is RNA. The virus particles are spherical with an external diameter of about 300 Å. The coat proteins form a shell with icosahedral symmetry with 60 protomers, each composed of a single copy of VP1, VP2, VP3, and VP4 (Fig. 1) with approximate relative molecular masses of 34,000, 30,000, 25,000, and 7,000 daltons, respectively. For Mengo virus, the proteins consist of 277, 256, 231, and 70 amino acids, respectively. On degrading Mengo virus, the virions separate into 13.4*S* pentamers and then into 6*S* protomers (*3, 4*) consistent with structural observations (*5*). Traditionally, the cardiovirus capsid proteins have been designated α, β, γ, and δ in order of decreasing size; the VP1 (α), VP2 (β), VP3 (γ), VP4 (δ) nomenclature is used in this article in order to facilitate comparison with other picornaviruses. The viral

M. Luo, G. Vriend, G. Kamer, I. Minor, E. Arnold, and M. G. Rossmann, who did the crystallographic analysis, are in the Department of Biological Sciences, Purdue University, West Lafayette, IN 47907. U. Boege and D. G. Scraba, who produced and purified the 60 milligrams of virus used, are in the Department of Biochemistry, University of Alberta, Edmonton, Alberta T6G 2H7, Canada. G. M. Duke and A. C. Palmenberg, who determined the sequence of the viral RNA, are in the Biophysical Laboratory of the Graduate School, University of Wisconsin, Madison, WI 53706.

*Present address: Department of Structural Chemistry, University of Groningen, Nijenborgh 16, 9747 AG Groningen, The Netherlands.

OnCusp
Ex. 1002

was observed. Finally, the conjugated drug caused 90% reduction in the size of the lesion 11 days after the initiation of drug treatment. The greatest effect on the regression of the lesions by the conjugated drug was observed at a dose of 1 mg/kg per footpad. The lack of effect at higher concentrations probably reflects saturation of the receptor-mediated uptake process for Mtx-MBSA. The footpad regressed to nearly normal size when Mtx-MBSA was used. In contrast, administration of free Mtx did not significantly affect the footpad lesion. The lesions did not reappear even 4 weeks after the last injection of Mtx-MBSA. During the experimental period all the animals remained healthy with no apparent weight loss. No antibody against MBSA or Mtx-MBSA was detectable in these animals after 3 weeks as determined by the Ouchterlony immunodiffusion technique.

In conclusion, our results show that effective delivery of drug to macrophages can be achieved by using the "scavenger" receptor-mediated endocytic pathway to achieve selective killing of intracellular parasites residing in macrophages, both in vitro and in vivo. A similar approach may be useful for effective delivery of drugs in the treatment of other diseases in which macrophages are the primary target, including tuberculosis, leprosy, monocytic leukemia, and heavy metal storage diseases.

REFERENCES AND NOTES

1. M. L. Chance, *Br. Med. J.* **283**, 1245 (1981).
2. J. A. Walsh and K. S. Warren, *N. Eng. J. Med.* **301**, 967 (1979).
3. K. P. Chang, *Int. Rev. Cytol* (Suppl.) **14**, 267 (1983).
4. J. D. Berman, in *Leishmaniasis*, K. P. Chang and R. S. Bray Eds. (Elsevier, Amsterdam, 1985), vol. 1, pp. 111–138.
5. J. J. Marr, in *Parasitic Diseases*, J. M. Mansfield, Ed. (Dekker, New York, 1984), vol. 2, pp. 201–227.
6. C. D. V. Black, G. J. Watson, R. J. Ward, *Trans. R. Soc. Trop. Med. Hyg.* **71**, 550 (1977).
7. C. R. Alving, E. A. Steck, W. L. Hanson, P. S. Loizeaux, W. L. Chapman, Jr., *Life Sci.* **22**, 1021 (1978).
8. R. R. C. New, M. L. Chance, S. C. Thomas, W. Peters, *Nature* **272**, 55 (1978).
9. R. R. C. New, M. L. Chance, S. Heath, *J. Antimicrob. Chemother.* **8**, 371 (1981).
10. C. R. Alving and G. M. Swartz, Jr., in *Liposome Technology*, G. Gregoriadis, Ed. (CRC Press, Boca Raton, FL, 1984), vol. 2, pp. 55–68.
11. C. R. Alving *et al.*, *Proc. Natl. Acad Sci. U.S.A.* **75**, 2959 (1978).
12. J. L. Goldstein, Y. K. Ho, S. K. Basu, M. S. Brown, *ibid.* **76**, 333 (1979).
13. M. S. Brown, S. K. Basu, C. R. Falk, Y. K. Ho, J. L. Goldstein, *J. Supramol. Struct.* **13**, 67 (1980).
14. O. Stein and Y. Stein, *Biochim. Biophys. Acta* **620**, 631 (1980).
15. A. N. Glazer, R. S. Delange, D. S. Sigman, Eds., *Chemical Modification of Proteins* (North-Holland, Amsterdam, 1975), pp. 79–81.
16. H. J. P. Ryser and W. C. Shen, *Proc. Natl. Acad. Sci. U.S.A.* **75**, 3867 (1978).
17. A. Mukhopadhyay, G. Chaudhuri, S. K. Basu, unpublished data. In some receptor systems chloroquine, especially at relatively high concentrations, inhibits uptake of the ligand. In our case, however, chloroquine primarily affected degradation of ^{125}I-labeled Mtx-MBSA as shown from the following observation. Hamster peritoneal macrophages were incubated at 37°C in medium containing ^{125}I-labeled Mtx-MBSA (10 μg per milliliter of protein). The cellular content of radioactivity and that released into medium (acid-soluble) were measured as a function of time in the presence and absence of chloroquine (3 μ*M*). Cellular content of radioactivity continued to increase in chloroquine-treated cultures but release of acid-soluble radioactivity in the medium was arrested. These results suggested that at this concentration chloroquine inhibited the degradation of Mtx-MBSA and not its uptake.
18. M. Rabinowitch, V. Zilberfarb, C. Ramazeilles, *J. Exp. Med.* **163**, 520 (1986).
19. S. Sehgal and S. K. Arora, *Ind. J. Med. Res.* **82**, 202 (1985).
20. B. Phillips and J. C. Gazer, *Nature* **220**, 1140 (1968).
21. J. D. Berman and D. J. Wyler, *J. Infect. Dis.* **142**, 83 (1980).
22. We thank V. K. Kalra and G. C. Mishra for critically reviewing the manuscript, and the Council of Scientific and Industrial Research and Indian Council of Medical Research for award of fellowships to A.M. and G.C.

13 September 1988; accepted 20 February 1989

Studies of the HER-2/*neu* Proto-oncogene in Human Breast and Ovarian Cancer

DENNIS J. SLAMON,* WILLIAM GODOLPHIN, LOVELL A. JONES, JOHN A. HOLT, STEVEN G. WONG, DUANE E. KEITH, WENDY J. LEVIN, SUSAN G. STUART, JUDY UDOVE, AXEL ULLRICH, MICHAEL F. PRESS

Carcinoma of the breast and ovary account for one-third of all cancers occurring in women and together are responsible for approximately one-quarter of cancer-related deaths in females. The HER-2/*neu* proto-oncogene is amplified in 25 to 30 percent of human primary breast cancers and this alteration is associated with disease behavior. In this report, several similarities were found in the biology of HER-2/*neu* in breast and ovarian cancer, including a similar incidence of amplification, a direct correlation between amplification and over-expression, evidence of tumors in which overexpression occurs without amplification, and the association between gene alteration and clinical outcome. A comprehensive study of the gene and its products (RNA and protein) was simultaneously performed on a large number of both tumor types. This analysis identified several potential shortcomings of the various methods used to evaluate HER-2/*neu* in these diseases (Southern, Northern, and Western blots, and immunohistochemistry) and provided information regarding considerations that should be addressed when studying a gene or gene product in human tissue. The data presented further support the concept that the HER-2/*neu* gene may be involved in the pathogenesis of some human cancers.

PROTO-ONCOGENES REPRESENT A family of normal cellular genes that were identified on the basis of their similarity to genetic sequences with known tumorigenic or transforming potential (*1*). Considerable circumstantial evidence now exists that alterations in either the structure, copy number, or expression of one or another of these genes may play a role in the pathogenesis of some human malignancies (*2*). One such gene, called HER-2/*neu* or c-*erb* B2, was first identified by transfection studies in which NIH 3T3 cells were transformed with DNA from chemically induced rat neuroglioblastomas (*3*). The gene encodes a protein that has extracellular, transmembrane, and intracellular domains (*4*) which is consistent with the structure of a growth factor reception.

Recently, we found a 28% incidence of amplification of HER-2/*neu* in 189 primary human breast cancers (*5*). Patients with multiple copies of the gene in DNA from their tumors had a shorter time to relapse as well as a shorter overall survival indicating that gene amplification was prognostic for disease behavior in these individuals. Moreover, multivariate survival analysis showed HER-2/*neu* amplification to be more predictive for clinical outcome than all other known prognosticators with the exception of positive lymph nodes (*5*). Since that initial report, a number of studies have been published on the amplification of this gene

D. Slamon, S. G. Wong, D. E. Keith, W. J. Levin, Division of Hematology-Oncology, Department of Medicine, and the Jonsson Comprehensive Cancer Center, U.C.L.A. School of Medicine, Los Angeles, CA 90024.
W. Godolphin, Department of Clinical Chemistry, Vancouver General Hospital, Vancouver, Canada V5Z1M9.
L. A. Jones, Department of Gynecology, M. D. Anderson Hospital, Houston, TX 77030.
J. A. Holt, Department of Obstetrics and Gynecology, University of Chicago Medical Center, Chicago, IL 60637.
S. G. Stuart, Triton Biosciences, Inc., Alameda, CA 94501.
J. Udove and M. F. Press, Department of Pathology, University of Southern California, School of Medicine, Los Angeles, CA 90033.
A. Ullrich, Department of Molecular Biology, Genentech, Inc., South San Francisco, CA 94080.

*To whom correspondence should be addressed.

in human breast cancer and the association of gene amplification with clinical behavior (*6–8*). There is considerable variability in both the reported incidence of amplification and the correlation of gene amplification with patient outcome (*5–10*). Some groups have found amplification rates as low as 10% and no correlation to outcome data while others have found rates as high as 33% and a strong association with outcome (*7, 10*). Given the variable natural history and heterogeneity of human breast cancer, all studies published to date suffer from a similar problem, which is small numbers of evaluated cases (*5–10*). Perhaps a more significant shortcoming of most prior studies of oncogenes in human tumors including our own is that only one aspect of the gene in question (DNA, RNA, or protein status) is evaluated (*5, 11, 12*). The potential errors introduced by dilution of tumor cell macromolecules with macromolecules from surrounding normal vascular, stromal, or inflammatory cells is a general problem in human tumor tissue and a particular problem in breast cancer where these non-malignant cells can account for more than 50% of the tissue. All solid matrix–blotting techniques (Southern, Western, or Northern) are susceptible to these errors. Similarly, these techniques cannot determine whether an observed alteration is specific for only the malignant cells in the tissue.

Studies of the rat *neu* gene isolated from the chemically induced neuroglioblastomas revealed it to contain a single mutation in the transmembrane domain that differentiated it from the nontransforming *neu* gene found in normal rat tissues. This mutation is critical in the conversion of the normal gene into a transforming gene (*13*). To address

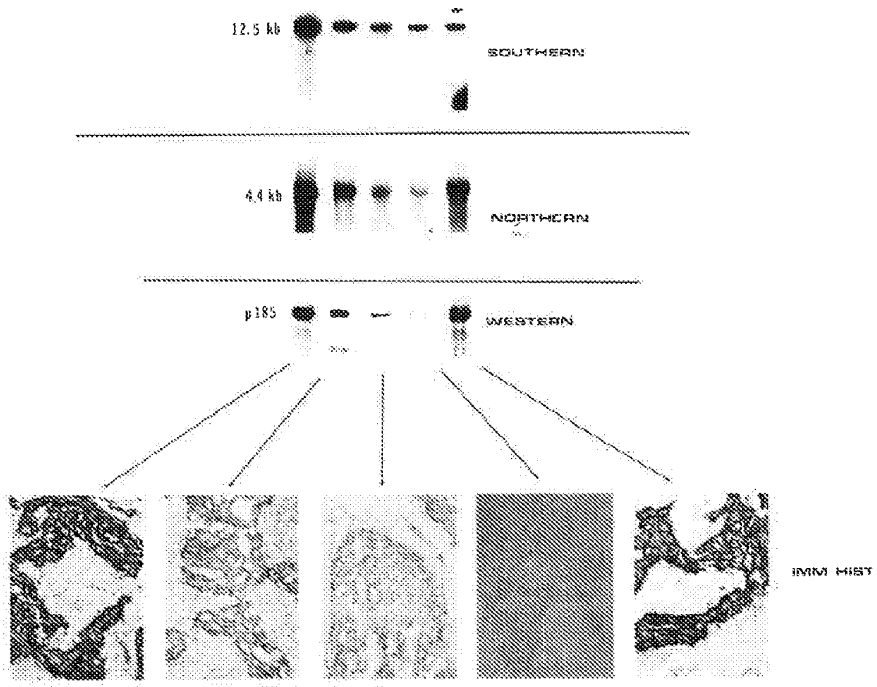


Fig. 1. Examples of the correlation between HER-2/*neu* gene amplification and expression. Southern blot analyses show the 12.5-kb HER-2/*neu* band seen with Eco RI cut DNA. All DNA samples were checked for integrity of high molecular weight species and samples showing evidence of DNA degradation were not evaluated (*9*). Southern blots and HER-2/*neu* copy number determinations were as described (*5, 9*). Hybridizations were done with a 1.4-kb, 3′ Eco RI fragment of the human HER-2/*neu* cDNA clone. Northern blot analyses show the 4.5-kb HER-2/*neu* transcript. All RNA samples were checked for integrity of the 28*S* and 18*S* ribosomal RNA species. Total RNA (20 μg) from samples with intact RNA were run on an agarose gel, transferred to a nylon filter, and hybridized with a ^{32}P-labeled HER-2/*neu* probe as described (*11*). Samples with intact DNA but showing some degradation of the RNA were evaluated by slot-blot analysis by loading 12 μg of total RNA on the filter and hybridizing as above. Samples showing degradation of both DNA and RNA were not used for RNA analysis. The relative optical density (O.D.) of bands was determined by soft laser densitometry scanning and ranged from a low of 0.1 O.D. units to a high of 3.8 O.D. units. Tumors were grouped into RNA expression categories as follows: 0.1 to 0.5 O.D. units, 1+; >0.5 to 1.0 O.D. units, 2+; >1.0 to 1.5 O.D. units, 3+; and >1.5 O.D. units, 4+. Western blot analyses show the 185-kD HER-2/*neu* protein band. The relative O.D. of bands ranged from a low of 0.1 O.D. units to a high 4.5 O.D. units. Tumors were grouped into protein expression categories as follows: 0.1 to 0.5 O.D. units, 1+; >0.5 to 1.0 O.D. units, 2+; >1.0 to 1.5 O.D. units, 3+; >1.5 O.D. units, 4+. Immunohistochemical analysis was done as described (*20*) with the anti-HER-2/*neu* specific antibody and frozen sections (*14*). Tissues were scored and placed in one of the four staining categories shown on the basis of the relative level of specific staining as judged by microscopic examination as follows: negative to weak, 1+, 2+, 3+. The five samples analyzed here are arranged in identical order from left to right in each panel. The HER-2/*neu* copy numbers (from left to right) were >20, 5 to 20, 2 to 5, 1, and 1, respectively. The corresponding O.D. readings from the Northern blots were 4.3, 1.4, 0.9, 0.2, and 2.8, respectively. The corresponding O.D. readings from the Western blots were 2.0, 1.1, 0.6, 0.12, and 2.1, respectively. The corresponding immunohistochemistry readings were 3+, 2+, 1+, weak, and 3+, respectively.

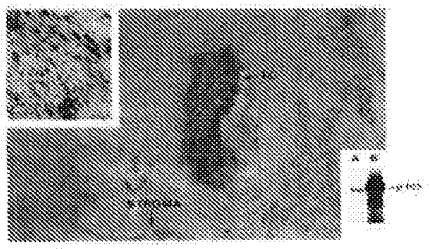


Fig. 2. Comparison of immunoperoxidase staining with Western blot on stroma-rich breast cancer. The inset (upper left) is a hematoxylin-eosin stain of a breast tumor rich in stromal tissue. Note the absence of significant numbers of tumor cells. Large middle panel is the immunoperoxidase staining of tumor cells (TC) found in this tissue. The staining is 3+, placing this tumor in the highest category of HER-2/*neu* expression as judged by immunostaining. Southern analysis revealed two to five copies of the gene in the DNA and Northern blot analysis gave an O.D. reading of 0.6 (2+). Western blot of protein from this sample is shown in lane A of the lower right inset. The O.D. reading for this sample was 0.18 (1+), while the Western blot of protein from another specimen with amplified HER-2/*neu* and greater numbers of tumor cells is shown in lane B. The O.D. reading for this tumor (lane B) was 3.2 (4+). Eight of the 11 tumors found to have inappropriately low Western blot data in comparison to other data were similar in that they were stromal-rich tumors.

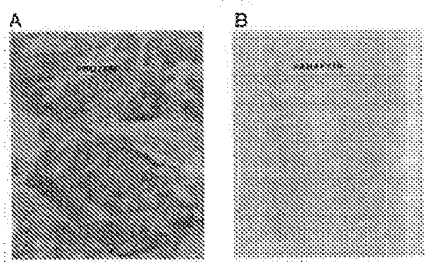


Fig. 3. Comparison of immunohistochemical staining of HER-2/*neu* protein in the same breast cancer specimen evaluated with frozen tissue and formalin-fixed, paraffin-embedded tissue. Tissue shown in panels A and B are from the same tumor which was found to have 5 to 20 copies of the gene and a 2+ expression level by Northern and Western blot analyses. Panel A is the frozen section and shows 2+ immunostaining. Panel B is the formalin-fixed, paraffin-embedded section of the same tumor and shows negative immunostaining.

OnCusp
Ex. 1002

the question of whether or not a similar change had occurred in an amplified HER-2/*neu* gene found in human breast cancer, cDNA clones from tumor tissue rather than cell lines were generated by means of the Okayama-Berg vector (*14, 15*). Tissue was used to circumvent acquired genetic changes which can occur in vitro. Analysis of the transmembrane domain of eight clones from two separate tumors showed the identical sequence. There was no glutamic acid for valine substitution as reported in the transforming *neu* gene from the chemically induced rat tumors (*13*). There was, however, a neutral change of isoleucine for valine at position 655 in the transmembrane domain, which is similar to the sequence found in breast cancer cell lines (*16*). Analysis of the entire coding sequence of full-length clone and comparison with the published placental sequence (*3*) showed no other significant changes (*14*). These data are consistent with the concept that overexpression of a normal HER-2/*neu* gene product rather than mutation to an abnormal gene may be an important pathogenic event for some tumors.

Having obtained and sequenced a full-length cDNA clone from a human breast tumor, we next wanted to generate antisera to the human gene product. The generation and characterization of this antiserum is described elsewhere (*14*) and the antibody is capable of identifying the gene product both by Western blot analysis of tissue homogenates and immunohistochemically in tissue sections.

In the current study, we collected a total of 668 human breast cancer specimens. Of these, 526 had sufficient clinical follow-up to allow for evaluation of an association between gene amplification and disease outcome. As in our initial study (*5*), we performed Southern analysis on samples without knowledge of the clinical outcome. All DNA blots were stripped and reprobed with both p53 and myeloperoxidase probes to evaluate the relative loading of DNA in each lane and to exclude the possibility that "amplification" was caused by partial or complete duplication of chromosome 17 (*9*). Blots were scanned by soft laser densitometry and the level of HER-2/*neu* amplification was determined by the ratio of the HER-2/*neu* signal relative to the single-copy p53 signal.

We evaluated 345 patients with node-positive disease in a blinded fashion (Table 1). Of these, 101 (27%) had evidence of HER-2/*neu* amplification. Univariate survival analysis showed amplification of the HER-2/*neu* gene to be a significant predictor of both disease-free survival and overall survival for these patients (Table 1). Tumor size was slightly better than HER-2/*neu* amplification in the univariate analysis but lost its significance on multivariate analysis, which indicates that it was not independent of nodal status (Table 1). Multivariate analysis showed HER-2/*neu* amplification to be an independent predictor of both disease relapse and overall survival ($P = 0.006$ and $P = 0.045$, respectively) and superior to all other known prognostic factors with the exception of a number of positive lymph nodes for this group of patients (Table 1). We also evaluated DNA from tumors of 181 node-negative patients with a median follow-up of 59 months (62 months for those still alive). Of these, 45 (25%) had amplification of the HER-2/*neu* gene. Univariate and multivariate analysis did not show an association between gene amplification and disease outcome in this group of patients.

Table 1. Univariate and multivariate survival analyses comparing disease-free (relapse) and overall survival to prognostic factors in 345 node-positive breast cancer patients. Statistical analyses were performed by the χ^2 test and by Cox's partially nonparametric regression analysis to evaluate the predictive power of various combinations and interactions of prognostic factors in a multivariate manner as described (*5*). Prognostic parameters evaluated include number of nodes (Nodes), HER-2/*neu* gene amplification (HER-2/*neu*), estrogen receptor (ER), progesterone receptor (PGR), size of primary tumor (Size), and age of patient at diagnosis (Age). The median follow up was 57 months (60 months for those still alive).

	Disease free survival		Overall survival	
	Univariate (P)	Multivariate (P)*	Univariate (P)	Multivariate (P)*
Nodes	<0.0001	<0.0001 [0.0818 ± 0.0214]	<0.0001	<0.0001 [0.0912 ± 0.0346]
HER-2/*neu*	0.01	0.006 [0.1142 ± 0.0413]	0.041	0.045 [0.0864 ± 0.0288]
ER	0.235	0.60	0.091	0.157
PGR	0.045	0.07	0.20	0.24
Size	0.003	0.15	0.006	0.16
Age	0.92	0.96	0.20	0.11

*Regression coefficients ± SE are shown in square brackets.

There were 187 tumor samples of sufficient size and integrity to allow for multiple studies in the same specimen. This group of specimens was representative of the overall group in that lesions from both node-negative as well as node-positive patients were included as well as tumors of varying sizes (<1 cm to >2.5 cm). The availability of a cDNA clone for HER-2/*neu* from a human tumor as well as antisera that could identify the protein in both Western blots and tissue sections allowed for a comprehensive evaluation of the gene and its products (RNA and protein) in these tissues. Such a study addresses several critical issues regarding HER-2/*neu* in human breast cancer. First, the correlation between a given level of amplification and relative expression for both RNA and protein is important. Some genes that are amplified in breast cancer, such as *erb* A (*6*), are not expressed; these genes may serve as useful markers but are unlikely to be involved in the pathogenesis of the disease. Second, it should be possible to address the issue of whether amplification and over-expression of HER-2/*neu* is specific to tumor cells in these specimens. When blotting techniques alone are used, there is the risk of dilutional effects, which make it impossible to distinguish signals from tumor cells versus those from normal cells. Third, this approach should give some indication of the relative strengths and weaknesses of the various techniques used in assessing the status of the HER-2/*neu* gene and its products in the same primary human tissue. Studies at both the RNA and protein levels are important since there are examples of human tumors in which transcripts of a particular gene are present but no protein can be detected (*17*). Fourth, if gene expression correlates closely with amplification, a separate assessment of the incidence of amplification can be made.

The samples used for the comprehensive analysis were between 0.5 and 1 g in size and had been stored for various periods of time at −70° to −140°C. Tumor tissue was fractured in liquid nitrogen to obtain a representative piece suitable for cryostatic sectioning and immunohistochemical analysis. The remainder of the entire specimen was ground to powder in liquid nitrogen with a mortar and pestle. This process allowed for an even distribution of tumor cells in all subsequent analyses. A portion of the tissue powder (50 mg) was stored for Western blot analysis and the remainder was extracted for DNA and RNA simultaneously. As in our clinical correlation studies, each procedure was conducted separately and without knowledge of the results obtained by other modalities of evaluation. Southern blots with appropriate p53 and myeloperoxidase controls were performed and HER-2/*neu* copy number determined as described (Fig. 1). Northern blots were performed on 20 μg of total RNA extracted from the sample and were analyzed for the presence and relative intensity of the 4.5-kb HER-2/*neu* messenger RNA using soft laser densi-

tometry and grouped into one of four RNA expression categories depending on the densitometry results (Fig. 1). Western blots were performed on 100 μg of total protein extracted from each sample and were analyzed for the presence and relative intensity of the 185-kD HER-2/*neu* gene product by soft laser densitometry and grouped into one of four protein expression categories (Fig. 1). Immunohistochemical analysis was performed by an immunoperoxidase staining technique on frozen sections of the tumor tissue. The immunohistochemical specificity of the antibody was previously shown (*14*).

After completion of testing of all samples by each modality, the study was unblinded and a direct correlation analysis between gene amplification and expression was performed. Of the 187 samples evaluated in this manner there was almost complete concordance of the data, with a few notable exceptions. Fifty-one samples (27%) of the cases were called amplified by the Southern blot analyses, and in every instance the amplified samples were shown to over-express the HER-2/*neu* gene product relative to nonamplified cases. In 46 of the amplification-positive samples (90%) there was complete concordance of all tests, that is, amplification correlated with overexpression as determined by Northern, Western and immunohistochemistry. In all 51 cases with amplification, two of the three measures of expression were concordant in showing overexpression.

The Western blot analysis was most discordant, being inconsistent with data obtained by Southern blot, Northern blot, and immunohistochemistry in 11 of the 187 cases (6%). A possible explanation for this phenomenon is that samples showing a weak signal by Western blot may do so because of a relatively large amount of stroma in the tissue. In 8 of the 11 cases in which the Western was discordant, histologic examination confirmed the presence of excessive stromal elements (Fig. 2). DNA and RNA analyses were less sensitive to this problem since there was evidence of amplification and increased transcript levels in these tumors. The increased susceptibility of the Western blot to dilutional effects is likely due to the fact that large amounts of noncellular connective tissue can substantially contribute to the total protein in a sample by adding significant amounts of extracellular matrix proteins such as collagen to the lysate. The stroma, however, is relatively poor in cellularity and will make only minimal contributions to the total DNA or RNA extracted from the same specimen.

The Northern blot analysis was discordant in only four cases (2%) judged amplified at the DNA level, and the immunohistochemical data were inconsistent in only two cases (1%). In each of these cases, the other two modalities used showed overexpression. The correlation between amplification and overexpression ($P < 0.0001$) shown in the comprehensive analysis confirms previously published amplification rates of 25 to 30% for HER-2/*neu* in human breast cancer. There were 18 cases (10%) which were judged as single copy by DNA analysis but which showed clear over-expression at the RNA and protein levels (Fig. 1, lane 5). These cases may represent examples of alterations that occur in control mechanisms for gene expression, rather than increases in gene copy number. Alternatively, these cases may represent instances of true gene amplification at low levels (two- to fivefold) which are missed because of dilution of the tumor cell DNA with DNA from nonmalignant tissue.

Some studies have used only immunostaining of formalin-fixed, paraffin-embedded tissue to assess the status of the HER-2/*neu* product (*8, 10, 18*). This approach presents some problems, since fixation and embedding of tissue frequently decreases or totally destroys reactivity for many antigens (*19*). Furthermore, the degree of loss can vary considerably depending on the duration of fixation with the same fixative (*19, 20*). For 42 of the 187 cases in the comprehensive analysis, formalin-fixed, paraffin-embedded tissue was available. This allowed for a comparison of immunohistochemical staining of the HER-2/*neu* protein in the same specimen prepared in different ways. Evaluation of HER-2/*neu* immuno-reactivity showed that in virtually every case there was some decrease in immunohistochemical staining with the rabbit polyclonal antiserum when comparing fixed to frozen tissue. In tumors expressing very high levels (3+ to 4+), the protein was visible by immunostaining in tissue prepared by either method. The problem was more significant in samples expressing moderate levels of protein (2+) since many completely lost their immunohistochemical reactivity when fixed in formalin and embedded in paraffin (Fig. 3). The majority of these tumors were amplified for the HER-2/*neu* gene at levels of two- to fivefold. However, occasional tumors with 5- to 20-fold amplification that expressed moderate to high levels of protein appeared negative in fixed tissue.

To determine if the same or similar alterations in the HER-2/*neu* gene found in breast cancer occurred in other human malignancies, we screened DNA from 60 non–small cell lung cancers, 40 colon carcinomas, 35 neuroblastomas, and 18 ovarian cancers. There was no significant incidence of HER-2/*neu* gene amplification or rearrangement in any of these groups except for ovarian cancer, where gene amplification was found in 6 of the 18 tumors analyzed. There are several similarities between carcinomas of the ovary and breast. Like breast cancer, the vast majority (>90%) of ovarian malignancies are of epithelial rather than stromal origin (*21*). Also, like breast cancer, steroid hormone receptors are found in the tumor cells of many ovarian malignancies (*22*). Finally, epidemiologic studies suggest that some carcinomas of the breast and ovary may share common etiologic factors since women with breast cancer have twice the expected incidence of ovarian cancer and women with ovarian cancer have a three- to fourfold increased risk of developing carcinoma of the breast (*21*). These similarities and the findings of HER-2/*neu* amplification in the initial cases examined prompted us to evaluate a larger number of ovarian cancers for incidence of gene amplification,

Table 2. Median survival time of patients with ovarian cancer as well as various degrees of HER-2/*neu* gene amplification and expression. All samples were analyzed by both the Kaplan-Meier method and the Cox proportional hazards regression model to provide an assessment of the association of the various assays with survival. The median follow-up was 75 months for those patients still alive. Subgroup categories were as described (Fig. 1).

Assay	Subgroup	Number of cases	Median survival time (days)	Log rank test (P)	Cox proportional hazards regression model (P)*
DNA	1 copy	64	1879		
	2 to 5	17	959	<0.0001	<0.0001 [0.1479 ± 0.0320]
	>5	6	243		
RNA	1+	44	1960		
	2+	16	919	0.0710	0.0244 [0.4537 ± 0.1969]
	3+ to 4+	7	531		
Protein	1+	27	1960	0.1866	0.0628 [0.5437 ± 0.2944]
	2+ to 4+	10	959		
Histochem.	Neg. to 1+	36	1960		
	2+	32	1093	0.0126	<0.0001 [0.4276 ± 0.1163]
	>2+	4	417		

*Regression coefficients ± SE are shown in square brackets.

correlation between amplification and over-expression; and an association between amplification/over-expression and clinical behavior of the malignancy.

DNA from 120 primary ovarian malignancies of epithelial origin were evaluated by Southern blot analysis using the same criteria and techniques described for the breast cancer cohort. Identical controls (rehybridization of blots with p53 and myeloperoxidase probes) were performed. Thirty-one (26%) of the cases showed evidence of HER-2/*neu* amplification (23 were amplified two- to fivefold and 8 were amplified >fivefold). Intact RNA was available for 72 of the 120 cases and, as with breast cancer cases, they were grouped into one of four expression categories. Sufficient material was available to prepare tissue powder for 37 of the 120 cases. Western blot analysis of these samples with the anti-HER-2/*neu* antibody revealed the p185 HER-2/*neu* protein, which was quantitated by densitometry as described (see legend to Fig. 1). A fragment of frozen (nonfixed) tumor was available for 75 of the 120 cases and immunohistochemical analysis was performed with the HER-2/*neu* antibody. Samples were again grouped into various expression categories based on microscopic evaluation of the tumor cells in the tissue sections. Unlike the breast study, there were only 37 cases from which sufficient material was available to perform a comprehensive analysis (DNA, RNA, protein, and immunohistochemistry) on the same samples. However, the data regarding the correlation between amplification and expression from this smaller number of ovarian cases were identical to those found in the larger breast cancer cohort. There was a complete correlation between gene amplification and over-expression ($P < 0.0001$). Every ovarian cancer judged amplified without knowledge of the expression data had evidence of over-expression. In 50 of the 120 cases sufficient material was available for analysis of expression by at least two techniques, Northern blot analysis and immunohistochemistry. Again, there was a perfect correlation between amplification and overexpression, that is, HER-2/*neu* amplification resulted in high levels of expression of the membrane protein (see cover photo of this issue). In addition, there were six cases (12%) in which the gene copy number was determined to be single but which had evidence of over-expression. This is similar to the incidence of single-copy over-expression found in the breast cancer specimens.

Ovarian cancer, unlike breast cancer, has no good prognostic factors for predicting biologic behavior of the tumor or eventual clinical outcome in patients afflicted with the disease. Clinical stage (extent of disease) has some predictive value but the vast majority of ovarian cancer patients (>70%) have regional or distant spread of disease at initial diagnosis which makes this factor less useful for most patients. The only parameter that has been used with some success has been histologic grading, the determination of the degree of cellular differentiation within the tumor (*21, 23*). As with other malignancies, however, histologic grading of ovarian cancer suffers from a lack of standardization and considerable observer-related variability (*21*).

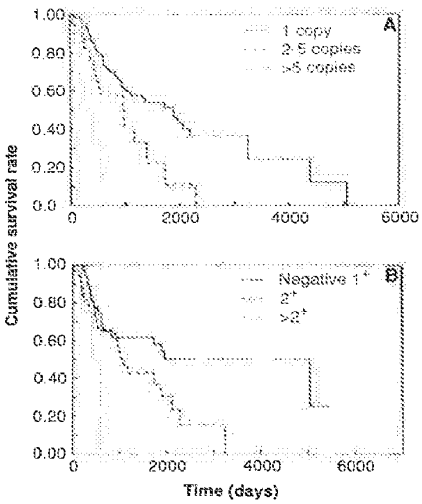


Fig. 4. Actuarial survival curves for patients with ovarian cancer evaluating (**A**) the association of HER-2/*neu* gene amplification with survival and (**B**) the association of HER-2/*neu* expression as determined by histochemical analyses and survival. The *P* values for these two curves are <0.0001 and 0.0126, respectively. The Kaplan-Meier method was used to estimate the survival distribution for each subgroup. Patients were grouped on the basis of the assay values, that is, gene copy number (1, 2–5, or >5) or level of expression as determined by immunohistochemical staining (negative to 1+, 2+, or >2+). The log rank test was used to evaluate the equality of the survival curves.

In our study, long-term follow-up (median 75.4 months) was available for 87 of the 120 ovarian malignancies. Again the molecular and cellular analyses were performed without knowledge of clinical information. For the 87 cases in which both DNA data and long-term follow-up were available, there was a statistically significant ($P < 0.0001$) correlation between gene amplification and survival with median survivals of 1879, 959, and 243 days for patients having one copy, two to five copies, and more than five copies of the gene, respectively (Table 2 and Fig. 4). In addition, in the 72 cases for which follow-up data and expression analysis based on immunohistochemistry were available, a significant ($P < 0.0126$) association between HER-2/*neu* expression and survival was found (Table 2 and Fig. 4). There were a smaller number of cases (67 total) for which both intact RNA and follow-up were available and even fewer (37 total) for which both Western blot data and follow-up were available. Median survival time of these cases showed the negative relationship between survival and increased expression (Table 2) but the data did not reach statistical significance for Western analysis (most likely due to the small number of samples in the group).

Several conclusions regarding HER-2/*neu* in human breast and ovarian cancer can be drawn from these data. For breast cancer, we confirmed our earlier conclusions that amplification of the gene is a predictor of both relapse and survival in node-positive patients and is superior to all other prognosticators with the exception of positive lymph nodes (*5*). The data, however, do not address the possible influence of therapy in this group. To do this would require a study of an even larger series of patients given the various methods of treatment used for the disease. In 181 node-negative patients, there was no evidence of an association between gene amplification and outcome. This may be due to some fundamental difference in the basic biology of node-negative disease or alternatively may represent a statistical artifact introduced by the relatively small number of patients studied. The overall incidence of disease recurrence in node-negative patients is only 15 to 25% and, as a result, there may not be a sufficient number of events, that is, relapse or death in our cohort, to reveal an association. Recent data from another study indicate that over-expression of HER-2/*neu* is predictive of a poor clinical outcome in node-negative breast cancer (*10*).

Similarities in the biology of the HER-2/*neu* gene in human breast and ovarian cancer are considerable and include the fact that amplification of the gene occurred in 25 to 30% of both malignancies, amplification was uniformly associated with over-expression in both tumor types, approximately 10% of both breast and ovarian cancers had evidence of a single gene copy with over-expression of the gene product, and (in both malignancies) there was an association between amplification and clinical outcome. Few of the 187 breast cancer cases studied in the comprehensive analysis had significant follow-up and an even smaller number showed amplification/over-expression, making it impossible to perform the necessary statistical analyses to evaluate the association of gene expression with outcome. However, the correlation between amplification and

over-expression ($P < 0.0001$) would strongly suggest that measurement of HER-2/*neu* expression should also be predictive of disease survival in breast cancer. This notion is completely supported by the results of the ovarian cancer cohort, where long-term follow-up data were available for almost all cases studied and both amplification and overexpression were associated with decreased survival.

For studies assessing any gene product in human tumor tissue, it is critical to evaluate the specificity of the reagents used, the condition of the molecule under study, and the ability of the assay method to detect the alteration in question with certainty. Studies using only one of the solid matrix modalities are prone to errors introduced by both technique and nature. Technical problems are likely to occur as a result of the considerable variability in handling the tissue specimens post-operatively since this can result in degradation of macromolecules. The condition of the DNA and RNA in a given sample must be evaluated by some method such as gel electrophoresis and ethidium bromide staining prior to subsequent analysis. Assessment of the integrity of the DNA is crucial if Southern blot analysis is to be used, since as previously shown, even small amounts of DNA degradation can result in significant decreases in signal intensity on a Southern blot (*9*). All solid matrix blotting techniques are subject to errors introduced by the variability in content of tumor cells in a specimen. Merely assessing a sample for the presence or absence of malignant cells is insufficient, as it is the relative number of these cells which is important.

Immunohistochemical analysis of HER-2/*neu* in frozen tissue sections correlated best with all other analytic data for both breast and ovarian cancer. There are several advantages to this technique. Most importantly, it assesses the status of the protein in tumor cells specifically, and is not subject to dilutional effects introduced by surrounding nonmalignant cells and stromal proteins. In addition, with the advent of earlier diagnosis for breast cancer, tissue specimens are becoming smaller. Even the most sensitive techniques for solid matrix blots currently require milligram quantities (5 to 50 mg) of tumor to assess DNA, RNA, or protein. The small primary samples available (fine needle biopsies of lesions or cytologic specimens) that are used in breast cancer diagnostics (*24*) make such analyses virtually impossible. The issue of specimen size is of lesser concern for ovarian cancer since most of these lesions are diagnosed late in their course and, as a result, large amounts of tumor tissue are available at surgery. In either tumor type, histochemical evaluation offers the advantage that only a microscopic section of the tumor sample is required to assess HER-2/*neu* expression.

There are, however, at least two disadvantages of the immunohistochemical approach. One is the problem of loss of antigenic immunoreactivity during fixation which occurs for almost all proteins. This phenomenon is particularly significant in tumors expressing moderate levels of the gene product. Data generated from archival material should be interpreted with this caveat in mind, since it could significantly reduce both the incidence and intensity of immunostaining and may be responsible for some of the variability in reported percentages of HER-2/*neu* expression in tumors and correlation with outcome (*5, 7, 18*). This problem can be overcome by using frozen tissue samples. The second disadvantage is the difficulty in quantitating expression levels precisely. Recent advances in digital image processing of tissue sections stained for specific cellular proteins has circumvented this problem. Proteins that are frequently evaluated in breast cancer, such as the estrogen receptor, can be carefully and critically quantitated with these techniques (*25*).

It is projected that in 1989 a total of 162,000 new cases of breast and ovarian cancer will occur (*26*). This constitutes one-third of all cancers in women. In addition, these two malignancies will account for 55,000 deaths or approximately one-quarter of cancer-related deaths in women. The fact that the HER-2/*neu* gene is altered in 25 to 30% of these cases and that the alteration is associated with poor patient outcome indicates that HER-2/*neu* may play a role in the pathogenesis of a significant number of human tumors. This does not preclude the possibility that other genes or genetic elements may be of importance in these diseases; however, there is already strong supporting evidence from experimental in vitro and in vivo systems that alterations in the HER-2/*neu* gene are important in transformation and tumorigenesis. Subsequent to our initial studies in human breast malignancies, studies were published reporting that over-expression of the normal, nonmutated, HER-2/*neu* gene could induce transformation in NIH 3T3 cells (*16, 27*). In one study, over-expression was achieved by amplification of the normal gene to levels similar to those seen in human breast and ovarian cancers, and cells transformed in this way were tumorigenic in nude mice (*27*). Most recently, the mutated rat *neu* gene placed in transgenic mice resulted in development of adenocarcinomas of the breast in 100% of female and male animals expressing the transgene (*28*). Moreover, the tumors arose synchronously, were polyclonal in origin and the malignant process involved the entire epithelium of each gland. No normal mammary tissue was present in these animals. These data indicated that the altered *neu* gene was capable of inducing malignant transformation in breast epithelium of the mouse in a single-step fashion. We would concur with Muller *et al.* (*28*) that this oncogene should be a focus of attention for diagnosis and therapy in human breast cancer; our current findings would extend this idea to ovarian cancer.

REFERENCES AND NOTES

1. J. M. Bishop, *Annu. Rev. Biochem.* **52**, 301 (1983); H. E. Varmus, *Annu. Rev. Genet.* **18**, 553 (1984).
2. D. J. Slamon, *N. Engl. J. Med.* **317**, 955 (1987).
3. C. Shih *et al.*, *Nature* **290**, 261 (1981).
4. A. L. Schechter *et al.*, *ibid.* **312**, 513 (1984); L. Coussens *et al.*, *Science* **230**, 1132 (1985).
5. D. J. Slamon *et al.*, *Science* **235**, 177 (1987).
6. M. van de Vijver *et al.*, *Mol. Cell. Biol.* **7**, 2019 (1987).
7. M. S. Berger *et al.*, *Cancer Res.* **48**, 1238 (1988); D. J. Venter *et al.*, *Lancet* **ii**, 69 (1987); J. M. Varley *et al.*, *Oncogene* **1**, 423 (1987); I. U. Ali, G. Campbell, R. Lidereau, R. Callahan, *Science* **240**, 1795 (1988); D. Zhou *et al.*, *Cancer Res.* **47**, 6123 (1987); D. Zhou *et al.*, *Oncogene* **4**, 105 (1989); M. J. van de Vijver *et al.*, *Eur. J. Surg. Oncol.* **14**, 111 (1988).
8. M. J. van de Vijver *et al.*, *N. Engl. J. Med.* **319**, 1239 (1988).
9. D. J. Slamon and G. M. Clark, *Science* **240**, 1796 (1988).
10. C. Wright *et al.*, *Cancer Res.* **49**, 2087 (1989).
11. D. J. Slamon *et al.*, *Science* **224**, 256 (1984).
12. T. Tanaka *et al.*, *Cancer Res.* **46**, 1465 (1986).
13. C. I. Bargmann, M. C. Hung, R. A. Weinberg, *Cell* **45**, 649 (1986); C. I. Bargmann and R. A. Weinberg, *EMBO J.* **7**, 2043 (1988).
14. D. J. Slamon *et al.*, *Cancer Cells* **7**, 371 (1989).
15. D. J. Slamon *et al.*, *Science* **232**, 768 (1986); D. J. Slamon *et al.*, *ibid.* **233**, 347 (1986).
16. P. P. DiFiore *et al.*, *ibid.* **237**, 178 (1987).
17. J. Yokota *et al.*, *Oncogene* **3**, 471 (1988).
18. B. A. Gusterson *et al.*, *Mol. Cell. Probes.* **2**, 383 (1988); D. M. Barnes *et al.*, *Brit. J. Cancer* **58**, 448 (1988); B. A. Gusterson *et al.*, *ibid.*, p. 453.
19. H. Battifora and M. Kopinski, *J. Histochem. Cytochem.* **34**, 1095 (1986); H. Battifora, *Am. J. Surg. Pathol.* **12**, 24 (1988); L. A. Sternberger, in *Immunocytochemistry* (Wiley, New York, 1986), pp. 211–218; M. F. Press and G. L. Greene, *Lab Invest.* **50**, 480 (1984).
20. M. F. Press and G. L. Greene, *Endocrinology* **122**, 1165 (1988).
21. R. C. Young *et al.*, in *Cancer: Principles and Practices of Oncology*, V. T. DeVita, S. Hellman, S. A. Rosenberg, Eds. (Lippincott, Philadelphia, PA, 1985), pp. 1083–1117.
22. J. A. Holt *et al.*, *Obstet. Gynecol.* **53**, 50 (1979); M. F. Press, J. A. Holt, A. L. Herbst, G. L. Greene, *Lab. Invest.* **53**, 349 (1985).
23. T. C. Day, H. S. Gallager, F. Rutledge, *Natl. Cancer Inst. Monogr.* **42**, 15 (1975).
24. J. A. Linsk and S. Franzen, in *Clinical Aspiration Cytology* (Lippincott, Philadelphia, 1983), pp. 105–135; L. G. Koss, in *Diagnostic Cytology and its Histopathologic Bases* (Lippincott, Philadelphia, 1979), pp. 991–995.
25. S. Bacus *et al.*, *Am. J. Clin. Pathol.* **90**, 233 (1988).
26. E. Silverberg and J. A. Lubera, *Cancer J.* **39**, 3 (1989).
27. R. M. Hudziak, J. Schlessinger, A. Ullrich, *Proc. Natl. Acad. Sci. U.S.A.* **84**, 7159 (1987).
28. W. J. Muller *et al.*, *Cell* **54**, 105 (1988).
29. Supported by U.S. Public Health Service grants CA 36827 and CA 48780. D.J.S. is a recipient of an American Cancer Society Faculty Research Award. We thank L. Ramos, P. Haran, H.-J. Wang, and P. Bluford for their technical assistance.

23 February 1989; accepted 6 April 1989

OnCusp
Ex. 1002

THE JOURNAL OF BIOLOGICAL CHEMISTRY

Vol. 269, No. 20, Issue of May 20, pp. 14661–14665, 1994
Printed in U.S.A.

Coexpression of *erb*B2 and *erb*B3 Proteins Reconstitutes a High Affinity Receptor for Heregulin*

(Received for publication, March 2, 1994, and in revised form, March 22, 1994)

Mark X. Sliwkowski‡§, Gabriele Schaefer‡, Robert W. Akita‡, Julie A. Lofgren‡, V. Danial Fitzpatrick‡, Andrew Nuijens‡, Brian M. Fendly‡, Richard A. Cerione¶‖, Richard L. Vandlen‡, and Kermit L. Carraway III

*From ‡Genentech, Inc., South San Francisco, California 94080, the ¶Department of Pharmacology, Cornell University, Ithaca, New York 14853, and the **Harvard Medical School, Division of Signal Transduction, Beth Israel Hospital, Boston, Massachusetts 02115*

The heregulin/*neu* differentiation factor gene products were purified and cloned based on their ability to stimulate the phosphorylation of a 185-kDa protein in human breast carcinoma cell lines known to express *erb*B2. However, not all cells that express *erb*B2 respond to heregulin, indicating that other components besides *erb*B2 may be required for heregulin binding. Cells that are transfected with the closely related receptor, *erb*B3, display a single class of lower affinity heregulin binding sites than has been previously observed on breast carcinoma cell lines. Little or no stimulation of tyrosine phosphorylation in response to heregulin occurs in cells that are transfected with *erb*B3 alone. Transfection of cells with *erb*B3 and *erb*B2 reconstitutes a higher affinity binding receptor, which is also capable of generating a tyrosine phosphorylation signal in response to heregulin. A monoclonal antibody to *erb*B2 will inhibit heregulin activation of tyrosine phosphorylation and binding in cells transfected with both receptors but not with *erb*B3 alone. In cells expressing *erb*B2 and *erb*B3, both proteins become tyrosine-phosphorylated upon interaction with heregulin. Direct interaction between heregulin and the two proteins was demonstrated by chemical cross-linking experiments using ^{125}I-heregulin followed by immunoprecipitation with antibodies specific for *erb*B2 or *erb*B3.

Several diverse biological activities have recently been attributed to a family of related proteins that can arise from alternative RNA splicing of a single gene product (1). Included in this family are the heregulins (HRG)[1] (2), *neu* differentiation factor (3), acetylcholine receptor inducing activity (4), and glial growth factor. The HRGs and *neu* differentiation factor (the rat homologue of HRGα) (5) were originally purified based on their ability to stimulate the phosphorylation of a 185-kDa protein that was expressed in a number of breast carcinoma cell lines. This 185-kDa protein was shown to be p185^{erbB2}, also known as HER-2 or *neu*, based on the observation that a tyrosine-phosphorylated form of p185^{erbB2} could be immunoprecipitated from cell lines following HRG treatment. Furthermore, a radiolabeled EGF-like domain of HRGβ1 (residues 177–244) can be chemically cross-linked to a 180–185-kDa protein on breast carcinoma cell lines and immunoprecipitated with anti-p185^{erbB2} antibodies (2). These data argued that *erb*B2 is a target/receptor for HRG. However, additional studies revealed that HRG binding and activation of p185^{erbB2} was not always observed in cells that expressed *erb*B2 (6). Thus, these observations indicated that another cellular component, perhaps closely related to *erb*B2, was necessary for conferring full HRG responsiveness. Recently, we obtained data suggesting that the *erb*B3 (HER-3) protein is a candidate for such a component (7). Specifically, a single class of HRG binding sites was observed when bovine *erb*B3 was expressed in insect cells using a baculovirus expression system. However, the affinity for the HRG-*erb*B3 binding interaction (K_D ~ 0.9–3.0 nM) was significantly weaker than that measured for the binding of HRG to breast carcinoma cell lines (K_D ~ 0.1 nM) (2). Moreover, no increase in *erb*B3 protein tyrosine phosphorylation was observed upon HRG treatment of insect cells expressing *erb*B3. These findings, together with those implicating *erb*B2 as a target for HRG, raised the possibility that *erb*B3 may work together with *erb*B2 to provide a high affinity receptor for HRG with tyrosine kinase capability. The present study addresses whether direct interaction between HRG and p185^{erbB2} can be mediated by *erb*B3 and if p185^{erbB2} is required to generate a phosphorylation signal.

EXPERIMENTAL PROCEDURES

Antibodies to erbB2 and erbB3 Proteins—The anti-p185^{erbB2} monoclonal antibodies 3E8, 2C4, and 2H11 have been described previously (8). Western blot analysis for p185^{erbB2} was performed using the anti-*c-neu* monoclonal antibody, Ab-3, obtained from Oncogene Sciences. Western blot analysis for the *erb*B3 protein was performed using an anti-*erb*B3 polyclonal (rabbit) antibody obtained from Transduction Laboratories. Antibodies to the synthetic peptide ELEPELDLDLDLDLE, corresponding to residues 986–998 of the human *erb*B3 protein, were raised in rabbits and affinity-purified essentially as described by Prigent *et al.* (9).

Recombinant Heregulins—The data presented here were generated using the 68-amino acid peptide corresponding to the EGF-like domain of HRGβ1. The EGF-like domain of HRGβ1 corresponding to residues 177 to 244 was expressed in *Escherichia coli* and purified to homogeneity as described previously (2). We have verified that the full-length versions of HRGβ1 and HRGα produced and purified from mammalian cells both bind to *erb*B3 and exhibit the high affinity binding elicited by the presence of *erb*B2 together with *erb*B3. Thus, in agreement with previous observations (2), the EGF-like domain appears to be sufficient for HRG binding and the specificity of binding is not detectably α or β1 isoform-specific in this system.

Expression Vectors and Transfections—The cDNA encoding bovine *erb*B3 was subcloned into the pRK7 expression vector containing the cytomegalovirus promoter (10). The cDNA encoding human *erb*B2 also in pRK7 was obtained from Sharon Erickson, Genentech, Inc. COS-7

* The costs of publication of this article were defrayed in part by the payment of page charges. This article must therefore be hereby marked "*advertisement*" in accordance with 18 U.S.C. Section 1734 solely to indicate this fact.

§ To whom correspondence should be addressed: Genentech, Inc., 390 Point San Bruno Blvd., Mail Stop 63, South San Francisco, CA 94080. Tel.: 415-225-1247; Fax: 415-225-5945.

‖ Supported by Grant GM40654 from the National Institutes of Health.

[1] The abbreviations used are: HRG, heregulin; r, recombinant; EGF, epidermal growth factor.

OnCusp
Ex. 1002

cells (ATCC CRL 1651) were transfected using the LipofectAMINE™ protocol obtained from Life Technologies, Inc. Cells were transfected in 15-cm plates using a total of 18 μg of DNA. When cells were transfected with both *erbB2* and *erbB3*, 9 μg of each expression plasmid was used. Single transfections were performed using 9 μg of the specific cDNA-containing plasmid and 9 μg of the pRK7 vector control plasmid. Transfections were carried out for 24–36 h, and experiments were initiated immediately.

^{125}I-HRG Binding Assay—Purified rHRG was iodinated using the lactoperoxidase method, and the radiolabeled protein was then purified by reversed phase high performance liquid chromatography using a C4 column. The average specific activity of the radiolabeled, purified protein was 300 μCi/μg. Cells were removed from 15-cm dishes 24–36 h after transfection using 2 mM EDTA in phosphate-buffered saline. Binding reactions were performed on ice for 12–16 h using 1–3 × 10^5 cells/incubation. Cell-bound ^{125}I-rHRGβ1 was separated from free by centrifugation through silicon-paraffin oil (11). Data were analyzed using a nonlinear regression program (12).

Tyrosine Phosphorylation Assay—For tyrosine phosphorylation assays, COS-7 cells were transfected in 12-well plates. Cells were stimulated with the indicated concentrations of HRG for 8 min at room temperature. Supernatants were decanted, and reactions were stopped by the addition of 200 μl of SDS sample buffer. Samples (50 μl) were electrophoresed on 4–12% polyacrylamide gradient gels (Novex) and then electroblotted onto nitrocellulose. Blots were probed with anti-phosphotyrosine monoclonal antibody-horseradish peroxidase conjugate (Transduction Laboratories), and immunoreactive bands were visualized using enhanced chemiluminescence with reagents obtained from Amersham Corp.

Chemical Cross-linking and Immunoprecipitation—Cells (1.0 × 10^6) were suspended in Hank's balanced salts containing 20 mM HEPES, pH 7.4, and incubated for 20 min at room temperature with ^{125}I-rHRGβ1 (0.5 nM) in the presence or absence of 200 nM unlabeled rHRGβ1. Bis(sulfosuccinimidyl)suberate was then added to a final concentration of 1.0 mM, and the samples were incubated for an additional 20 min. Samples were run on SDS-polyacrylamide gels (5%), and radioactive, cross-linked complexes were visualized by autoradiography.

For immunoprecipitation experiments, COS-7 cells were transfected with *erbB3* alone or *erbB2* and *erbB3* and chemical cross-linking was performed as described above, except that cells were pretreated with rHRGβ1 (200 nM), buffer 2C4 (200 nM), or control antibody 2H11 (200 nM) for 20 min at room temperature. Lysates were then prepared in 0.1% SDS, 1% Triton X-100 in Tris-buffered saline containing 10% glycerol, 1 mM EDTA, 0.5 mM Na_3VO_4, 0.2 mM phenylmethylsulfonyl fluoride, 50 trypsin inhibitory units/liter aprotinin, 10 μM leupeptin. Immunoprecipitations were performed with anti-p185$^{c-erbB2}$ (3E8) or anti-*erbB3* COOH-terminal peptide antibody. Immune complexes were purified by absorption on protein A/G-agarose (Pierce Chemical Co.). Samples were analyzed by electrophoresis on polyacrylamide gels as described above.

RESULTS AND DISCUSSION

We chose to study the potential interaction of *erbB2* and *erbB3* proteins using transient transfections in COS-7 cells. Northern and Western blot analyses revealed that COS-7 cells expressed very low but detectable levels of *erbB2* (data not shown); however, as shown in Fig. 1A, COS-7 cells transfected with a control expression plasmid (10) showed no detectable binding of ^{125}I-rHRGβ1. When COS-7 cells were transfected with an *erbB2* expression plasmid, no increase in HRG binding was observed. Expression of the *erbB2* protein was confirmed by Western blot analysis of the transfected COS-7 cell lysates (data not shown). Cells transfected with *erbB3* alone displayed a single affinity binding site (4.3 × 10^5 sites/cell) with a K_D = 1.9 ± 0.3 nM. This dissociation constant for HRG is similar to that measured for insect cells expressing *erbB3* (7). When COS-7 cells were transfected with equal amounts of *erbB2* and *erbB3* expression plasmids, an increase in HRG binding affinity was observed. These cells also exhibited a single class of HRG binding sites (1.6 × 10^5 sites/cell) with a K_D for HRG binding of 0.13 ± 0.01 nM. Thus, co-transfection with both expression vectors generated a HRG binding site with similar affinity to that measured for HRG binding to the breast carcinoma cell line MCF-7 (2). Double transfections of *erbB2* and *erbB3* were then conducted, varying the ratio of *erbB2* to *erbB3* expression plas-

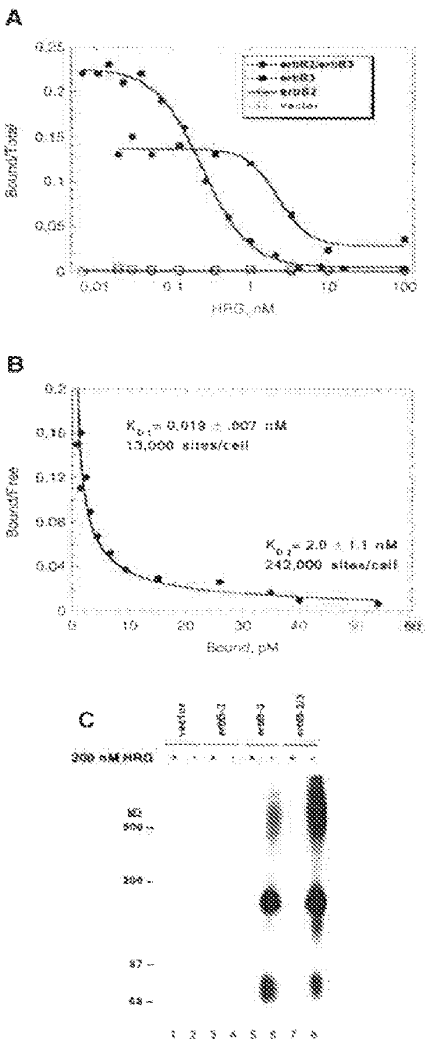


FIG. 1. Binding of ^{125}I-rHRGβ1$_{177-244}$ to COS-7 cell transfectants. *A*, displacement curves of ^{125}I-rHRGβ1 binding with unlabeled rHRGβ1. Cells were transfected with pRK7 control expression plasmid (○), equal amounts of *erbB2* expression plasmid and control expression plasmid (▽), equal amounts of *erbB3* expression plasmid and control expression plasmid (■), or equal amounts of *erbB2* and *erbB3* expression plasmids (●). *B*, Scatchard analysis of HRG binding to *erbB2* and *erbB3* transfectants. A 10-fold excess of *erbB3* expression plasmid relative to *erbB2* was used for COS-7 cell transfections. Binding experiments were performed as described in *A*. *C*, chemical cross-linking of ^{125}I-rHRGβ1$_{177-244}$ to cell surface receptors on COS-7 cell transformants. Transfection conditions were the same as described for panel *A*. Cells (1.0 × 10^6) were detached in 2 mM EDTA, PBS and then resuspended in Hank's balanced salts containing 20 mM HEPES, pH 7.4, and incubated for 30 min at room temperature with ^{125}I-rHRGβ1 (0.5 nM) in the presence (+) or absence (−) of 200 nM unlabeled rHRGβ1. Bis(sulfosuccinimidyl)suberate was then added to a final concentration of 1.0 mM, and the samples were incubated for an additional 20 min. Samples were run on SDS-polyacrylamide gels (5%), and radioactive, cross-linked complexes were visualized by autoradiography. *Lanes 1* and *2* are COS-7 cells transfected with control expression plasmid, *lanes 3* and *4* with *erbB2*, *lanes 5* and *6* with *erbB3*, and *lanes 7* and *8* with equal amounts of *erbB2* and *erbB3* expression plasmids.

OnCusp
Ex. 1002

mids used for transfection. The total amount of expression plasmids used for transfection remained constant at all ratios throughout a given experiment. Scatchard analysis of HRG binding to cells transfected with a 10-fold excess of *erb*B3 over *erb*B2 is shown in Fig. 1*B*. The curvilinear nature of this Scatchard plot indicates the presence of two binding sites with different affinities. The high affinity sites (1.3×10^4 sites/cell) had a K_D value of 0.02 ± 0.01 nM, while the lower affinity binding sites (2.4×10^5 sites/cell) had a K_D of 2.0 ± 1.1 nM. The latter value was similar to that measured for COS-7 cells transfected with *erb*B3 alone. Increasing the amount of *erb*B2 expression plasmid to *erb*B3 expression plasmid used for transfection caused an increase in the number of high affinity binding sites. Moreover, when an expression plasmid for *erb*B3 was transfected into DHFR/C8 cells, a fibroblast cell line that overexpresses *neu* (13) but does not normally bind HRG, only high affinity HRG binding sites were observed (K_D = 0.02 nM; data not shown). Taken together these data indicate that, while the *erb*B3 protein alone binds HRG, a higher affinity receptor is generated when *erb*B2 is expressed together with *erb*B3.

Chemical cross-linking experiments were utilized to study the interaction of HRG with the *erb*B3 protein in the presence and absence of the *erb*B2 protein. As shown in Fig. 1*C*, HRG-specific cross-linked products in the 175–190-kDa range were observed when COS-7 cells were transfected with the *erb*B3 expression plasmid (Fig. 1*C*, *lanes 6* and *8*). No detectable cross-linked proteins were observed with the vector control or the *erb*B2 alone transfectants (Fig. 1*C*, *lanes 2* and *4*). Higher molecular mass complexes (Fig. 1*C*, *lanes 6* and *8*) were also observed when cross-linking was performed on COS-7 cells transfected with *erb*B3. This complex migrated more slowly on a 5% polyacrylamide gel than purified, recombinant apolipoprotein(a), a protein with an apparent molecular mass of 500 kDa (14). The intensity of this high molecular size complex compared to the 175–190-kDa product is greater in cells transfected with *erb*B2 and *erb*B3 than in cells transfected with *erb*B3 alone, indicating a greater propensity to form multimeric species upon HRG binding to the double transfectants.

The direct role of *erb*B2 in the formation of a high affinity HRG receptor was further addressed using a panel of monoclonal antibodies previously developed against $p185^{erbB2}$ (8). We have determined that several anti-$p185^{erbB2}$ monoclonal antibodies were capable of inhibiting HRG binding and tyrosine phosphorylation of $p185^{erbB2}$ in breast carcinoma cell lines.[2] One of these antibodies, 2C4, was tested for its ability to block HRG binding to cells transfected with *erb*B3 alone or with *erb*B2 and *erb*B3. As seen in Fig. 2*A*, HRG binding to COS-7 cells expressing both *erb*B2 and *erb*B3 was inhibited by 2C4 in a dose-dependent manner. The residual HRG binding remaining, in the presence of saturating concentrations of 2C4, was due to HRG binding to *erb*B3, since the amount of binding observed was similar to that measured in COS-7 cells expressing *erb*B3 alone. In contrast, HRG binding to COS-7 cells expressing *erb*B3 alone was not significantly inhibited by 2C4.

The identity of the cross-linked species was examined by immunoprecipitation experiments using a monoclonal antibody 3E8 directed against $p185^{erbB2}$ (8) and a rabbit polyclonal antibody raised against a synthetic peptide corresponding to residues 986–998 of the human *erb*B3 protein. Chemical cross-linking experiments were performed as in Fig. 1*C*, but cells were subsequently solubilized with 0.1% SDS and 1% Triton X-100, which dissociates non-covalent interactions between *erb*B2 and *erb*B3 (data not shown). As shown in Fig. 2*B* (*lanes 1–4*), we were not able to demonstrate a significant immunoprecipitation of protein cross-linked to ^{125}I-rHRGβ1, using the anti-*erb*B2 antibody, in COS-7 cells transfected with *erb*B3 alone. This was expected because although HRG will bind and cross-link to *erb*B3, this complex should not be precipitated by a specific anti-*erb*B2 antibody. However, the immunoprecipitation of cross-linked proteins with the anti-*erb*B2 antibody was observed in COS-7 cells transfected with both *erb*B2 and *erb*B3 (Fig. 2*B*, *lanes 6* and *8*). These data indicate that in the *erb*B2/*erb*B3 COS-7 transfectants, the ^{125}I-rHRGβ1-cross-linked complexes contain *erb*B2. Similar experiments were performed using the anti-*erb*B3 antibody (Fig. 2*B*, *lanes 9–16*). In these cases, a predominant ^{125}I-rHRGβ1 cross-linked band of ~175–190 kDa was immunoprecipitated both from cells expressing *erb*B3 alone (*lanes 10–12*) and from cells expressing *erb*B3 and *erb*B2 (*lanes 14–16*). Other than the relative intensity of the very high molecular size complex, cells expressing both *erb*B2 and *erb*B3 and immunoprecipitated with anti-*erb*B3 (*lane 14*)

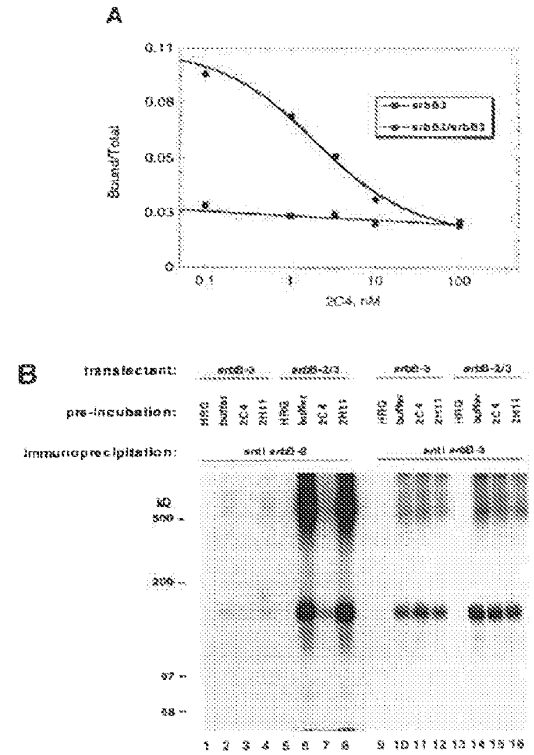


FIG. 2. **Inhibition of HRG binding by 2C4 monoclonal antibody to $p185^{erbB2}$.** *A*, COS-7 cells expressing *erb*B3 or *erb*B2 and *erb*B3 were incubated with the indicated concentrations of 2C4 on ice for 4 h. ^{125}I-rHRGβ1 (10 pM) was then added, and binding reactions were performed as described in Fig. 1*A*. Binding of ^{125}I-rHRGβ1 was 0.1% of input in the presence of 100 nM unlabeled HRG. Transfections were performed using 9 μg of *erb*B3 expression plasmid and 9 μg of control expression plasmid for *erb*B3 cells or 9 μg of *erb*B3, 0.9 μg of *erb*B2, and 8.1 μg of control expression plasmid for *erb*B2/*erb*B3 cells. *B*, effect of 2C4 on chemical cross-linking of ^{125}I-rHRGβ1 to COS-7 cell transfectants. COS-7 cells were transfected with *erb*B3 alone or *erb*B2 and *erb*B3, and chemical cross-linking was performed as described for Fig. 1*C*, except that cells were preincubated as indicated with rHRGβ1 (200 nM), buffer, 2C4 (200 nM), or control antibody 2H11 (200 nM) for 20 min at room temperature. Lysates were prepared in buffer containing 0.1% SDS, 1% Triton X-100 as described under "Experimental Procedures." Immunoprecipitations were performed with anti-$p185^{erbB2}$ (3E8) or anti-*erb*B3 COOH-terminal peptide antibody. Samples were analyzed by electrophoresis on polyacrylamide gels as described in Fig. 1*C*.

[2] M. X. Sliwkowski, J. A. Lofgren, and B. M. Fendly, unpublished data.

OnCusp
Ex. 1002

show a nearly identical pattern to cells expressing *erb*B3 alone. The relatively low level of high molecular size complex that is immunoprecipitated with the anti-*erb*B3 antibodies suggests that the *erb*B3 protein may be inefficiently cross-linked to itself.

After cross-linking the electrophoretic mobilities of the *erb*B2 and *erb*B3 proteins were not distinguishable in these gel systems. This is in agreement with a recent report that demonstrated the molecular size of the *erb*B3 protein is approximately 180 kDa in breast carcinoma cell lines (15). To definitively determine whether HRG was directly bound to *erb*B2, as well as to *erb*B3, we performed cross-linking experiments in the presence of an *erb*B2 antibody, 2C4, that specifically blocks HRG binding to *erb*B2 (but not to *erb*B3). To do this, the COS-7 transfectants were incubated with the 2C4 or with a control *erb*B2 antibody (2H11) that does not inhibit HRG binding, prior to incubation with ^{125}I-*r*HRGβ1 and chemical cross-linking reagents. The HRG cross-linked products were then immunoprecipitated with anti-*erb*B2 or anti-*erb*B3 antibodies. The results presented in Fig. 2*B* (*lane 7*) illustrate that 2C4 antibody prevented the immunoprecipitation of a HRG cross-linked band in cells that were transfected with both *erb*B2 and *erb*B3 and then immunoprecipitated with an anti-*erb*B2 antibody. No inhibition was observed with the control antibody (*lane 8*). No inhibition was observed by the 2C4 antibody of the immunoprecipitation of a HRG cross-linked band when cells were transfected with *erb*B3 alone, or with *erb*B2 and *erb*B3, when immunoprecipitations were performed with the specific anti-*erb*B3 antibody (Fig. 2*B*, *lanes 11* and *15*). These data support the specificity of the 2C4 monoclonal antibody for *erb*B2. Thus, *erb*B2 will directly bind (and cross-link) to HRG, but only when *erb*B3 is expressed in the same cell.

The HRG stimulation of receptor tyrosine kinase activity of the different COS-7 cell transfectants was examined using immunoblotting with anti-phosphotyrosine antibodies. As shown in Fig. 3*A*, cells transfected with a control expression plasmid (*lane 1* in each panel) or an expression plasmid for *erb*B2 (*lane 2* in each panel) showed no HRG-dependent increase in tyrosine phosphorylation. Cells transfected with *erb*B3 alone (*lane 3* in each panel) showed a slight phosphorylation signal in response to HRG. However, a marked HRG-dose dependent tyrosine phosphorylation signal was obtained with COS-7 cells expressing both *erb*B3 and *erb*B2 (*lane 4* in each panel).

To further investigate the role of *erb*B2 in the generation of a tyrosine phosphorylation signal, COS-7 cells that had been transfected with *erb*B3 alone or with *erb*B2 and *erb*B3 were incubated in the presence of the anti-*erb*B2 antibody, 2C4, and then assayed for HRG-dependent tyrosine phosphorylation activity. As seen from Fig. 3 (*panel B*), incubation with 2C4 significantly decreased the HRG-stimulated tyrosine phosphorylation in the *erb*B2/*erb*B3 transfectants. Although the *erb*B3 protein is capable of binding HRG alone, this binding event does not appear to generate a strong tyrosine phosphorylation signal. There are other reasons to question whether *erb*B3 is capable of autophosphorylation or tyrosine kinase activity. Foremost among these is that the comparison of the sequences of a number of protein kinases indicates that *erb*B3 differs from all other kinases at four positions; particularly noteworthy is the presence of an asparagine residue at position 834 of *erb*B3, which is an aspartic acid in all other kinases and which is thought to be an essential residue in the active center of protein kinase A (16–18). Similar amino acid substitutions when present in *hst* (19) or *fps* (20) result in a protein that is kinase-defective. It is perhaps significant that the carboxyl-terminal domain of *erb*B3 contains 13 potential phosphorylation sites (21, 22), whereas other members of this receptor family contain four or five. Thus, even if *erb*B3 is incapable of autophosphorylation or tyrosine kinase activity, it may be phosphorylated

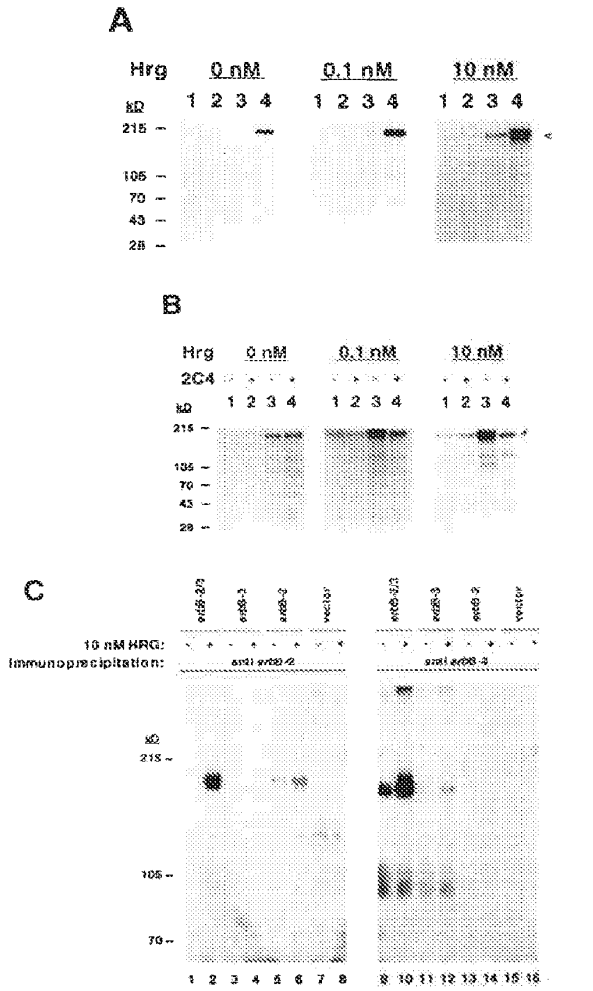


FIG. 3. **HRG stimulation of tyrosine phosphorylation.** *A*, COS-7 cells in 12-well plates were transfected with control expression plasmid (*lane 1*) or *erb*B2 alone (*lane 2*), *erb*B3 alone (*lane 3*), or *erb*B2 and *erb*B3 (*lane 4*, 10-fold excess of *erb*B3 expression plasmid over *erb*B2 was used for transfection). *B*, inhibition of tyrosine phosphorylation by anti-p185^{erbB2} monoclonal antibody 2C4. COS-7 cells transfected as described in *A* with *erb*B3 alone (*lanes 1* and *2*) or *erb*B2 and *erb*B3 (*lanes 3* and *4*) were incubated first with 2C4 (110 nM, *lanes 3* and *4*) for 30 min at room temperature and then with the indicated concentrations of HRG for 8 min. Blots were probed with anti-phosphotyrosine and developed as described for *panel A*. *C*, immunoprecipitation of HRG-stimulated COS-7 cells. COS-7 cells transfected with *erb*B2 and *erb*B3 (as described in *A*) were incubated in the presence (+) of rHRG (10 nM) or control buffer (−). Reactions were conducted as described in *A* except that samples were immunoprecipitated as described in *B* with anti-p185^{erbB2} (3E8) or anti-*erb*B3 COOH-terminal peptide antibody and then electrophoresed and immunoblotted with anti-phosphotyrosine monoclonal antibody.

by other receptor tyrosine kinases and perhaps recruit other SH-2-containing proteins to the membrane.

To determine whether tyrosine phosphorylation occurred on one or both of these proteins when they were complexed with HRG, immunoprecipitation experiments were performed on lysates from HRG-treated cells using the specific anti-*erb*B2 or anti-*erb*B3 antibodies. COS-7 cells transfected with both the *erb*B2 or *erb*B3 expression plasmids were first stimulated with

HRG, precipitated with anti-*erb*B2 and anti-*erb*B3 antibodies, and then the precipitates were Western blotted with anti-phosphotyrosine antibody. The data presented in Fig. 3*C* show that both *erb*B2 (*lane 2*) and *erb*B3 (*lane 10*) are recognized by the anti-phosphotyrosine antibody in a HRG-stimulated manner. This type of dual phosphorylation could occur through a number of possible mechanisms. For example, HRG binding to *erb*B2 within a *erb*B2-*erb*B3 complex could stimulate *erb*B2 to undergo an intramolecular autophosphorylation event as well as to trans-phosphorylate *erb*B3. It is also possible that, although *erb*B3 alone shows little if any tyrosine kinase activity, the presence of a high local concentration of a potential substrate, *erb*B2, within an *erb*B2-*erb*B3 complex may enable the weak kinase (*erb*B3) to trans-phosphorylate *erb*B2. A somewhat similar situation has been described by Spivak-Kroizman *et al.* (23), who studied the interaction of a kinase negative point mutation of EGF receptor and its interaction with *erb*B2.

In summary, we show that the formation of a HRG-stimulated *erb*B2-*erb*B3 interaction provides for a potentially novel signaling system, where one of the participants (*erb*B3) alone has little or no tyrosine kinase activity, but when expressed with *erb*B2, contributes to a high affinity growth factor binding site and provides unique tyrosine residues, which, when trans-phosphorylated, may recruit specific signaling molecules. This differs from other interactions that have been characterized such as EGF-stimulated EGF receptor-p185^{erbB2} complex (24–27), and the more recently reported *erb*B2-*erb*B4 (HER4) complex (28), where in both cases, each of the protein components making up the heterodimer is a fully active tyrosine kinase and capable of autophosphorylation. Nonetheless, given the potential for a number of different HRG-stimulated heterodimeric complexes, it may be that these different combinations are partially responsible for the pleiotropic biological activities that have been associated with the large number of HRG/*neu* differentiation factor/acetylcholine receptor inducing activity/glial growth factor gene products.

Acknowledgments—We thank N. Abadi, R. Hayes, and H. Heinsohn for their assistance in the development of rHRG purification procedures; K. Neote and G. Bennett for technical advice; and D. Eaton for recombinant apolipoprotein(a). K. L. C. acknowledges Dr. Lewis C. Cantley for support, advice, and encouragement.

REFERENCES

1. Marchionni, M. A., Goodearl, A. D. J., Chen, M. S., Bermingham-McDonogh, O., Kirk, C., Hendricks, M., Danehy, F., Misumi, D., Sudhalter, J., Kobayashi, K., Wroblewski, D., Lynch C., Baldassare, M., Hiles, I., Davis, J. B., Hauan, J. J., Totty, N. F., Otsu, M., McBurney, R. N., Waterfield, M. D., Stroobant, P., and Gwynne, D. (1993) *Nature* **362**, 312–318
2. Holmes, W. E., Sliwkowski, M. X., Akita, R. W., Henzel, W. J., Lee, J., Park J. W., Yansura, D., Abadi, N., Raab, H., Lewis, G. D., Shepard, M., Kuang, W. J., Wood, W. I., Goeddel, D. V., and Vandlen, R. L. (1992) *Science* **256**, 1205–1210
3. Wen, D., Peles, E., Cupples, R., Suggs, S. V., Bacus, S. S., Luo, Y., Trail, G., Hu, S., Silbiger, S. M., Levy, R. B., Koski, R. A., Lu, H. S., and Yarden, Y. (1992) *Cell* **69**, 559–572
4. Falls, D. L., Rosen, K. M., Corfas, G., Lane, W. S., and Fischbach, G. D. (1993) *Cell* **72**, 801–815
5. Peles, E., Bacus, S. S., Koski, R. A., Lu, H. S., Wen, D., Ogden, S. G., Ben Levy, R., and Yarden, Y. (1992) *Cell* **69**, 205–216
6. Peles, E., Ben-Levy, R., Tzahar, E., Liu, N., Wen, D., and Yarden, Y. (1993) *EMBO J.* **12**, 961–971
7. Carraway, K. L., III, Sliwkowski, M. X., Akita, R. W., Platko, J. V., Guy, P. M., Nuijens, A., Diamonti, A. J., Vandlen, R. L., Cantley, L. C., and Cerione, R. A. (1994) *J. Biol. Chem.* **269**, 14303–14306
8. Fendly, B. M., Winget, M., Hudziak, R. M., Lipari, M. A., Napier, M. A., and Ullrich, A. (1990) *Cancer Res.* **50**, 1550–1558
9. Prigent, S. A., Lemoine, N. R., Hughes, C. M., Plowman, G. D., Selden, C., and Gullick, W. J. (1992) *Oncogene* **7**, 1279–1286
10. Gorman, C. M., Gies, D. R., and McCray, G. (1990) *DNA Protein Eng. Tech.* **2**, 3–10
11. Robb, R. J., Greene, W. C., and Rusk, C. M. (1984) *J. Exp. Med.* **160**, 1126–1146
12. Munson, P., and Rodbard, D. (1980) *Anal. Biochem.* **107**, 220–239
13. Hung, M.-C., Schechter, A. L., Chevray, P.-Y. M., Stern, D. F., and Weinberg, R. A. (1986) *Proc. Natl. Acad. Sci. U. S. A.* **83**, 261
14. Koschinsky, M. L., Tomlinson, J. E., Zioncheck, T. F., Schwartz, K., Eaton, D. L., and Lawn, R. M. (1991) *Biochemistry* **30**, 5044–5051
15. Kraus, M. H., Fedi, P., Starks, V., Muraro, R., and Aaronson, S. A. (1993) *Proc. Natl. Acad. Sci. U. S. A.* **90**, 2900–2904
16. Knighton, D. R., Zheng, J., Ten Eyck, L. F., Ashford, V. A., Xuong, N.-H., Taylor, S., and Sowadski, J. M. (1991) *Science* **253**, 407–414
17. Gibbs, C. S., and Zoller, M. J. (1991) *J. Biol. Chem.* **266**, 8923–8931
18. Chou, Y.-H., and Hayman, M. J. (1991) *Proc. Natl. Acad. Sci. U. S. A.* **88**, 4897–4901
19. Tan, J. C., Nocka, K., Ray, P., Traktman, P., and Besmer, P. (1990) *Science* **247**, 209–212
20. Moran, M. F., Koch, C. A., Sadowski, I., and Pawson, T. (1988) *Oncogene* **3**, 665–672
21. Kraus, M. H., Issing, W., Miki, T., Popescu, N. C., and Aaronson, S. A. (1989) *Proc. Natl. Acad. Sci. U. S. A.* **86**, 9193–9197
22. Plowman, G. D., Whitney, G. S., Neubauer, M. G., Green, J. M., McDonald, V. L., Todaro, G. J., and Shoyab, M. (1990) *Proc. Natl. Acad. Sci. U. S. A.* **87**, 4905–4909
23. Spivak-Kroizman, T., Rotin, D., Pinchasi, D., Ullrich, A., Schlessinger, J., and Lax, I. (1992) *J. Biol. Chem.* **267**, 8056–8063
24. King, C. R., Borrello, I., Bellot, F., Comoglio, P., and Schlessinger, J. (1988) *EMBO J.* **7**, 1647–1651
25. Connelly, P. A., and Stern, D. F. (1990) *Proc. Natl. Acad. Sci. U. S. A.* **87**, 8054–8057
26. Goldman, R., Levy, R. B., Peles, E., and Yarden, Y. (1990) *Biochemistry* **29**, 11024–11025
27. Qian, X., Decker, S. J., and Greene, M. I. (1992) *Proc. Natl. Acad. Sci. U. S. A.* **89**, 1330–1334
28. Plowman, G. D., Green, J. M., Culouscou, J.-M., Carlton, G. W., Rothwell, V. M., and Buckley, S. (1993) *Nature* **366**, 473–475.

Nonclinical Studies Addressing the Mechanism of Action of Trastuzumab (Herceptin)

Mark X. Sliwkowski, Julie A. Lofgren, Gail D. Lewis, Timothy E. Hotaling, Brian M. Fendly, and Judith A. Fox

HER2 is a ligand-less member of the human epidermal growth factor receptor or ErbB family of tyrosine kinases. In normal biological systems, HER2 functions as a co-receptor for a multitude of epidermal growth factor-like ligands that bind and activate other HER family members. HER2 overexpression is observed in a number of human adenocarcinomas and results in constitutive HER2 activation. Specific targeting of these tumors can be accomplished with antibodies directed against the extracellular domain of the HER2 protein. One of these antibodies, 4D5, has been fully humanized and is termed trastuzumab (Herceptin; Genentech, San Francisco, CA). Treatment of HER2-overexpressing breast cancer cell lines with trastuzumab results in induction of $p27^{KIP1}$ and the Rb-related protein, p130, which in turn significantly reduces the number of cells undergoing S-phase. A number of other phenotypic changes are observed in vitro as a consequence of trastuzumab binding to HER2-overexpressing cells. These phenotypic changes include downmodulation of the HER2 receptor, inhibition of tumor cell growth, reversed cytokine resistance, restored E-cadherin expression levels, and reduced vascular endothelial growth factor production. Interaction of trastuzumab with the human immune system via its human immunoglobulin G_1 Fc domain may potentiate its antitumor activities. In vitro studies demonstrate that trastuzumab is very effective in mediating antibody-dependent cell-mediated cytotoxicity against HER2-overexpressing tumor targets. Trastuzumab treatment of mouse xenograft models results in marked suppression of tumor growth. When given in combination with standard cytotoxic chemotherapeutic agents, trastuzumab treatment generally results in statistically superior antitumor efficacy compared with either agent given alone. Taken together, these studies suggest that the mechanism of action of trastuzumab includes antagonizing the constitutive growth-signaling properties of the HER2 system, enlisting immune cells to attack and kill the tumor target, and augmenting chemotherapy-induced cytotoxicity.

Semin Oncol 26 (suppl 12):60–70. Copyright © 1999 by W.B. Saunders Company.

From Genentech, Inc, South San Francisco, CA
All authors are employees of Genentech, Inc
Address correspondence and reprint requests to Mark Sliwkowski, PhD, Department of Molecular Oncology, Genentech, Inc, 1 DNA Way, Mail Stop 63, South San Francisco, CA 94080.
Copyright © 1999 by W.B. Saunders Company
0093-7754/99/2604-1208$10.00/0

THE EPIDERMAL growth factor (also known as HER or ErbB) family of receptor tyrosine kinases are important mediators of cell growth, differentiation, and survival.[1,2] As shown in Fig 1, the receptor family is composed of four distinct members, including epidermal growth factor receptor (EGFR; HER1 or ErbB1), HER2 (*neu* or ErbB2), HER3 (ErbB3), and HER4 (tyro2 or ErbB4). Within a given tissue, these receptors are rarely, if ever, expressed alone, but are found in various combinations.[3] At present there are nine ligands that bind directly to EGFR, HER3, or HER4. HER2 also becomes activated as a result of ligand binding to other HER family members. Furthermore, blocking the association of HER2 with these receptors inhibits ligand-mediated signaling.[4-8] Thus, HER2 is an essential component of these receptor complexes, although no ligand has been characterized at the molecular level that interacts with HER2 alone.

Recently, the HER receptors have been studied either alone or in specific combinations.[9-11] Ligand-receptor complexes that include HER2 appear to be more potent than other receptor combinations. Features of HER2-containing complexes that may account for enhanced receptor signaling include the conversion from a low-affinity to a high-affinity growth factor binding site,[12] which results from a decrease in ligand dissociation from the complex.[5] Second, the internalization rate of HER2 receptor complex is nearly an order of magnitude lower than that observed for EGFR.[13] The higher-affinity binding state and the decreased internalization rate may result in a receptor–ligand complex that resides longer on the plasma membrane and prolongs the duration of receptor signaling. Third, HER2 is a very active tyrosine kinase[14] that also can be constitutively activated by mutation or overexpression. In addition to transphosphorylating other HER receptors, activated HER2 phosphorylates PLCγ,[15] activates the Ras/Raf/MEK/MAPK pathway,[16-18] and associates with the cytoplasmic tyrosine kinases src[19-21] and CHK.[22] Heterodimerization of HER receptors[23-25] appears to increase the diversity of cellular

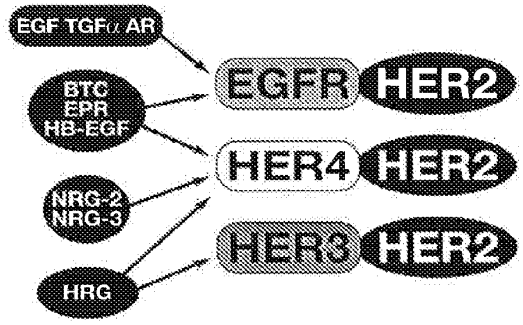


Fig 1. Schematic representation of the human epidermal growth factor receptor (HER) family and their ligands.[5]

responses to a variety of proteins that serve as ligands for these receptors.[9,10]

Activation of nonmutated HER2 occurs through self-association and by transactivation with other related receptor family members. In breast cancer, gene amplification results in HER2 protein levels in tumor cells that are 10- to 100-fold greater than that found in the adjacent normal breast epithelium.[26] Since *HER2* is localized in the plasma membrane, its diffusion is limited to two dimensions; thus, even moderate overexpression of HER2 can lead to a constitutively activated receptor.[27] Soon after the HER2 gene was cloned, and well before its role as a common subunit was appreciated, compelling clinical data were generated demonstrating that HER2 gene amplification predicts a poor clinical outcome.[28] Although these data were controversial at first, at present the general consensus is that HER2 overexpression is a negative prognostic indicator for breast cancer.[29,30] Subsequent studies have shown that HER2 overexpression correlates with shorter disease-free interval and overall survival.[31] Moreover, comprehensive studies have shown that the presence of this molecular alteration is predictive of aggressive disease regardless of disease stage or node status.[32-34]

A role for HER2 as an oncogene was first appreciated in rodent systems. The activated form of the rodent homolog of the HER2 gene, *c-neu*, was initially identified as an extremely potent transforming oncogene in DNA isolated from rats treated with ethylnitrosourea.[35] This version of the *neu* oncogene contained a point mutation in the transmembrane domain, which resulted in the *neu* protein existing in a constitutively activated state. To date, no analogous mutations have been found in human tumors.[28,29,36,37] Rather, the molecular alteration that occurs in human cancers is overexpression of the normal gene product. Overexpression generates a constitutively activated receptor and leads to transformation of both NIH3T3 cells and human breast cells, suggesting that this alteration may play a pathogenic role in tumorigenesis.[38-41] Additionally, female transgenic animals that are engineered to overexpress the nonmutated *neu* oncogene in their breast tissue develop breast tumors after puberty with a high degree of penetrance.[42] Taken together, these data suggest that HER2 overexpression has an active role in neoplastic transformation.

TARGETING HER2-OVEREXPRESSING CANCERS

A number of approaches have been used to therapeutically target HER2-overexpressing cancers.[43] A common approach, based on similar studies with the closely related EGFR, has been the generation of antibodies that inhibit the growth of cells which possess activated HER2/*neu* receptors.[44-49] Analysis of one of these panels of anti-HER2 monoclonal antibodies led to the identification of the murine monoclonal, 4D5.[50] This antibody recognizes an extracellular epitope (amino acids 529 to 627) in the cysteine-rich II domain that resides very close to the transmembrane region. Treatment of breast cancer cells with 4D5 partially blocks heregulin activation of HER2-HER3 complexes, as measured by receptor phosphorylation assays.[6] To allow for chronic human administration, murine 4D5 was fully humanized to generate trastuzumab (Herceptin; Genentech, San Francisco, CA). Solution-phase binding studies determined that trastuzumab binds to the recombinant HER2 extracellular domain with an affinity (Kd) of 0.1 nmol/L, which is threefold greater than 4D5.[51]

IN VITRO EFFECTS OF ANTI-HER2 MONOCLONAL ANTIBODIES

All the antibodies generated against HER2 were assessed for their ability to inhibit the anchorage-dependent growth of human cancer cell lines. Several of these antibodies exhibited antiproliferative activity toward cell lines that expressed higher-than-normal levels of HER2. This observation was

also extended to include assays performed in soft agar or in an anchorage-independent format, and similar results were obtained.[52] The most potent growth-inhibitory antibody of this panel was 4D5. Cell cycle analysis following treatment of SK-BR-3 breast cancer cells, which express high levels of HER2, is shown in Fig 2. Trastuzumab or 4D5 significantly reduces the percentage of SK-BR-3 cells undergoing S-phase and increases the percentage of cells in G0/G1. In contrast, HER2 antibody treatment does not affect the cell line MCF-7, which expresses normal amounts of HER2. The effect of these antibodies on the cell cycle is dose-dependent, with maximal inhibitory activity occurring at antibody concentrations greater than 1 μg/mL.[53] To address the molecular basis for growth arrest, SK-BR-3 cells were treated with trastuzumab; cell lysates were then probed by immunoblot analysis with reagents specific for known inhibitors of the cell cycle. As shown in Fig 3, treatment of SK-BR-3 cells with trastuzumab resulted in marked induction of the CDK2 kinase inhibitor, $p27^{KIP1}$. Moreovet, a similar induction of the retinoblastoma-related protein, p130, was

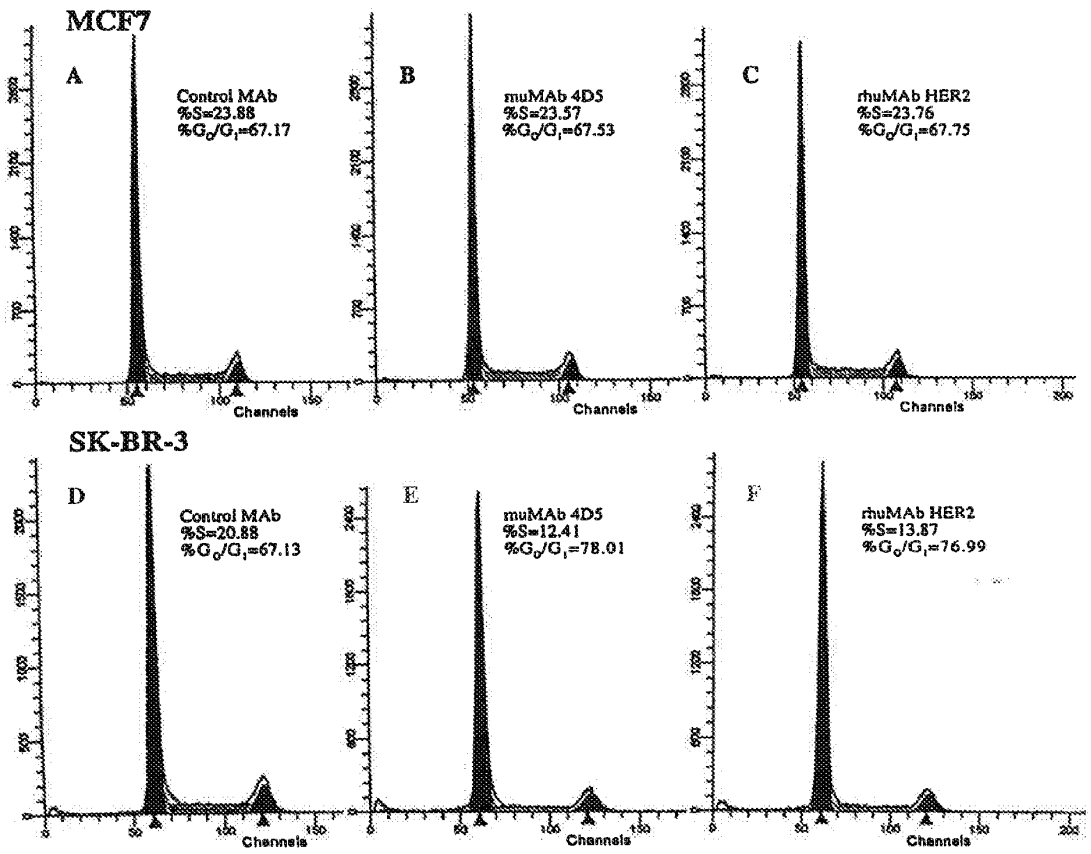


Fig 2. MCF-7 (A-C) or SK-BR-3 (D-F) cells were plated at a density of 2 × 10^6/dish in 60 mm × 15 mm culture dishes and allowed to adhere overnight. Monolayers were washed with phosphate-buffered saline (PBS) and incubated with media containing trastuzumab or control antibodies at a concentration of 10 μg/mL. Following a 72-hour incubation, cells were trypsinized, washed with PBS, fixed in ice-cold methanol, and stored at -20°C. Fixed cells were then washed twice with PBS and allowed to incubate with RNAse 100 μg/mL (Worthington Biochemical, Lakewood, NJ) for 30 minutes at 37°C. Following centrifugation, nuclei were subjected to propidium iodide 50 μg/mL (Molecular Probes, Inc, Eugene, OR) staining in PBS. Samples were analyzed by flow cytometry (Epics Elite; Coulter Corporation, Miami, FL) using Modfit LT software (Verity Software House, Sunnyvale, CA).

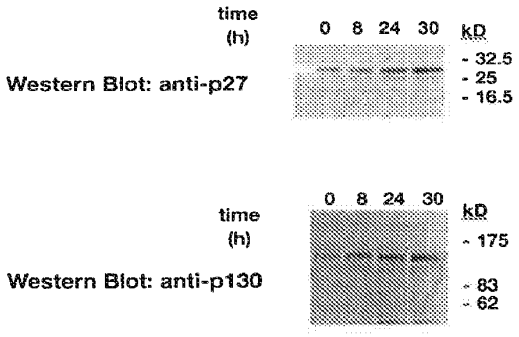


Fig 3. Induction of the cell cycle inhibitor $p27^{KIP1}$ and the retinoblastoma-related p130 protein in SK-BR-3 cells treated with trastuzumab. Cells (1.5×10^5 cells/well) were plated in six-well dishes and grown to approximately 50% confluence in medium containing 10% fetal bovine serum. The medium was removed and treatments (trastuzumab, 16 μg/mL) were prepared in fresh medium containing 10% fetal bovine serum and added to the culture dishes. Incubations were stopped by the addition of 0.5 mL sodium dodecyl sulfate sample buffer (5% sodium dodecyl sulfate, 2% β-mercaptoethanol, 10% glycerol, 50 mmol/L Tris HCl, pH 6.8). Samples (20 μg of protein/lane) were electrophoresed on an 8% to 16% Tris-glycine gel (Novex, San Diego, CA). Protein was transferred from the gels to nitrocellulose. Western blot analysis and detection were done following the manufacturer's instructions (ECD; Amersham, Buckinghamshire, UK). Primary antibodies used for $p27^{KIP1}$ and the retinoblastoma-related p130 protein immunoblots were rabbit polyclonals (SC-317 and SC-528, respectively; Santa Cruz, Santa Cruz, CA) and were used at 0.1 μg/mL. Both proteins were detected with an anti-rabbit horseradish peroxidase-conjugate secondary antibody used at a titer of 1:10,000 (ALI 3404; Biosource International, Carmarillo, CA).

also observed. These data are consistent with the observation that treatment of HER2-overexpressing cells is antiproliferative and that cytostasis results from an inhibition of cell cycle progression.

Cells that overexpress HER2 are intrinsically resistant to the cytotoxic effects of tumor necrosis factor-α.[54] This observation suggests that HER2 overexpression may potentiate tumorigenesis by inducing tumor cell resistance to host defense mechanisms. Furthermore, when HER2-overexpressing cells are treated with the murine monoclonal 4D5, they become sensitized to tumor necrosis factor-α treatment.[49]

Molecules involved in cell adhesion are also thought to play a critical role in malignant progression. One of these molecules, E-cadherin, plays a central role in maintaining epithelial cell morphology.[55] A reduction in E-cadherin synthesis can be correlated with increased invasiveness.[56] Overexpression of HER2 in normal human breast epithelial cells reduces morphogenesis in vitro.[57] These HER2 transfectants express significantly lower levels of E-cadherin as well as the α2 integrin subunit. Treatment of these HER2 transfectants with 4D5 restores E-cadherin and α2 integrin to normal levels.[58] Taken together, these data suggest that HER2 overexpression affects adhesion molecule synthesis, which in turn may contribute to the metastatic process and malignant progression. Targeting HER2 overexpression with monoclonal antibodies such as 4D5 and trastuzumab may be effective in controlling metastatic potential.

Angiogenesis is a critical survival function for solid tumors.[59,60] Vascular endothelial growth factor is one of the more important mediators of tumor angiogenesis.[61] Recently, it has been demonstrated that treatment of HER2-overexpressing tumor cells with 4D5 decreases vascular endothelial growth factor production.[62] Suppression of angiogenesis may enhance the activity of anti-HER2 monoclonal antibody therapy in vivo.

AGONIST PROPERTIES OF TRASTUZUMAB

Several reports have suggested that binding of 4D5 to HER2 activates the receptor, as monitored by an increase in tyrosine autophosphorylation.[63] In addition, c-fos induction[64] and increases in inositol polyphosphate and diacyl glycerol synthesis[65] following 4D5 treatment also have been reported. These agonistic properties are difficult to reconcile the potent cytostatic activity of 4D5 or trastuzumab on the growth of human tumor cells that overexpress HER2.[6,52]

With recent recognition of the role of HER2 as a shared signaling subunit with other HER receptor family members, the ligand-like properties of trastuzumab have been re-examined. MCF-7 cells express normal/low levels of HER2 and are not growth inhibited by trastuzumab treatment. MCF-7 cells were treated with trastuzumab, 4D5, or recombinant heregulin (rHRG). Cell lysates were prepared using denaturing (sodium dodecyl sulfate) or nondenaturing (nonionic detergent, Triton X-100) conditions. These latter conditions are frequently used for examination of receptor activation or co-immunoprecipitation of mediators involved in signal transduction. As shown in Fig 4, treatment of MCF-7 cells with rHRG results in HER2 tyrosine phosphorylation, regardless of the manner in which the cells are lysed. In con-

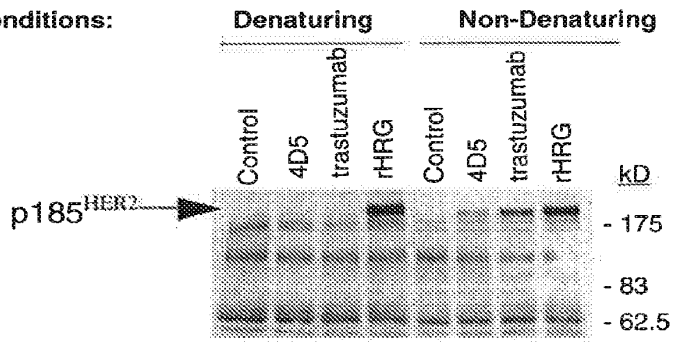


Fig 4. Phosphotyrosine analysis of HER2. MCF-7 cells were seeded in 24-well plates at 1.5 × 10^5 cells/well and allowed to grow for 2 days. Before treatment, cells were transferred to medium without serum. Cells were treated for 30 minutes at room temperature with 4D5 (16 μg/mL), trastuzumab (16 μg/mL), or rHRG (300 pmol/L). Cell lysates were then prepared using denaturing or nondenaturing conditions and allowed to remain at room temperature for 3 hours. For nondenaturing conditions, lysates were prepared in 0.5% Triton X-100, 50 mmol/L Hepes, 150 mmol/L NaCl, 1 mmol/L phenylmethylsulfonyl fluoride, 2 mmol/L $NaVO_4$, and 5 KIU/mL aprotinin. Sodium dodecyl sulfate-polyacrylamide electrophoresis buffer was used for denaturing conditions. Samples were prepared for electrophoresis by adding an equivalent volume of 5% sodium dodecyl sulfate and 2% β-mercaptoethanol to each sample and then heated at 100°C for 5 minutes. Following sodium dodecyl sulfate-polyacrylamide electrophoresis, proteins were transferred to nitrocellulose membranes and probed with anti-phosphotyrosine monoclonal antibody (#E120H; Transduction Labs, San Diego, CA) linked to horseradish peroxidase used at a final concentration of 0.125 ng/mL.

trast, 4D5 or trastuzumab results in HER2 tyrosine phosphorylation only when lysates are prepared in nonionic detergent. Although biochemically interesting, this phosphorylation event does not appear to be physiologic. A similar artifact has been reported for anti-EGFR monoclonal antibodies.[66] When similar experiments are performed with SK-BR-3 cells, which overexpress HER2 and are growth inhibited by trastuzumab treatment, the results are confounded by a high degree of basal tyrosine phosphorylation that exists on HER2. Taking this high baseline phosphotyrosine level into account, trastuzumab treatment of SK-BR-3 cells results in a modest but reproducible increase in tyrosine phosphorylation content, which is in agreement with previous published studies.[63]

To assess whether trastuzumab treatment causes further activation of the HER2 signal transduction pathway, the common adapter molecule, shc, was examined. MCF-7 or SK-BR-3 cells were treated with trastuzumab, 4D5, or rHRG, and cell lysates were then prepared using denaturing conditions. Immunoprecipitates of shc were prepared and immunoblots were then probed with anti-phosphotyrosine antibody to determine the level of shc tyrosine phosphorylation. As shown in Fig 5, rHRG treatment of either MCF-7 or SK-BR-3 cells results in a rapid increase in shc phosphorylation that is sustained for approximately 120 minutes. In contrast, neither trastuzumab nor 4D5 treatment causes a significant increase in shc phosphorylation. Mitogen-activated protein kinases are common mediators of growth factor receptor signal transduction pathways. To further investigate potential differences in downstream signaling, mitogen-activated protein kinase activation was examined after exposure to trastuzumab or rHRG. As shown in Fig 6, strong mitogen-activated protein kinase activation occurs in either MCF-7 (Fig 6, top) or SK-BR-3 cells (Fig 6, bottom) only after rHRG treatment. These data suggest that while trastuzumab or 4D5 may cause autophosphorylation under some conditions, downstream signaling pathways are not significantly activated.

Other detailed investigations have been undertaken with well-characterized panels of anti-HER2 monoclonal antibodies in an attempt to correlate agonistic activities of these antibody panels with the desired biological outcome, ie, cytostasis.[47,48,67,68] To date, no strict correlation exists between any one measured biochemical parameter and antiproliferative activity. Rather, a number of attributes emerge as components in assessing anti-HER2 cytostatic activity. These include antibody affinity, bivalency, pH dependence of binding, downmodulation, internalization, and the ability to block HER2 association with other HER family members. It appears that the more potent antipro-

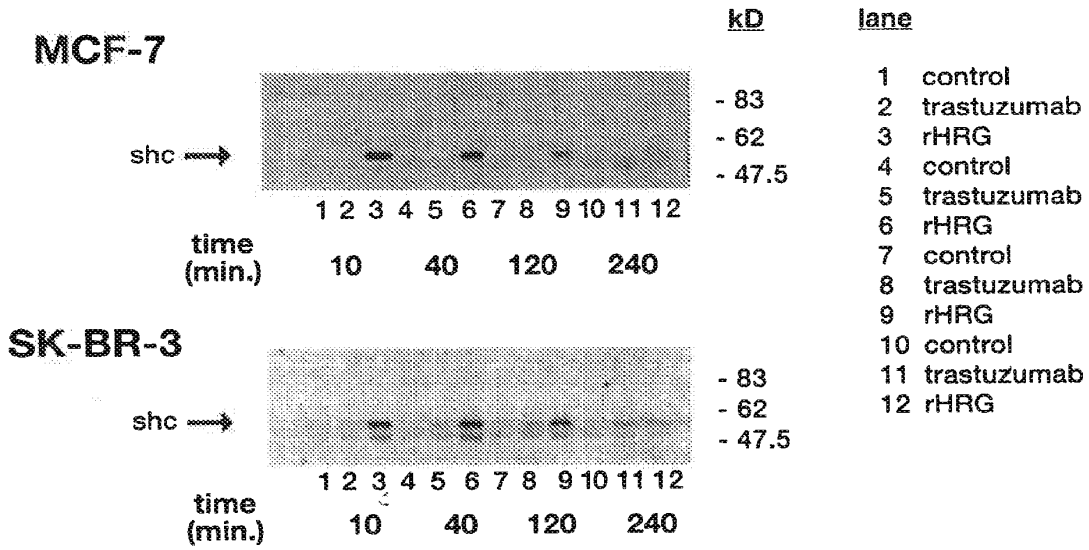


Fig 5. Effects of trastuzumab or rHRG treatment on shc phosphorylation in MCF-7 or SK-BR-3 cells. Cells were grown in six-well dishes. They were serum-starved 24 hours before treatment and then lysed under denaturing conditions. Cell lysates were immunoprecipitated with anti-shc pAb (#S14630; Transduction Labs) and immunoblotted with anti-phosphotyrosine monoclonal antibodies as described in Fig 3.

liferative HER2 antibodies share a number of these characteristics, which together diminish the contribution of HER2 to ligand-dependent and independent signaling.

TRASTUZUMAB-MEDIATED RECEPTOR DOWNMODULATION

Downmodulation of receptor–ligand complexes is thought to be a major attenuation mechanism for receptor-induced signaling. Recently, it has been shown that HER2, HER3, and HER4 are impaired relative to EGFR with regard to their ability to undergo ligand-mediated endocytosis.[13] Although the rate and precise mechanism for downmodulation of HER2 are vastly slower than observed for EGFR, significant removal of HER2 from the plasma membrane occurs with 4D5 treatment.[49,65,69]

In summary, these data are consistent with the notion that trastuzumab or 4D5 induces obligate formation of HER2 homodimers, particularly in cells that overexpress HER2, and that these homodimers are capable of receptor transphosphorylation. However, antibody-induced receptor activation does not appear to induce effective downstream signaling. Instead, trastuzumab treatment leads to downmodulation of HER2 from the tumor cell surface. The removal of HER2 from the plasma membrane presumably results in less receptor available for dimerization with itself or other HER family members, which in turn diminishes the HER2-initiated constitutive growth signal.

COMPLEMENT-DEPENDENT CYTOTOXICITY

Because trastuzumab contains a human immunoglobulin G1 (IgG1) Fc region, it may be capable of activating the human complement cascade. Immunochemical and functional analysis demonstrated that trastuzumab activated complement after binding to its target antigen HER2 on five of six breast adenocarcinoma cell lines (M. Kirschfink, University of Heidelberg, personal communication, July 1996). However, trastuzumab-induced complement-mediated tumor cell lysis was not observed, which is likely due to the presence of membrane-associated complement regulatory proteins such as CD35 (complement receptor 1), CD55 (decay accelerating factor), or CD46 (membrane cofactor protein).[70] Complement-ac-

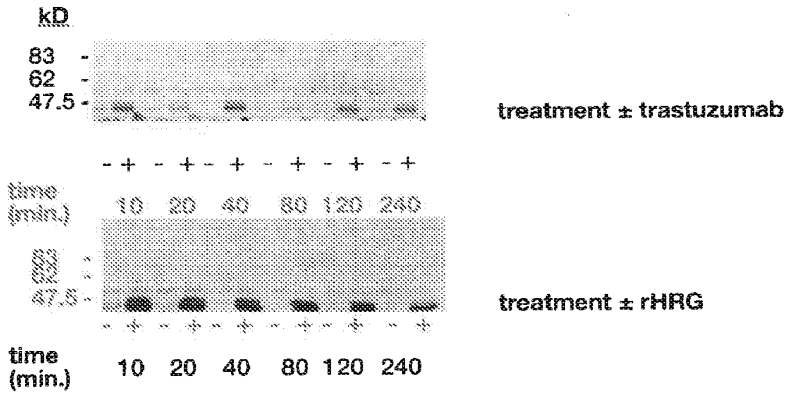


Fig 6. Detection of MAP kinase activation in MCF-7 or SK-BR-3 cells. Cells (1.2 × 10⁵ cells/well) plated in 12-well dishes were changed to low serum-containing medium (0.1% fetal bovine serum) 24 hours after adhering. After an additional 48 hours, the medium was changed again to serum-free for 1.5 hours to minimize any mitogen activated protein kinase activation in the untreated cells. Cells were treated for various times as indicated at 37°C with trastuzumab (10 μg/mL) or rHRG (10 nmol/L). Incubations were stopped by the addition of 0.4 mL sodium dodecyl sulfate sample buffer with reducing agent. Lysates were heated to 100°C for 5 minutes and then 25 μL was electrophoresed on a 4% to 20% Tris-glycine gel (Novex, San Diego, CA). Western blots were probed with a polyclonal antibody recognizing the dually phosphorylated form (#V667A; Promega, Madison, WI) or antibodies that recognize the unactivated forms of ERK1 and ERK2, each used at a dilution of 1:2,000 (SC-094-G and SC-154-G; Santa Cruz).

tivating ability of the antibody was further supported by results from solid-phase binding assays. On binding of trastuzumab to the immobilized purified extracellular domain of HER2, the complement cascade reaction could be demonstrated to occur up to the binding of the C5b-9 (membrane attack complex) (M. Kirschfink, University of Heidelberg, personal communication, July 1996).

ANTIBODY-DEPENDENT CELL-MEDIATED CYTOTOXICITY

Antibody-dependent cell-mediated cytotoxicity (ADCC) is triggered when antibody-coated (opsonized) target cells interact with Fc receptors that are present on effector cells. Activated effector cells destroy their targets by release of cytoplasmic granules that contain perforin and granzymes. Previously, it was reported that trastuzumab-mediated ADCC was very effective against tumor cells that overexpress HER2.[51,52] In these studies, human peripheral blood mononuclear cells were used as effector cells and were pretreated with interleukin-2. Since trastuzumab contains an IgG1 Fc, trastuzumab-dependent ADCC was expected to be mediated by Fcγ receptors , which are present on peripheral blood mononuclear cells. To assess the type of Fcγ receptors that are primarily responsible for mediating trastuzumab-dependent ADCC without prior interleukin-2 treatment, cytotoxicity assays were performed in the presence of antibodies known to block the interaction of human IgG1 Fc with specific Fcγ receptors. Data from these experiments demonstrated that trastuzumab-dependent ADCC occurred primarily through interactions with the type III receptor, or CD16. FcγRIII is expressed primarily on natural killer cells, some monocytes, and activated T cells. As shown in Fig 7, specific types of effector cells were isolated and tested in ^{51}Cr release cytotoxicity

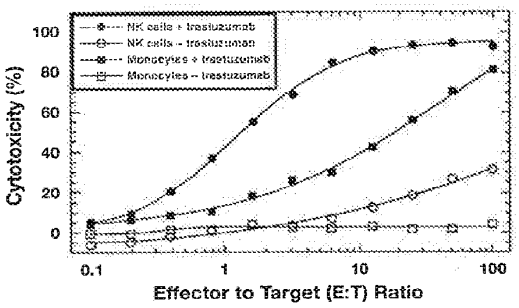


Fig 7. Trastuzumab-mediated ADCC using purified natural killer (NK) cells or monocytes as effector cells and ^{51}Cr-labeled SK-BR-3 cells as targets.

assays using the HER2-overexpressing breast cancer cell line, SK-BR-3, as a target. By varying the effector to target ratios from 0.1 to 100, the effector to target ratio where half-maximal cytotoxicity occurred could be determined by four-parameter fit analysis. For natural killer cells and monocytes, these values were determined to be 1 and 3, respectively, suggesting that these effector cells are extremely potent in killing trastuzumab-coated target cells.

The precise role of ADCC in vivo is difficult to assess in cancer patients undergoing immunotherapy or in animal models. Arming of natural killer cells by tumor-specific antibody has been postulated as a mechanism for directing these effector cells to tumors.[71] Since the binding of human IgG1 with FcγRIII is a relatively weak interaction and the concentration of IgG is high in serum, effector cell arming with trastuzumab is unlikely to occur in vivo. In contrast, the binding between trastuzumab and HER2 is governed by a very high-affinity interaction. To determine whether trastuzumab-mediated ADCC was affected by physiologic concentrations of IgG, cytotoxicity assays were performed in the presence or absence of 10 mg/mL human IgG. The results of these experiments demonstrated that serum level concentrations of IgG did not affect either the half-maximal effector to target ratio or the degree of cytotoxicity. Moreover, since trastuzumab is bivalent and HER2 protein density is very high in these tumor cells, an avidity component also likely contributes to the near-irreversible binding of trastuzumab to cells that overexpress HER2. Furthermore, overexpressing tumor cell lines were more susceptible to cytotoxic damage than intermediate- or low-expressing tumor cell lines. Taken together, these data suggest that the affinity and avidity of the trastuzumab-HER2 interaction may also contribute to the safety profile of trastuzumab in patients, since HER2-overexpressing tumor cells would likely be preferentially targeted for ADCC rather than tissues that express normal levels of HER2.

EFFICACY IN HUMAN BREAST TUMOR XENOGRAFTS

To determine the relative potency of trastuzumab, both MCF-7-HER2 and BT-474 xenograft models have been used. In these experiments, animals bearing HER2-overexpressing MCF-7-HER2 xenografts were treated with trastuzumab at total doses of 3, 10, 30, and 100 mg/kg. As shown in Fig 8, dose-dependent antitumor activity was observed with 3 to 100 mg/kg trastuzumab treatment compared with mice treated with control antibody. Nude mice bearing BT-474 xenografts were treated with trastuzumab doses ranging from 0.1 to 30 mg/kg. In this case, dose-dependent antitumor activity was observed with 0.1, 0.3, and 1 mg/kg trastuzumab treatment compared with mice treated with control antibody. Antitumor activity appeared to plateau at doses above 1 mg/kg.[73] The BT-474 xenograft model is thus more sensitive to trastuzumab treatment than the MCF-7-HER2 xenograft model.[53]

COMBINATION EFFICACY STUDIES WITH CYTOTOXIC CHEMOTHERAPEUTIC AGENTS

Treatment of human cancer typically involves a multidisciplinary approach that frequently includes surgery, radiation, chemotherapy, and/or hormonal manipulation. To determine how to use trastuzumab both alone and in combination with established therapeutic agents, a series of in vitro and in vivo studies was conducted. These studies were based on previously published reports of enhanced activity of cisplatin when used in combination with antibodies directed against the EGFR.[73] Combination studies with cisplatin revealed that trastuzumab, 4D5, or other anti-HER2 monoclonal antibodies potentiate cytotoxicity by decreasing DNA repair following cisplatin-induced DNA damage.[74,75]

The median-effect principle and combination-

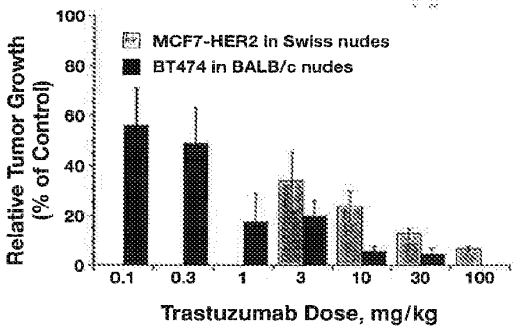


Fig 8. Effect of trastuzumab on the growth of HER2-overexpressing MCF-7-HER2 or BT-474 xenografts. Tumor measurements were made after 21 days of trastuzumab treatment. Data are summarized from Pegram et al[53] and Baselga et al.[72]

index isobologram method of multiple drug effect analysis were used to further characterize the effects of combinations of trastuzumab and other cytotoxic chemotherapeutic agents used in breast cancer therapy. In vitro experiments with the human breast cancer cell line, SK-BR-3, were conducted combining trastuzumab and eight drugs representing seven different classes of cytotoxic chemotherapeutics. The drugs studied include the anthracycline antibiotic doxorubicin, the taxane paclitaxel, the topoisomerase II inhibitor etoposide, the platinum analog cisplatin, the vinca alkaloid vinblastine, the alkylating agents thiotepa and cyclophosphamide, and the antimetabolite 5-fluorouracil. In cell culture studies, cisplatin, thiotepa, and etoposide were found to be synergistic with trastuzumab. Additive interactions were observed with doxorubicin, paclitaxel, methotrexate, and vinblastine. One drug, 5-fluorouracil, was found to exhibit an antagonistic interaction with trastuzumab.[53]

Since SK-BR-3 cells are not tumorigenic in athymic mice, parallel studies were conducted in vivo testing the same trastuzumab/drug combinations with HER2-transfected MCF-7 breast cancer xenografts. Due to the number of athymic mice required, it was not possible to comprehensively study the multiple drug effects model in vivo. Instead, cytotoxic drug doses were based on independent dose-escalation studies and were at or near the maximum tolerated dose reported in the literature for each drug. Trastuzumab doses were chosen to achieve serum concentration of more than 10 μg/mL in animals bearing HER2-overexpressing xenografts of 50 to 500 mm^3. This concentration of trastuzumab is approximately fivefold greater than that required to achieve maximal antiproliferative activity in vitro.[51] Statistically superior antitumor efficacy was observed with trastuzumab in combination with doxorubicin, paclitaxel, cyclophosphamide, methotrexate, etoposide, and vinblastine. For the drug 5-fluorouracil, which was antagonistic with trastuzumab in vitro, the combination in vivo was superior to trastuzumab alone but not to 5-fluorouracil alone.[53]

To further assess the antitumor activity of trastuzumab with cytotoxic chemotherapy, an alternative experimental system was explored using the human breast cancer cell line, BT-474. This cell line is not engineered, and like SK-BR-3, overexpresses HER2. A derivative of the BT-474 cell line has been selected for enhanced tumorigenicity. In combination studies, treatment with trastuzumab and doxorubicin or paclitaxel resulted in greater inhibition of tumor growth than observed with any agent alone. The combination of paclitaxel and trastuzumab resulted in the highest tumor growth inhibition and had a significantly superior complete tumor regression rate compared with paclitaxel or trastuzumab alone.[72]

SUMMARY

In conclusion, nonclinical pharmacology studies suggest that trastuzumab may antagonize the function of the growth-signaling properties of the HER2 system, enlist immune cells to attack and kill the tumor target, and augment chemotherapy-induced cytotoxicity.

ACKNOWLEDGMENT

The authors thank their collaborators who have contributed to the development of trastuzumab. In particular, they are grateful to Mark Pegram, Richard Pietras, and Dennis Slamon from UCLA, and Jose Baselga and John Mendelsohn from Memorial Sloan-Kettering Cancer Center for their expertise in evaluating the activity of trastuzumab in xenograft models.

REFERENCES

1. Groenen LC, Nice EC, Burgess AW: Structure-function relationships for the EGF/TGF-alpha family of mitogens. Growth Factors 11:235-257, 1994

2. Lemke G: Neuregulins in development. Mol Cell Neurosci 7:247-262, 1996

3. Carraway KL III, Cantley LC: A neu acquaintance for erbB3 and erbB4: A role for receptor heterodimerization in growth signaling. Cell 78:5-8, 1994

4. Morrissey TK, Levi AD, Nuijens A, et al: Axon-induced mitogenesis of human Schwann cells involves heregulin and p185erbB2. Proc Natl Acad Sci U S A 92:1431-1435, 1995

5. Karunagaran D, Tzahar E, Beerli RR, et al: ErbB-2 is a common auxiliary subunit of NDF and EGF receptors: Implications for breast cancer. EMBO J 15:254-264, 1996

6. Lewis GD, Lofgren JA, McMurtrey AE, et al: Growth regulation of human breast and ovarian tumor cells by heregulin: Evidence for the requirement of ErbB2 as a critical component in mediating heregulin responsiveness. Cancer Res 56:1457-1465, 1996

7. Graus-Porta D, Beerli RR, Hynes NE: Single-chain antibody-mediated intracellular retention of ErbB-2 impairs neu differentiation factor and epidermal growth factor signaling. Mol Cell Biol 15:1182-1191, 1995

8. Graus-Porta D, Beerli RR, Daly JM, et al: ErbB-2, the preferred heterodimerization partner of all ErbB receptors, is a mediator of lateral signaling. EMBO J 16:1647-1655, 1997

9. Riese DJ, van Raaij TM, Plowman GD, et al: The cellular response to neuregulins is governed by complex interactions of the erbB receptor family. Mol Cell Biol 15:5770-5776, 1995

10. Pinkas-Kramarski R, Soussan L, Waterman H, et al: Diversification of Neu differentiation factor and epidermal growth factor signaling by combinatorial receptor interactions. EMBO J 15:2452-2467, 1996

11. Plowman GD, Green JM, Culouscou JM, et al: Heregulin induces tyrosine phosphorylation of HER4/p180erbB4. Nature 366:473-475, 1993

12. Sliwkowski MX, Schaefer G, Akita RW, et al: Coexpression of erbB2 and erbB3 proteins reconstitutes a high affinity receptor for heregulin. J Biol Chem 269:14661-14665, 1994

13. Baulida J, Kraus MH, Alimandi M, et al: All ErbB receptors other than the epidermal growth factor receptor are endocytosis impaired. J Biol Chem 271:5251-5257, 1996

14. Segatto O, Lonardo F, Pierce JH, et al: The role of autophosphorylation in modulation of erbB-2 transforming function. New Biol 2:187-195, 1990

15. Di Fiore PP, Segatto O, Taylor WG, et al: EGF receptor and erbB-2 tyrosine kinase domains confer cell specificity for mitogenic signaling. Science 248:79-83, 1990

16. Jallal B, Schlessinger J, Ullrich A: Tyrosine phosphatase inhibition permits analysis of signal transduction complexes in p185HER2/neu-overexpressing human tumor cells. J Biol Chem 267:4357-4363, 1992

17. Ben-Levy R, Paterson HF, Marshall CJ, et al: A single autophosphorylation site confers oncogenicity to the Neu/ErbB-2 receptor and enables coupling to the MAP kinase pathway. EMBO J 13:3302-3311, 1994

18. Segatto O, Pelicci G, Giuli S, et al: Shc products are substrates of erbB-2 kinase. Oncogene 8:2105-2112, 1993

19. Muthuswamy SK, Siegel PM, Dankort DL, et al: Mammary tumors expressing the neu proto-oncogene possess elevated c-Src tyrosine kinase activity. Mol Cell Biol 14:735-743, 1994

20. Muthuswamy SK, Muller WJ: Direct and specific interaction of c-Src with Neu is involved in signaling by the epidermal growth factor receptor. Oncogene 11:271-279, 1995

21. Luttrell DK, Lee A, Lansing TJ, et al: Involvement of pp60c-src with two major signaling pathways in human breast cancer. Proc Natl Acad Sci U S A 91:83-87, 1994

22. Zrihan-Licht S, Lim J, Keydar I, et al: Association of csk-homologous kinase (CHK) (formerly MATK) with HER-2/ErbB-2. J Biol Chem 272:1856-1863, 1997

23. Earp HS, Dawson TL, Li X, et al: Heterodimerization and functional interaction between EGF receptor family members: A new signaling paradigm with implications for breast cancer research. Breast Cancer Res Treat 35:115-132, 1995

24. Pinkas-Kramarski R, Alroy I, Yarden Y: ErbB receptors and EGF-like ligands: Cell lineage determination and oncogenesis through combinatorial signaling. J Mammary Gland Biol Neoplasia 2:97-107, 1997

25. Burden S, Yarden Y: Neuregulins and their receptors: A versatile signaling module in organogenesis and oncogenesis. Neuron 18:847-855, 1997

26. Kraus MH, Popescu NC, Amsbaugh SC, et al: Overexpression of the EGF receptor-related proto-oncogene erbB-2 in human mammary tumor cell lines by different molecular mechanisms. EMBO J 6:605-610, 1987

27. Schaefer G, Fitzpatrick VD, Sliwkowski MX: γ-Heregulin: A novel heregulin isoform that is an autocrine growth factor for the human breast tumor cell line, MDA-MB-175. Oncogene 15:1385-1394, 1997

28. Slamon DJ, Clark GM, Wong SG, et al: Human breast cancer: Correlation of relapse and survival with amplification of the HER-2/neu oncogene. Science 235:177-182, 1987

29. Slamon DJ, Godolphin W, Jones LA, et al: Studies of the HER-2/neu proto-oncogene in human breast and ovarian cancer. Science 244:707-712, 1989

30. Hynes NE: Amplification and overexpression of the erbB-2 gene in human tumors: Its involvement in tumor development, significance as a prognostic factor, and potential as a target for cancer therapy. Semin Cancer Biol 4:19-26, 1993

31. Seshadri R, Firgaira F, Horsfall D, et al: Clinical significance of HER-2/neu oncogene amplification in primary breast cancer. The South Australian Breast Cancer Study Group. J Clin Oncol 11:1936-1942, 1993

32. Press MF, Pike MC, Chazin VR, et al: HER-2/neu expression in node-negative breast cancer: Direct tissue quantitation by computerized image analysis and association of overexpression with increased risk of recurrent disease. Cancer Res 53:4960-4970, 1993

33. Pauletti G, Godolphin W, Press MF, et al: Detection and quantitation of HER-2/neu gene amplification in human breast cancer archival material using fluorescence in situ hybridization. Oncogene 13:63-72, 1996

34. Press MF, Bernstein L, Thomas PA, et al: HER-2/neu gene amplification characterized by fluorescence in situ hybridization: Poor prognosis in node-negative breast carcinomas. J Clin Oncol 15:2894-2904, 1997

35. Shih C, Padhy LC, Murray M, et al: Transforming genes of carcinomas and neuroblastomas introduced into mouse fibroblasts. Nature 290:261-264, 1981

36. Lemoine NR, Staddon S, Dickson C, et al: Absence of activating transmembrane mutations in the c-erbB-2 proto-oncogene in human breast cancer. Oncogene 5:237-239, 1990

37. Lofts FJ, Gullick WJ: c-erbB2 amplification and overexpression in human tumors. Cancer Treat Res 61:161-179, 1992

38. Di Fiore PP, Pierce JH, Kraus MH, et al: erbB-2 is a potent oncogene when overexpressed in NIH/3T3 cells. Science 237:178-182, 1987

39. Hudziak RM, Schlessinger J, Ullrich A: Increased expression of the putative growth factor receptor p185^{HER2} causes transformation and tumorigenesis of NIH 3T3 cells. Proc Natl Acad Sci U S A 84:7159-7163, 1987

40. Pierce JH, Arnstein P, DiMarco E, et al: Oncogenic potential of erbB-2 in human mammary epithelial cells. Oncogene 6:1189-1194, 1991

41. Chazin VR, Kaleko M, Miller AD, et al: Transformation mediated by the human HER-2 gene independent of the epidermal growth factor receptor. Oncogene 7:1859-1866, 1992

42. Guy CT, Webster MA, Schaller M, et al: Expression of the neu protooncogene in the mammary epithelium of transgenic mice induces metastatic disease. Proc Natl Acad Sci U S A 89:10578-10582, 1992

43. Baselga J, Mendelsohn J: Receptor blockade with monoclonal antibodies as anti-cancer therapy. Pharmacol Ther 64: 127-154, 1994

44. Drebin JA, Link VC, Stern DF, et al: Down-modulation of an oncogene protein product and reversion of the transformed phenotype by monoclonal antibodies. Cell 41:697-706, 1985

45. Hancock MC, Langton BC, Chan T, et al: A monoclonal antibody against the c-erbB-2 protein enhances the cytotoxicity of cis-diamminedichloroplatinum against human breast and ovarian tumor cell lines. Cancer Res 51:4575-4580, 1991

46. Kasprzyk PG, Song SU, Di Fiore PP, et al: Therapy of an animal model of human gastric cancer using a combination of anti-erbB-2 monoclonal antibodies. Cancer Res 52:2771-2776, 1992

47. Stancovski I, Hurwitz E, Leitner O, et al: Mechanistic aspects of the opposing effects of monoclonal antibodies to the ERBB2 receptor on tumor growth. Proc Natl Acad Sci U S A 88:8691-8695, 1991

48. Harwerth I-M, Wels W, Marte BM, et al: Monoclonal antibodies against the extracellular domain of the erbB-2 receptor function as partial ligand agonists. J Biol Chem 267: 15160-15167, 1992

49. Hudziak RM, Lewis GD, Winget M, et al: p185HER2 monoclonal antibody has antiproliferative effects in vitro and sensitizes human breast tumor cells to tumor necrosis factor. Mol Cell Biol 9:1165-1172, 1989

50. Fendly BM, Winget M, Hudziak RM, et al: Characterization of murine monoclonal antibodies reactive to either the human epidermal growth factor receptor or HER2/neu gene product. Cancer Res 50:1550-1558, 1990

51. Carter P, Presta L, Gorman CM, et al: Humanization of an anti-p185HER2 antibody for human cancer therapy. Proc Natl Acad Sci U S A 89:4285-4289, 1992

52. Lewis GD, Figari I, Fendly B, et al: Differential responses of human tumor cell lines to anti-p185HER2 monoclonal antibodies. Cancer Immunol Immunother 37:255-263, 1993

53. Pegram M, Hsu S, Lewis G, et al: Inhibitory effects of combinations of HER-2/neu antibody and chemotherapeutic agents used for treatment of human breast cancers. Oncogene 14:2241-2251, 1999

54. Hudziak RM, Lewis GD, Shalaby MR, et al: Amplified expression of the HER2/ERBB2 oncogene induces resistance to tumor necrosis factor alpha in NIH 3T3 cells. Proc Natl Acad Sci U S A 85:5102-5106, 1988

55. Nose A, Tsuji K, Takeichi M: Localization of specificity determining sites in cadherin cell adhesion molecules. Cell 61:147-155, 1990

56. Oka H, Shiozaki H, Kobayashi K, et al: Expression of E-cadherin cell adhesion molecules in human breast cancer tissues and its relationship to metastasis. Cancer Res 53:1696-1701, 1993

57. D'Souza B, Berdichevsky F, Kyprianou N, et al: Collagen-induced morphogenesis and expression of the alpha 2-integrin subunit is inhibited in c-erbB2-transfected human mammary epithelial cells. Oncogene 8:1797-1806, 1993

58. D'souza B, Taylor-Papadimitriou J: Overexpression of ERBB2 in human mammary epithelial cells signals inhibition of transcription of the E-cadherin gene. Proc Natl Acad Sci U S A 91:7202-7206, 1994

59. Folkman J: What is the evidence that tumors are angiogenesis dependent? J Natl Cancer Inst 82:4-6, 1990

60. Weidner N, Semple P, Welch W, et al: Tumor angiogenesis and metastasis-correlation in invasive breast carcinoma. N Engl J Med 324:1-8, 1991

61. Ferrara N, Davis-Smyth T: The biology of vascular endothelial growth factor. Endocr Rev 18:4-25, 1997

62. Petit AM, Rak J, Hung MC, et al: Neutralizing antibodies against epidermal growth factor and ErbB-2/neu receptor tyrosine kinases down-regulate vascular endothelial growth factor production by tumor cells in vitro and in vivo: Angiogenic implications for signal transduction therapy of solid tumors. Am J Pathol 151:1523-1530, 1997

63. Kumar R, Shepard HM, Mendelsohn J: Regulation of phosphorylation of the c-erbB-2/HER2 gene product by a monoclonal antibody and serum growth factor(s) in human mammary carcinoma cells. Mol Cell Biol 11:979-986, 1991

64. Scott GK, Dodson JM, Montgomery PA, et al: p185HER2 signal transduction in breast cancer cells. J Biol Chem 266:14300-14305, 1991

65. Sarup JC, Johnson RM, King KL, et al: Characterization of an anti-p185 HER2 monoclonal antibody that stimulates receptor function and inhibits tumor cell growth. Growth Regul 1:72-82, 1991

66. Pan Z, Mendelsohn J, Masui H, et al: Regulation of epidermal growth factor receptor in NIH3T3/HER14 cells by antireceptor monoclonal antibodies. J Biol Chem 268:21073-21079, 1993

67. Shawver LK, Mann E, Elliger SS, et al: Ligand-like effects induced by anti-c-erbB-2 antibodies do not correlate with and are not required for growth inhibition of human carcinoma cells. Cancer Res 54:1367-1373, 1994

68. Klapper LN, Vaisman N, Hurwitz E, et al: A subclass of tumor-inhibitory monoclonal antibodies to ErbB-2/HER2 blocks crosstalk with growth factor receptors. Oncogene 14: 2099-2109, 1997

69. De Santes K, Slamon D, Anderson SK, et al: Radiolabeled antibody targeting of the HER-2/neu oncoprotein. Cancer Res 52:1916-1923, 1992

70. Devine DV: The regulation of complement on cell surfaces. Transfus Med Rev 5:123-131, 1991

71. Sung MW, Yasumura S, Johnson JT, et al: Natural killer (NK) cells as effectors of antibody-dependent cytotoxicity with chimeric antibodies reactive with human squamous-cell carcinomas of the head and neck. Int J Cancer 61:864-872, 1995

72. Baselga J, Norton L, Albanell J, et al: Recombinant humanized anti-HER2 antibody (Herceptin) enhances the antitumor activity of paclitaxel and doxorubicin against HER2/neu overexpressing human breast cancer xenografts. Cancer Res 58:2825-2831, 1998

73. Aboud-Pirak E, Hurwitz E, Pirak ME, et al: Efficacy of antibodies to epidermal growth factor receptor against KB carcinoma in vitro and in nude mice. J Natl Cancer Inst 80:1605-1611, 1988

74. Pietras RJ, Fendly BM, Chazin VR, et al: Antibody to HER-2/neu receptor blocks DNA repair after cisplatin in human breast and ovarian cancer cells. Oncogene 9:1829-1838, 1994

75. Arteaga CL, Winnier AR, Poirier MC, et al: $p185^{c\text{-}erbB2}$ signaling enhances cisplatin-induced cytotoxicity in human breast carcinoma cells: Association between an oncogenic receptor tyrosine kinase and drug-induced DNA repair. Cancer Res 54:3758-3765, 1994